Processing Xylan Rich Residue to Produce Prebiotic- Xylooligosaccharides

Submitted in partial fulfillment of the requirements

of the degree of

Doctor of Philosophy

of the
Indian Institute of Technology Bombay, India
and
Monash University, Australia

by

Ramkrishna Singh

Supervisors:

Prof. Amit Arora (IIT Bombay)

Prof. Jane Muir (Monash University)

The course of study for this award was developed jointly by
Monash University, Australia and the Indian Institute of Technology Bombay, India
and was given academic recognition by each of them.
The programme was administrated by The IITB-Monash Research Academy

(2019)

Approval

This thesis, entitled “Processing Xylan Rich Residues to Produce Prebiotic-Xylooligosaccharides” by Ramkrishna Singh is approved for the degree of Ph.D.

Assoc. Prof. Amit Arora

Supervisor
IIT-Bombay

Assoc. Prof. Jane Muir

Supervisor
Monash University

Examiner

Declaration

I declare that this written submission represents my ideas in my own words and where others' ideas or words have been included, I have adequately cited and referenced the original sources. I also declare that I have adhered to all principles of academic honesty and integrity and have not misrepresented or fabricated or falsified any idea/data/fact/source in my submission. I understand that any violation of the above will be cause for disciplinary action by the Institute and can also evoke panel action from the sources which have thus not been properly cited or from whom proper permission has not been taken when needed.

Signature

Ramkrishna Singh

Roll number:

IITB: 144354002

Monash: 26849771

Date: 7th June 2019

Acknowledgment

A Ph.D. is a long haul, albeit an exciting one, wherein the journey is equally or even more valuable as the destination. A doctoral study is not a lonely journey and cannot be done in isolation. It is an endeavor which requires association between the researchers, supervisors, institutions, infrastructure, and people supporting that infrastructure, knowingly or unknowingly. At the end of my study, I have not only learned the science but also got trained with the three M's: Man, Material, and Machine.

My Ph.D. journey started with admission into the competitive research program by the Indian Institute of Technology Bombay- Monash Research Academy. I sincerely thank the past CEO *Prof. Mohan Krishnamoorthy*, the current CEO, *Prof. Murali Sastry*, the COO *Dr. K.S. Nagabhushana*, and the entire staff for enabling smooth functioning and support during my research tenure. The program allowed me to work on multi-disciplinary research, thereby broadening my area of interest. I express my gratitude to the Centre for Technology Alternatives for Rural Areas (CTARA), IITB for providing the necessary infrastructure. I would sincerely thank *Prof. Milind Sohoni*, *Prof. Satish Agnihotri,* and *Prof. Narendra Shah* for providing the required research infrastructure. I express my heartfelt regards to my supervisors, *Prof. Amit Arora* (IITB) and *Prof. Jane Muir* (Monash University). I am extremely grateful for the extent of freedom and confidence they provided to encourage and stimulate independent thinking while giving crucial inputs at times necessary, which is highly valuable for a budding researcher.

I deeply acknowledge the guidance and inputs of the Research Progress Committee members, *Prof. Yogendra Shastri* (IITB) and *Prof. Antonio F. Patti*. They played a critical role in evaluating the work; their experience and comments have helped to increase the quality of the thesis. Prof. Tony as a mentor is exceptional, and I am thankful that he allowed me to use his lab facilities during my Monash stay, and also for the Christmas dinner and other celebratory treats. The discussion session with him was rewarding. He has a great research team, and I am glad I had an opportunity to interact with them.

On the student side, over the last four years, I got to interact with many research students and interns. During the initial days, having people like *Jhumur Banerjee* and *Karishma Bhuyan* was great. Jhumur (the first "Dr." from our group) was a great colleague. I will cherish the experience we shared in the lab, be it going to field visits or devouring delicious mangoes (a small part of her project work, the major part was valorizing the mango waste). I will remember Karishma Bhuyan for her chirpy and ever smiling nature and for gathering arecanut husk (biomass for my study). Over the four years, our research group increased from 4 members to about 25 or more and brought in different interesting characters and personalities. I am thankful to my colleagues *Priyabrata*

Pradhan, Sachin Talekar, Shivali Banerjee, Mayur Nilawar, Aniket Deo, Subramoni Hariharan, Ankur Khanpara, Kusumika Sinha-Roy, Poornima V, Dr. Richa Katiyar and Dr. Ipshita Das for their assistance. The diverse research topic each one of us works on and explains efficiently spikes the research interest, and I also thank you for keeping up the fun quotient, which helps maintain the sanity in the otherwise arduous task of research.

I sincerely thank all the research interns who were part of our group over the years. I am glad to have shared space and time with *Manshu Kapoor, Siva Ramakrishnan, Pushpani Sharma, Ashwini Kedari, Sonia Sasmal, Robina Rai, Swastika Das, Cresha Gracy Nadar* (now a Ph.D. colleague), *Tejaswini Deshmukh, Urvi Gangar and Nidhi Verma*. In assisting you guys, I and others had the opportunity to learn and update our knowledge too. It was a reciprocal learning experience. Moreover, a lot did happen on the tea-samosa breaks. I also thank my Academy batchmates and CTARA colleagues; it was fun sharing time with you all.

I express my sincere thanks to the entire team of Prof. Jane and Department of Gastroenterology, Monash University. *Daniel So* is a great researcher I had the chance to interact with; he was valuable in the successful completion of my work. I sincerely acknowledge his efforts to perform *in-vitro* human fecal fermentation study, and data analysis. I am thankful to *Paul Gill* for his help with GC analysis and also thankful to *Alex Bogatyrev, Elizabeth Ly,* and *Ally Heywood*. My sincere thanks to Prof. Tony's group, including *Dr. Karen Little, Gavin Styles, Temma Carruthers-Taylor, Cuyler Borrowman, and Dr. Wong Yong Foo,* for accommodating me in their lab and office space. I am also thankful to the School of Chemistry for providing required lab and instrument facility and to *Vu Dao, Sinuo Tan* for their help with GPC and Freeze dryer.

A great thanks to the staff members who help run the IITB, Monash University, CTARA, and the Academy efficiently. A notable mention and thanks to the non-academic staff at IITB, the PRO staff, the security, the cleaning staff, the hostel management, the various student bodies, and the various eateries. They consciously or sub-consciously contributes to an efficient and healthy organization and keep us sound and safe.

My most sincere thank goes to my family for their belief, support, encouragement, and understanding when I was absent during important events and not putting the usual societal pressure.

Yours,
Ramkrishna

Abstract:

The human gastrointestinal tract hosts an army of billions in the form of microbes in the gut. These microbes, belonging to about 1000 different types live in symbiotic association with the human host. These “good bacteria” uses undigested protein, non-digestible carbohydrates, and other undigested fraction of food reaching the distal part of the gut as an energy source. The presence of a healthy number of the good bacteria and the metabolites produced by them confer health benefits to the host like good overall gut health, reduced risk of pathogenic infection in the gut, improved metabolic control, improved immunity, etc. Non-digestible carbohydrates such as fructooligosaccharides, galactooligosaccharides, inulin, xylooligosaccharides, termed as prebiotics, can be as an energy source by gut bacteria. Xylooligosaccharides, a prebiotic, is obtained from hemicellulose, a component of the plant cell wall. Interestingly, billions of tonnes of residue result from agricultural, forestry, industrial and allied practices, comprising of cellulose, hemicellulose, and lignin along with other bioactive. The surplus quantum of such residue scores millions of tonnes. Also, with increased emphasis and incentive for cellulosic ethanol production, the availability of residue may see a further rise. Thus, xylooligosaccharides, has the advantage of being produced from abundantly available, cheaper starting material.

In this work, underutilized sources such as arecanut husk and almond shell were used for their potential valorization into prebiotic xylooligosaccharides. The alkaline pretreatment process was studied for maximal recovery of hemicellulose while achieving delignification of husk. The hydrothermal treatment (1 h) of biomass soaked in 20% NaOH was able to recover about 82% of available hemicellulose while causing 69% delignification. When the biomass suspended in alkali solution was treated with hydrothermally for 1 h (without soaking), only 75% of hemicellulose was recovered with 65% lignin removal. Further, when the hydrothermal time was increased to 1.5 h (without soaking of biomass), 83-86% of hemicellulose could be recovered with 15% w/v NaOH. Further optimization of alkaline pretreatment process was performed by evaluating incubation time (8, 16, 24 h), incubation temperature (25, 50, 65^{o}C), alkali concentration (5, 10, 15, 20% w/v) and assistance of hydrothermal treatment. The results indicate that 10% alkali can recover more than 90% of available hemicellulose when the biomass is incubated at 65^{o}C for 8 h and then treated hydrothermally for 1 h. However, when microwave irradiation was used as a heat source, 52% hemicellulose could be recovered within 3 min at 900 W with 15% alkali. Also, the alkali treated husk residue was concentrated in cellulose and could be enzymatically

converted to glucose. Upon enzymatic treatment of residue with cellulase and β- glucosidase, 75-79% reducing sugar was obtained containing 69% glucose. Thus, the husk could be fractionated into hemicellulose and cellulose using alkaline pretreatment.

For the almond shell, the effect of particle size on hemicellulose recovery and alkali concentration was evaluated. The shell was subjected to ball milling or grinding to reduce the particle size. Upon alkali treatment at 4 and 8% w/v, the observation indicates that irrespective of the method of grinding, more than 90% hemicellulose can be recovered with 8% alkali when the particle size is less than 120 µm. The optimum reaction condition was 121^{o}C, 1 h. Thus, the energy-intensive process of ball milling can be replaced with grinding while still achieving near complete hemicellulose recovery. It has been suggested that alkali pretreatment is effective for biomass with low lignin content, and thus 12-16% alkali has been reported for above 90% hemicellulose recovery. However, in this work, we have demonstrated that optimization of process, or reduction in particle size can achieve more than 90% hemicellulose at alkali concentration below 10%, even when lignin content is about 25%. As enzymes are an important cost determining factor of a process, in this work, efforts were made to optimize enzymatic reactions. An iron oxide-based magnetic nanoparticle was prepared and used as support for endoxylanase immobilization. The immobilized enzyme was found to be at par with the free enzyme in terms of pH and temperature profile, reaction kinetics. The immobilized enzyme, however, gave a lower yield of XOS as compared to free enzyme. However, when the enzymatic reaction was conducted at 50 and 60^{o}C, immobilized enzyme gave similar XOS yield, whereas the yield of free enzyme decreased at 60^{o}C as compared to 50^{o}C. Interestingly, the immobilized enzyme has limited reusability, as the XOS yield was reduced to 41% in cycle 3, as compared to the first cycle. This may be due to longer reaction time necessary to maximize XOS yields. The response surface methodology based optimization of enzyme dose and substrate concentration indicates that 10 U of the enzyme is optimum to maximize XOS yield. The analysis of RSM data indicates that substrate concentration below 2% is optimal, as an increase in substrate concentration decreases the desirability of higher XOS yield.

The enzymatically produced XOS was refined using membrane assisted separation and Diaion WA 30 resin treatment. The filtration using 10 kDa membrane allowed permeation of more than 90% of xylobiose, xylotriose, xylose, and acetic acid while decreasing the colour intensity of liquor. This is due to the retention of higher molecular weight impurities including enzyme and higher molecular weight hemicellulose or undissolved hemicellulose.

The filtration with 1 kDa did not produce a significant difference in terms of composition or colour intensity. Finally, the liquor was refined using 150 Da membrane, which retains 79% of xylobiose, 41% xylotriose along with 36-40% of xylose and acetic acid. At the end of membrane filtration, about 80% of initial low DP XOS was recovered. The resin treatment could remove colour impurities as indicated by a decrease in absorption at 230 and 280 nm from 3.8 to 1. The final colourless XOS concentrate was composed of 77% xylose based molecules, out of which 72% was present as XOS (xylobiose and xylotriose). The concentrate also contains about 10% acetic acid.

The almond shell XOS was similar to commercial corncob derived XOS in term of fermentation. The in-vitro fermentation using human fecal samples shows that XOS is rapidly fermented to produce short chain fatty acids and gases. Among, the acids, acetate was predominantly produced in case of XOS as compared to longer chain oligosaccharides such as fructooligosaccharides or inulin. The total gas produced upon XOS fermentation was not significantly different from that obtained by fermentation of commercial XOS, inulin or FOS. The in-vitro bacterial fermentation using Lactobacillus, suggest that XOS can be used as an energy source by the bacteria, as the bacterial population increases ten-fold in 48 h. Also, similar to human fecal fermentation, acetate was predominant SCFA. It was observed that the bacteria utilized xylobiose more as compared to xylotriose and xylotetrose. Thus, this study suggests that the almond shell can be used for the production of prebiotic XOS and justifies production of low DP.

As a green approach, autohydrolysis of the almond shell was studied for XOS production. For this a sequential autohydrolysis, enzymatic hydrolysis and membrane purification process was developed to obtain a low degree of polymerization xylooligosaccharides. The treatment of shell at 200^{o}C for 5 min, corresponding to severity factor of 3.64, could hydrolyze 65% of xylan to produce oligosaccharides or 10.97g XOS/ 100g biomass was obtained. However, the percentage of low DP XOS (Xylobiose and xylotriose) was 3.5% of the biomass. Upon enzymatic hydrolysis, the contribution of low DP XOS increases to 8.5% of the biomass. Further membrane separation using 1 kDa and 250 Da membrane could recover 69% of low DP XOS.

Thus, the present work provides two approaches for the production of low DP XOS. A techno-economic evaluation of the developed process will help to realize the most economical and suitable process.

Contents

Chapter 1 Introduction 1
1. Background 1
1.1. Motivation and objective of the study 3
Chapter 2 Prebiotics 5
2.1. Overview 5
2.2. Physical properties of prebiotics 6
2.3. Metabolism of prebiotics 6
2.4. SCFA and host metabolism 11
2.5. Is prebiotic supplementation required? 12
Chapter 3 Literature Review 14
3.1. Xylooligosaccharides as Prebiotics 14
3.2. Bacterial fermentation of XOS: 15
3.3. Health Benefit of XOS 16
3.3.1. Effect of XOS on Gut health 16
3.3.2. Effects on metabolic disorder 18
3.3.3. Antioxidant activity 19
3.3.4. Effect on the immune system 20
3.4. Advantages of XOS over other prebiotics 21
3.5. Prospects of XOS as a food ingredient: 22
3.6. Xylooligosaccharides production 22
3.6.1. Lignocellulosic biomass as raw material: 22
3.6.2. Tertiary Structure of lignocellulose biomass 24
3.6.3. Pretreatment methods for lignocellulosic biomass 24
3.6.3.1. Physicochemical pretreatment methods: 25
a. Autohydrolysis 25
b. Steam explosion 26
3.6.3.2. Chemical pretreatment methods 26
a. Acid hydrolysis 26
b. Alkaline pretreatment 27
3.6.4. Enzymatic Production of XOS 29
3.7. Separation and purification of XOS 34
3.7.1. Solvent extraction 35
3.7.2. Adsorption 35

3.7.3. Chromatographic methods....36
3.7.4. Membrane-based technology....37
3.8. Status of research on XOS....38
3.8.1. National status of research....38
3.8.2. International status on xylooligosaccharides research....40
3.9. Scope and objectives of the work....43
Chapter 4 Material and Methods....45
4.1. Materials:....45
4.1.1. Raw materials and chemicals....45
4.1.2. Equipment....46
Weighing balance....46
Hot air oven....46
Incubator shaker....46
pH meter....46
Centrifuge....46
Rotary evaporator....47
Freezer 47
Magnetic Stirrer....47
Hydrothermal Reactor....47
Autoclave....47
Microwave....48
High-speed grinder....48
Shredder....48
4.2. Biomass characterization....48
4.2.1. Determination of extractives in biomass....48
4.2.2. Determination of the lignocellulosic composition of biomass....49
a. Neutral Detergent Fiber....49
b. Acid detergent fiber:....50
c. Acid-insoluble lignin determination:....51
4.3. Alkaline pretreatment for extraction of hemicellulose....52
4.4. Analytical techniques....53
4.4.1. Fourier Transform Infrared Spectroscopy analysis:....53
4.4.2. Scanning Electron Microscopy....53

4.4.3. Thermal Gravimetric Analysis 53
4.4.4. Reducing sugar determination 53
4.4.5. Chromatographic method 54
Chapter 5 Preliminary study on Alkaline extraction of hemicellulose from arecanut husk 55
5.1. Biomass characterization: 56
5.2. Alkaline extraction of hemicellulose 56
5.2.1. Protocol 1: Incubation 56
5.2.2. Protocol 2: Incubation and hydrothermal assisted extraction 57
5.2.3. Protocol 3: Hydrothermal assisted alkaline extraction 57
5.3. Microwave-Assisted alkaline pretreatment 57
5.4. Enzymatic hydrolysis of alkali pretreated residue 57
5.5. Characterization of extracted hemicellulose: 58
5.6. Results and Discussion 58
5.6.1. Biomass Characterisation 58
5.6.2. Alkaline extraction of hemicellulose 59
5.6.3. Microwave-assisted fractionation of arecanut husk 61
5.6.4. Compositional analysis of pretreated residue 63
5.6.5. Enzymatic hydrolysis of residue 64
5.6.6. Characterization of extracted hemicellulose 66
5.6.6.1. Fourier Transform Infrared Spectroscopy 66
5.6.6.2. Thermal Gravimetric Analysis 67
5.6.6.3. Scanning Electron Microscopy 69
5.6.6.4. Chemical composition of extracted hemicellulose 70
5.7. Conclusion 71
Chapter 6 Process optimization for XOS production from arecanut husk 73
6.1. Optimization of a process for XOS production 73
6.1.1. Optimization of alkaline pretreatment for hemicellulose recovery 73
6.1.2. Hydrothermal assisted alkaline extraction of hemicellulose 73
6.1.3. Enzymatic hydrolysis of extracted hemicellulose 75
6.2. Results and Discussion 76
6.2.1. Optimization of alkali assisted hemicellulose extraction 76
6.2.2. Hydrothermal assisted alkali pretreatment for hemicellulose recovery 78
6.2.3. Enzymatic hydrolysis of extracted hemicellulose 84

6.3. Conclusion 89
Chapter 7 Production of Xylooligosaccharides from Almond Shell 90
7.1. Part A: alkaline pretreatment of almond shell 91
7.1.1. Determination of lignocellulosic composition of almond shell 91
7.1.2. Ball milling and alkaline extraction shell hemicellulose 91
7.1.3. Grinding and alkaline extraction of shell hemicellulose 92
7.2. Results and discussion 92
7.2.1. Lignocellulosic composition of shell 92
7.2.2. Alkaline extraction of hemicellulose from ball milled samples 92
7.2.3. Alkaline extraction of hemicellulose from ground shells 94
7.2.4. Hemicellulose characterization 96
7.3. Part B: Production of xylooligosaccharides 97
7.3.1. Immobilized enzyme assisted XOS production 97
7.3.1.1. Synthesis and activation of magnetic nanoparticles 97
7.3.1.2. Immobilization of endoxylanase 98
7.3.1.3. Characterization of immobilized enzyme 98
7.3.1.4. Production of Xylooligosaccharides 99
7.4. Results and Discussion 99
7.4.1. Synthesis of enzyme coated magnetic nanoparticles 99
7.4.2. Characterization of immobilized xylanase 100
7.4.2.1. Effect of pH on enzyme activity 100
7.4.2.2. Reaction Kinetics: 102
7.4.2.3. Storage Stability of immobilized enzyme 103
7.4.2.4. Enzymatic production of Xylooligosaccharides 107
Part C: RSM based optimization of enzyme dose and substrate concentration 111
7.5. Optimization of enzymatic hydrolysis 111
9.6. Results: Optimization of enzymatic hydrolysis 113
7.7. Conclusion: 117
Chapter 8 Autohydrolysis pretreatment for XOS production 119
8.1. Methodology 120
8.1.1. Reactor system and autohydrolysis 120
8.1.2. Enzymatic hydrolysis of original liquor 121
8.1.3. Membrane assisted refining of XOS liquor 122

8.2. Result and Discussion....122
8.2.1. Effect of autohydrolysis on xylan hydrolysis....122
8.2.2. Composition of autohydrolysis liquor....126
8.2.3. Enzymatic hydrolysis of liquor....127
8.2.4. Membrane assisted refining of enzymatic XOS liquor....131
8.3. Conclusion....136
Chapter 9 Membrane assisted refinement and *in-vitro* fermentation of XOS....137
9.1. Methodology....138
9.1.1. Membrane assisted refinement of enzymatic XOS liquor....138
9.1.2. *In-vitro* human fecal fermentation study....139
9.1.2.1. Participants....139
9.1.2.2. In vitro fermentation....139
9.1.2.3. Assessment of gas production in response to fiber substrates....140
11.1.2.4. Short chain fatty acid concentrations....140
9.1.2.5. Statistical analysis:....140
9.1.3. *In-vitro* bacterial fermentation....141
9.2. Results and discussion....142
9.2.1. Membrane assisted refinement of XOS....142
9.2.2. *In-vitro* human fecal fermentation....149
9.2.3. *In-vitro* bacterial fermentation....152
9.3. Conclusion....156
Chapter 10 Conclusion and Future work....157
11. References....164
Appendix (i)....178
Appendix ii....183

List of Figures:

Figure 2.1: The metabolic route for utilization of non-digestible carbohydrates by gut microbiota (den Besten et al., 2013b) 10
Figure 2.2: The metabolic route for the production of butyrate upon carbohydrate fermentation (den Besten et al., 2013b) 10
Figure 5.1: Glucose release during enzymatic hydrolysis of pretreated arecanut husk (hydrothermal treatment for 1.5 h and alkali concentration 15%) 65
Figure 5.2: FTIR spectra of extracted hemicellulose a) hydrothermal pretreatment of alkali soaked biomass b) hydrothermal pretreatment of alkali steeped and c) (16 h) biomass microwave irradiated 66
Figure 5.3: TGA profile of untreated and hydrothermally pretreated biomass 68
Figure 5.4: SEM images of biomass a) untreated, b) hydrothermal pretreatment of alkali soaked biomass and c) hydrothermal pretreatment of alkali steeped biomass and d) microwave irradiated 69
Figure 6.1: Process flow diagram for optimization and production of XOS from arecanut husk 74
Figure 6.2: (A) Main and (B) Interaction plots for hemicellulose recovery 81
Figure 6.3: Relative recovery at (a) different alkali concentrations (5 and 10%) and hydrothermal treatment periods (1, 1.5 and 2h) for incubation period of 8h and (b) different alkali concentrations (5 and 10%) and incubation periods (8, 16, 24 h) 83
Figure 6.4: Time course study of xylose, xylobiose, xylotriose, xylotetrose, XOS and acetic acid production at optimal experimental conditions (Temperature: 50°C, pH: 4, Enzyme dosage: 10 U) 88
Figure 7.1: Particle size range obtained after ball milling of the almond shell for different time. 93
Figure 7.2: Effect of particle size on hemicellulose recovery at the studied alkali concentration 94
Figure 7.3: FTIR Spectra of extracted hemicellulose and its comparison with commercial corncob derived xylan 96
Figure 7.4: Pictorial Representation for activation of magnetic nanoparticles using APTES and enzyme immobilization 97
Figure 7.5: Xylanase activity upon immobilization on magnetic nanoparticles using different concentration of glutaraldehyde 100
Figure 7.6: Characterisation of immobilized enzyme, a) effect of pH on the activity of free and immobilized xylanase, b) effect of Temperature on the activity of free and immobilized xylanases 101
Figure 7.7: Enzymatic activity of free enzyme and immobilized enzyme at different substrate concentration, pH 5.8 and 50^{o}C 103
Figure 7.8: Percentage residual activity after storage for 30 days at 4^{o}C 104
Figure 7.9: FTIR spectra of MNP, APTES-MNP and E-MNP showing characteristic peaks 105
Figure 7.10: FEG-SEM images of (a) MNP, (b) APTES-MNP, (c) E-MNP 106
Figure 7.11: XRD pattern of iron oxide MNP, APTES-MNP, and E-MNP 107

Figure 7.12: Comparison of XOS produced by free xylanase and xylanase immobilized on magnetic nanoparticles at: a) 50oC and b) 60oC. The bar graph represents XOS yield concerning hemicellulose, and line graph denotes XOS yield concerning xylan.....108
Figure 7.13: XOS yields produced after three successive cycles of enzymatic hydrolysis using same immobilized enzyme on fresh substrate.....110
Figure 7.14: Contour, 3D surface plot and desirability estimate of XOS production. A) Contour plot describing the effect of enzyme dose and substrate concentration on XOS yield; B) 3D surface plot describing the effect of enzyme dose and substrate concentration on XOS yield; C) Response optimization plot describing the desirability of XOS production at enzyme dose of 10 U and 1.17% substrate concentration; D) Response optimization plot describing the desirability of XOS production at enzyme dose of 10 U and substrate 2%.....117
Figure 8.1: Schematic description of the process for autohydrolysis and maximizing low DP XOS production.....121
Figure 8.2: The effect of temperature and holding time on depolymerization of xylan and formation of oligosaccharides (% of xylan).....123
Figure 8.3: The influence of severity factor upon xylan depolymerization and generation of oligosaccharides (% of xylan). represents 180^{o}C, represents 200^{o}C and represents 220^{o}C.....125
Figure 8.4: The percentage of total XOS and the corresponding levels of xylobiose and xylotriose produced upon autohydrolysis at different experimental conditions.....125
Figure 8.5: Enzymatic hydrolysis of autohydrolysate to increase the composition of low DP XOS (sum of xylobiose and xylotriose) at three different enzyme doses of 5 U, 10 U, and 15 U.....128
Figure 8.6: Statistical analysis of enzymatic hydrolysis of autohydrolysate showing (a) main plot (b) interaction plot and (c) contour plot.....131
Figure 8.7: The flux rate observed during membrane filtration using 1 kDa and 250 Da membrane.....132
Figure 8.8: Mass balance of constituent upon membrane assisted refining using 1 kDa and 250 Da membranes. X2: Xylobiose, X3: Xylotriose, X: Xylose, G: Glucose, A: Arabinose and Aa: Acetic acid. Y axis is in g/100g biomass.....134
Figure 9.1: Schematic of membrane filtration sequence and the observed flux.....143
Figure 9.2: Mass balance of membrane separation of enzymatically produced XOS.....145
Figure 9.3: The percentage permeation of each component with time upon filtration through 150 Da.....146
Figure 9.4: Colour of (a) feed (b) 150 Da retentate and (c) Diaion treated liquor 147
Figure 9.5: UV-Vis spectra of membrane refined XOS at different stages of filtration.....148
Figure 9.6: FEG-SEM images of membranes after filtration process (a) 10 kDa, (b) 1 kDa and (c) 150 Da.....149
Figure 9.7: Kinetics of total gas production over four hours for different fiber substrates. Values are mean (n = 3) ± SD.....151
Figure 9.8: Optical density measured upon fermentation of carbohydrates by Lactobacillus spp.....152
Figure 9.9: Drop in pH as measured upon fermentation of carbohydrates by Lactobacillus spp.....154

Figure 9.10: The residual XOS content at the end of fermentation 155

List of Tables

Table 2.1: Dietary oligosaccharides with occurrence, chemical characteristics, production process, dose, calories, sweetness and marketed product. 7
Table 2.2: Examples of acetate, propionate, and butyrate-producing bacteria and the physiological effect ascribed to SCFAs 12
Table 3.1: Study of bacterial fermentation of prebiotic XOS 15
Table 3.2 : Lignocellulose composition of some biomass and availability of their residue in a million tons……..….23
Table 3.3: Examples of pretreatment method for isolation and separation of xylan and XOS from lignocellulose material…….27
Table 3.4: Literature review on the use of enzymatic hydrolysis for XOS production……...30
Table 3.5: Examples of immobilization techniques used for immobilization of endoxylanase for XOS production……..…32
Table 5.1: Chemical composition of arecanut husk 58
Table 5.2: Ultimate analysis of arecanut husk 59
Table 5.3: Relative recovery of hemicellulose from arecanut husk under different experimental conditions 60
Table 5.4: Hemicellulose recovery upon microwave irradiation of alkali biomass mixture ..62
Table 5.5: Compositional analysis of pretreated residue depicting % cellulose and % delignification 64
Table 6.1: Relative recovery of hemicellulose under studied conditions 77
Table 6.2: Analysis of variance (ANOVA) test for experimental response for hydrothermal experiment.....79
Table 6.3: Optimization constraints and solutions for maximum relative recovery of hemicellulose 83
Table 6.4: Experimental design layout of enzymatic hydrolysis (Box-Behnken design) and average yields of various oligomers 85
Table 6.5: a) Analysis of Variance (ANOVA) test for an experimental response for enzymatic hydrolysis of hemicellulose into XOS, b) evaluation of regression coefficients of determinations.....87
Table 7.1: Percentage relative recovery of hemicellulose upon alkaline extraction of different fractions.....95
Table 7.2: Kinetic parameter (Km and Vmax) of free and immobilized enzyme.....103
Table 7.3: Central composite design generated for variables, predicated and experimental values of XOS yield 112
Table 7.4: Analysis of Variance (ANOVA) test for the experimental XOS yield obtained from hemicellulose hydrolysis 114
Table 8.1: The content of monosaccharide, acetic acid and corresponding liquor pH upon autohydrolysis 127
Table 8.2: Analysis of Variance test for experimental response upon enzymatic hydrolysis 128
Table 8.3: Mass balance of components upon membrane assisted refining of XOS liquor .133

Table 9.1: The composition of permeate and retentate upon membrane filtration using different molecular weight cut-off.....143
Table 9.2: Absorbance at 230 and 280 nm of samples at a different stage of membrane refining.....148
Table 9.3: Magnitude of gas production, differences in pH and SCFA at the end of the four hours experimental period for each fiber substrate.....150
Table 9.4: The SCFA level produced upon fermentation of carbohydrates by Lactobacillus spp.....155

Abbreviations

($\overline{(DP)}$): average degree of polymerization
Acetyl CoA: Acetyl Coenzyme A
ADF: Acid Detergent Fiber
AIL: Acid insoluble lignin
ANOVA: Analysis of Variance
AXOS: arabinoxylooligosaccharides
DDGS: Distiller's dried grains with solubles
DP: Degree of Polymerisation
EMP: Embden-Meyerhof-Parnas
FEG-SEM: Field Emission Gun- Scanning Electron Microscopy
FOSHU: Food for Specified Health Use
FTIR: Fourier Transform Infrared Spectroscopy
GIT: gastrointestinal tract
IBD: Inflammatory Bowel Disease
IBS: Irritable Bowel Syndrome
MWCO: Molecular Weight Cut-off
NADH: Nicotinamide adenine dinucleotide
NADPH: Nicotinamide adenine dinucleotide phosphate
NDF: Neutral Detergent Fiber
PEP: phosphoenolpyruvate
RPM: Rotations per minute
RSM: Response Surface Methodology
SCFA: Short chain fatty acids
SEM: Scanning Electron Microscopy
TGA: Thermal Gravimetric Analysis
X2: Xylobiose
X3: Xylotriose
X4: xylotetrose
XOS: Xylooligosaccharides

Chapter 1 Introduction

1. Background:

A complex ecosystem of "superorganism" or microbiome, comprising of bacteria, archaea, yeast, and filamentous fungi, is thought to have co-evolved with human beings. These microbiomes reside on and inside of humans, and many a time presents symbiotic associations. The host gastrointestinal tract (GIT) acts as a barrier between environmental factors, food and host, and contains about 10^{14} microbial cells, which is about ten times more than the human cell (Gill et al., 2006). A recent study estimated that about 3.8×10^{13} bacterial cells are present as compared to 3.0×10^{13} human cells, thereby giving a ratio of about 1:1-1:1.3. The study also suggested that the bacterial cells total mass is about 0.2 kg in a 70 kg individual (Sender, Fuchs, & Milo, 2016). The gastrointestinal tract of an individual is thought to harbor more than 1000 bacterial species, most of which are strict anaerobes. It is believed that strict anaerobes are abundant and predominate facultative anaerobes and aerobes (Gorbach, 1996). Research has also indicated the presence of above 50 bacterial phylotypes in the human gut. However, *Bacteroidetes* and *Firmicutes* are predominantly present (Schloss & Handelsman, 2004).

The consensus about the development of the gut microbiota indicates birth as a point of origin. However, few studies argue the detection of microbes in placenta (Aagaard et al., 2014). The microbial composition of infants is thought to be influenced by the mode of delivery, wherein, the *Lactobacillus* flora from the vagina is reflected in infants upon vaginal delivery (Aagaard et al., 2012). Whereas, most of the C-section delivered infants shows the presence of facultative anaerobes such as *Clostridium* species (Jakobsson et al., 2014). Also, the colonization of such infant gut with *Bacteroides* genus is observed to be delayed. It has also been observed that about 72% of vaginally delivered babies and 41% of C-section delivered babies have microbiota, which is representative of the mother's (Bäckhed et al., 2015). Initially, the microbiota is predominantly belonging to Actinobacteria and Proteobacteria phyla, but with age the microbial diversity and number increases and by the age of 2.5 years, it represents adult-like capabilities (Rodríguez et al., 2015). The microbiota serves as a protective barrier and contributes to the first line of defense provided by the gut, by preventing the adhesion of pathogenic bacteria and competing for available nutrition (Hooper, Xu, Falk, Midtvedt, & Gordon, 1999). Also, they are also responsible for the production of vitamins and the development of the immune system (Canny & McCormick,

2008). The presence of a healthy bacterial colony is associated with host metabolism, physiology, immune development and response, energy balance, disease/ disorder, and behavior (Stearns et al., 2011). Various intervention studies to modulate and enforce the development of healthy gut microbiota has shown to restore gut-related disorders including inflammatory bowel disease (IBD), irritable bowel syndrome (IBS), metabolic disorders including diabetes, obesity (O'Mahony, 2015; Galisteo, Duarte, & Zarzuelo, 2008).

The gut microbiome is dependent on fermentation of undigested substrates from the diet including undigested carbohydrates, undigested proteins, non-digestible oligosaccharides, dietary fiber, host-derived glycoprotein, epithelial cells, and pancreatic secretions, for energy and metabolism. It has been observed that fermentation of carbohydrates is energetically favorable as compared to protein, and hence upon entering the colon, it is preferentially fermented. Also, fermentation of protein produces a range of chemicals which can cause irritation, cytotoxicity, and genotoxicity (De Filippo, C.; Lionetti, 2016; Richardson, McKain, & Wallace, 2013). The metabolites produced upon fermentation include short-chain fatty acids (SCFA), gases, and heat. The SCFA's including acetate, propionate, butyrate are claimed to be involved in improving gut health, maintaining gut integrity, inhibiting growth and proliferation of pathogenic bacterium, aid in mineral absorption and produce putative peripheral benefits on liver, adipose and muscle tissue and brain (Lunn & Buttriss, 2007; Tremaroli & Bäckhed, 2012).

Along with the mode of delivery, host genetics, immunological factor, antibiotic usage, and diet influence the development and composition of gut microbiota. In recent years, a change in lifestyle reflected in a sedentary lifestyle, decreased physical activity accompanied by increased energy intake, the host energetic balance has disrupted (den Besten et al., 2013a). With an increased preference for a refined and processed food product, the intake of fiber as part of a natural diet has decreased, thereby reducing the substrate available for microbial fermentation. The altered diet and microbial balance are among the reason for the higher incidence of metabolic and lifestyle-related diseases and disorders. Such metabolic disorders are on the rise in both developing and developed countries. In India, the medical expenses incurred due to chronic conditions like heart disease, diabetes, and cancer is estimated to be $236.6 billion (Sharma & Majumdar, 2009).

Prebiotics are a class of non-digestible carbohydrates which can serve as a source of energy for the gut microbiome. Xylooligosaccharides (XOS), as a prebiotic, can be obtained from the

hydrolysis of hemicellulose, the second most abundant bio-polysaccharides after cellulose. Annually, tonnes of lignocellulosic residues are generated due to agricultural, horticultural, and allied activities in the form of cob, bagasse, straw, husk. These residues are rich in cellulose, hemicellulose, and lignin and abundantly discarded as waste. Due to the presence of about 25% hemicellulose in lignocellulosic residues, they can act as potential raw material for the production of prebiotic oligosaccharide, xylooligosaccharides.

1.1. Motivation and objective of the study

Most of the commercially available prebiotics such as fructooligosaccharides, inulin, are either synthesized chemically or obtained from limited natural sources. Xylooligosaccharides, on the other hand, can be obtained from abundantly available lignocellulosic residues. Out of the tonnes of biomass generated, a significant amount is either burned or discarded without value addition, thereby representing a loss of resource and contributing to environmental pollution. Valorization of such residues for the production of prebiotic oligosaccharide can minimize environmental impact while providing monetary returns and health benefits.

Thus, the current work is concerned with the valorization of lignocellulosic residue for the generation of xylooligosaccharides. In this work, two substrates of different physical forms, i.e., husk (arecanut husk) and shell (almond shell) were used. The rationale for selecting two different substrates was the potential difference in energy and efforts required for particle size reduction. The shells are more natural to grind into micron size as compared to the husk. As particle size is an important variable in a chemical process, alkaline pretreatment protocol was developed for these two substrates to minimize chemical usage. The other criteria for selection of biomass was the lignin content. The substrate with lignin content above 20% was selected to develop the process for hemicellulose extraction. As lignin content is one of the governing factors for the success of the pretreatment process, it is proposed that an efficient process for biomass with high lignin content will be equally useful for lower lignin content biomass. In addition, to the best of my knowledge, no reports are available on valorisation of arecanut husk to produce XOS. Although, for almond shell, autohydrolysis has been studied for production of XOS, however, a broad degree of polymerisation range product was reported. The objective of the work is to evaluate two different pretreatment approaches. For alkaline pretreatment, the objective is to minimize chemical requirements for extracting maximum available hemicellulose. As enzymatic hydrolysis is an essential step for XOS production and as enzymes contribute significantly to a process cost, in this work, efforts were made to optimize the enzymatic hydrolysis. The enzyme immobilization on magnetic

nanoparticles was evaluated for its feasibility to enable reuse of enzyme upon full enzymatic reaction cycle. Also, substrate concentration and enzyme dose were optimized using response surface methodology. The physicochemical pretreatment (Autohydrolysis), was studied as a greener alternative to XOS production. In this process, efforts were directed to obtain narrow range, low degree of polymerization (DP) XOS. The work has also dwelled in developing a membrane bio-separation and resin assisted, separation and refining process for concentration of produced xylooligosaccharides. Upon fermentation, gas and short chain fatty acids are produced as primary metabolites. Hence, the last part of work includes studying the fermentation of XOS using bacteria and human faecal matter to estimate the levels of gas and short chain fatty acid produced.

Chapter 2 Prebiotics

2.1. Overview:

The famous saying of Hippocrates "let food be thy medicine and medicine be thy food" was embraced many centuries ago and has received new limelight from the 20th century. With the assistance of sophisticated technology and greater understanding, scientists have started identifying bioactive or physiologically active ingredients of food that have putative health claims. Such research activity has translated into the introduction of health supplements and health-promoting products, health-aware consumers, introduction, and modification of existing guidelines and regulations and introduction of the term "functional foods"(Hasler, 2002). The concept of functional food came into existence in the 1980s, when Japan introduced the term "Food for Specified Health Use (FOSHU)," under which certain foods with demonstrated health benefits were approved for its aging population (Arai, 1996). Functional foods are thus basic nutrition food with demonstrable physiological benefits and can include: a) food with natural bioactive, b) derived foods such as prebiotics and c) bioactive added to food as supplements such as antioxidants, probiotics (Grajek, Olejnik, & Sip, 2005).

Prebiotics are considered as food ingredients which are either non-digestible or has low digestibility, can selectively stimulate the growth of beneficial gut microbiota, thereby providing health benefits to the host. The criteria's by which a product is considered as prebiotics are as follows (Roberfroid, 2007; Roberfroid & Slavin, 2010; Broekaert et al., 2011):

a) Resistant to gastric acidity or hydrolysis by mammalian digestive enzymes and absorption
b) Fermentation and utilization as an energy source by gut microbiota
c) Ability to induce growth or activity of beneficial gut bacteria to confer a health benefit to the host

The listed criteria's result in all prebiotics being considered as dietary fiber, but not all fiber can be considered as prebiotics. Prebiotics can be dietary nondigestible carbohydrates (resistant starch, dextrins), non-starch polysaccharides (such as pectin, gums, hemicellulose), non-digestible oligosaccharides such as fructans, mannans, raffinose, stachyose; undigestible disaccharides (lactose/lactulose) and sugar alcohols such as isomalt, lactitol (Bajury, Nashri,

King Jie Hung, & Sarbini, 2018). Table 2.1 presents examples of some of the prebiotics along with their source, chemical characteristics, production process, and marketed products.

2.2. Physical properties of prebiotics:

As outlined in the above paragraph and Table 2, prebiotics are structurally oligosaccharides obtained either from natural sources or synthesized using chemical and enzymatic routes. Being oligosaccharides, they are composed of 2-9 molecules of monosaccharides linked via β- glycosidic linkages. Owing to the difference in glycosidic linkage as compared to digestible starch, prebiotic oligosaccharides are resistant to action by digestive enzymes, except for lactose, which is digestible by mammalian digestive enzymes. Prebiotics are available as a dried powder, and their thermophysical properties depend on their molecular weight. Prebiotics are water soluble with relative sweetness in the range of 0.3-0.6 when compared to sucrose. As they are non- digestible by mammalian enzymes and hence possess limited to none absorption, they are considered as food of low or zero calories (Roberfroid & Slavin, 2010).

2.3. Metabolism of prebiotics:

As non-digestible carbohydrates, prebiotics mostly reaches the lower part of the gut in intact form and are then fermented by gut microbiota as a source of energy. The product of carbohydrate fermentation includes short-chain fatty acids (SCFA) such as acetic acid, propionic acid, butyric acid, lactic acid along with gases and heat. The SCFAs are present in the range of 70-130 mmol/L, thereby contributing to two-thirds of colonic anion concentration. The general reaction of a carbohydrate (e.g., hexose) fermentation is as depicted below:

$$59C_6H_{12}O_6 + 38H_2O \rightarrow 60CH_3COOH + 22CH_3CH_2COOH + 18CH_3CH_2CH_2COOH + 96CO_2 + 268H^+ + \text{Heat} + \text{additional bacteria}$$

It is postulated that the percentage and distribution of SCFA upon fermentation is dependent on colonic microflora; type, amount and structural features of carbohydrates, but generally shows a similar trend to that of hexoses.

Table 2.1: Dietary oligosaccharides with occurrence, chemical characteristics, production process, dose, calories, sweetness and marketed product.

Type of OS	Natural occurrence	Chemical structure	Chemical composition	Production process	Daily dose (g/day)	Calorie (Kcal/g)	Sweetness	Marketed product	Reference
Lactulose	Cow milk	Ga-Fr	4-*O*- β-D-galactopyranosyl-D-fructose	Alkali Isomerization of lactose	10	-	48-62% of sucrose		(Mussatto & Mancilha, 2007; Bouhnik, et al., 2004)
Inulin	Chicory roots, onion, asparagus, artichoke	GuFr*n*	FOS having DP from 3- 60. Fructosyl-glucose and fructosyl-fructose linked by β-(2→1) & β-(1→2) respectively	Diffusion in hot water, refining and spray drying	10-20	1-2	30% of sucrose	Raftilose (Orafti, USA); Inulin FOS (Jarrow Formulas, USA)	(Niness, 1999; ; Murphy, 2001; Kelly, 2009; Costabile, et al., 2010; (Apolinario, et al., 2014)
FOS	Artichoke, garlic, onion, asparagus, chicory	(Fr)n-Gu	β-(2→1) linked fructosyl unit with terminal glucose. Chain length of 2-10 with average DP of 4	Inulin hydrolysis, synthesis from sucrose	10	2	20-40% of sucrose	Aktifit (Emmi, switzerland) ; probioplus (Migros, Switzerland	(Guio, Rodriguez, Almeciga-Diaz, & Sanchez, 2009; Niness, 1999; Yun, Jung, Oh, & Lee, 1990; Bornet, Brouns, Tashiro, & Duvillier, 2002)
GOS	Human milk, cow milk	(Ga)n-Gu	2-8 galactose uint with terminal glucose having 1→4, 1→6 linkages	Enzymatic tranglycosylation from lactose	5-10	1.73	30-60% of sucrose	Oligomate (Yakult, Japan); Cup-Oligo (Nissin, Japan)	(McVeagh & Miller, 1997; Chockchaisawasdee, Athanasopoulos, Niranjan, & Rastall, 2004; Sako, Matstumoto,

									& Tanaka, 1999; Voragen, 1998; Lamsal, 2012; Torres, Goncalves, Teixeira, & Rodrigues, 2010)
IMO	Starch from wheat, barley, potato, rice, cassava, honey	(Gu)n	4-7 units of α-(1,6) linked (6-*O*- α-D-glucopyranosyl -D-glucose)	Enzymatically transformed from starch	8-10	2.8-3.2	40% of sucrose	Vitafiber (BioNeurta, USA), IMO	(Lee, Wang, & Lin, 2008; Goulas, Fisher, Grimble, Grandison, & Rastall, 2004; Patel, Patel, & Krishnamurthy, 2013)
Soybean oligosaccharides	Soybean	Raffinose, stachyose,	α-(1,6) linked galactose bonded via α-(1,3) to terminal sucrose	Extracted from soybean whey	-	-	-	Oligo CC (Calpis, Japan)	Espinosa-Martos & Ruperez, 2006
XOS	Hardwood, corncob, wheat straw, rice hull, barley straw	Xy*n*	β-(1→4) linked xylopyranose, with arabinofuranosyl, 4-O-methylglucuronic acid, acetyl, phenolics substituted at C2 or C3.	Hydrolysis of Hemicellulose	2-5	-	30% of sucrose	Llife-Oligo (Lifebridge, USA)	(Moure, Gullon, Dominguez, & Parajo, 2006; Vazquez, Alonso, Dominguez, & Parajo, 2000); (Aachary & Prapulla, 2009)

SCFA production is dependent on the type of carbohydrates and the bacterium species (Macfarlane & Macfarlane, 2003). In vitro fermentation of individual carbohydrates using faecal microbiota have shown a difference in the rate of fiber fermentation. It was observed that polysaccharides such as starch and pectin, undergo rapid fermentation as compared to xylan or arabinogalactan. Also, the difference in concentration of metabolite was also observed, with acetate being produced predominantly upon pectin and xylan fermentation, while acetate and propionate produced upon arabinogalactan fermentation. Upon fermentation of glucose-based polysaccharide (Starch), the major SCFA produced was butyrate (Englyst, Hay, & Macfarlane, 1987). It is observed that the primary metabolite produced by phylum Bacteroidetes is acetate and propionate, whereas Firmicutes produces butyrate predominantly upon carbohydrate fermentation.

The gut microbiota possesses the ability to breakdown non-digestible carbohydrates and oligosaccharides into monosaccharides, which are fermented to harness energy. Depending on the sugar, two metabolic pathways are utilized: the Embden-Meyerhof-Parnas (EMP) pathway (glycolysis) for hexose sugars or the Pentose-Phosphate pathway (PPP) for pentoses. As shown in Figure 2.1, the metabolite produced at the end of these pathway includes phosphoenolpyruvate (PEP) and the electron carrier NADH or NADPH. The pyruvate obtained at the end of the EMP or PPP route acts as a precursor for generation of SCFAs. The pyruvate can undergo decarboxylation to produce acetyl-CoA, which can result in acetate.

Additionally, the liberated carbon dioxide can undergo the Wood-Ljungdahl pathway to produce acetate. As shown in figure 2.1, pyruvate can be converted to lactate, which then undergoes the acrylate pathway to produce propionate. Alternatively, the oxaloacetate generated from PEP can undergo a series of reaction to produce succinate which is then converted to propionate. In the classical pathway, two molecules of acetyl-CoA can undergo condensation to produce butyryl-CoA, which is a precursor for butyrate (Figure 2.2).

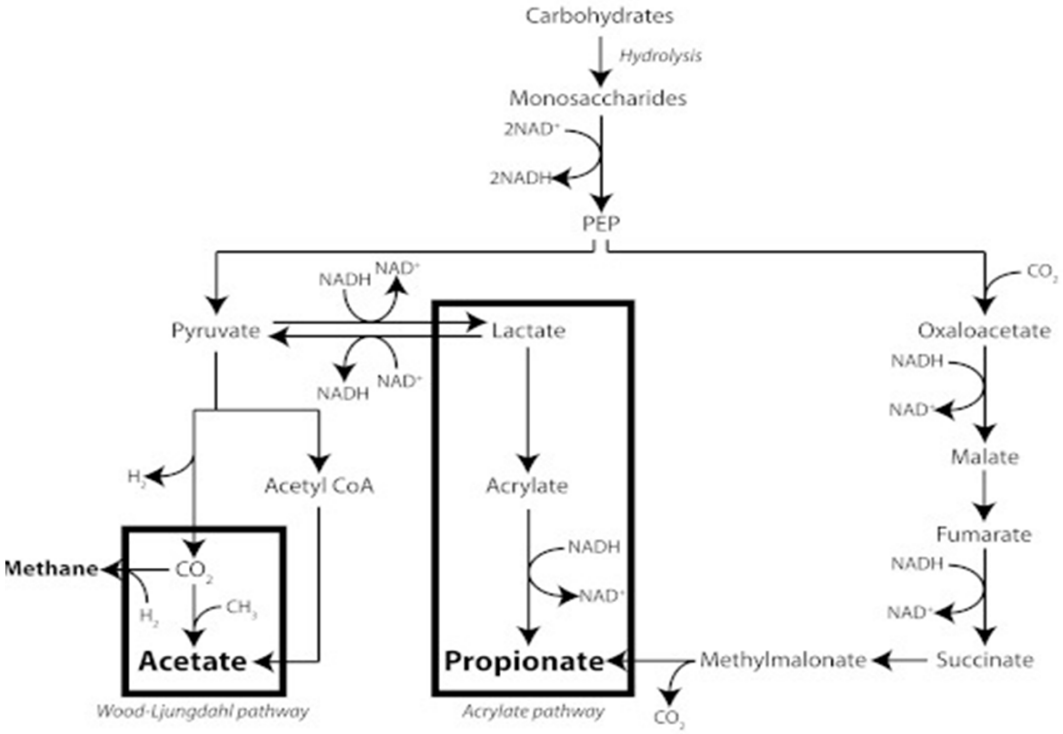

Figure 2.1: The metabolic route for utilization of non-digestible carbohydrates by gut microbiota (den Besten et al., 2013b)

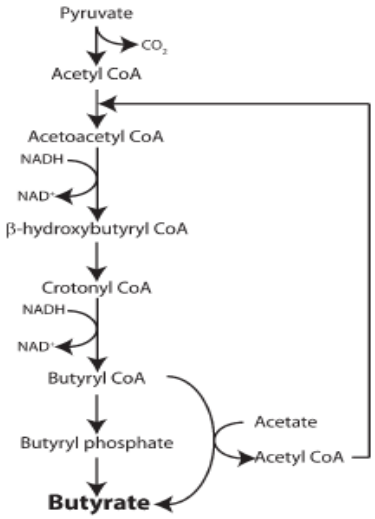

Figure 2.2: The metabolic route for the production of butyrate upon carbohydrate fermentation (den Besten et al., 2013b)

However, a cross-feeding between acetate producing and butyrate-producing bacteria is observed; wherein, exogenous acetate is used to produce butyrate using butyryl-CoA:acetate-CoA transferase. This alternative pathway is thought to be predominant in human gut microbes (Duncan, Barcenilla, Stewart, Pryde, & Flint, 2002; Venema, 2010).

2.4. SCFA and host metabolism:

These SCFAs create an osmotic load, decreases pH of the lumen, stimulates intestinal cell growth and proliferation, and contributes as an energy source to cells. Various receptors and mechanisms have been proposed governing the uptake of produced SCFA including the SCFA-HCO_3^- exchange and monocarboxylate transporters. Upon uptake, it is considered that SCFA contributes about 5-10% of host energy requirement, whereas, colonocytes derive about 60-70% of its energy from SCFA metabolism. Butyrate is preferentially used as a source of energy by colonocytes, which oxidized it to ketone bodies and carbon dioxide (Bergman, 1990; Roediger, 1982). Acetate resulting from bacterial fermentation is absorbed into the bloodstream, and a significant fraction (~70%) is used up by the liver as an energy source, for the synthesis of cholesterol, triacyl-glycerides and as co-substrate for glutamine and glutamate synthesis (Bloemen et al., 2009). The liver clears most of the propionate from blood circulation, wherein it is used as a precursor for gluconeogenesis (Pereira & Gibson, 2002). It has also been proposed that the ratio of acetate/propionate is important concerning the cholesterol-lowering ability of prebiotics (Pereira & Gibson, 2002). The SCFA via a complex signaling pathway tends to reduce free fatty acid in plasma by activating fatty acid oxidation in tissues and inhibiting de-novo synthesis, lipolysis and fat storage in white adipose tissue. This effect is beneficial for diet-induced obesity. Butyrate is considered as the primary source of energy for colonocytes, regulating their growth and proliferation. Also, it has also be implied in inhibiting the growth of colorectal cancerous cells and inducing apoptosis, thereby being preventive of colon cancer (Cruz-Bravo et al., 2014; Heerdt, Houston, & Augenlicht, 1997). Table 2.2 gives the example of bacterium suggested to maximize a specific SCFA production and also summarizes the physiological effects of SCFA (Fernández et al., 2016).

2.5. Is prebiotic supplementation required?

A difference in diet is observed between the developed and underdeveloped or developing countries, with a westernized diet being rich in animal protein, fat, sugar while having low fiber content. In contrast, most of the developing or rural communities have higher dietary fiber intake due to the consumption of vegetables and fruits. It has been observed that in the US adults consume about 12-18g fiber per day, whereas it is about 14g/day in the UK and 16-29g/day in Europe (Holscher, 2017).

Table 2.2: Examples of acetate, propionate, and butyrate-producing bacteria and the physiological effect ascribed to SCFAs

SCFA	Producer microbe	Beneficial effect
Acetate	*Bifidobacterium adolescentis* *Lactobacillus spp.* *Bacteroides thetaiotaomicron*	Energy source Induction of cholesterol biosynthesis
Propionate	*Roseburia insulinovorans* *Veillonella spp* *Ruminococcus obeum* *Bacteroides spp* *Dialister spp* *Phascolarctobacterium spp*	Energy Gluconeogenesis Inhibition of cholesterol biosynthesis
Butyrate	*Roseburia spp* *Eubacterium rectale* *Eubacterium hallii* *Faecalibacterium prausnitzii* *Anaerostipes caccae* *Coprococcus eutactus*	Energy in colonocytes Anti-inflammatory Induction of immunosuppressive cytokines and GLP-2 Apoptosis induction in tumor cells Overexpression of detoxifying enzymes Enhancement of mucosal barrier function

Though fiber consumption can be increased by increasing the consumption of fruits and vegetables such as apple, peaches, onion, garlic, chicory, cabbage. However, most of these sources contain about 1-3g fiber per serving and hence, a large quantity of such food needs to be consumed to meet the daily requirement of

fiber intake (25g/2000 Kcal). Dietary fiber and prebiotics though differ in their physiological properties, including fermentability. Insoluble fiber possesses limited to none fermentability and owes their therapeutic effects to solubility and viscosity. Some of the fermentable fiber

do impact the gut microbiota. Prebiotics, on the other hand, produce a significant impact on the gut microbes owing to their fermentability.

It has been suggested that the oligosaccharides with DP below 5 stimulate the gut bacteria to greater extent as compared to oligosaccharides above DP 5. Similarly, polymeric xylan has limited ability to act as an energy source to gut microbes, whereas the hydrolyzed products show prebiotic activity (Singh, Banerjee, & Arora, 2015). The fiber content of the diet can be increased by consumption of fiber-rich fruits, grains, and vegetables. However, they possess limited prebiotic content. Thus, based on the above arguments and the beneficial effect of prebiotic on human health, introducing prebiotic as supplements can be an option towards improved gut health.

Chapter 3 Literature Review

The chapter describes the prospect of xylooligosaccharides as a prebiotic and the literature supporting the health benefits. It also presents a broad description of the literature available for production and purification of XOS. The later part of the chapter includes the national and international work conducted on XOS and concluding with the scope of XOS as a prebiotic candidate.

3.1. Xylooligosaccharides as Prebiotics:

Xylooligosaccharides (XOS), the hydrolysis product of xylan, are oligomers of β- 1, 4- linked xylose residues with various substituents including acetyl, phenolic, and uronic acid. They are thought to be present in fruits, vegetables, bamboo, honey, milk (though the percentage is not reported) (Vazquez, et al., 2003; Gupta, Agarwal, & Hegde, 2013) thus making xylan rich lignocellulosic material obtained from agricultural, forestry and industrial waste as a significant source. XOS is available as a white powder containing two to nine xylose molecules, however, in some reports, molecules with DP $\leq$ 20 are also considered as XOS (Makelainen, et al., 2010). However, for food application, XOS with DP 2-4 are preferred (Loo, et al., 1999; Vazquez, Alonso, Dominguez, & Parajo, 2000). These oligosaccharides are stable over a wide pH range of 2.5-8.0, gastric pH and temperatures up to 100^{o}C. The XOS with average DP of 3-5 are more sensitive to alkaline decomposition as compared to longer chain XOS with an average DP of about 15. XOS has good thermal stability during pasteurization and autoclave sterilization at low pH (Wang, J., et al., 2009) as compared to FOS which are more susceptible for decomposition at low pH and higher temperature (Courtin, Swennen, Verjans, & Delcour, 2009). In food processing, XOS is advantageous over inulin in terms of heat and acidity resistance, allowing their utilization in low pH juices (Vazquez, Alonso, Dominguez, & Parajo, 2000).

As a food ingredient, XOS is non- carcinogenic, stimulate bacterial growth and fermentation, and improve intestinal mineral absorption. They also possess antioxidant, antiallergenic,

antimicrobial, immunomodulatory and selective cytotoxic activity, as well as blood and skin health-related effects (Moure, Gullon, Dominguez, & Parajo, 2006)

3.2. Bacterial fermentation of XOS:

Utilization of XOS as prebiotic has been studied extensively with *Bifidobacterium spp* and *Lactobacillus spp*. Table 3.1 enlist bacterial strains which have demonstrated the prebiotic activity with XOS. It has been observed that Bifidogenic activity of XOS is dependent on the considered strain. Among the *Bifidobacterium spp*., *B. adolescentis* can utilize both xylobiose and xylotriose as substrate (Hopkins, Cummings, & Macfarlane, 1998).

Table 3.1: Study of bacterial fermentation of prebiotic XOS

Substrate	Bacterial genera	Remark	Reference
Rice husk	*B.adolsecentis* CECT 5781 *B. longum* CECT 4503 *B. infantis* CECT 4551 *B. breve* CECT 4893	*B. adolescentis* was stimulated higher as compared to other utilizing 77% of XOS in 24 h	(Gullón et al., 2008)
Wheat bran	*B. adolscentis* DNRI 236, *B. bifidum* ATCC 29521 *B. bifidum* NCDO 2715 *L.plantarum,* *L. brevis* 01 NDRI *strain* RTS *Pedicoccus pentosaceus* NCDO813 *P. pentosaceus* ATCC 8081	Butyrate was detected only in culture of *B. bifidum* ATCC29521.	(Manisseri & Gudipati, 2010)
Corn cob	*Enterococcus fecalis* CCD10 *E. faecium* TCD3 *L. maltromicus* MTCC108 *L. viridisens* NCIM2167	Prebiotic activity was higher with *E. faecium* followed by *L. maltromicus* and *L viridiscens*	(Samanta, Senani, et al., 2012)
Corn cob	*B. adolescentis* *B. bifidum* *L. fermentum* *L acidophilus*	Growth of *Bifidobacterium* was higher as compared to *lactobacillus*, owing to their expression of mixture of xylosidase enzymes	(Chapla, Pandit, & Shah, 2012)
Birch wood	*Weissela spp*	*Weissella* strain isolated from fermented food and evaluated for	(Patel et al., 2013)

		utilization of XOS as prebiotics	
Wheat straw	*L. brevis* DSM 1269	In- vitro fermentation	(Faryar et al., 2015)
Corn cob	*L. plantarum* S2	XOS combined with *L. plantarum* increase bifidogenic activity while decreasing *Enterococcus, Enterobacter* and *Clostridia spp* population, in vivo. The symbiotic preparation showed in- vitro antioxidant activity.	(Yu et al., 2015)
Wheat bran	*Lactobacillus*	Symbiotic combination of XOS with *Lactobacillus* increased the antioxidant capacity of milk	(Lasrado & Gudipati, 2015)
Sugarcane bagasse	*B. bifidum* *B. infantis* *B. breve*	*B. breve* produce a higher level of formate as compared to the other two	(Reddy & Krishnan, 2016)

3.3. Health Benefit of XOS

3.3.1. Effect of XOS on Gut health

XOS is preferentially utilized by *Bifidobacterium* spp, especially *B. adolescentis*, *B. longum* in rat intestine (US Patent, 005939309). Differences in microbial flora were observed when fed with XOS and FOS; FOS primarily stimulated the growth of *Lactobacilli*, whereas XOS was found to be more bifidogenic, although both contribute to a healthy environment of the colon. The bifidogenic activity of XOS produces acetic acid and lactic acid, which was comparable to glucose and more pronounced than inulin, a commercial prebiotic. Three-Fold increases in the population of *Bifidobacterium* species was noted following oral administration of 5g/ day XOS obtained from birch wood xylan to healthy volunteers for two weeks (Okazaki, Fujikawa, & Matsumoto, 1990). The increase in *Bifidobacterium* population was accompanied by a decrease of pH and maintenance of normal water content (between 70-80%) of faeces promoting intestinal cell proliferation and peristalsis, thus providing benefit against constipation. XOS intake was associated with a reduction in faeces hardness in healthy young women (Na & Kim, 2007), increased faecal water content in elderly with no effect on stool consistency and frequency (Chung, Hsu, Ko, & Chan, 2007). Moreover, 4.2g/day XOS was found to be safe and effective in normalizing the bowel movements in

pregnant women. XOS supplementation was accompanied with increased frequency of stool formation with a reduction in the occurrence of hard or loose stool, thus providing an alternative intervention for the treatment of severe constipation during the third trimester of pregnancy (Kiso, et al., 2005).

The catalytic activity of enzymes is dependent on substrate structure, and substitution, hence XOS fermentation by bacterial enzymes in human faeces vary with the degree of substitution. Linear XOS and Arabino-XOS are fermented preferably and more quickly to produce small chain fatty acids and lactate as compared to highly substituted XOS having acetyl and 4-o-methylglucuronic acid substituents (Voragen, Kabel, Kortenoveven, & Schols, 2002).

A high concentration of acid in the form of lactate, acetate, and fatty acid decreases the intestinal pH, thus hindering the growth of potentially pathogenic and putrefactive bacterial species. Butyrate is speculated to inhibit histone hyperacetylation and p21 induction, impair epidermal growth factor responsiveness of colon cell thus preventing cells from entering G_o phase of the cell cycle, causing a permanent cell cycle arrest and inhibiting colon cell carcinoma (Archer, et al., 1998). Butyrate is also used as an energy source for colonocytes (Roediger, 1982), stimulates epithelial cells, and increases the absorptive capacity of epithelial cells (Topping & Clifton, 2001). XOS and FOS were observed to reduce colonic aberrant crypt foci, an early marker of tumor diagnosis by 76% and 48% respectively, indicating better tumor-suppressing activity of XOS over FOS in DMH induced colonic lesion (Hsu, et al., 2004). Supplementation of 5.4% XOS and FOS improved colon health as indicated by increased cecal weight, a result of the bifidogenic activity of dietary fibers. A significant increase in body weight, normalcy of colon epithelial cells, reduced colonic lipid peroxidation, restoration of antioxidant enzyme activity was observed in DMH treated rats.

An effective daily dose of oligosaccharides (pure form) for XOS is 0.7g and that for FOS is 3.0g, indicating that XOS may be effective at lower doses as compared to FOS (Tomomatsu, 1994). This is supported by a study wherein XOS at a dose of 1.4g/day in adults was found to be efficacious as prebiotic as compared to FOS or GOS (≥10 g per day) (Bouhnik, et al.,

1999). Also, consumption of FOS increases flatulence, intestinal bloating, and intestinal irritation (Ten Bruggencate, et al., 2006). XOS being given at lower dose compared to FOS has not been reported for such side effects and however need further studies.

3.3.2. Effects on metabolic disorder:

The beneficial effect of XOS in the metabolic condition of diabetes can be attributed to the production of SCFA in the colon which increases sodium and water absorption in distal intestine (Roediger & Moore, 1981) thus improving polydipsia. Also, acetate is absorbed into the systemic circulation and transported to muscles to be used as energy source thereby reducing degradation of muscle protein for energy production (Knowles, Jarrett, Filsell, & Ballard, 1974; Skutches, Holroyde, Myers, & Reichard, 1979). XOS included in the diet was shown to improve growth, hyperphagia, polydipsia along with reducing desaturation index and improving serum glucose, triglyceride and cholesterol profile in streptozocin-induced diabetes in Wistar rats (Imaizumi, et al., 1991). The XOS from corncob and FOS from cane sugar significantly decreases the mortality rate in streptozocin-induced diabetes in Wistar rats and provide an improvement in a clinical condition associated with diabetes (Prapulla, et al., 2010). Supplementation of 10% dietary fiber restored the antioxidant activity and reduced the accumulation of advanced glycation end products (AGE), thus ameliorating function of nephrons, reversing hyperglycemia, and hypercholesterolemia. Wheat bran derived AXOS provide an improvement in high fat-induced body weight gain and fat mass development by increasing satietogenic peptides including GLP 1 and PYY, insulin resistance in diet-induced obese mice (Neyrinck, et al., 2012).

Stimulation of bifidogenic bacteria by prebiotics suppress protein fermentation in colon, thereby reducing the toxic catabolites like ammonia, amines, phenols, indoles and thiols produced as a result of amino acid degradation pathways which contributes to reduced risk of inflammatory diseases of colon (Bone, Tamm, & Hill, 1976; Ramakrishna, Roberts-Thomson, Pannall, & Roediger, 1991). XOS but not inulin has been shown to possess protective activity against high protein diet-induced genotoxicity and DNA strand breakage

of the colon (Conlon, Licht, Petersen, & Christophersen, 2013). The geno-protective effect was attributed to the production of short chain fatty acids including acetate and butyrate, produced upon fermentation of carbohydrates by colonic bacteria and stimulation of *B. fragilis*, *E. coli* and sulfur reducing bacteria. XOS fed to human subjects for eight weeks, was found to reduce blood glucose, HbA1c and fructosamine concentration, along with a reduction in the level of total cholesterol, LDL cholesterol, and oxidized low-density lipoprotein. Furthermore, there was a beneficial effect on the activity of oxidative enzymes indicated by an increase in the level of glutathione peroxidase, superoxide dismutase and reduced level of catalase (Sheu, Lee, Chen, & Chan, 2008).

Prebiotics such as XOS alters the structure, physicochemical properties of membrane bilayer and brings about changes in sphingomyelin/ cholesterol ratio in rat liver plasma membranes (Staneva, et al., 2013). These effects modify the functioning of various membrane receptors and cell signaling, thus providing a beneficial effect in glucose and lipid metabolism.

3.3.3. Antioxidant activity:

The *in- vitro* antioxidant activity in the range of 48-80% at a dose of 1.25-2.1 mg has been reported for xylan obtained from the almond shell by DPPH radical scavenging test (Ebringerova, Hromadkova, Kostalova, & Sasinkova, 2008). Similarly, XOS derived from sugarcane bagasse shows dose-dependent antioxidant activity with an IC_{50} value of 1.6 (Bian, et al., 2013). Concentration-dependent antioxidant activity has been found for ragi XOS in range of 12% to 70% for a concentration of 10 µg- 60 µg (Veenashri & Muralikrishna, 2011). The antioxidant activity for ragi was higher as compared to XOS derived from wheat, rice, and maize, possibly due to the higher content of bound phenolics. The antioxidant activity is attributed to the presence of ester linked hydroxycinnamic acid derivatives such as ferulic acid and syringic acid residue on the xylan chain. Study on Wistar rat fed with wheat bran feruloyl oligosaccharides supports the utility of ferulic acid as an antioxidant (Wang, Sun, Cao, & Wang, 2010). Thus, xylooligosaccharides with ferulic acid substituents can be

evaluated for their incorporation in food products as an antioxidant and as a natural substitute for synthetic agents such as BHA and BHT.

Wheat bran XOS was found to be active against protection from high fat-induced oxidative stress in rats via modulation of lipid metabolism and antioxidant defense system (Wang, Cao, Wang, & Sun, 2011). In this study, XOS supplementation decreased malondialdehyde and oxidized glutathione levels with an increase in reduced glutathione level. Furthermore, the activity of oxidative enzymes, including SOD, CAT, and GSH-Px in serum, liver, and heart, was improved. An *in- vitro* radical scavenging activity was found in water-soluble arabinoxylan extracted from wheat bran comprising of phenolic residues (Hromadkova, et al., 2013). Similarly, *in- vitro* antioxidant activity of XOS have been reported for enzymatic derived XOS from sunflower and wheat stalk (Akpinar, et al., 2010), XOS from endo- β-Xylanase treated corncob (Yamani, Kristanti, & Puspaningsih, 2012).

3.3.4. Effect on the immune system:

An *In- vitro* complement- fixing assay of alkali extracted wheat bran xylan showed ICH_{50} values of 57.2 µg/ml and 17.6 µg/ml for two fractions WB2 and WB1, respectively. WB2 fraction showed 60% higher hemolysis inhibitory activity as compared to the positive control, immunogenic polysaccharide PMII (ICH_{50}- 44 µg/ml) (Hromadkova, et al., 2013). Wheat bran arabinoxylans were found to possess immunostimulatory activity, which contributed to antitumor activity. It promoted thymus and spleen indexes, splenocyte proliferation, natural killer cell and macrophage phagocytosis activity, interleukin-2 production and delayed type hypersensitivity reaction. It significantly inhibited the growth of transplantable tumors in S180 tumor-bearing mice (Cao, et al., 2011). Extraction with chemical and enzymatic method produces products with a different chemical group which can affect the functionality of the xylan. It was observed that AX obtained by enzymatic treatment of wheat bran had higher macrophage phagocytosis and delayed hypersensitivity reaction as compared to AX derived from the chemical method. However, no significant difference in enhancing lymphocyte proliferation was observed (Zhou, et al., 2010). AX from green leaves of *Litsea glutinosa*

(Lauraceae) induced splenocyte and thymocyte proliferation at a dose of 25µg/ml and 50µg/ml in mouse culture medium (Das, Maiti, Maiti, & Islam, 2013). Also, a dose-dependent increase in macrophage activation was observed, indicating potential tumor inhibitory activity. However, the low immunological activity was reported for arabinoxylan and mixed- linked β-glucans from barley on cell cultures (Samuelsen, et al., 2011). Wheat bran AXs improves humoral response in chickens indicated by the increased titre of immunoglobulins after being challenged by Eimera infection (Akhtar, et al., 2012). The result indicates that wheat bran AX can be used as an allopathic alternative for the treatment of Coccidiosis in broiler chickens.

Furthermore, AXOS improves immune response in fish, which is attributed to the enhancement of beneficial microbiota in the hindgut (Geraylou, et al., 2012). The effect was more pronounced with XOS of a higher degree of polymerization which is in confirmation with the immunomodulatory effect of AX from wheat bran with a molecular weight above 5kDa (Monobe, Maeda- Yamamoto, Matsuoka, Kaneko, & Hiramoto, 2008)

3.4. Advantages of XOS over other prebiotics:

I. Xylan rich lignocellulose biomasses are abundantly available and are utilized to a limited extent. Thus, valorization of such residues for the production of XOS is a viable option. This is advantageous in comparison for other prebiotics like GOS, FOS, and inulin, which are either obtained from food sources or derived synthetically.
II. XOS is found to be stable in the pH range of 2-8 and temperatures up to 100^{o}C even in low gastric pH. On the other hand, FOS are susceptible to degradation at low pH and higher temperature conditions (Courtin, Swennen, Verjans, & Delcour, 2009). Thus, XOS is a potential ingredient for formulating different health drinks.
III. It has been observed that XOS are effective at a daily dose as low as 0.7 g/day in comparison to FOS, which has an effective daily dose of 3 g/day (Tomomatsu, 1994). Thus, XOS produces bifidogenic activity at lower doses. However, studies are limited and need to be proved.

IV. As fermentation of prebiotics produces gases, the lower effective dose can be beneficial to reduce the incidence of flatulence, bloating upon consumption, which are significant side effects observed upon consumption of inulin and FOS (Bruggencate, Bovee-oudenhoven, Lettink-wissink, Katan, & Meer, 2006).

Prebiotics also tend to overcome the shortcomings of probiotics. Probiotics need careful handling and processing to keep the bacteria alive. Also, the dosage needs to be carefully controlled to provide the required amount of bacterial population in a viable state upon consumption by the end user. Also, limited strains can be delivered as probiotic formulation and the benefits is specifically related to the strain being consumed, prebiotics, on the other hand, serves as food for multiple strains of the bacterium in the gut.

3.5. Prospects of XOS as a food ingredient:

XOS can act as potential candidate ingredient for functional foods such as health drinks, fortified bread, health bars, jam, and symbiotic preparations. It can be evaluated as an adjuvant for pharmaceutical preparation in case of colon cancer, diarrhea, gut inflammation, and disorders. As gut flora makeup is dependent on age, genetic makeup and disease state, a detailed study concerning the utilization of XOS under such diverse condition can enable to realize the full extent of the prebiotic potential of XOS. Also, studies related to appropriate dosage under different disease conditions, the effect of substituent pattern on XOS, the effect of the ratio of arabinose to xylose on health outcome can be realized. Though XOS has good physicochemical attributes, little effort has been directed to use it as an ingredient in food products.

3.6. Xylooligosaccharides production

3.6.1. Lignocellulosic biomass as raw material:

Annually billions of tonnes of residues abundant in lignocellulose, in the form of straw, husk, bagasse, stalk, bran is produced and discarded (Saini, Saini, & Tewari, 2014; Anwar, Gulfraz, & Irshad, 2014). Table 3.2 enlists examples of certain lignocellulosic biomass. Lignocellulose is the primary building block of the plant cell wall. Lignocellulose material

(LCM) comprises of three major polymers, i.e. cellulose (40-50%), hemicellulose (25-30%) and lignin (15-20%) along with pectin, protein, extractives, and ash. Cellulose is a linear polymer of β- glucose linked via 1→4 glycosidic linkages, whereas hemicellulose is a heteropolysaccharide made up of pentoses and hexoses. Lignin is the non- carbohydrate component of LCM structure and comprises of three major phenolic components viz, p-coumaryl alcohol, coniferyl alcohol, and sinapyl alcohol. Hemicelluloses are a heterogeneous group of polysaccharides having β- (1→4) linkages and include xyloglucans, xylans, etc (Scheller & Ulvskov, 2010). Xylans are most abundant polymer present in hemicellulose and have a linear β- (1→4)-D-xylopyranose backbone and have various substituents including arabinofuranosyl, glycopyranosyl, uronic acid, ferulic acid, coumaric acid derivatives which may be ester or ether-linked to the hydroxyl group of xylan.

Table 3.2: Lignocellulose composition of some biomass and availability of their residue in a million tons (Van Dyk & Pletschke, 2012; Saini, Saini, & Tewari, 2014)

Biomass	Cellulose (%)	Hemicellulose (%)	Lignin (%)	Residue available (million tons)
Rice straw	28-36	23-28	12.14	731.3
Corn stover	39-40	19.1	15	128.02
Wheat straw	30-44	23-32	17-19	354.34
Bagasse	33-43	25-30	18-24	180.73
Leaves	15-20	80-85	0	-

Depending on the source, the method of extraction, xylan of different structure can be obtained, which have potential health benefits as exhibited by prebiotics (Otieno & Ahring, 2012; Jensen, Johnson, & Wilkerson, 2013). Current utilization of such residues includes paper-making, as a binder, as packaging material, composite. Recently, bioethanol production from such residues has attracted increased interest in the realization of limited fossil fuel availability. However, bioethanol production uses cellulose as a substrate, and in most bioethanol plants, hemicellulose is discarded as waste (Saha, 2003; Wyman, 2007). Thus, hemicellulose valorization via isolation of xylan from LCM and its hydrolysis to XOS would provide an alternative for effective waste utilization. However, isolation of xylan from LCM has practical difficulties owing to the lignocellulosic framework.

3.6.2. Tertiary Structure of lignocellulose biomass:

The tertiary frame of lignocellulose is modulated by the presence of various covalent and non- covalent linkages between the constituents. Cellulose is composed of β-1-4-glycosidic linkages of D- glucose to form a cellulose chain. These long-chain cellulose polymers are bound together by hydrogen and vanderwaal forces, causing cellulose to form a tightly packed microfibril structure. Cellulose microfibrils are stabilized by intra- and inter molecular hydrogen bonds, giving cellulose a pseudo-crystalline structure. Hemicellulose differs from cellulose in that it has branches of short lateral chains of different sugars including arabinose, mannose, uronic acids, acetyl groups, etc. Lignin comprises of a complex cross-linked polymer of phenolic monomers which coats the polysaccharide structure. The coniferyl alcohol, coumaryl alcohol, and sinapyl alcohol are interlinked via alkyl-aryl, alkyl- alkyl and aryl- aryl ether bonds to form the backbone of lignin. It provides support, impermeability, and resistance against microbial attack. Xylan is the interface between lignin and other carbohydrates. The ferulic groups on xylan are thought to bind hydrophobic lignin with hydrophilic polysaccharides via alkali sensitive ester bonds. The presence of lignin and the alkali resistant ether bonds acts as a shield, thereby preventing enzymatic access for hemicellulose hydrolysis (Kumar, Barrett, Delwiche, & Stroeve, 2009; Malherbe & Cloete, 2002). Using native substrates, it has been observed that less than 20% of the polysaccharide is enzymatically hydrolyzed to constituent sugar. Thus, the presence of an intricate framework makes pretreatment via physical, chemical, enzymatic, or combination a necessity for efficient recovery of underlying polysaccharides.

3.6.3. Pretreatment methods for lignocellulosic biomass

It is assumed that the drawback of no pretreatment of biomass is higher as compared to the cost of pretreatment. Thus, various pretreatment approaches have been reported to achieve one of the following effects:

- The decrease in particle size of the substrate
- Partial or complete removal of lignin, thereby decreasing hydrophobicity and increasing porosity of biomass

- Disruption of linkages between lignin and other carbohydrates
- Partial solubilization of hemicellulose structure
- Reduction of cellulose crystallinity and degree of polymerization

The presence of lignin is considered as the limiting factor for access to hemicellulose as well as cellulose and their hydrolysis. The hydrophobic lignin barrier not only serves as physical hinderance but also inactivates enzymes by adsorption (Berlin et al., 2006; Qi, Chen, Su, & Wan, 2011). Thus, the removal of lignin is considered as an important step in the valorization of lignocellulosic biomass.

With respect to hemicellulose utilization, pretreatment approaches can be classified into physicochemical, chemical, and enzymatic routes.

3.6.3.1. Physicochemical pretreatment methods:

Physicochemical pretreatments can be achieved via hydrothermal treatments such as autohydrolysis, steam explosion, wet oxidation. The hydrothermal process employs temperature in the range of 150^{o}C to 220^{o}C as below 100^{o}C; there is no hydrolytic effect on biomass, whereas above 220^{o}C, cellulose degradation occurs.

a. **Autohydrolysis**:

This process employs temperature in the range of 160-220^{o}C and pressures more than saturation point to hydrolyze hemicellulose in minutes. In this process, lignin is not significantly solubilized, nor sugars are decomposed to a more considerable extent. Thus, the process yields liquid fraction, which is rich in the oligomeric form of hemicellulose with minimum inhibitor compounds. During autohydrolysis, hydronium ions (H_3O^+) generated from water at high temperature catalyze the depolymerization of hemicellulose. Subsequently, cleavage of acetic acid from xylan backbone produces addition hydronium ion, thereby improving the kinetics of the reaction. The *in- situ* generated acids catalyze the hydrolysis of bonds between carbohydrates and lignin and convert hemicellulose to soluble saccharides. Also, low concentration of inhibitors is produced, thus giving a hemicellulose oligosaccharide rich liquid fraction and residue rich in cellulose and lignin. The process is

economical as no additional catalyst is required thereby minimizing environmental impact and reducing labor cost (Heitz et al., 1986; Overend, Chornet, & Gascoigne, 1987; Rubio, Tortosa, Quesada, & Gómez, 1998).

b. **Steam explosion**:

In this process, the biomass is treated with high pressure saturated steam (20-25 bar) for a few seconds to minutes. At high pressure, the steam condenses on the biomass, thereby wetting the material and also penetrates the structure. After the desired time, steam is removed through a small nozzle by induced force. The sudden evaporation caused by a decrease in pressure brings about the desegregation of LCM matrix, breaking of inter, and intra-molecular linkages. The steam explosion causes high hemicellulose solubilization and low lignin solubility, thus giving oligosaccharide rich liquid fraction.

3.6.3.2. Chemical pretreatment methods

a. **Acid hydrolysis**:

Acid-catalyzed hydrolysis can be divided into two types based on the concentration of acid viz., dilute acid, and strong acid catalyzed hydrolysis. In concentrated acid-catalyzed hydrolysis, sulphuric acid is generally employed as a catalyst. However, other mineral acids such as hydrochloric acid, nitric acid, phosphoric acid have also been used. Solubilization of polysaccharides has been achieved by using 72% sulphuric acid, 41% hydrochloric acid, or 100% trifluoroacetic acid. Use of concentrated acid generally removes cellulose and hemicellulose, leaving behind lignin-rich solid phase. Use of concentrated acid allows operating at low/ medium temperature and pressure, thus producing a lower quantity of degradation products. However, precise control of temperature and pressure is essential, as the rate of degradation of polysaccharides to furfural is severely affected by a slight change in temperature. Also, the use of concentrated acid requires corrosion resistant equipment, thereby increasing the cost of production (Carvalheiro, Duarte, & Gírio, 2008).
In the dilute acid pretreatment process, dilute acid (0.2-2.5% w/w) is applied to biomass at a temperature range of 130^{o}C - 210^{o}C for few minutes to hours. An advantage of acid

hydrolysis is that subsequent enzymatic hydrolysis is not required. However, the reaction conditions need to be stringently controlled to prevent the formation of inhibitors and degradation products (Brodeur et al., 2011).

b. **Alkaline pretreatment**:

Alkaline pretreatment involves the use of bases such as sodium hydroxide, potassium hydroxide, calcium hydroxide, and ammonium hydroxide. Alkali causes degradation of ester and glycosidic side chains, thereby causing structural disruption of lignin, partial solvation of hemicellulose, breaking of linkages between lignin and hemicellulose and cellulose swelling. Structural disruption of lignin followed by saponification of ester bonds that links hemicellulose to other components liberates hemicellulose, thereby increasing enzymatic accessibility for hydrolysis of hemicellulose to oligosaccharides (Macdonald et al., 1983; McIntosh & Vancov, 2010). Alkaline pretreatment is generally carried out using 0.05- 0.15 g alkali/g biomass, the temperature in the range of 30^{o}C to 130^{o}C and period of 10 min to 18 h. The advantage of alkaline pretreatment includes low cost of equipment. Use of lime is cost-effective as compared to another alkali, as it can be recovered and recycled (Silverstein, Chen, Sharma-Shivappa, Boyette, & Osborne, 2007; Wyman et al., 2005).

Table 3.3 presents examples of lignocellulosic substrates used for xylan extraction and XOS production using different pretreatment strategies.

Table 3.3: Examples of pretreatment method for isolation and separation of xylan and XOS from lignocellulose material

Feedstock	**Pretreatment Method**	**XOS production method**	**Xylan yield (%)**	**XOS (%)**	**Reference**
Poplar wood	Alkaline hydrolysis	-	78.16-69.23	-	Sun, R. C., et al., 2001
Olive Stones (whole stone and seed husk)	Steam Explosion	-	63	-	Fernandez-Bolanos, J., et al., 2001
Corncob	Autohydrolysis	-	30.9	70	Parajo, J. C., et al., 2001

Beech	Alkaline Extraction	-	66.9	-	Puls, J., et al., 2001
	DMSO extraction		65.14	-	
Wheat straw	Steam	-	46.65	-	
Oat Spelt	Alkaline hydrolysis	-	66.9	-	
Hymenaea courbaril leaves	Alkaline extraction	-	28.4	-	Busato, A. P., et al., 2001
Almond shell		Autohydrolysis	-	63	Nabarlatz, D., et al., 2005
Corncob	Alkali Pretreatment	Enzymatic Hydrolysis	40.8	81	Aachary, A. A., and Prapulla, S. G., 2009
Corncob	Acid Pretreatment	-	39.2	52	Aachary, A. A., and Prapulla, S. G., 2009
Corncob	Steam Cooked	Enzymatic hydrolysis	40.0	77	Aachary, A. A., and Prapulla, S. G., 2009
Brewer's spent grain		Microwave superheated water and dilute alkali extraction	-	62	Coelho, E., et al., 2014
Corncob	Alkaline extraction		66.3	-	Egues, I., et al., 2014
Sugarcane bagasse	Alkaline extraction	Enzymatic hydrolysis	85	-	Jayapal, N., et al., 2013
Sweet sorghum stem	Aqueous and alkali extraction		76.3	-	Sun, S. L., et al., 2013
Sugarcane bagasse	Alkali hydrolysis	Enzymatic hydrolysis		31.8	Bian, J., et al., 2013
Wheat bran		Microwave assisted enzymatic		6.4 (Pure)	Wang, T. H., and Lu, S., 2013

		hydrolysis			
Oil Palm empty Fruit bunch fibre	Non-isothermal extraction		63	17.6	Ho, A. L., et al., 2013
Wheat Straw	Cold Alkaline extraction		45.2		Garcia, J. C., et al., 2013
Bamboo Leaves	Aqueous and Alkaline extraction		67.83		Peng, H., et al., 2013
Bamboo culm	Non-isothermal autohydrolysis		47.49		Xiao, X., et al., 2013
Sehima nervosum grass	Alkaline hydrolysis	Enzymatic hydrolysis	98	11	Samanta, A. K., 2012
Corncob	Alkaline hydrolysis	Acid Hydrolysis	83.5	68.5-86.6	Samanta, A. K., 2012
Corncob	Alkali treatment	Enzymatic hydrolysis	17.8	6.73	Chapla, D., et al., 2012
Miscanthus giganteus	Autohydrolysis			65	Ligero, P., et al., 2012
Corncob	Steam explosion	Enzymatic hydrolysis	22.8	28.6	Teng, C., et al., 2010
Maize bran		Microwave irradiation		50	Rose, D. J., and Inglett, G. E., 2010

3.6.4. Enzymatic Production of XOS:

XOS can be produced after extraction of xylan by alkali, such as NaOH and KOH, using xylanase enzymes which hydrolyzes β-1, 4-glycosidic linkages in xylan, and possess low exo-xylanase and *β*-xylosidase activity (Akpinar, O., et al., 2007). Enzymes with high exo-xylanase or *β*-xylosidase activity produce a higher concentration of xylose, which can cause end-product inhibition, thereby affecting XOS production (Vazquez, M. J., et al., 2002). Xylanases belong to family 5, 7, 8, 10, 11 and 43 of glycoside hydrolases, differing in their amino acid sequence, physicochemical properties, mode of action and substrate specificity (Collins, T., et al., 2005). Xylanases can be produced from a variety of microorganisms

including *Aspergillus, Trichoderma, Streptomycetes, Phanerochaetes, Chytridiomycetes, Ruminococus, Fibrobacter, Clostridium, Bacillus, Thermoascus,* and *Penicillium*, using various agricultural wastes (Carvalho, A.F. A., et al., 2013). In contrast to autohydrolysis, enzymatic production of XOS is advantageous as it does not produce undesirable by-products, high concentration of monosaccharides and furthermore, no specialized equipment is required. However, enzymatic hydrolysis requires a longer reaction time, as compared to acid hydrolysis or autohydrolysis. This can be overcomed by using different xylanases and side group removal enzymes (Akpinar, O., 2010). Also, xylanases differ in substrate specificity, thus producing different hydrolysis end products, and control of the production of XOS with desired DP range can be challenging (Qing, Q., et al., 2013).

Table 3.4: Literature review on the use of enzymatic hydrolysis for XOS production

Feedstock	Enzyme used	Operating Condition	XOS yield	Reference
Cornhusk	*Rapidase Pomaliq*	50^{o}C, 4 h, pH 5.0	8.21	Yoon, K.Y., et al., 2006
Corncob		50^{o}C, 4 h, pH 5.0	9.90	
Oat spelt xylan		50^{o}C, 4 h, pH 5.0	18.3	
Oat spelt xylan	Endoxylanase (*T. fusca*)	60^{o}C, 24 h, pH 7.0	40.1	Yang, C. H., et al., 2007
Corncob		60^{o}C, 24 h, pH 7.0	29.5	
Bagasse		60^{o}C, 24 h, pH 7.0	23.7	
Wheat bran		60^{o}C, 24 h, pH 7.0	7.60	
Peanut shell		60^{o}C, 24 h, pH 7.0	10.1	
Corncob	Endoxylanase (*Tricoderma sp*)	50^{o}C, 12 h, pH 7.0	46.5	Chen, L. L., et al., 2009
Wheat bran	*B. subtilis*	50^{o}C, 16 h, pH 5.0	31.2	Wang, J., et al., 2009
Corncob	Endoxylanase (*A. oryzae*)	50^{o}C, 6 h, pH 5.4	86.7	Aachary, A. A and Prapulla, S. G., 2009
*Populas tomentosa*chips	*Pichia stipites* xylanase	50^{o}C, 24 h pH 5.4	36.8	Haiyan, Y., et al., 2011
Corncob	*Streptomyces thermovulgaris* TISTR1948 (Endoxylanase)	55^{o}C, 24 h, pH 6.5	60.3	Boonchuay, P and Chaiyaso, T., 2012

Thus, xylanases capable of acting on a wide range of substrate are finding increasing interests. These enzymes can be added directly to the media (Pellerin, P., et al., 1991), as an immobilized system (Suwa, Y., et al., 1999) or produced in- situ by microorganisms (Cai, J., et al,.1997).Enzymatic hydrolysis has been applied to the various lignocellulosic substrate after suitable pretreatment for XOS production, as exemplified in Table 3.4. Enzyme preparation from the medium of *Aspergillus foetidus* was found to hydrolyze corncob xylan primarily to xylobiose with no production of D-xylose (Whistler, R. L and Masak, Jr. E., 1955). Similarly, xylanases from *Streptomyces rameus* produces xylobiose (X2) and xylotriose (X3) as the major products, from birchwood and oat spelt xylan. Due to the intrinsic endoxylanase activity, it hydrolyzed xylotetrose (X4) and xylopentose (X5) without hydrolyzing xylobiose and xylotriose (Xiuting, Li., et al., 2012) providing a potential enzyme for the functional food industry.

A thermostable xylanase obtained from *Streptomyces chartreusis* L1105, showed specific activity towards different xylan substrate. The xylanase found to be stable in the pH range of 5-11, with an optimum temperature of 70^{o}C and produced xylobiose and xylotriose as a principle product from hydrolysis of oat-spelt and corncob xylan (Zhu, Y., et al., 2012). Hydrolysis of alkali treated xylan from corncob (6%) using endoxylanase from *Aspergillus oryzae* MTCC 5154 at 50^{o}C, pH 5.4 and 14 hr produced 79.7% XOS with 70.5% xylobiose (Aachary, A., and Prapulla, S., 2009). In contrast, hydrolysis of mild alkali pretreated corncob xylan (17.9%) with xylanase from *Aspergillus foetidus* MTCC 4898, gave 60% XOS after 8 hr, 45^{o}C (Chapla, D., et al., 2012). Moreover, hydrolysis of xylan from tobacco stalk, cotton stalk, sunflower stalk, and wheat straw for XOS production using 200 U/g of xylanase from *A. niger* at 50^{o}c over 24 h was compared. Tobacco stalk gave the best results with XOS yield of 13.8%, comprising of X2 (7.95%), X3 (5.9). Also, xylanase from *A. niger* gave a higher yield of XOS as compared to xylanase from *Trichoderma longibachiatum* for extracted xylan (Akpinar, O., et al., 2009). Above studies indicates that xylanase type, substrate, xylan composition, pretreatment method, reaction time, and temperature affect the XOS yield and composition.

Immobilization of enzyme has gained increased importance as can be exemplified from Table 3.5, to improve the economics of XOS production. Immobilization of xylanase from *Bacillus pumilus* exhibited higher pH stability (up to 28%) in range of 7-10, higher optimum temperature (68^{o}C) as compared to the free enzyme (60^{o}C). The immobilized enzyme from *Talaromyces thermophiles* produced xylobiose as a major product from hydrolysis of wheat bran xylan, in contrast to crude xylanase which produced mainly xylose (Maalej-Achouri, I., et al., 2009). Contrasting results were obtained for endoxylanase from *Bacillus halodurans,* wherein free enzyme was more efficient in XOS production as compared to the immobilized enzyme. The free enzyme converted xylan to higher oligomers with DP above 4 with 32.5% X2 and X3 in comparison to an immobilized enzyme which produced XOS with a shorter length and 25.2% X2 and X3 mixture (Lin, Y. S., 2011). This suggests that immobilization may limit the accessibility of enzyme to xylan backbone.

Table 3.5: Examples of immobilization techniques used for immobilization of endoxylanase for XOS production

Source	Immobilization substrate	Remark	Reference
Talaromyces thermophiles stolk	Gelatin	Retained 94% activity even after 13 successive cycles. X2 as major product	Maalej-Achouri, I., et al., 2009
Bacillus pumilus strain MK001	Gelatin	Less than 50% activity after four cycles	Kapoor, M., Kuhad, R. C., 2007
	Chitin		
	Q- speharose	70% activity after seven cycles	
	HP- 20 Beads		
Bacillus halodurans	Lewatit MonoPlus MP64 (ion exchange resin)	71% activity retained after five cycles	Lin, Y. S., et al., 2011
Streptomyces olivaceoviridis E-86	Eudragit S100	81% activity retained after four cycles	Ai, Z., et al., 2005

Penicillium occitanis xylanases 3 expressed in *Pichia pastoris* was immobilized on chitosan using glutaraldehyde. The optimum pH of immobilized enzyme was in the range of 2-4 as compared to the free enzyme (pH 3); also, the optimum temperature was found to be 65^{o}C in

contrast to 50^{o}C of the free enzyme (Driss, D., et al., 2014). From these studies, it can be concluded that immobilization of enzymes allows for the use of a wide range of pH, higher processing temperature and reusability of enzymes, a factor which governs processability and cost of manufacturing. The endoxylanase immobilized on anion exchange resin was found to convert 80.9% of the insoluble substrate (corncob xylan) into soluble oligomers (XOS) as compared to 99.8% for the free enzyme at the end of 24 h (Lin et al., 2011). Continuous production of XOS was achieved using xylanase from *Aspergillus versicolor* immobilized on glyoxyl- agarose support. The immobilized enzyme had higher stability at 60^{o}C as compared to the free enzyme and can be used for ten cycles of 1 h each (Aragon, Santos, et al., 2013). The xylanase immobilized on chitosan was found to have more than 95% activity recovery and immobilization yield along with enhanced thermostability. Also, the XOS was primarily composed of xylobiose and xylotriose (Driss, Zouari-Ellouzi, et al., 2014a). Thus, it can be observed that various substrates have been utilized as immobilization support or carrier for performing the enzymatic reaction. However, such supports require centrifugation or filtration to separate them from enzymatic liquor. At commercial scale, such interventions introduce additional unit operations in the process, which increases the processing cost. Magnetic nanoparticles (MNP) prepared from Fe_3O_4 as immobilization support provides an advantage of the ease of magnetic separation of the enzyme from the reaction mixture. The surface activation of chemically inert MNP with (3- aminopropyl)- trimethoxysilane (APTES) grafts aminopropyl silane groups and enables cross-linking of the enzyme via glutaraldehyde (GDA) (Ozalp et al., 2015; Wang et al., 2013). The Fe_3O_4 coated chitosan MNP obtained using a layer by layer assembly for immobilization of *Aspergillus niger* xylanase A was found to have the high binding capacity and recovery activity along with thermal and storage stability. The immobilized enzyme could retain 87.5% of activity after seven consecutive cycles (Liu et al., 2014). However, the residual activity was not evaluated for consecutive cycles after the end of 24-48 h. Most of the available literature measure enzyme reuse for one h cycle. From a practical understanding and economic feasibility

viewpoint, it is worthwhile to evaluate the reusability of enzymes for the whole process when xylan hydrolysis stabilizes in 24- 48 h.

Recently, there has been increased interest in the production of xylanase *in- situ* or by using lignocellulose substrate, to make the XOS production cost effective. Xylanase produced by *Aspergillus terreus* cultivated on finely grounded wheat straw (10g/flask) in solid-state fermentation, showed high specificity towards oat spelt xylan with apparent *Vmax* and K_m of 333.3 U/mg and 16.7 mg xylan/ml respectively. The enzyme had an optimum pH of 7.0 and temperature of 50^{o}C (Ghanem, N. B., et al., 2000). The ability of mesophilic xylanases from *Bacillus subtilis, Aspergillus niger, Hypocrea jecorina* and thermophilic xylanase of *H. jecorina* for in situ production of arabinoxylooligosaccharide (AXOS) from arabinoxylan during wheat meal bread making was compared. Thermophilic *H. jecorina* xylanase was maximally active during the baking process and produced about 2.1% AXOS without affecting dough consistency as compared to other mesophilic xylanases (Damen, B., et al., 2012). Lignocellulosic wastes were used to induce extracellular xylanases from *Thermobifida fusca* NTU22 to produce xylanases, β- xylosidase, and acetyl esterase. Heat treatment of crude enzymes at 70^{o}C for 30 min inhibited 90% β- xylosidase activity and the enzyme produced about 40.1% XOS containing 61% X2, 13% X3 and 26% X4 (Yang, C. H., et al., 2007).

3.7. Separation and purification of XOS:

XOS obtained from hydrothermal or enzymatic process usually contains a wide DP range of oligomers along with monosaccharides, acetic acid, extractives, lignin fraction, degradation products such as furfural, protein derived products, which appears in the reaction system. Hence, the purification of XOS is a complex problem, and a variety of strategies have been proposed for refining crude liquor to obtain a product with desired DP range of oligomers. The usual purity range of commercial XOS lies between 75- 95% (Moure, et al., 2006), and requires multistage processing. Pretreatments and enzymatic processes facilitate purification of XOS.

3.7.1. Solvent extraction:

Solvent extraction is employed to remove non-saccharide components and recover XOS from the liquors (Vegas, R., et al., 2005). The process yields a refined aqueous phase, and a solvent soluble fraction made up of phenolics, and extractive derived compounds. Thus maximum compounds can be extracted via a single step. The degree of purification and yield depends on the solvent and lignocellulose raw material and its composition and substitution pattern, usually, solvents such as ethanol, acetone, 2- propanol are employed (Vazquez, M. J., 2005, Vegas, R., et al., 2004). Also, vacuum evaporation may be applied before solvent extraction and precipitation to concentrate the crude liquor.

Along with the concentration of liquor, evaporation allows for the removal of acetic acid, flavors and other volatile components (Eden, J., et al., 1998). Since the presence of water may affect the extraction, and purification step, hence solvent extraction of freeze-dried autohydrolysis liquors can be used (Vazquez, M. J., 2005, Vegas, R., et al., 2004). Extraction of freeze-dried liquor of Eucalyptus wood shows that ethanol gives intense purification but with lower recovery yield (52.3%) as compared to 2- propanol (93.8%) (Vazquez, M. J., 2005).

3.7.2. Adsorption:

Adsorption by surface active materials has been used in combination with other purification steps to separate oligosaccharides from monosaccharides (Vazquez, M. J, 2000, Sanz, M. L., 2005), removal of undesired compounds (Kokubo, I., and Ikemizu, S., 2004). Most commonly used adsorbents include activated charcoal, acid clay, bentonite, aluminum hydroxide, silica, or porous materials (Vazquez, M. J., 2000). After adsorption on activated charcoal, elution with different concentration of ethanol in water can be used to fractionate oligosaccharides based on their molecular weight (Pellerin, P., et al., 1991). XOS from aqueous ammonia-treated corn cob and stover were purified using 1- 10% activated carbon and eluted using 0- 50% ethanol in water (Sluiter, J. B., 2010). The highest yield was

obtained for elution using a 15- 30% ethanol solution. Active carbon at a dosage of 0.15g/g (based on total solids) was used for decoloration of alkali treated wheat straw XOS. The decolorization ratio was found to be 87.5% with XOS yield of 91.5% (Xu, M., et al., 2012). Adsorption equilibrium of XOS obtained from autohydrolysis of the almond shell was studied in a batch system using activated carbon (20g/L). It was observed that lignin was more selective than carbohydrates for the three commercial activated carbons at slightly different acidic pH. Also, low concentration of basic surface groups, low volume of mesopore diameter limited XOS adsorption whereas highly microporous structure and acidic surface group favored lignin adsorption (Montane, D., et al., 2006). Ethanol precipitation and activated carbon adsorption were compared for purification of liquor obtained after microwave-assisted enzymatic hydrolysis of wheat bran. It was found that; activated carbon adsorption gave X2 and X3 as a major product with the small amount of X4 in contrast to ethanol precipitation, wherein higher amount of X4 and higher oligosaccharides were obtained (Wang, T. H.and Lu, S., 2013). This study indicates that carbon adsorption has the potential for producing food grade XOS with a higher proportion of X2 and X3.

3.7.3. Chromatographic methods:

XOS with a high level of purity with a wide range of DP values can be obtained by using chromatographic separations. This is advantageous as the XOS could be separated or combined as required to evaluate their prebiotic potential and optimize the functional properties (Ho, A. L., et al., 2014). Gel filtration chromatography has been employed for purification of autohydrolysis liquor of corncob to obtain product composed of X2, X3, and X4 (Moura, P., et al., 2007); for purification of XOS obtained from oil palm fruit bunch fibre by non- isothermal process with purity of 74% (Ho., A. L., et al., 2014); for fractionation of olive tree pruning hydrolysate (Cara, C., et al., 2012); for purification of XOS obtained enzymatic hydrolysis of alkali pretreated corn cob, which was found to contain xylobiose as major product (Aachary, A. A., and Prapulla, S. G., 2009). Gel permeation chromatography uses polyacrylamide-based columns such as Bio-Gel, which is not susceptible to microbial

degradation and does not leak carbohydrate during elution. Furthermore, since deionized water is used as eluent, it eliminates the need for removal of buffers after separation, and the XOS fractions can be concentrated by evaporation. However, GPC is not cost effective for large scale production of XOS due to the high cost of the process. Size exclusion chromatography (SEC) have been used for refining of XOS obtained from hydrothermal processing of agricultural wastes (Kabel, M. A., et al., 2002); flax shives (Jacobs, A. et al., 2003). Ion exchange chromatography has been used for purification of XOS from rice husks (Gullon, P., et al., 2011); rice husk autohydrolysis liquors (Vegas, R., et al., 2004); barley grains and spent barley grains (Vegas, R., et al., 2005). Activated charcoal column chromatography using 10% charcoal was used for refining of XOS obtained from corncob by fungal xylanase. Elution with distilled water gave a recovery of 80% with X2 and X3 as a major product (Chapla, D., et al., 2012). Similar results were obtained for autohydrolysis explosion liquor of corncob using immobilized enzyme, with X2 as a major product (Tan, S. S., et al., 2008). Centrifugal partition chromatography has also been employed for purification of XOS from birchwood xylan. More than 85% of XOS with DP 1 and 2 were separated using a solvent system containing dimethyl sulfoxide, tetrahydrofuran, and water in a ratio of 1:6:3 (Lau, C. S., et al., 2011).

3.7.4. Membrane-based technology:

There has been increased interest in using ultrafiltration and nanofiltration, for refining, purification, and concentration of oligosaccharides. Size-dependent separation mechanism of such techniques provides product concentrates with different molecular weights, whereby removing impurities such as monosaccharides, phenolics, etc (Meyer, A. S., et al., 2009). Membrane separation has advantages of low energy requirements, ease of manipulation of operational variables and relative ease of scale-up (Czermak, P., et al., 2004, Cano, A., and Palet, C., 2007).

Ultrafiltration using commercial thin film polymeric membrane was employed for purification of autohydrolysis liquor of almond shells (Nabarlatz, D., et al., 2007); for

separation of xylan rice straw XOS using commercial membrane of molecular weight cut-off (MWCO) at 5 KDa (Wang, F., et al., 2011); for separation and purification of XOS from enzymatic hydrolysate of cotton stalk xylan (Akpinar, O., et al., 2007); refining XOS of tobacco stalk (Akpinar, O., et al., 2010). Ultrafiltration and ethanol precipitation for fractionation of AXOS obtained from enzymatic processing of wheat was compared. It was observed that ultrafiltration produces a heterogeneous, polydisperse fraction as compared to ethanol precipitation, wherein a gradient ethanol precipitation was able to separate XOS in a narrow range of DP based on solubility (Swennen, K., et al., 2005). This indicates that ethanol precipitation is better at achieving separation in a narrow range of DP; however, the process requires large volumes of ethanol. Thus, a cost-effective and efficient method for purification by ultrafiltration can be designed using a careful selection of membranes of narrow pore size distribution and optimization of operational parameters.

Nanofiltration has been used for refining barley waste XOS obtained after hydrothermal processing using a polymeric spiral membrane with a cut-off of 1000 Da. The process was able to reduce monosaccharide content, producing more than 70% XOS in the filtrate (Gullon, P., et al., 2011). Similarly, membrane processing was used to refine XOS obtained from wheat bran using a regenerated cellulose spiral membrane (MWCO 1000 Da). The process recovered more than 50% of XOS with limited monosaccharides and non-saccharide components (Gullon, B., et al., 2014). Nanofiltration using ceramic membrane (MWCO 1000 Da) provided for simultaneous concentration and purification *via* preferential removal of monosaccharides and non-saccharides (Vegas, R., et al., 2006).

3.8. Status of research on XOS

3.8.1. National status of research:

In India, researchers have focused on the production of xylooligosaccharides from substrates such as corncob, wheat bran, pigeon pea, natural grass, and bagasse. Alkaline pretreatment was the method of choice for disruption of the lignin-carbohydrate complex to facilitate

extraction of xylan from the substrates. Extracted xylan was further converted to XOS using enzymatic hydrolysis.

Lignocellulosic structure of corncob was found to be altered to a significant extent via alkaline pretreatment as compared to mild acid and pressure cooking. The extracted xylan was hydrolyzed with commercial endoxylanase from *Aspergillus oryzae* MTCC 5154 to produce XOS (81 ± 3.9%) with xylobiose as a major component (Aachary & Prapulla, 2009). Similarly, alkaline pretreatment using 16% NaOH followed by steam application in autoclave could recover about 90% xylan, which was enzymatically converted to XOS with xylobiose and xylotriose as major products. The prebiotic potential of obtained XOS was evaluated *in vitro* by measuring the growth of the bacterial colony (Samanta et al., 2012, 2014). Researchers have also compared acid pretreatment followed by steam application, delignification followed by alkaline extraction, alkali extraction, and autohydrolysis for extraction of xylan from corncob. The alkali-based extraction method was observed to enable the highest recovery of xylan (178.73 ± 5.8 g/kg corn cob). Enzymatic hydrolysis of extracted xylan was carried out using fungal xylanase to yield xylobiose and xylotriose, which were purified using activated charcoal (Chapla et al., 2012). Alkaline pretreatment supplemented with the steam application was found to be suitable for extraction of about 98%, 96% and 85% xylan from natural grass (Samanta et al., 2012), pigeon pea stalk (Samanta et al., 2013) and sugarcane bagasse (Jayapal et al., 2013). Commercial endoxylanase was utilized for conversion of xylan to XOS, thus enabling value addition to such agro waste.

XOS derived from wheat bran and Bengal gram husk was found to stimulate the growth of *Bifidobacteria*, *Lactobacillus* spp, to produce short-chain fatty acids such as acetate, propionate, and butyrate (Madhukumar & Muralikrishna, 2012; Manisseri & Gudipati, 2010). However, the prebiotic potential of XOS is not only limited to stimulating the growth of *Bifidobacteria* and *Lactobacillus*, in a recent study the strains of *Weissella* spp have been shown to utilize XOS as a source of energy (Patel et al., 2013). This study thus increases the spectrum of bacterial species, which possess the ability to ferment XOS. Also, XOS derived

from cereal; millet brans have been shown to impart antioxidant activity *in- vitro* (Veenashri & Muralikrishna, 2011).

XOS has also been evaluated for its effectiveness as an adjunct in food and dairy products. XOS from corncob was found to improve fermentation rate, sensory profile, and batter quality when used as an ingredient for the preparation of legume-based food, *idli* (Aachary, Gobinath, & Prapulla, 2011). Also, incorporation of XOS in milk as symbiotic preparation along with *Lactobacillus* was found to increase the antioxidant potential of milk (Lasrado & Gudipati, 2015). Thus, XOS provides a useful alternative for the fortification of fermented food and as a dietary supplement.

3.8.2. International status on xylooligosaccharides research:

Agricultural wastes such as tobacco stalk, cotton stalk, sunflower stalk, and wheat straw have been evaluated for their feasibility of value addition using alkaline extraction followed by enzymatic hydrolysis. The degree of polymerization of XOS generated using the above substrate was found to be dependent on substrate structure and enzyme specificity (Akpinar, Erdogan, & Bostanci, 2009)

Autohydrolysis has been used recently for the generation for XOS from various substrates including *Miscanthus giganteus*, corncob, rice husk, rice straw, wheat straw, bamboo culm, olive palm. Yield of XOS obtained from autohydrolysis of agricultural residues such as corncob (60%), almond shell (55%), olive stone (43%), rice husk (30%), wheat straw (43%) and barley straw (43%) was found to be dependent on the structure and substituents on xylan in substrates (Nabarlatz, Ebringerová, & Montané, 2007). Autohydrolysis of bamboo culm was found to be effective for the recovery of 47.5% of XOS in the reaction media, while the residue was enriched in lignin and cellulose. Also, under the reaction conditions of 180^{o}C and 30 min, minimum degradation products were produced (Xiao et al., 2013). Similarly, autohydrolysis of rice straw at 210^{o}C could recover 40% xylan producing 12.86 g/L XOS with a minimum concentration of xylose and furfural (Moniz, Pereira, Duarte, & Carvalheiro,

2014). A study on Miscanthus x giganteus has corroborated the effectiveness of autohydrolysis for XOS production. Under optimal conditions, XOS up to 13% w/w of initial biomass could be obtained. The XOS liquor was further concentrated based on the degree of polymerization using activated charcoal and elution with ethanol and ethanol-water mixture (Chen et al., 2014). Fiber separated from ground corn flour (FC), and DDGS was evaluated for XOS production using autohydrolysis. Reaction at 108^{o}C for 20 min and 190^{o}C for 10 min could recover 71.5% and 54.6% of XOS from xylan for FC and DDGS respectively (Samala, Srinivasan, & Yadav, 2015).

Microwave irradiation as an extraction method provides advantages of reduced reaction time and improved hydrolysis efficiency. Hence, currently, researchers have tried to utilize microwave irradiation for hydrolysis and extraction of hemicellulose for the generation of XOS. Microwave-assisted enzymatic extraction of XOS from wheat bran was evaluated to reduce extraction time. A process consisting of repeated microwave assisted enzymatic extraction and purification by activated carbon was found to yield 6.4% of XOS from dried wheat bran (Wang & Lu, 2013). Alkali extracted hemicellulose from sugarcane bagasse was converted to XOS via microwave-assisted acid hydrolysis. Response surface analysis of microwave-assisted acid hydrolysis indicated that maximum XOS yield of 290 mg/g could be obtained using 0.24 M sulphuric acid and 31 min (Bian et al., 2014). Microwave irradiation, along with sulfonated bamboo-based catalyst was evaluated for feasibility of conversion of bamboo hemicellulose to XOS. It was observed that in the temperature range of 140- 160^{o}C, the addition of catalyst gave higher XOS yield of 49% as compared to hydrolysis in the absence of catalyst where XOS was unnoticeable (Bai, Xiao, & Sun, 2015).

Newer pretreatment techniques such as steam explosion, ammonia fiber explosion, aqueous ammonia have been used with relation to lignin and cellulose fraction. However, there are limited reports on the utilization of such technique for hemicellulose isolation. Steam explosion of corncob at 196^{o}C for 5 min resulted in 22.8% hemicellulose recovery. Enzymatic hydrolysis of recovered hemicellulose produced a liquor with 28.6g XOS/ 100g

xylan, rich in xylobiose and xylotriose (Teng, Yan, Jiang, Fan, & Shi, 2010). Similarly, 71.58- 79.59% of hemicellulose could be recovered by a combination of alkali and steam pretreatment on the corn stalk. The pretreatment also enabled extensive delignification, wherein 64- 71.8% of lignin was removed (Sun et al., 2015).

Enzymatic hydrolysis of isolated xylan to XOS is advantageous over other chemical methods as it avoids the production of degradation products. However, the utilization of enzymes adds to the overall cost of production of XOS. Hence, to develop economic process, researches have evaluated the feasibility of enzyme immobilization to allow reuse of xylanase for the conversion of xylan to XOS. Substrates such as gelatin (Maalej-Achouri, Guerfali, Gargouri, & Belghith, 2009), Silicon-dioxide nanoparticles (Dhiman et al., 2012), glyoxyl- agarose (Aragon, Mateo, et al., 2013), chitosan (Driss, Zouari-Ellouzi, et al., 2014b) have been used for immobilization of xylanase. In all reported cases, immobilization of enzyme was observed to give higher pH stability, thermostability, and retention on enzyme activity even after multiple uses, this may enable to reduce the cost of production of XOS. A packed bed enzymatic reactor with xylanase from *Aspergillus versicolor* was immobilized on glyoxyl-agarose was evaluated for the continuous production of XOS. The immobilized enzyme could produce 2.5fold higher xylobiose as compared to the soluble enzyme while retaining full catalytic activity up to 10 cycles (Aragon, et al., 2013).

Both nationally as well as internationally, studies related to XOS have focused on the utilization of different agricultural, industrial, forestry residues for the generation of XOS. However, there are various under-utilized sources such as areca husk, almond shell, bamboo stalk, cotton stalk, jackfruit rind, pomegranate peel which can be evaluated for their hemicellulose content, xylan structure and feasibility of XOS production. Microwave irradiation is capable of inducing structure disruption as well as reducing reaction time, a process for the production of XOS with microwave irradiation in combination with the alkali, acid pretreatment can be studied.

3.9. Scope and objectives of the work:

As outlined in the above paragraphs, chemical pretreatment primarily, alkaline pretreatment and physicochemical pretreatment such as autohydrolysis have been commonly employed for the production of prebiotic xylooligosaccharides. Alkaline pretreatment can enable separation of lignocellulosic components to achieve a biorefinery concept. However, in literature, an alkali concentration of 12-16% has been reported, the use of a high concentration of chemical will result in higher production cost. Also, the waste alkaline liquor generated at the end of the process is challenging to handle and will require extensive downstream processing for effective disposal or recovery of alkali. Another unit operation in alkaline pretreatment includes enzymatic hydrolysis of extracted hemicellulose to produce XOS. As the use of enzyme contributes significantly to a process cost, efforts are warranted to minimize the same. This work tries to optimize the alkaline pretreatment protocol, by investigating the pretreatment parameters including alkali concentration, incubation temperature, incubation time, the assistance of hydrothermal treatment, to minimize the alkali loading.

Additionally, the effect of particle size on alkali loading for maximum recovery of hemicellulose was also evaluated. For enzymatic hydrolysis, immobilization of enzyme onto magnetic nanoparticles was used to enable recycling of enzyme. As outlined in the literature review, a limited study has studied enzyme reuse after full enzymatic reaction period. Hence in this work, the enzymatic reaction was performed for a full cycle (48 h) which is necessary to maximize XOS yield, and then the ability of the immobilized enzyme to be re-used for next cycle was evaluated. Also, response surface methodology was employed to understand the interplay between substrate concentration and enzyme dose. The objective of which was to determine a suitable minimum enzyme dose which can efficiently convert a suitable maximum substrate concentration, producing high XOS yield.
The autohydrolysis process provides a green approach for the generation of XOS, as no chemical is required. However, as suggested in the literature review, the process produces XOS with a wide range of DP and a possibly high degree of contamination arising from

degradation products and monosaccharides. Also, as outlined, low DP XOS are better utilized as an energy source by gut microbiota. Hence, in this work, autohydrolysis in a combination of enzymatic hydrolysis was evaluated to produce a maximum of low DP XOS.

The metabolite upon fermentation of prebiotics includes short-chain fatty acids and gases. The SCFA are responsible for putative health claims. However, gas can lead to some discomfort. Hence, in this work, the fermentation of produced XOS was carried out using human fecal samples, and the total gas produced along with total and individual SCFA was measured and compared to commercial prebiotics. The in-vitro bacterial fermentation of produced XOS was also performed using *Lactobacillus* species to ascertain the prebiotic property of XOS.

Chapter 4 Material and Methods

The current chapter describes the materials used during the study. It also describes the general method used for alkaline extraction, autohydrolysis, and characterization techniques.

4.1. Materials:

4.1.1. Raw materials and chemicals:

Areca nut husk was obtained from Sirsi district of Karnataka, during the month of May-June 2015 and 2016. The husk was dried to constant moisture content at 50^{o}C, then stored in an airtight container till further use. The husk was milled using hammer mill (located at Reaction Engineering, F1 Shed, IITB) to obtain smaller particle size. The fraction of husk which could not be converted to a smaller size was manually trimmed using scissors.

Almonds with shells were procured from local markets in Melbourne, Australia and shells were separated from kernel manually. The shells were dried to constant moisture content at 50^{o}C, coarsely ground and stored in airtight containers. In India, finely powdered almond shells were procured from a local vendor (Shree Agrovet, Pune, Maharashtra), dried and stored.

All chemicals and reagents were obtained as the analytical grade from Sigma, USA unless specified. Sodium hydroxide pellets (low chloride) was procured from Merck Millipore, USA. All the reagents, buffers, and standard solutions were prepared using double distilled water. The high pure standards for xylobiose, xylotriose and xylotetrose were procured from Megazyme, USA. The xylanase from *Trichoderma oryzae* and *Thermomyces lanuginosus* was obtained from Merck, USA. The pure standards for glucose, xylose, arabinose was obtained from Sigma, USA. Pure standards of acetic acid, propionic acid, butyric acid was obtained from SD fine Chem, India. The MRS broth and individual components of MRS broth were obtained from Sigma, USA. The Bifidobacterium broth was obtained from Hi-Media, India. The bacterial cultures of *Lactobacillus* were procured from National Dairy Research Institute, Karnal, Haryana, India.

All the glassware used in the study were made of borosilicate and cleaned thoroughly before usage.

4.1.2. Equipment:

Weighing balance

An analytical balance from Mettler Toledo (ME 204), USA or Shimadzu (ATX224), Japan. The balance has a maximum weigh capacity of 220g, with a minimum of 0.1g.

Hot air oven

A custom-made hot air oven (18"×18"×18") with PID controller and motorized air circulation blower was fabricated and supplied by Chemtek Scientific, India was used for all drying purpose. Unless otherwise stated, all materials were dried at 50^{o}C

Incubator shaker

A custom-made incubator shaker having a temperature range of 5-80^{o}C with digital RPM indicator up to 200 rpm and frequency control AC motor drive was fabricated by Priya Enterprises, India and supplied by Chemtek Scientific, Thane, India. The temperature could be adjusted and controlled using microprocessor-based PID temperature controller. The shaker could hold nine conical flasks of 250-500 ml capacity.

pH meter

The pH measurements were made using Eutech pH 700, Thermo Scientific, USA. The pH meter was periodically calibrated using a standard buffer solution of pH 4 ± 0.05, 7 ± 0.05, and 9.2 ± 0.05. The buffer solutions were prepared by dissolving buffer capsules (Merck, USA) in double distilled water.

Centrifuge

Two types of centrifuge were used for the work. A lab-scale centrifuge R24 (400×500×455 mm) procured from Remi, India and a microcentrifuge, Labquest DCF 06 VT (260×244×205 mm) obtained from Borosil. The R24 has stepless speed regulator with zero start interlock, digital speed indicator, dynamic brake along with 0-99 min digital count down timer,

imbalance detector with cut-off and safety lid interlock to prevent cover opening during centrifugation. The R24 centrifuge has a maximum speed of 17300 rpm (max. RCF of 27440). The R24 was provided with rotors, which could hold six tubes of 50 ml capacity and twelve tubes of 15 ml capacity. The DCF06VT was equipped with a fixed angle rotor capable of holding 5,7, 9 and 15 ml tubes. The maximum rpm of the centrifuge was 6500 with digital display, imbalance detection and lid lock safety.

Rotary evaporator

The rotavap Superfit PBU-7 was obtained from Superfit, India. The assembly consists of double wall, thermostatically controlled water bath (up to 100^{o}C), double coiled glass condenser with three openings to assist cooling and vacuum application, a pear-shaped evaporating flask of 800 ml capacity and a reservoir flask of 1 l capacity. The vacuum was applied using an oil free portable vacuum pump having a capacity of 27" Hg.

Freezer

A home refrigerator manufactured by LG, South Korea was used for regular storage of chemicals, standards, and other solutions. For storage at -20^{o}C, a freezer having CFC free hermetically sealed Emerson Copeland make compressor, PID based microprocessor and constructed with stainless steel was procured from Tempo Instruments Pvt Ltd, India.

Magnetic Stirrer

A 1-liter capacity stirrer 1 MLH was obtained from REMI, India and used for the mixing and preparation of the required solution.

Hydrothermal Reactor

The hydrothermal reactor having a 1 L SS vessel, temperature capacity up to 500^{o}C, pressure range of 1-100 bar having overhead drive was obtained from Trident Labotek, Thane.

Autoclave

A 16 L capacity portable autoclave fabricated using die pressed stainless steel was procured from Equitron Medica Private Limited, India.

Microwave

A home use microwave from LG (ME3283FMPG), South Korea was used for microwave irradiation experiments.

High-speed grinder

An M20 universal mill from IKA-Werke GmbH and Co. KG, Germany, was used at Monash University for size reduction of the almond shell.

Shredder

Two stationary hammer type shredders (Make: CRPL) were used for size reduction of arecanut husk. The coarse shedder had a mill screen size of 25.4 mm, power requirement: 15 hp, capacity of 160-180 kg/h and the fine shredder had a mill screen size of 6.35 mm, the power requirement of 7.5 hp and capacity of 80-100kg/h was used.

4.2. Biomass characterization:

4.2.1. Determination of extractives in biomass:

The n-hexane soluble, alcohol (95%) soluble, water-soluble extractive content of the biomass was determined by extraction using soxhlet apparatus (Borosil, India), using the protocol defined by NREL (Sluiter, R. Ruiz, C. Scarlata, J. Sluiter & Templeton, 2008). The detailed procedure is as follows:

1. The residual moisture content of the biomass was determined using a moisture balance. In this procedure, 10 g of the biomass was placed in the extraction thimble of soxhlet apparatus.
2. About 150-200 ml of the required solvent (based on the extractive determination) was placed in the receiving flask and kept on the heating mantle. The temperature of the heating mantle was adjusted to the boiling point of the solvent in use.
3. The entire assembly was set-up by attaching the condenser and required tubes for water circulation and the extraction process was continued for 4-6 h.

4. At the end of extraction time, the solvent was collected, and the biomass left in the extraction thimble for extraction with the next solvent.
5. The collected extract was concentrated using rotary evaporator, and the concentrated extract was placed on a pre-weighed evaporating dish and dried at 105^{o}C.
6. The weight of dried residue obtained from the extract was then used to calculate the percentage of extractives by using the formula:

% extractive: (weight of dried residue/ weight of dried biomass) * 100

The temperature used of each extraction solvent is as shown below

n-hexane: 40^{o}C

95% ethanol: 70^{o}C

Water: 100^{o}C

4.2.2. Determination of the lignocellulosic composition of biomass:

The estimation of cellulose and hemicellulose of the biomass was performed by determination of the neutral detergent fiber (NDF) and the acid detergent fiber (ADF). Van Soest protocol was used for the determination of NDF and ADF (Van Soest, Robertson, & Lewis, 1991). The acid-insoluble lignin content of the biomass was determined by using the NREL protocol for structural carbohydrates and lignin (Sluiter et al., 2008).

a. **Neutral Detergent Fiber**:

Preparation of neutral detergent solution:

The neutral detergent solution was prepared by mixing 18.61 g of disodium ethylene diaminetetracetic acid (EDTA) with 6.81 g of sodium borate decahydrate in a beaker containing 200 ml of water and heated until a clear solution was obtained. A solution of 30 g sodium lauryl sulfate and 10 ml of 2- ethoxyethanol in 100-200 ml water was added to the above mixture and mixed well. Then, 4.56 g of sodium hydrogen phosphate was added to the above solution, and the volume made up to 1 L with distilled water. The pH of the solution was adjusted to be between 6.9- 7.1.

Determination of NDF:

1. The glass filtering crucibles were dried in a muffle furnace (Temperature up to 1200^{o}C, Nirmala Scientific Industries, India) to constant weight and empty weight recorded (Wt).
2. The dry biomass (1 g) (Ws) was weighed accurately and transferred to 150 ml round bottom flask.
3. To the flask, 100 ml of neutral detergent solution was added and mixed to ensure complete wetting of biomass
4. Next, 0.5 of sodium sulfite was added to the above mixture.
5. The mixture was subjected to reflux (40-60^{o}C) for to 1 h while adjusting the temperature as necessary to prevent excessive foaming. The mixture was heated to boil, and then the temperature decreased to 40-60^{o}C to prevent excessive foam formation.
6. After refluxing, the hot mixture was filtered through pre-weighed glass crucibles and then washed thrice with hot water (50 ml).
7. The residue was finally rinsed with acetone until the drained liquid was colorless and dried overnight in an oven at 105^{o}C.
8. The weight of the glass crucible with residue was measured after cooling in a desiccator (Wo).
9. The %NDF was calculated after taking moisture content into account by using the following formula,

$$\%NDF = [(Wo-Wt)/Ws] * 100$$

b. Acid detergent fiber:

Preparation of Acid detergent solution:

The acid detergent solution was made by dissolving 20 g of cetyl-trimethylammonium bromide (CTAB) in 1L of 1N sulphuric acid and mixed well to ensure complete dissolution of CTAB.

Determination of ADF:

1. The glass filtering crucibles were dried in a muffle furnace to constant weight, and empty weight was also recorded (Wt).
2. The dry biomass (1 g) (Ws) was weighed accurately and transferred to 150 ml round bottom flask.
3. To the flask, 100 ml of acid detergent solution was added and mixed to ensure complete wetting of biomass
4. The mixture was subjected to reflux for to 1 h while adjusting the temperature as necessary to prevent excessive foaming.
5. After refluxing, the hot mixture was filtered through pre-weighed glass crucibles and then washed thrice with hot water (50 ml).
6. The residue was finally rinsed with acetone until the drained liquid was colorless and dried overnight in an oven at 105^{o}C.
7. The weight of the glass crucible with residue was measured after cooling in a desiccator (Wo).
8. The %ADF was calculated after taking moisture content into account by using the following formula,

$$\%ADF = (Wo-Wt)/Ws * 100$$

c. Acid-insoluble lignin determination:

1. To a vessel, 300 mg of accurately weighed dried biomass was added and mixed with 3 ml of 72% sulphuric acid
2. The mixture was incubated at 30^{o}C for 1 h with occasional stirring.
3. After 1 h, 84 ml of water (at room temperature) was added to the above mixture to bring the acid concentration to 4% wt and mixed well.
4. The above mixture was then subjected to the autoclaving at 121^{o}C, 15 psi for 1 h.
5. After autoclave treatment, the mixture was cooled to room temperature and filtered using pre-weighed glass crucibles, under vacuum when necessary.

6. The residue was then rinsed three times with hot water (50 ml), followed by rinsing with acetone.
7. The residue along with the crucible was dried overnight at 105^{o}C, and the final weight recorded after cooling in a desiccator.
8. The percentage of acid insoluble lignin was determined by the following formula after considering the ash content and moisture content:

%AIL: (weight of residue/ weight of dried biomass) * 100

4.3. Alkaline pretreatment for extraction of hemicellulose:

The general protocol for alkaline pretreatment of biomass for extraction of hemicellulose is described in the following section. Necessary adjustments were made during individual protocols and have been mentioned where required.

1. The dry biomass was mixed with an alkaline solution of desired concentration at 1:10 solid to liquid ratio and mixed thoroughly to ensure complete wetting of the biomass and to prevent the formation of clumps.
2. The biomass-alkali mixture was then incubated or treated at the desired temperature for the desired time.
3. After pretreatment, the mixture was filtered using a muslin cloth to separate the solid and liquid fraction
4. The liquid fraction was then centrifuged at 5000 rpm for 10 min to obtain a clear alkaline liquor.
5. The pH of alkaline liquor was adjusted to 5 using glacial acetic acid to induce precipitation of the dissolved hemicellulose
6. To the pH adjusted liquor, ice-cold ethanol was added and allowed to stand overnight to bring about settling of polysaccharide; the dissolved lignin remains in the liquor in a soluble form.
7. The settled polysaccharide was then recovered by centrifugation, washed three times with room temperature ethanol (95%) and finally with water.

8. The washed pellet was collected, dried at 50^{o}C, and weighed to determine hemicellulose yield. The recovery was expressed as % True recovery and % Relative recovery, which was calculated as follows:

Hemicellulose yield = (weight of dried pellet/weight of dried biomass) * 100

% True Recovery = [Hemicellulose yield (g)/ Dry biomass (g)] *100

% Relative Recovery = [% true recovery/ % hemicellulose in biomass] * 100

4.4. Analytical techniques:

4.4.1. Fourier Transform Infrared Spectroscopy analysis:

Fourier Transform Infrared (FTIR) analysis of the extracted hemicellulose was determined by recording the wavelength in the range of 400-4000cm^{-1} using 3000 Hyperion Microscope with Vertex 80 FTIR system, Bruker, Germany, situated at the Sophisticated Analytical Instrument Facility, IIT Bombay. The ground samples were mixed with potassium bromide, preferably in 1:100 ratio of sample to KBr and pressed into a disk before analysis for detection of the functional groups.

4.4.2. Scanning Electron Microscopy:

The morphology of biomass before and after pretreatment was visualized by capturing images using Field Emission Scanning Electron Microscopy (SEM), JSM-7600F. The samples were affixed on to disk and subjected to platinum coating before analysis.

4.4.3. Thermal Gravimetric Analysis:

The thermal behavior of untreated and pretreated biomass was examined using Diamond TG/DTA (Perking Elmer, USA) at a heating rate of 10◦C/min in the temperature range of 0–600◦C under a nitrogen atmosphere (200 ml/min).

4.4.4. Reducing sugar determination:

The total sugar content and reducing the sugar content of the samples were determined by using the phenol-sulphuric acid method and the di-nitrosalicylic acid (DNS) method, respectively using UV-Vis Spectrophotometer, Shimadzu Corporation, Japan.

4.4.5. Chromatographic method:

The High-Pressure Liquid Chromatography (HPLC) method was developed for detection of xylobiose, xylotriose, xylotetrose, xylose, glucose, arabinose, acetic acid, propionic acid, and butyric acid by using pure standards. The HPLC method was developed on an Infinity 1290 chromatographic system (Agilent, USA) equipped with a quaternary pump, autosampler, column thermostat, refractive index detector (RID) and diode array detector (DAD). The mobile phase used was 5mM sulphuric acid in HPLC grade water at a flow rate of 0.7ml/min. The analysis was performed using Hi-Plex H (300*4.6 mm) column held at 65^{o}C and RID held at 50^{o}C under positive signal detection. The calibration curve of each standard was prepared by measuring the peak area of suitably serially diluted stock solution. The equation obtained from the calibration curve was used to determine the concentration of unknown samples.

For furfural, the method was developed on a C18 column (250*4.6 mm) held at room temperature using methanol: HPLC water (5:95 v/v) at 1 ml/min.

Chapter 5 Preliminary study on Alkaline extraction of hemicellulose from arecanut husk

This chapter describes the process and outcome for alkaline extraction of hemicellulose and production of xylooligosaccharides using enzymatic hydrolysis from arecanut husk. Arecanut husk is generated as a waste by-product during processing of areca to obtain nut; it represents about 60-80% of the total weight of the nut. In India, the quantum of husk generated in 2013-2014 was recorded as 0.5 million metric tonnes (MMT) (National Horticultural Database, 2015) from 0.62 MMT areca produced. A fraction of the husk is used as a solid fuel for the household application while the major part is discarded as waste. The disposal of husk is a challenge due to its slow degradation rate and low bulk density; moreover, if left unmanaged, it attracts pests. Thus, a common practice is the burning of the husk, which contributes to environmental pollution. Also, as the husk is a good source of lignocellulose, it leads to loss of valuable biopolymer.

As outlined in the literature review section, alkaline pretreatment and steam assisted alkaline pretreatment has been used to extract hemicellulose from biomass such as corn cobs (Samanta et al., 2014), natural grass (Samanta, Jayapal, et al., 2012a), pigeon pea (Samanta et al., 2013b), sugarcane bagasse (Jayapal et al., 2013). However, in the above reports, about 12-16% alkali was optimum to extract about 90% hemicellulose. Also, an optimisation of alkali pretreatment process has been reported for bagasse to extract arabinoxylan. The report analysed 5, 10 and 24% KOH at different temperatures (35, 70 and 121^{o}C) and reaction time (0.5 and 3 h) (de Figueiredo, Carvalho, Brienzo, Campioni, & de Oliva-Neto, 2017). Thus, alkaline pretreatment involves the use of a high concentration of alkali, along with ethanol required for precipitation and washing of hemicellulose. This results in high chemical load and usage. Hence, in this work, the objective was to minimize the usage of alkali for high hemicellulose recovery and to minimize ethanol consumption in the downstream steps. Hence, the pretreatment parameters: alkali concentration, incubation time, incubation temperature, the assistance of hydrothermal were studied in detail. Also, hydrothermal

heating and microwave assisted heating was evaluated. To realise the maximum potential of biomass, a biorefinery approach was sought, wherein, the cellulosic portion of alkali pretreated residue was converted into glucose.

5.1. Biomass characterization:

The extractive content and ash content of dry arecanut husk was determined by using the National Renewable Energy Laboratory (NREL) analytical protocol TP 510-42619 and TP 510-42622, respectively (as described in section 4.2). The lignocellulosic content of the husk was determined by following NDF, ADF and acid insoluble lignin protocol (as described in section 4.2). The carbon, hydrogen, nitrogen and oxygen content of husk was determined by using CHNSO elemental analyzer (Flash EA 1112 Series, Thermo Finnigan, Italy). The calorific value of biomass was determined by Bomb Calorimeter (IKA, C200, IKA, China). The crude protein content in the raw material was estimated by conventional Kjeldahl method (AOAC, 2000).

5.2. Alkaline extraction of hemicellulose:

Alkaline extraction of hemicellulose was performed using three protocols. The process for alkaline extraction and calculation of the yield is described in section 4.3, however necessary changes were made as desired in each protocol. The alkali concentration used in the study was 5, 10, 15, 20% w/v Sodium hydroxide. The protocols are as described below:

5.2.1. Protocol 1: Incubation

To 5 g of extractive-free biomass, 50 ml of the desired concentration of sodium hydroxide was added, and the mixture was mixed to ensure even wetting of particles and preventing clump formation. The mixture was then incubated at 35^{o}C for 16 h at 150 rpm. The remaining process for hemicellulose extraction is as described in section 4.3.

5.2.2. Protocol 2: Incubation and hydrothermal assisted extraction

In this protocol, the biomass was mixed with 1:10 solid to liquid ratio with an alkali solution and incubated at 35^{o}C for 16 h. After incubation, the mixture was subjected to hydrothermal treatment for 1 h at 121^{o}C. The remaining steps are as mentioned in section 4.3

5.2.3. Protocol 3: Hydrothermal assisted alkaline extraction

Hydrothermal assisted alkaline extraction was performed at three reaction time, i.e. 1 h, 1.5 h, and 2 h. The extractive free biomass was mixed with the alkaline solution at 1:10 w/v (solid to liquid) ratio and mixed well. The mixture was then heated in an autoclave at 121^{o}C for different reaction time. The remaining process is as mentioned in section 4.3.

5.3. Microwave-Assisted alkaline pretreatment:

Microwave-assisted alkaline extraction was studied using a general purpose home microwave oven (Model MC3283FMPG, LG, South Korea). The microwave operates at 2450 MHz, with adjustable microwave power in range of 100-900 W. For the pretreatment, the biomass was mixed with alkali solution at 1:10 w/v and subjected to heating at three power levels (180 W, 540 W and 900 W) to cover the lower, medium and higher heating value of microwave. Each pretreatment at designated power level was performed for two reaction time, i.e., 1 and 3 min. The final temperature of the mixture at the end of each reaction time was measured using an infrared thermometer (DIT-130, Sonel, Poland).

5.4. Enzymatic hydrolysis of alkali pretreated residue:

The residue obtained after alkaline pretreatment was used for enzymatic hydrolysis of cellulose into glucose. A fraction of biomass was bleached using 5% w/v hydrogen peroxide containing 0.05% w/v magnesium sulphate and 5% w/v sodium silicate, at 70^{o}C for 1 h at 1:10 solid to liquid ratio, under continuous stirring. The bleached biomass was then washed thoroughly with de-ionized water and dried in an oven at 60^{o}C. The enzymatic hydrolysis of

bleached and unbleached biomass was carried out using the protocol defined by National Renewable Energy Laboratory (NREL) (Resch, Baker, & Decker, 2015). For hydrolysis, 60 ml of the reaction mixture was incubated with enzymes at 50^{o}C for 72 h at 120 rpm. The reaction mixture was composed of 0.05 mol/L citrate buffer (pH 4.8), 40 µg/ml tetracycline, 30 µg/ml cycloheximide, along with Cellulase from *Trichoderma reesei* (Celluclast 1.5L, Sigma) at an enzymatic activity of 60 FPU/g cellulose and β- glucosidase from *Aspergillus niger* (Novozyme 188, Sigma) having an enzyme activity of 30 CBU/g cellulose. The reducing sugar released upon hydrolysis was measured spectrophotometrically using the DNS method, whereas the amount of glucose was estimated using HPLC.

5.5. Characterization of extracted hemicellulose:

The structural and thermal characterization of extracted hemicellulose was done by obtaining FTIR spectra and TGA data. The SEM images of the pretreated residue were obtained to visualize the effect of chemical treatment on the morphology. The extracted hemicellulose was hydrolyzed using sulphuric acid to determine the neutral sugar composition and the acid-insoluble lignin content by following the protocol for acid insoluble lignin determination. The sugar content of hemicellulose was estimated using HPLC.

5.6. Results and Discussion:

5.6.1. Biomass Characterisation:

The lignocellulosic composition of arecanut husk is as shown in Table 5.1, and the ultimate analysis results in Table 5.2.

Table 5.1: Chemical composition of arecanut husk

Biomass component	Value (%)
Cellulose	28.3±1.5
Hemicellulose	24.6±1.2
Lignin	24.7±2.7
Crude protein	7.8± 0.02
Total extractives	14.6± 1.2
Ash	7.1± 0.3
Organic matter	92.9± 0.3

Table 5.2: Ultimate analysis of arecanut husk

Parameter	Average value (%)
Carbon	45.5
Hydrogen	5.2
Oxygen	22.4
Nitrogen	0.5
Gross calorific value (MJ/kg)	16.6

The hemicellulose content of husk was similar to that of sugarcane bagasse (25%), corn stover (18.2%), rice straw (24%) and wheat straw (20-25%). The lignin content of husk was higher as compared to that reported for corn cobs (15%), corn stover (14.2%), but in accordance to that measured for bagasse, sorghum, wheat straw (20-21%). The cellulose content of husk was found to be lower as compared to other biomass such as hardwood, softwood, straws, and bagasse (33.4%). The ultimate analysis measured using CHNSO analyzer gave a carbon content of 45.5% and hydrogen content of 5.2%. These values are similar to that reported for Napier grass, pinewood bark, timothy grass, and wheat straw. The oxygen content of husk was 22.42%, which is low as compared to the biomass mentioned above.

5.6.2. Alkaline extraction of hemicellulose:

As alkaline pretreatment brings about the disruption of lignin and hemicellulose bonds, cell wall disruption, cellulose swelling, dissolution of hemicellulose and some of the lignin, it can be useful for fractionation of biomass into its constituent fractions. However, often the high concentration of alkali has been used (12-16%) to achieve the high hemicellulose recovery without valorization of other components (Singh, Bhuyan, Banerjee, Muir, & Arora, 2017). Secondly, the high amount of liquor generated is difficult to handle. Thus, alkaline pretreatment in the presence or absence of hydrothermal treatment as evaluated to achieve fractionation of arecanut husk. The relative recovery of hemicellulose is as shown in Table 5.3. As can be seen, the relative recovery of hemicellulose was dependent on the alkali concentration and increased with increase in concentration.

Table 5.3: Relative recovery of hemicellulose from arecanut husk under different experimental conditions

Process	Alkali Concentration (%)	Hemicellulose yield (%)	Relative recovery (%)*
Incubation 16 h)	5	3.1± 0.3	12.6 ± 1.4^{n}
	10	5.9 ± 0.1	$24.1 \pm 0.2^{j,k}$
	15	6.3 ± 0.3	$25.7 \pm 1.1^{i,j}$
	20	6.9 ± 0.4	28.1 ± 1.7^{i}
Alkali incubation (16 h) + hydrothermal (1 h)	5	5.4 ± 0.1	$21.9 \pm 0.5^{k,l}$
	10	13.1 ± 0.4	53.2 ± 0.7^{g}
	15	19.0 ± 0.6	$77.2 \pm 2.5^{b,c}$
	20	20.2 ± 0.1	82.1 ± 0.5^{a}
Hydrothermal (1 h)	5	4.9 ± 0.5	$19.9 \pm 2.1^{l,m}$
	10	11.9 ± 0.4	48.2 ± 1.7^{h}
	15	14.7 ± 0.2	59.9 ± 0.7^{f}
	20	18.4 ± 0.3	74.9 ± 1.3^{c}
Hydrothermal (1.5 h)	5	4.3 ± 1.0	17.6 ± 4.1^{m}
	10	15.9 ± 0.3	64.8 ± 1.1^{f}
	15	20.5 ± 1.0	83.5 ± 4.2^{a}
	20	19.7± 0.5	$79.9 \pm 1.9^{a,b}$
Hydrothermal (2 h)	5	6.2 ± 0.1	$25.3 \pm 0.5^{i,j,k}$
	10	17.4 ± 0.3	70.6 ± 1.1^{d}
	15	18.9 ± 0.3	$76.6 \pm 1.3^{b,c}$
	20	20.2 ± 0.3	82.3 ± 1.1^{a}

*results are expressed as mean ± sd. Relative recovery values sharing an alphabet are not significantly different ($p<0.005$)

It was observed that soaking of the biomass (protocol 1) in 20% w/v alkali for 16 h could extract only 28.1% of the available hemicellulose. However, when hydrothermal treatment was used after soaking (protocol 2), the recovery could be increased to 82.1 ± 0.5%. Thus, it seems likely that heat plays a crucial role along with the alkali concentration.

These results are in accordance to those obtained for bagasse (85%) (Jayapal et al., 2013) and corn cob (83%) (Samanta et al., 2014) under similar conditions. Another observation from the table 5.1 is that the recovery of hemicellulose increases with increasing alkali concentration when only hydrothermal treatment was applied for 1 h and reaches a maximum of 74.9 ±

1.9% for 20% w/v NaOH. Thus, as reaction temperature, time, and alkali concentration are the critical variables, the effect of increasing the reaction time on hemicellulose recovery was evaluated while keeping reaction temperature constant. For 1.5 h and 2 h hydrothermal time, at 10% w/v NaOH concentration, 64.8% and 70.6% of hemicellulose was recovered. The hemicellulose recovery at 10% w/v NaOH with 1.5 and 2 h was significantly different ($p < 0.05$). Also, the recovery at 1.5 and 2 h were significantly different in comparison to hemicellulose recovery observed at 1 h hydrothermal treatment time (Table 5.3). With an increase in NaOH concentration to 15% w/v, hemicellulose recovery was observed to be 83.5% and 76.6% at 1.5 and 2 h, respectively. Similarly, for 15% w/v NaOH, hemicellulose yield at 1.5 and 2 h was significantly different from those obtained at 1 h. Using 20% w/v NaOH, 79.9% and 82.3% hemicellulose could be recovered at 1.5 and 2 h, respectively. It can be observed that hemicellulose recovery at 1, 1.5, and 2 h at 20% w/v NaOH concentration was not significantly different. However, at a hydrothermal pretreatment time of 1.5 h, the highest hemicellulose recovery was achieved. Thus, hydrothermal pretreatment of alkali soaked biomass for 1.5 h can be considered as economical as compared to the process involving alkali soaking (16 h) followed by hydrothermal treatment (1 h) (Table 5.3).

5.6.3. Microwave-assisted fractionation of arecanut husk:

The applicability of microwave irradiation as a heat source for the fractionation of lignocellulose from arecanut husk was evaluated using a conventional home microwave oven at two reaction time and three power levels. The recovery of hemicellulose upon microwave irradiation of alkaline solution is as shown in Table 5.4. As observed, recovery increases with an increase in the alkali concentration up to a threshold value, beyond which recovery tend to decrease. The observation may be due to degradation or hydrolysis of hemicellulose into oligosaccharides, monosaccharides, and degradation products. However, this was not estimated. Using two-way ANOVA analyses, a significant interaction between alkali concentration and the power level was observed for the recovery of hemicellulose, and reasons for such a response are not apparent. At a microwave power of 900 W, the maximum yield of hemicellulose was observed at 15% w/v alkali concentration for both 1 and 3 min. In

contrast, the maximum recovery of hemicellulose was obtained at 10% w/v alkali concentration for 1 and 3 min when exposed to 540W.

Table 5.4: Hemicellulose recovery upon microwave irradiation of alkali biomass mixture

Microwave irradiation time (min)	Power level (W)	Final temperature (°C)	Alkali concentration (%)	Yield (%)	Relative recovery (%)
1	180	48	5	1.0 ± 0.2	1.1 ± 0.8
		50	10	3.3 ± 0.5	13.5 ± 1.9
		50	15	2.5 ± 0.1	10.2 ± 0.4
		50	20	4.4 ± 0.5	17.9 ± 2.1
	540	72	5	4.4 ± 0.5	17.7 ± 1.9
		80	10	7.7 ± 0.7	31.3 ± 2.9
		80	15	4.9 ± 0.2	19.8 ± 0.8
		82	20	4.2 ± 0.3	17.1 ± 1.2
	900	82	5	5.6 ± 0.1	22.8 ± 0.6
		86	10	8.0 ± 0.2	32.6 ± 0.9
		88	15	9.2 ± 0.8	37.3 ± 3.4
		96	20	6.4 ± 0.1	25.8 ± 0.5
3	180	76	5	1.7 ± 0.1	6.7 ± 0.2
		92	10	4.5 ± 0.2	17.3 ± 0.7
		90	15	4.1 ± 0.3	16.6 ± 1.1
		90	20	5.9 ± 0.5	24.1 ± 1.9
	540	90	5	8.8 ± 0.2	37.1 ± 0.8
		92	10	10.1 ± 0.1	39.9 ± 0.5
		98	15	9.4 ± 0.1	38.1 ± 0.5
		104	20	7.7 ± 0.2	31.5 ± 0.8
	900	98	5	11.0 ± 1.3	44.7 ± 5.4
		108	10	12.1 ± 0.5	49.2 ± 2.2
		112	15	12.9 ± 0.7	52.5 ± 2.8
		116	20	5.6 ± 7.8	43.9 ± 1.7

*results of yield and % relative recovery are expressed as mean ± sd

With 180 W the maximum recovery of hemicellulose was observed at 20% w/v alkali concentration. The obtained results suggest that there is a decrease in hemicellulose yield with increasing alkali concentration at power levels of 540 and 900W. The findings may be due to the breakdown of the hemicellulose polymer into oligomers and monomers. However,

the anomaly in hemicellulose yield at 900W and 540W with increasing alkali concentration could not be explained and requires further study.

The highest yield of hemicellulose was found to be 52.5% of total xylan, at a microwave power of 900 W at 3 min reaction time. Thus, using microwave irradiation, a yield equivalent to 64% of that obtained using hydrothermal treatment of alkali soaked mixture with a reaction time of 17 h could be achieved within 3 min. This can be attributed to the heating mechanism of the microwave, which induces heat with direct interaction of electromagnetic waves through the sample. This is in contrast to conventional heating in an autoclave where heat transfer is through conduction/convection, which is slow but homogenous.

5.6.4. Compositional analysis of pretreated residue:

The residue obtained upon each pretreatment process was subjected to NDF, ADF, and acid insoluble lignin analysis to determine the percentage of cellulose and lignin. The lignin content of the residue was also translated into percent delignification upon pretreatment. The results are indicated in Table 5.5 The cellulose percentage (difference of ADF- AIL) was found to be in the range of 37.8-55.1% (dry basis). The percentage of cellulose was nearly twice in the residue as compared to raw biomass due to the removal of hemicellulose and lignin. This can be attributed to breakage of intermolecular ester linkages between carbohydrates and lignin during alkali pretreatment. The extent of delignification from biomass was found to increase with an increasing percentage of alkali in both pretreatment conditions, as shown in Table 5.5. For hydrothermally treated alkali soaked biomass (protocol 2), the extent of delignification increased from 32% to 69.7% with an increase in alkali concentration. Similarly, for the hydrothermally treated alkali-biomass mixture (protocol 3) the delignification percentage increases from 21.3% to 64.6% with an increase in alkali concentration from 5% to 20% w/v. It was observed that with hydrothermal treatment for 1.5 h, about 49% delignification could be achieved. The extent of delignification was found to be highest in case of soaking with 20% w/v NaOH followed by hydrothermal treatment. However, there was no significant difference in lignin removal in the case of hydrothermal treatment of soaked and non- soaked biomass at 20% w/v NaOH. With

microwave treatment, a maximum delignification value of 82% could be achieved at a power level of 900 W for 1 min and 15% w/v alkali concentration. The extent of lignin removal was found to be higher in the case of microwave irradiation as compared to hydrothermal assisted heating. Thus, hydrothermal and microwave assisted alkaline pretreatment method can fractionate biomass into a cellulose-rich residue, liquor rich in lignin, and recoverable hemicellulose.

Table 5.5: Compositional analysis of pretreated residue depicting % cellulose and % delignification

Process	Condition	Cellulose (%)	Lignin (%)	Delignification (%)
Alkali Soaking for 16 h + hydrothermal (1 h)	5% NaOH	39.2 ± 1.4	16.8 ± 0.7	32.0 ± 2.9
	10% NaOH	49.2 ± 0.1	12.2 ± 0.2	50.8 ± 0.9
	15% NaOH	48.2 ± 2.9	12.8 ± 2.1	48.1 ± 8.8
	20% NaOH	55.1 ± 1.3	7.5 ± 1.6	69.7 ± 6.6
Hydrothermal (1 h)	5%% NaOH	37.8± 1.0	19.5 ± 1.6	21.3 ± 6.6
	10%% NaOH	48.3 ± 0.5	10.3 ± 0.4	58.3 ± 1.9
	15%% NaOH	47.5 ± 0.7	9.3 ± 0.9	62.4 ± 3.8
	20%% NaOH	52.5 ± 1.3	8.8 ± 0.6	64.6 ± 2.6
Hydrothermal (1.5 h)	15% NaOH	49.8 ± 0.9	12.5 ± 0.7	49.43 ± 2.9
Hydrothermal (2 h)	20% NaOH	45.9 ± 0.9	9.6 ± 0.3	61.0 ± 1.3
Microwave assisted alkaline pretreatment	900W, 1 min, 15%	54.9 ± 2.7	4.3 ± 0.4	81.8 ± 0.9
	540W, 1 min, 10%	52.1 ± 0.8	10.5 ± 1.17	55.9 ± 2.4
	900W, 3 min, 15%	48.6 ± 1.3	16.0 ± 1.8	32.6 ± 3.8

*results are expressed as mean ± sd

5.6.5. Enzymatic hydrolysis of residue:

As hydrothermal treatment at 15% alkali, 1.5 h and 121oC gave the highest hemicellulose recovery with about 49.4% delignification; this residue was selected to observe further the extent of glucose produced upon enzymatic hydrolysis. The kinetics of reducing sugars released from the residue is shown in Figure 5.1. The percentage of reducing sugars released

from pretreated biomass at the end of 72 h using cellulase and glucosidase was evaluated at the following parameters: 50◦C, pH 4.8, and 120 rpm. At the end of 72 h, reducing sugars released from biomass was found to be 75.5 ± 3.5%. The pretreated cellulose was further bleached to remove residual lignin and study the effect on biomass hydrolysis. It was observed that after bleaching about 79.2 ± 2.1% of cellulose-rich biomass could be converted to reducing sugars. The obtained results indicated that there is no significant difference ($p < 0.05$) between reducing sugars released from pretreated samples and bleached samples. The HPLC analysis revealed that enzymatic hydrolysis of untreated biomass could release only 2.2 ± 0.1% glucose as compared to 71.5 ± 1.9% glucose released from pre-treated biomass.
On the other hand, xylose yields were 1.3 ± 0.4% and 4.3 ± 0.7% for untreated and pretreated samples, respectively. Other reducing sugars, such as mannose, galactose, and arabinose were found to be below the detection limit in both untreated and pre-treated biomass. Thus, this study showed that the highest amount of glucose released during enzymatic hydrolysis was ~ 21 g glucose for each 100 g of dry arecanut husk obtained using pretreatment at 121◦C, 15% w/v NaOH and 1.5 h of reaction time.

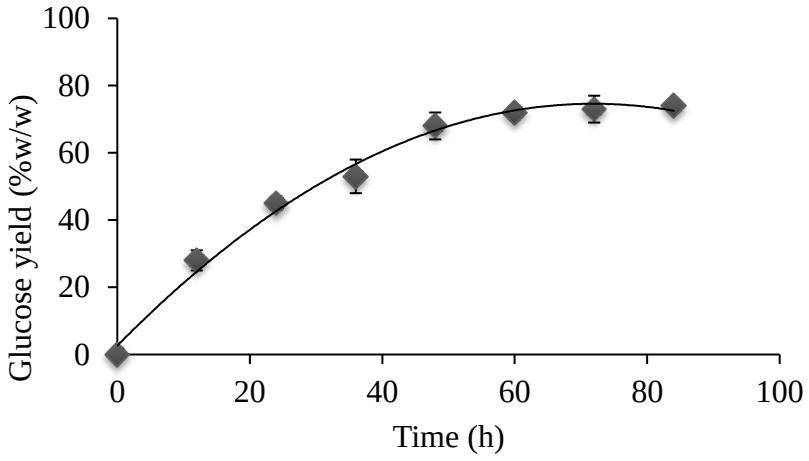

Figure 5.1: Glucose release during enzymatic hydrolysis of pretreated arecanut husk (hydrothermal treatment for 1.5 h and alkali concentration 15%)

5.6.6. Characterization of extracted hemicellulose:

5.6.6.1. Fourier Transform Infrared Spectroscopy:

FTIR is used for identifying physicochemical, conformational, and functional group characteristics of molecules in a biomass sample. Thus, FTIR spectra were collected and compared with the published literature to ascertain the extract as hemicellulose. The FTIR spectra of hemicellulose obtained from different pretreatment methods of hydrothermal or microwave assisted alkali extraction appeared to be similar (Fig. 5.2).

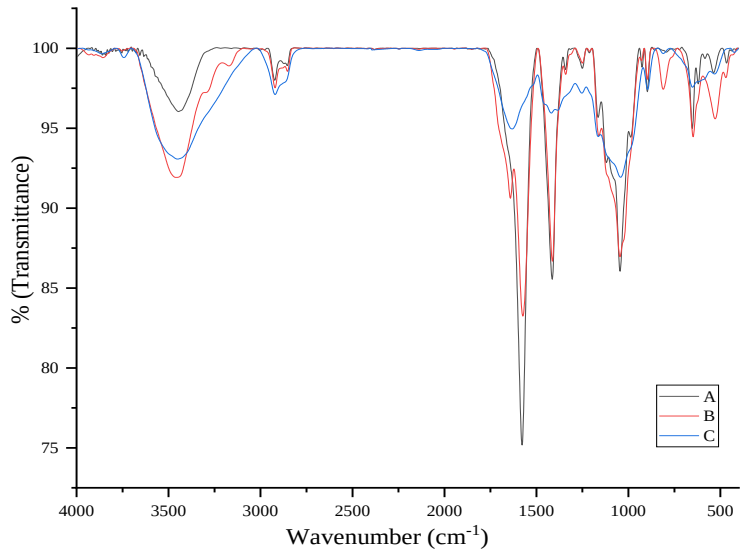

Figure 5.2: FTIR spectra of extracted hemicellulose a) hydrothermal pretreatment of alkali soaked biomass b) hydrothermal pretreatment of alkali steeped and c) (16 h) biomass microwave irradiated

The broad band in the region of 3600–3100 cm^{-1} can be attributed to a hydroxyl group in all samples; this agrees with FTIR spectra for xylan extracted from other biomass. The absorbance bands at 2917, 1422, 1219, 1166, and 1042 cm^{-1} are attributed to the xylan molecule. The band between 1166 and 1042 cm^{-1} are typical of xylan, and the band is arising at 896 cm^{-1} is characteristic of glycosidic linkage between sugar molecules (Buslov et al.,

2010). The complex absorption band with a principal maximum at 1042 cm^{-1} arises because of C-O, C-C stretching, or C-OH bending of hemicellulose. Also, the band in the region of 1200–1000 cm^{-1} are present in FTIR spectra of 4-O-methylglucuronoxylan (Kacuráková et al.,1999). The absence of a band at the 1520 cm^{-1} region indicates the absence of the pectin molecule in the extracted sample (Kacuráková, 2000). Also, a few extracted samples show absorbance bands in the region of 1560 $cm^{-1,}$ which can be ascribed to the presence of bound lignin (Maziero et al., 2012).

5.6.6.2. Thermal Gravimetric Analysis:

The thermal behavior of biomass is related to the physical characteristics and chemical composition of cellulose, hemicellulose, and lignin. The TGA analysis of untreated and pretreated biomass was conducted to examine the effects of alkali on the structure and composition. The thermal decomposition of lignocellulosic biomass has four stages: the first stage occurs in the temperature range of 50–120^{o}C due to loss of moisture and volatile constituents; stage two occurs between 180–320^{o}C where hemicellulose and some cellulose decomposition occurs; stage three is represented by cellulose decomposition between 320-400^{o}C; and stage four is where lignin decomposition takes place above a temperature of 400^{o}C (Phitsuwan et al., 2016; Subhedar and Gogate, 2014).

The hemicellulose structure is quite complex (branched polysaccharides) than cellulose and is thermally more unstable. As a consequence, these compounds decompose faster and at lower temperatures as compared to cellulose and lignin. Cellulose is a polymer composed of linear chains of glucose a degree of polymerization of ten to one hundred times higher than that of hemicellulose. Lignin, on the other hand, is a highly cross-linked polymer consisting of aromatic rings with multiple branches and functional groups, whose bonds cleave along with a wide range of temperatures. The thermal decomposition (mass loss) of untreated and pre-treated biomass is shown in Fig. 5.3. The initial decomposition occurred below 120^{o}C, which resulted in the mass loss of 7–8% for the untreated sample and 10–12% for the pretreated sample. This can be attributed to moisture loss. The second stage of decomposition occurred

between 230 and 330°C, representing about 42% and 26–28% mass loss for untreated biomass and pretreated samples, respectively. The decay in the sample corresponds to mainly hemicellulose and some cellulose decomposition. Xylan is predominant in hemicellulose in dicots and monocots (Scheller and Ulvskov, 2010) and due to its peculiar structure, its decomposition can be observed in two temperature ranges (Shen and Gu, 2009; Shen et al., 2009). The decomposition of residual side chains (4-O-methyl glucuronic acid and acetyl groups of xylan) was observed at 228°C while the rupture of the xylan main chain was observed at about 286°C.

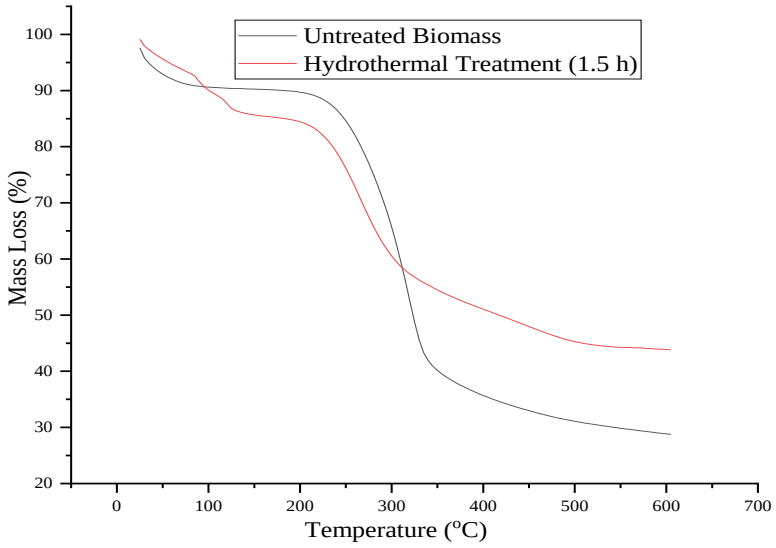

Figure 5.3: TGA profile of untreated and hydrothermally pretreated biomass

Any biomass tends to be quite complicated in their chemical composition, and thus the behavior under thermal environment is not predictive due to associated heterogeneity. The cellulose decomposition began at around 300°C (~15% mass loss before it reached 320°C) and the slope of the mass loss curve changed abruptly at 340°C, which is indicative of lignin decomposition. The lower mass loss for pretreated samples can be attributed to the lower content of hemicellulose due to recovery upon alkaline pretreatment. In untreated samples,

cellulose decomposition occurred between 280 and 300^{o}C. The final stage, above 340^{o}C, is associated with cellulose and lignin decomposition. The region shows a weight loss of 11–12% for untreated and 10–11% for pre-treated samples. Decomposition of pure components differs from real biomass because the reactions are less hindered by interactions with other components (Couhert et al., 2009).

5.6.6.3. Scanning Electron Microscopy:

The treated samples were visualized under a scanning electron microscope and the images compared to detect the morphological changes. The surface of the untreated samples (Fig. 5.4a) shows mostly a smooth surface. In comparison to untreated arecanut husk, the hydrothermal assisted alkali pretreated (Fig. 5.4b and c) and microwave-assisted alkali pre-treated fibers (Fig. 5.4d) show crevices, holes, and rough surfaces.

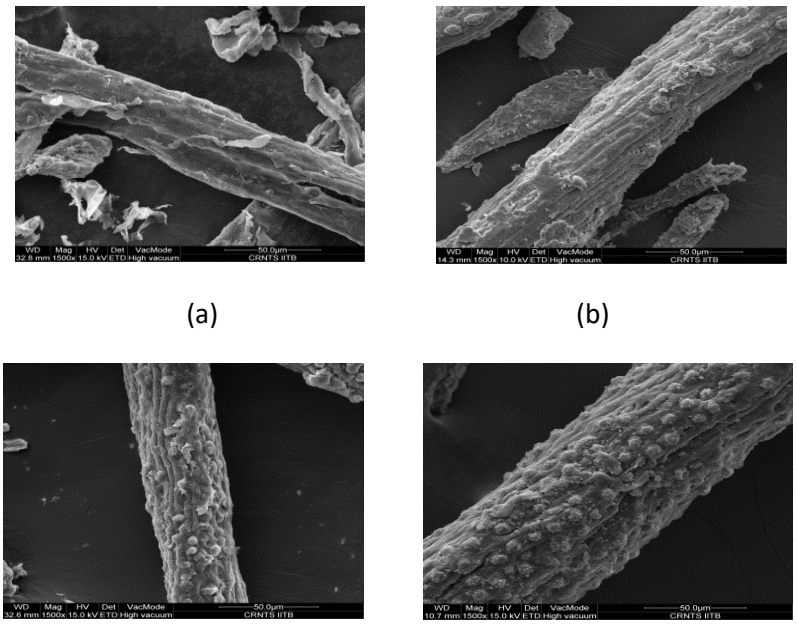

Figure 5.4: SEM images of biomass a) untreated, b) hydrothermal pretreatment of alkali soaked biomass and c) hydrothermal pretreatment of alkali steeped biomass and d) microwave irradiated

The upper surface ruptured, and lignin-hemicellulose complex may have been disrupted in case of alkali pre-treated biomass. With an increase in alkali concentration, the surface roughness increased in both pre-treatment methods. The droplet-like structure on the surface of fiber may be due to redeposition of some of the lignin after pre-treatment. The coarser surface in the case of samples treated with higher a percentage of alkali may be due to the removal of lignin to a larger extent. However, some of the lignin may have redeposited back on the surface. The images are in corroboration with previous studies, wherein hydrothermal and microwave assisted pretreatments caused the surface to loosen and become irregular (Kurian et al., 2015; Sun et al., 2014). The increase in porosity and surface area results in greater accessibility for enzymes during the hydrolysis stage to breakdown cellulose into glucose.

5.6.6.4. Chemical composition of extracted hemicellulose:

The xylan composition is variable and depends on the sources; however, it is thought to possess a backbone of D-xylose, linked via β- 1, 4- xylosidic linkages. The heterogeneity of xylan lies in the various sugar substituents such as glucose, arabinose, galactose, mannose or acidic groups such as uronic and acetic acid attached to the xylose backbone (Scheller & Ulvskov, 2010). The alkali extracted xylan was hydrolyzed with sulphuric acid to determine the monomer composition. It was observed that the extracted xylan was composed of 50.9 ± 3.2 % xylose, 9.8 ± 0.1% glucose and 1.72 + 0.5% acetic acid. This indicates a xylose to glucose ratio of 5.1. Other monomers such as arabinose were not detected upon acid hydrolysis. This may be due to the absence of arabinose or decomposition into degradation product.

In summary, xylan in arecanut husk is composed primarily of xylose units which constitute the backbone with glucose and acetic acid as substituents. The alkali extracted xylan was found to be contaminated with acid insoluble lignin to the extent of about 5.0 ± 0.5%. The presence of lignin is considered to be inhibitory, as it deactivates enzymes used for saccharification of xylan or cellulose. It is reported that lignin and hemicellulose are linked

via multiple bonds, including benzyl ester, benzyl ether, and phenyl glycosidic linkages to form lignin-carbohydrate-complex (Westbye, et al., 2007). The presence of such linkages possesses practical limitation for complete removal of lignin, and some may have been retained in the extracted xylan. In the present work, we can conclude that about 95% of pure xylan could be recovered under the optimized alkaline pretreatment.

5.7. Conclusion:

Hydrothermal and microwave assisted alkaline pretreatment approaches were utilized to fractionate arecanut husk into hemicellulose as a solid precipitate, cellulose-rich insoluble residue, and a dissolved lignin stream. Hydrothermal treatment of alkali soaked biomass (20% w/v) resulted in the recovery of 82% hemicellulose, with significant delignification (∼70%) of biomass. Whereas in the case of hydrothermal treatment of alkali biomass mixture (total reaction time of 1 h), 75% hemicellulose could be recovered at 20% w/v alkali concentration. However, by increasing the hydrothermal time to 1.5 h, at 15% w/v alkali, 83–86% hemicellulose recovery was obtained. Thus, it is possible to decrease the concentration of alkali use by increasing hydrothermal reaction time.

Similarly, under microwave-assisted alkali pretreatment, the best hemicellulose yield obtained was 52%. Delignification, however, was quite significant (∼82%) using this approach. Though the hydrothermal method recovered a higher fraction of hemicelluloses, significant lignin removal could be achieved in a shorter time using microwave irradiation, which can be attributed to the difference in their heating mechanisms. The residue obtained after pretreatment was observed to be rich in cellulose, making up to 69.2 ± 1.3% and was used for enzymatic hydrolysis. Enzymatic hydrolysis of pretreated biomass liberated 75–79% of reducing sugars from cellulose.

Furthermore, pretreatment of arecanut husk could achieve 71.5 ± 1.9% conversion of cellulose to glucose as compared to 2.2 ± 0.1% glucose released from untreated biomass. Thus, it is an indication of increased accessibility of enzyme after pretreatment. Chemical composition determination, morphological investigation using SEM, FTIR spectroscopy, and TGA confirmed the removal of non-cellulosic materials. Both methods can be used to

achieve fractionation of arecanut husk into its constituent fractions for value-added product generation. However, pilot level study and techno-economic analysis of both methods should be done to ascertain the feasibility of the methods for fractionation at an industrial level.

Chapter 6 Process optimization for XOS production from arecanut husk

In the previous chapter, the high recovery of hemicellulose was achieved by increasing the reaction time at 15% w/v NaOH. However, from a practical standpoint, 15% alkali is still high. As it was observed that alkali concentration, reaction temperature, and reaction time are important variables, further efforts were made to optimize the parameters. Also, as described in the previous chapter about 1.5x ethanol is required for precipitation of hemicellulose and additional quantity being consumed during washing of extracted hemicellulose. Hence, the option of decreasing ethanol requirement during precipitation and washing step was evaluated.

6.1. Optimization of a process for XOS production:

The protocol followed for optimization of alkaline pretreatment and enzymatic hydrolysis for XOS production is as shown in Figure 6.1.

6.1.1. Optimization of alkaline pretreatment for hemicellulose recovery:

For maximum hemicellulose recovery, the parameters of the alkali pretreatment process were optimized. The parameters include:

Alkali concentration: 5, 10, 15, 20% w/v

Incubation time: 8, 16, 24 h

Incubation temperature: 25^{o}C, 50^{o}C, and 65^{o}C

Briefly, the extractive-free biomass was mixed with the desired concentration of the alkali solution at 1:10 w/v ratio and subjected to the necessary incubation condition. After the reaction period, the hemicellulose was recovered, and recovery determined by following steps mentioned in section 4.3.

6.1.2. Hydrothermal assisted alkaline extraction of hemicellulose:

The experimental conditions from section 6.1.1, which resulted in the excellent recovery of hemicellulose were selected for hydrothermal assisted extraction. Briefly, the biomass was

subjected to the best incubation conditions, and after the incubation period, the mixture was heated at 121^{o}C, for 1 h, 1.5 h, and 2 h. After the entire reaction period, the hemicellulose was recovered, and recovery determined.

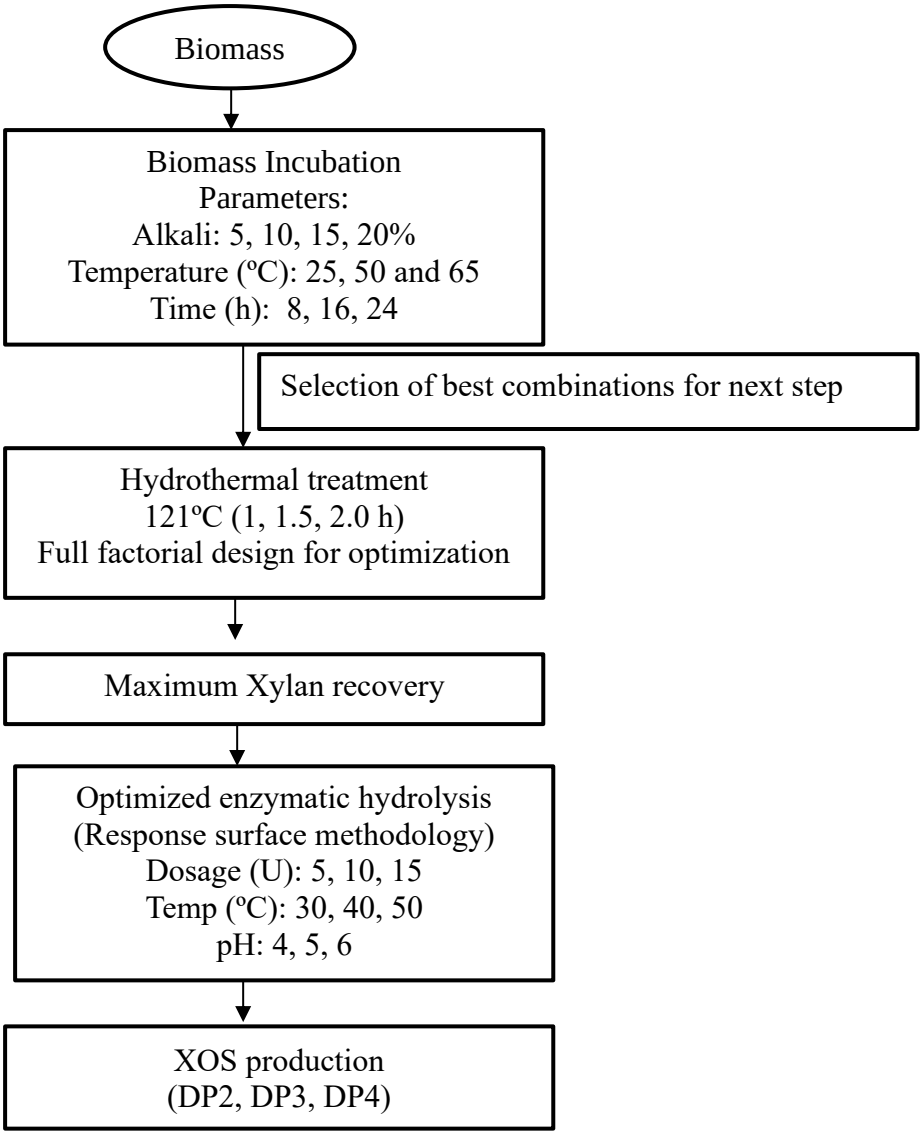

Figure 6.1: Process flow diagram for optimization and production of XOS from arecanut husk

The incubation time, alkali concentration, and the effect of hydrothermal reaction time were optimized using full factorial design study. The experiment order was randomized to minimize possible systematic errors. A full factorial design will have a total of 54

experiments (3 x 3 x 2 x 3) which would take an enormous amount of time, effort and chemicals. Hence, D-optimal design was chosen as the criteria to select the most important 25 design points from 54 points. The design allows to reduce the number of experiments without losing the representation of full factorial design. The advantage of choosing D optimal design is that it minimizes the variance in the regression coefficients of the fitted design model, thereby providing the most precise estimate of the effects (Carlson, 2001; Esbensen., et al., 1994). With the information of model specification, design points can be chosen that satisfy the D optimal criterion from a set of design points.

6.1.3. Enzymatic hydrolysis of extracted hemicellulose:

The extracted hemicellulose was hydrolyzed by using endo- 1, 4- β- xylanase M1 obtained from *Trichoderma viridea* (Megazyme, USA). The dried hemicellulose was dispersed in 50 mM citrate buffer at a concentration of 2% w/v and incubated at the desired temperature. Once the mixture reached the said temperature, the required dose of the enzyme was added to the mixture to initiate enzymatic hydrolysis. At fixed time interval of 15, 30, 45, 60, 120, 240, 480, 720 and 1440 min, an aliquot was withdrawn and kept in boiling water bath for 5 min to deactivate the enzyme. The aliquot was then filtered through a 0.2 µm cellulose nitrate membrane to obtain clear enzymatic liquor. The composition of liquor was determined using HPLC. The parameters studied include enzyme dose (5 U, 10 U, and 15 U), incubation temperature (30^{o}C, 40^{o}C and 50^{o}C), and pH (4, 5 and 6) for fixed incubation of 24 h. Response surface methodology was followed to optimize the above parameters using Box-Behnken design to achieve maximum XOS production as a response parameter. A total of 15 experiments were performed and the order of the experiments was fully randomized. The relationship between individual factors and response was calculated using the following equation:

$$Y = \beta_0 + \beta_1 X_1 + \beta_2 X_2 + \beta_3 X_3 + \beta_{11} X_1^2 + \beta_{22} X_2^2 + \beta_{33} X_3^2 + \beta_{11} X_1^2 + \beta_{12} X_1 X_2 + \beta_{23} X_2 X_3 + \beta_{13} X_1 X_3 + \beta_{123} X_1 X_2 X_3$$

where Y = predicted response (XOS yield), β_0 = constant, X_1 = temperature, X_2 = pH, X_3 = enzyme dosage, β_{12}, β_{23}, and β_{13} are interaction coefficients between the three factors; β_{11}, β_{22}, and β_{33} are quadratic coefficients.

6.2. Results and Discussion:

6.2.1. Optimization of alkali assisted hemicellulose extraction:

As can be observed from Table 6.1, the recovery of xylan was found to increase with an increase in temperature and incubation period. At 25^{o}C, the maximum recovery of xylan was 19.01 ± 0.58%, upon incubation with 20% w/v NaOH for 24 h. With an increase in the incubation temperature to 50^{o}C, we could recover 54.0 ± 2.6% of total xylan present in the arecanut husk within 24 h at 20% w/v NaOH. Further increase in incubation temperature to 65^{o}C enabled a relative recovery of 67.1 ± 1.4% in 24 h with 20% w/v NaOH. Upon analysis of data at 65^{o}C, it was observed that with 5% w/v NaOH, increasing the incubation time increases xylan recovery, to give a maximum of 42.0 ± 2.1% within 24 h which was much higher than recovered xylan at all 4 alkali levels at lower temperatures (except at 50^{o}C, 20% alkali, and 24 h incubation period). Similarly, at 10% w/v NaOH and 65^{o}C, increase in incubation time from 8 h to 24 h concomitantly increased the xylan recovery from 41.2 ± 0.8% to 51.3 ± 1.2%. Hence, it can be concluded that about 50% of available xylan in arecanut husk can be recovered under the mild condition of 65^{o}C and 10% NaOH. Further increase in relative recovery of xylan was noticed with an increase in alkali percentage (Table 6.1). Since the highest relative recovery of xylan was found at 65^{o}C, one way ANOVA analysis was performed for relative recovery obtained under incubation at 65^{o}C and means were compared for different alkali concentrations and incubation periods. It was observed that maximum recovery was achieved at 20% w/v NaOH, and 24 h incubation, which is significantly different from that obtained at 16 h incubation period. Also, the recovery at 65^{o}C, 15% w/v NaOH, 24 h, is significantly higher than that obtained at 65^{o}C, 20% NaOH and 16 h of incubation.

Table 6.1: Relative recovery of hemicellulose under studied conditions

Incubation temperature (ºC)	Alkali conc (%)	Incubation time (h)	Relative recovery (%) *
25	5	8	9.3 ± 0.1
		16	9.5 ± 0.1
		24	10.9 ± 0.2
	10	8	9.7 ± 0.3
		16	10.4 ± 0.2
		24	11.6 ± 0.2
	15	8	10.3 ± 0.7
		16	11.5 ± 0.5
		24	16.7 ± 0.7
	20	8	12.4 ± 0.3
		16	14.0 ± 0.5
		24	19.0 ± 0.6
50	5	8	10.5 ± 0.5
		16	11.9 ± 0.4
		24	14.6 ± 0.2
	10	8	16.1 ± 0.9
		16	27.1 ± 2.9
		24	30.3 ± 2.5
	15	8	20.6 ± 1.3
		16	29.7 ± 2.7
		24	36.8 ± 2.8
	20	8	29.7 ± 0.9
		16	37.5 ± 1.8
		24	54.0 ± 2.6
65	5	8	27.1 ± 0.9^{i}
		16	31.5 ± 0.4^{h}
		24	42.1 ± 2.1^{g}
	10	8	41.2 ± 0.8^{g}
		16	47.4 ± 1.4^{e}
		24	51.8 ± 1.2^{d}
	15	8	$43.3 \pm 2.1^{f,g}$
		16	$55.0 \pm 2.5^{c,d}$
		24	62.9 ± 1.1^{b}
	20	8	$46.2 \pm 0.7^{e,f}$
		16	56.5 ± 2.8^{c}
		24	67.1 ± 1.4^{a}

*values sharing different alphabets are significantly different ($p \leq 0.05$), values are expressed as means ± sd

It is interesting to note that relative recovery of xylan at 5% alkali (24 h incubation) was similar to yields obtained at 10%, 15% and 20% alkali concentration when incubated at 8h. To further improve the xylan yields in the second stage (hydrothermal treatment), alkali concentration of 5 and 10% w/v incubated at all periods were considered. Regarding ethanol use, no difference in xylan yield was observed upon precipitation of pH adjusted liquor by using 1 or 1.5 times of ice-cold ethanol (data not shown). In literature, 1.5 times of alcohol is prescribed for precipitation. However, we observed that 1:1 ratio (alcohol: alkali) could precipitate the dissolved xylan while leaving dissolved lignin in solution. Also, washing of precipitated xylan with 95% alcohol or water produced similar xylan yield. It was observed that in both cases washing the xylan thrice produced a clear supernatant. Since alkali extracted xylan is considered to be water insoluble due cleavage of uronic acid, acetyl groups (Rowley, et al., 2013), this may limit or prevent loss of xylan by dissolution.

Hence, it can be concluded that using cold ethanol in 1:1 ratio (to the alkaline solution) and washing with water produced similar results and prevented loss of dissolved xylan. Thus, the process can enable a reduction in the usage of alcohol, which in turn would help in reducing downstream processing cost.

6.2.2. Hydrothermal assisted alkali pretreatment for hemicellulose recovery:

In alkaline pretreatment, cost of alkali is one of the governing factors which may influence the economics of the process. As described in the previous chapter, heat assistance enables recovery of hemicellulose at reduced alkali concentration as compared to recovery obtained upon incubation only. Hence, hydrothermal assistance after alkali incubation was studied to reduce chemical usage. Based on results from alkaline pretreatment at different incubation temperature and period, the parameters at 65^{o}C, 5 and 10% w/v NaOH at all incubation periods (8, 16, 24 h) were further subjected to hydrothermal treatment (1, 1.5, 2 h). Analysis of variance table (ANOVA) for responses is shown in Table 6.2.

Table 6.2: Analysis of variance (ANOVA) test for experimental response for hydrothermal experiment

Source	Sum of Squares	df	Mean Square	F Value	p-value
Model	38612.1	17	2271.3	1059.9	<0.0001*
A-Hydrothermal treatment	19.7	2	9.8	4.60	0.017*
B-Alkali concentration	37393.3	1	37393.3	17449.8	<0.0001*
C-Incubation period	348.7	2	174.3	81.36	<0.0001*
AB	295.6	2	147.8	68.97	<0.0001*
AC	7.5	4	1.8	0.87	0.486
BC	523.8	2	261.9	122.2	<0.0001*
ABC	23.4	4	5.8	2.73	0.050
Residual	72.8	34	2.1		
Cor Total	38685.4	53			
R^2	0.99				
Adjusted R^2	0.98				

* p value < 0.05 means effect of treatment is significant.

According to the D-optimal design, 25 design points were chosen and analyzed for xylan yields. Statistical results of a model in which all parameters and interactions terms are significant were considered. As it can be seen from the table, the model contains seven terms namely, three main effects (A, B and C), three dual interaction terms (AB, BC, and AC) and one ternary interaction term (ABC).

The p-value of the model is considered to be significant when it falls below 0.05. The results of the model indicated that the individual terms, i.e., A, B, and C were significant according to the p-values of 0.017, <0.0001 and <0.0001, respectively, as shown in Table 6.2. Likewise, interaction terms associated with alkali concentration, i.e., AB and BC, were also significant ($p < 0.0001$). The R^2 and adjusted R^2 for this model was found to be 0.998 and 0.980, respectively, indicating a good fit between the regression model and the experimental values. Main effects and interaction effects plots are shown in Figure 2, and it is evident that alkali concentration was the most critical factor in xylan recovery. Increase in alkali concentration

significantly improved xylan recovery across all hydrothermal treatment times and incubation periods. Hydrothermal treatment time, though statistically significant, did not have a noticeable effect on xylan recovery (Figure 6.2a). In fact, hydrothermal treatment had a mixed effect on xylan recovery, as evident in interaction plots. Interaction plot between hydrothermal treatment time and incubation period clearly showed that no significant changes in xylan yields were observed (Figure 6.2b). Increase in hydrothermal treatment time increased xylan relative recovery at low alkali concentration (5%). However, the trend reversed when alkali concentration was 10% (Figure 6.3a). This can be possibly due to depolymerization of hemicellulose when exposed to higher alkali concentration and extended hydrothermal period (high severity factor). A similar trend was observed in case of alkali-incubation period interaction. Increasing incubation periods from 8 to 24 h at low alkali concentration resulted in higher xylan recoveries. At higher alkali concentration, no significant change in yields was observed when incubation periods increased from 8 to 24 h (Figure 6.3b). In the present optimization problem, there is a possibility of generating many solutions if the goal is to obtain >90% xylan recovery. However, it is important to minimize all inputs from an economics standpoint. Table 6.2 shows constraints and optimization solutions for given input parameters. Three solutions were found to be the best to achieve >94% xylan recovery. However, the most suitable solution is the one which minimizes incubation period (in first pretreatment step) and hydrothermal treatment time (Incubation period: 8h, Alkali Concentration: 10%, Hydrothermal treatment: 1 h) without compromising with the xylan recovery (Figure 6.3). The highest xylan recovery (95.4 ± 0.6%) was observed upon hydrothermal treatment (1 h) of husk incubated at 65^{o}C with 10% w/v NaOH, for 24 h.

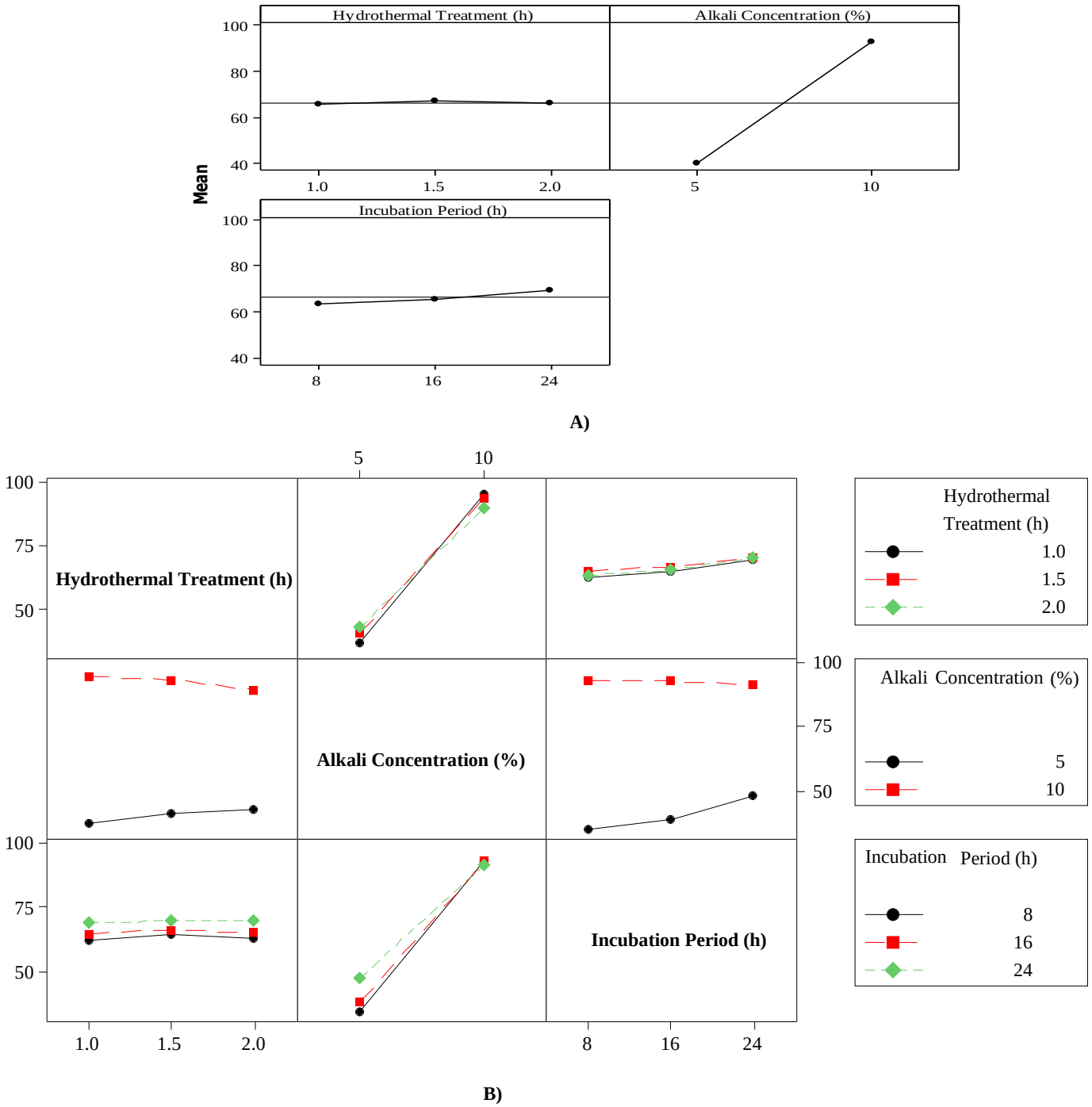

Figure 6.2: (A) Main and (B) Interaction plots for hemicellulose recovery

(a)

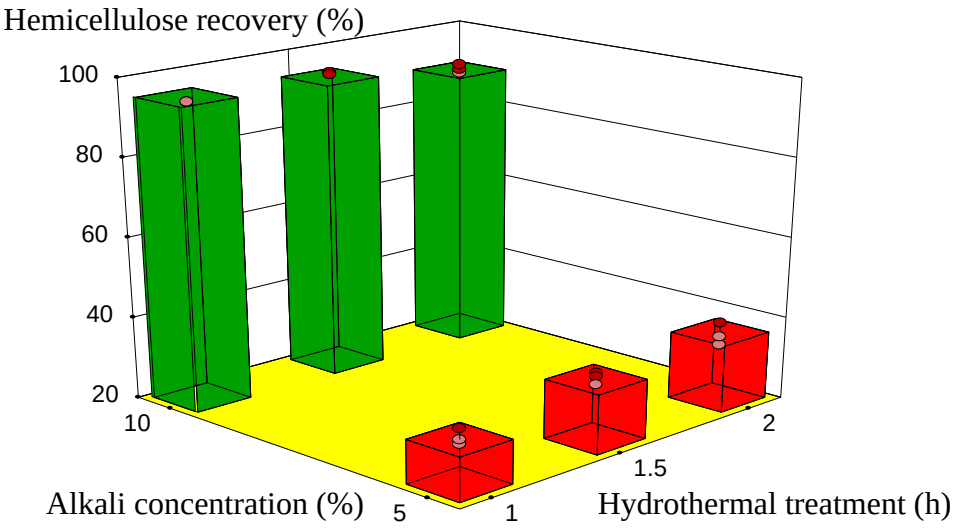
Hemicellulose recovery (%)
100
80
60
40
20
10
5
1
Alkali concentration (%)
2
1.5
Hydrothermal treatment (h)

(b)

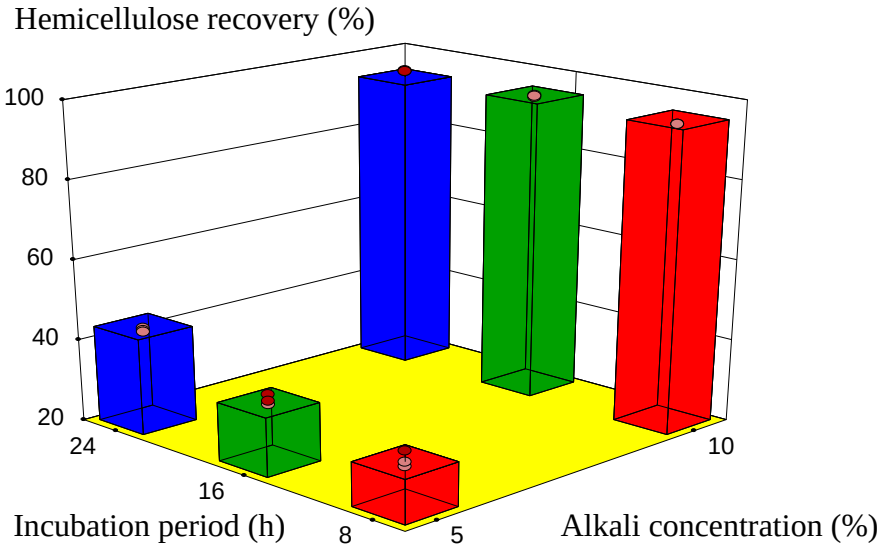
Hemicellulose recovery (%)
100
80
60
40
20
24
16
8
Incubation period (h)
10
5
Alkali concentration (%)

Figure 6.3: Relative recovery at (a) different alkali concentrations (5 and 10%) and hydrothermal treatment periods (1, 1.5 and 2h) for incubation period of 8h and (b) different alkali concentrations (5 and 10%) and incubation periods (8, 16, 24 h)

However, the recovery was not significantly different from that obtained under the same treatment, but for different incubation periods (8 and 16 h). Comparisons of means showed that there was no significant difference among xylan yields of three proposed solution schemes (Table 6.3). Thus, it can be concluded that a pretreatment process comprising of incubating arecanut husk with 10% w/v NaOH, at 65^{o}C for a period of 8 h, followed by hydrothermal treatment at 121^{o}C for an hour can help recover more than 94% of biomass xylan (Figure 6.3).

Table 6.3: Optimization constraints and solutions for maximum relative recovery of hemicellulose

Constraints			
Name	**Goal**	**Lower limit**	**Upper limit**
A: Hydrothermal treatment (h)	1	1	2
B: Alkali concentration (%)	5 to 10	5	10
C: Incubation period (h)	8	8	24
Relative recovery	Maximize	90	95.6
Optimization solutions			

Solutions	**Hydrothermal treatment (h)**	**Alkali concentration (%)**	**Incubation time (h)**	**Relative recovery (%) ***
1	1	10	24	95.4 ± 0.6^{a}
2	1	10	16	94.8 ± 0.7^{a}
3	1	10	8	94.2 ± 1.2^{a}

* Values with same alphabet in the last column are not significantly different (p> 0.05)

It is evident from the literature that efficiency of alkaline pretreatment and the consumption of alkali is governed by the amount of lignin present in the biomass (Chen, Stevens, Zhu,

Holmes, & Xu, 2013). The substrates such as corncob, pigeon pea, natural grass wherein 16% alkali was reported to extract more than 90% xylan, has low lignin content (~10%). However, in the present work, the lignin content of arecanut husk was on the higher side (~25%).

Higher lignin content presents practical difficulty in extraction of xylan. However, it has been demonstrated in this work that >90% xylan can be recovered at relatively higher lignin content by optimizing the process parameters.

6.2.3. Enzymatic hydrolysis of extracted hemicellulose:

The hemicellulose extracted using alkaline pretreatment of arecanut husk was subjected to enzymatic hydrolysis for production of XOS. The fermentability of oligosaccharides is dependent on their DP with short chain oligosaccharides having a faster rate of fermentation (Gullón et al., 2008). Among XOS, those with DP 2-6 are considered as low DP XOS (Xiao et al., 2013) and also, xylobiose is considered as prebiotic for food applications (Vázquez, et al., 2001). Hence, in this work, we consciously aimed at maximizing the production of XOS with DP range 2-4. The enzymatic hydrolysis was conducted at a different incubation temperature, pH, and enzyme dose using response surface methodology. The maximum XOS production was observed at 50^{o}C, pH , and 10 U enzyme dose (Table 6.4). At this condition, a total of 35.2 ± 1.3 XOS g/100g xylan could be produced with DP range 2-4. The hydrolysate was composed of xylobiose: 25.0 ± 1.2 g/100g xylan (~71% of total XOS), xylotriose: 9.2 ± 0.6 g/100g xylan (26.2% of XOS) and xylotetrose: 0.9 ± 0.1 g/100g xylan (2% of XOS). The yield of xylobiose is higher as compared to those reported for natural grass, 11g/ 100 g xylan (Samanta, et al., 2012). Also, as mentioned above, about 5% of lignin was present in extracted xylan. However, high conversion of xylan to XOS was observed. This indicates that the presence of the low amount of lignin in xylan has limited or no effect of hydrolysis of xylan into XOS. The concentration of xylobiose was significantly influenced by pH, temperature, and dose of the enzyme. However, none of the variables showed either increasing or decreasing trend on the concentration of xylobiose, xylotriose, and xylotetrose (Table 6.4). The ANOVA for responses for enzymatic hydrolysis of xylan is shown in Table

6.5. According to the standard Box Behnken design, statistical results of a model in which all parameters and interactions terms are significant were considered. Adjusted R^2 was used as a quality indicator to evaluate the fitness of the second order polynomial equation. Three-dimensional surface plots were employed to demonstrate the relationship and interaction between the independent variables and the response. Regression equation and response surface plots was used to obtain the optimal values of the selected variables.

Table 6.4: Experimental design layout of enzymatic hydrolysis (Box-Behnken design) and average yields of various oligomers

Run Order	Temperature (°C)	pH	Enzyme Dosage	X2[#*]	X3[#*]	X4[#*]	X1[#*]	XOS Yield[*$]
2	40	6	5	13.6	3.2	0.8	1.5	17.6 ±0.9
6	50	5	15	20.6	7.5	1.8	1.8	29.8 ±1.1
13	30	5	5	11.1	0.8	3.1	1.2	15.1 ±0.6
8	40	5	10	19.8	6.9	3.3	4.2	30.0 ±0.2
9	40	4	15	17.0	7.6	5.0	3.2	29.6 ±1.5
10	50	5	5	10.2	7.3	0.8	1.1	18.2 ±0.8
14	40	4	5	9.4	7.0	1.2	1.4	17.6 ±0.2
5	30	5	15	9.1	2.0	0.7	3.0	11.8 ±0.6
4	30	4	10	10.6	1.7	0.7	1.6	13.0 ±0.6
3	50	6	10	7.0	10.0	1.2	0.8	18.3 ±1.5
7	50	4	10	25.0	9.2	0.9	1.3	35.2 ±1.3
11	40	5	10	15.4	5.6	1.7	5.7	22.7 ±1.6
4	30	6	10	6.2	1.5	5.1	1.0	12.8 ±2
1	40	6	15	10.6	4.4	1.6	2.6	16.6 ±0.9
7	40	5	10	15.8	4.2	2.2	3.4	22.2 ±0.1

*Average yields are expressed in g/100g xylan. Xylan refers to a polymer of xylose which does not take in account any impurity. In this case, 50.9% of xylan was present in hemicellulose.
[#] X1 = Xylose, X2 = Xylobiose, X3 = Xylotriose, X4 = Xylotetrose.
[$] values are the standard error

It is clear from the table that temperature, pH, and their interaction effect played a significant role in predicting XOS production. Other model terms were found to be insignificant. Experimental data from the Box Behnken design were analyzed with RSM algorithm and fitted according to Eq. (1) As a second-order polynomial equation, including the main effects and interaction effects of each variable. The model's fit was confirmed based on two criteria,

viz. the $p < 0.05$ and the plausible agreement between the predicted and adjusted coefficient of determination.

Adjusted R^2 and Predicted R^2 were used as quality indicators to evaluate the fitness of the second order polynomial equation. Predicted R^2 is used in regression analysis to indicate how well the model predicted responses for new observations, whereas R^2 indicates how well the model fits the obtained data. Over-fitting refers to models that appear to explain the relationship between the predictor and response variables for the data set used for model calculation but fail to provide accurate predictions for new observations. Predicted R^2 is calculated by systematically removing each observation from the data set, estimating the regression equation, and determining how accurately the model predicts the removed observation. Larger values of predicted R^2 suggest models of greater predictive ability. To evaluate whether quadratic equation (2) is predicting correctly or over-fitting, the square terms were removed from the model (X_1^2, X_2^2, X_3^2) and coefficient of determination values (R^2, adjusted R^2 and predicted R^2) were recalculated. As shown in table 6.5 (b), it is apparent that reducing the number of terms reduced adjusted R^2 value, but it also showed improvement in predicted R^2 value. As shown in Table 6.5, square terms are insignificant, and by removing those terms, improved predicted R^2 signifies prevention of over-fitting of the model. It is more useful than adjusted R^2 for comparing models because it is calculated using observations not included in the model estimation.

Reduced equation with improved predicted R^2 and good adjusted R^2 is as follows-

$$Y = -184.07 + 4.76X_1 + 37.5X_2 + 3.04X_3 - 0.42X_1X_2 + 0.075X_1X_3 - 0.65X_2X_3$$

The optimal condition for this step was estimated at temp = 50°C, pH = 4 and ED =15 U. The predicted XOS concentration under the above condition was Y = 37.2 g/100 g pure xylan. To verify the prediction of the model, the optimal condition was applied to three independent replicates and the average XOS concentration obtained was 38.8 g/100g pure xylan, which is within the estimated value of the model equation. The deviations between the predicted and the observed values of the various responses were less than 10%, indicating the suitability of

the model. Time course study of oligomers (DP 2-4), xylose sugar, and acetic acid are presented in Figure 6.4. In the first 4 hours of enzymatic hydrolysis, the rate of xylotetrose production was highest among all oligomers. During this period, xylobiose production was negligible whereas xylotriose production reached to 7.7g/100g pure xylan.

Table 6.5: a) Analysis of Variance (ANOVA) test for an experimental response for enzymatic hydrolysis of hemicellulose into XOS, b) evaluation of regression coefficients of determinations

a)

Source	**DF**	**Sum of squares**	**Mean Square**	**F value**	**P value**
Regression	9	695.073	77.23	7.58	0.019*
Linear	3	456.36	152.12	14.94	0.006*
Temp	1	292.82	292.82	28.75	0.003*
pH	1	115.52	115.52	11.34	0.02*
ED	1	48.02	48.02	4.71	0.082
Square	3	67.963	22.654	2.22	0.203
Temp*Temp	1	40.413	40.413	3.97	0.103
pH*pH	1	9.551	9.551	0.94	0.377
ED*ED	1	27.083	27.083	2.66	0.164
Interaction	3	170.75	56.917	5.59	0.047*
Temp*pH	1	72.25	72.25	7.09	0.045*
Temp*ED	1	56.25	56.25	5.52	0.066
pH*ED	1	42.25	42.25	4.15	0.097
Residual Error	5	50.927	10.185		
Lack-of-Fit	3	8.26	2.753	0.13	0.935
Pure error	2	42.667	21.333		
Total	14	746			

* Values with same alphabet in the last column are not significantly different (p> 0.05)

b)

	R^2	Adjusted R^2	Predicted R^2
All quadratic terms were considered in the equation	98.30%	95.40%	79.30%
Square terms were removed from the equation	94.50%	89.60%	81.40%

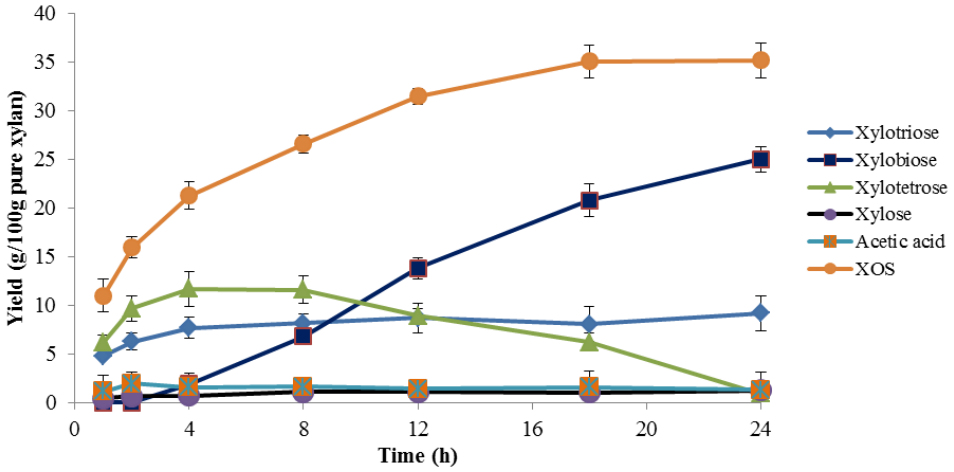

Figure 6.4: Time course study of xylose, xylobiose, xylotriose, xylotetrose, XOS and acetic acid production at optimal experimental conditions (Temperature: 50°C, pH: 4, Enzyme dosage: 10 U)

As hydrolysis continued, a marked increase in xylobiose production was observed with the concomitant reduction in xylotetrose concentration. The percentage of XOS in the hydrolysate was found to increase as the reaction time increased. This indicates that as the reaction time increases, XOS with a high degree of polymerization (including DP4) gets hydrolyzed into a lower degree of polymerization and monosaccharides. This is apparent from the Figure 6.4 that the rate of xylose monomer production increased from 0.4 to 1.3 g/100g of pure xylan and xylobiose production increased significantly from 1.9 to 25 g/100g of xylan as the reaction time increased to 24 h, respectively. However, a considerable reduction in the percentage of xylotetrose from a maximum value of 11.6 ±1.8 g/100g of xylan to 0.93±0.3 g/100g of xylan was observed. From the prebiotic potential standpoint, xylobiose and xylotriose concentration should be high in XOS, whereas xylose and acetic acid concentration should be minimum. Presence of acetic acid in XOS mixture may have an inhibitory effect on prebiotic activity and hence, requires separation. However, further study is warranted to ascertain the effect of the presence of a low quantity of acetic acid on prebiotic activity.

6.3. Conclusion:

The work described in this chapter presents a process for efficient and maximum extraction of hemicellulose and conversion into XOS using two-stage alkaline pretreatment and subsequent enzymatic hydrolysis. The importance of the two-stage process of alkaline pretreatment and hydrothermal treatment has enabled a reduction in usage of alkali to 10% for recovery of above 90% of available hemicellulose. This reduction in chemical load may be significant upon upscale or pilot level study, which will be reflected in a decrease in alkali procuring cost. Moreover, optimization of enzymatic hydrolysis enabled deciding experimental conditions for about 35.2% XOS (from 100g xylan basis). Importantly, the produced XOS liquor was rich in a low degree of polymerization containing xylobiose, xylotriose, and xylotetrose. As low DP XOS are considered prebiotic for food application, the work enables the production of food applicable product containing a narrow range of DP. Also, xylobiose was found to be the predominant oligosaccharide, representing 71% of the total XOS produced. Hence, the present chapter provides a process for efficient and maximum extraction of hemicellulose and its conversion into low DP rich XOS liquor.

Chapter 7 Production of Xylooligosaccharides from Almond Shell

This chapter describes the process for the production of XOS for almond shell using alkaline pretreatment and enzymatic hydrolysis. The chapter is divided into two parts. Part A studies the effect of particle size on the recovery of hemicellulose upon alkaline pretreatment. The shell was subjected to either ball milling or grinding in a high-speed grinder to achieve size reduction. The effect of size on hemicellulose recovery was evaluated. Part B focuses on enzymatic hydrolysis of hemicellulose into XOS. In this part, two alternatives were evaluated, such as the use of immobilized enzymes and optimization of enzyme dose: substrate concentration using response surface methodology.

The mechanical treatment (milling, grinding, ultrafine milling) has been studied in combination with chemical treatment to reduce the severity of pretreatment and reduce chemical usage. Ultrafine milling brings about structural changes including depolymerisation, deacetylation thereby allowing to reduce chemical usage. Such protocols has been evaluated for *Periplica sepium* (F. Xu et al., 2008), wheat straw (Qu et al., 2017), to obtain hemicellulose and lignin in high purity and yield. As enzyme cost adds significantly to the process economics, enzyme reutilization techniques such as immobilization has been evaluated. Various micron and sub-micron support such as resin (Lin et al., 2011), glyoxyl-agarose (Aragon, Santos, et al., 2013), chitosan-glyoxal (Milessi et al., 2016) has been utilized to immobilize xylanase to allow reuse. Alternatively, xylanase can be immobilized on magnetic nanoparticles, which can allow for easy separation of enzyme from liquor using magnet. In addition, magnetic nanoparticle provides higher surface area for enzyme attachment. Studies related to enzyme immobilization suggests that the system can be used for multiple enzymatic reaction cycle. However, in most of the studies, enzyme reusability was evaluated after enzyme reaction of 1 h, whereas, for maximum XOS production a higher reaction time is required. Thus, the reusability should be evaluated after full reaction period to better realise the suitability of enzyme immobilization.

The global production of almond without shell records about 1.4 million metric tons. The US was the highest producer contributing about 1.1 million tons, followed by the European

Union, Australia, India, Iran, Morocco, and China, among others (www.fas.usda.gov). The almond shell generated as a residue upon shelling contributes to 50% of the total produce. Thus, about 1.4 million metric tons of shell is obtained globally with limited to none value addition, representing a loss of lignocellulosic material. Almond shell has been reported to contain 72.3% carbon, 22.9% oxygen and low content of ash and hence used for the production of activated carbon (Li et al., 2018; Nabais et al., 2011). It also contains about 25-28% hemicellulose, thus can act as a potential source for the generation of xylooligosaccharides. As no reports are available wherein the effect of the particle size of the shell for hemicellulose recovery has been mentioned, in this work, it was studied.

The reduction in particle size was achieved by using a ball mill or grinding. The powder was then sieved through a mesh of different size to determine the particle size range. Each fraction was then extracted with alkali at 4 and 8% w/v sodium hydroxide and recovery determined.

7.1. Part A: alkaline pretreatment of almond shell:

7.1.1. Determination of lignocellulosic composition of almond shell:

The total extractive, moisture content, and lignocellulosic composition of the shell were determined as mentioned in chapter 4.

7.1.2. Ball milling and alkaline extraction shell hemicellulose:

The dried shells were coarsely ground to obtain particle in the range of 1-2 mm. The ground shells were then subjected to size reduction in a high energy shaker mill (SPEX SamplePrep, USA) containing six zirconium balls for a different time, and the particle size range determined. Briefly, about 10 g of material (occupying 50% of the mill volume) was loaded in the vessel along with zirconium balls and milled for a specified time. The milled samples were then passed through sieves to determine the particle size range. The material was then treated with alkali (1:10 w/v) of desired concentration at 121^{o}C for 1 h in an autoclave (Atherton cyber series, Australia). The parameters studied includes:

Ball mill time: 0.5 h, 1 h, 2 h, and 4 h

Alkali concentration: 4% and 8%

7.1.3. Grinding and alkaline extraction of shell hemicellulose:

The dried almond shell was ground in IKA M20 mill for size reduction. The ground material was sieved to collect fractions of the different size range. The mesh sizes used for fractionation were 50 µm, 75 µm, 120 µm, 500 µm, and 1000 µm. Each fraction was then extracted with alkali. Briefly, the dried shell of the desired particle size was suspended into alkali solution of desired concentration at solid: liquid ratio of 1:10. The mixture was then treated at 121^{o}C for 1 h with either 4 or 8% w/v NaOH.

7.2. Results and discussion:

7.2.1. Lignocellulosic composition of shell:

The percentage of shell from procured almonds was found to be 58.8% with about 40.9% kernel. The almond shell was characterized for determining the moisture content, total extractives, and lignocellulosic composition. The ground shell was found to contain 5.9 ± 0.1% moisture. The percentage total extractives in the ground almond shell was found to be 7.3 ± 0.1%, containing 0.08 ± 0.01% n-hexane soluble extractive; 1.0 ± 0.1% alcohol-soluble extractive and 5.5 ± 0.1% water soluble extractives. The lignocellulosic composition of the shell was 33.53 ± 2.08% cellulose, 30.7 ± 0.8% hemicellulose and 23.2 ± 1.3% of acid insoluble lignin.

7.2.2. Alkaline extraction of hemicellulose from ball milled samples:

The shell upon ball milling for a different time was subjected to sieving by attaching 500 µm 120 µm, 75 µm, 50 µm mesh size in series. The quantity of particle retained on each sieve was used to determine the percentage of that size range. The particle size range obtained can be visualized from Figure 7.1.

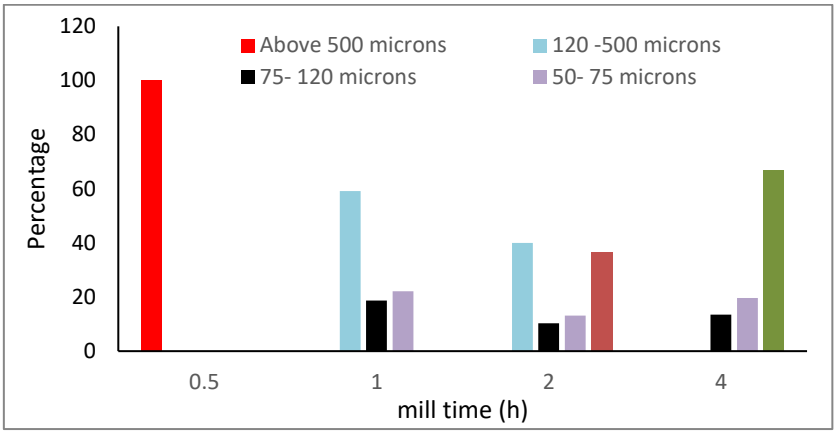

Figure 7.1: Particle size range obtained after ball milling of the almond shell for different time.

As can be observed, for ball mill time of 0.5 h, most of the particles were above 500 µm. With an increase in mill time, the particle size decreases as expected and produce a range of sizes at each mill time. Upon milling for 4 h, most of the particles were below 50 µm.

The hemicellulose from milled almond shells was extracted at two different alkali concentrations, namely 4 or 8% sodium hydroxide. As can be seen from Figure 7.2, the relative recovery of hemicellulose increases with a decrease in particle size for both alkali concentrations. At 4% NaOH, the recovery increases from 6.7 ± 1.4% to 41.8 ± 2.0%. Since at 4%, the relative recovery was found to be less than 50% of available hemicellulose, an increase in alkali concentration was evaluated to improve recovery. It was observed that by using 8% NaOH, there is a drastic increase in recovery of hemicellulose. At 8% NaOH concentration, the % relative recovery increases from 49.3 ± 2.2% to 97 ± 1.3%. Thus, the highest recovery of hemicellulose can be achieved by milling the sample to reduce particle size, preferably below 120 µm and extraction with 8% NaOH for 1 h. The higher recovery of hemicellulose at relatively lower alkali concentrations can be attributed to the modification of the surface, increase in the surface area upon milling thereby increasing accessibility and hence extraction capacity (Mayer-Laigle, Blanc, Rajaonarivony, & Rouau, 2018).

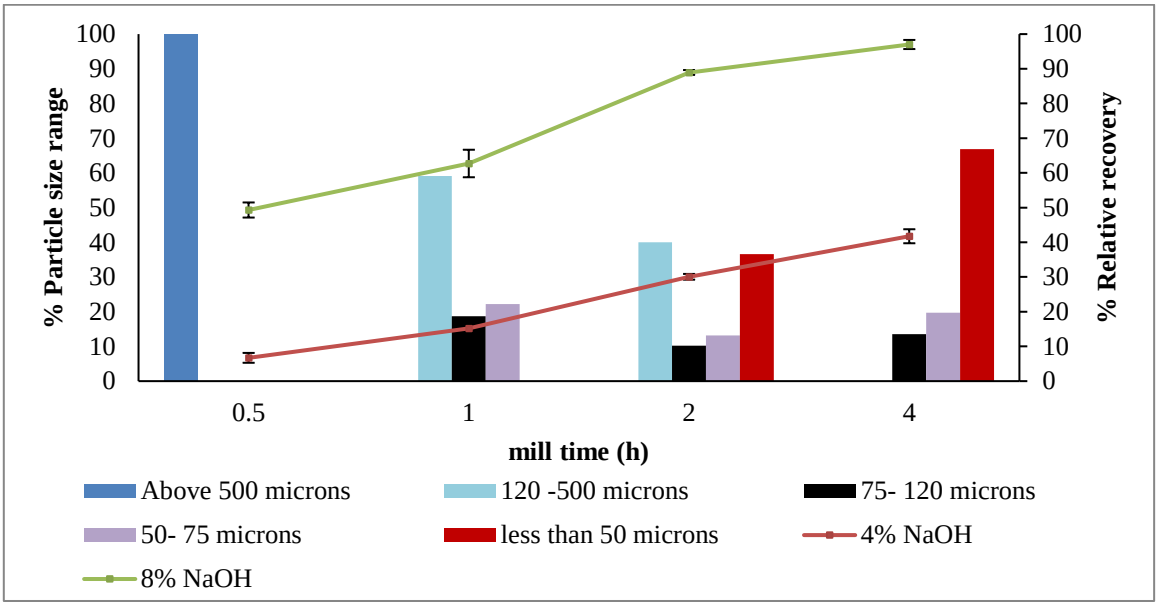

Figure 7.2: Effect of particle size on hemicellulose recovery at the studied alkali concentration

7.2.3. Alkaline extraction of hemicellulose from ground shells:

The particle size range obtained upon grinding and sieving was designation as fractions A to F. It was observed that fraction F possessed the particles above 1000 µm and particles of fraction A was lowest (less than 50 µm). The fraction B was composed of particles in the range of 50-75 µm, fraction C having a particle in the range of 75-120 µm, fraction D being comprised of 120-500 µm particles and the 500-1000 µm particle making fraction E. The relative recovery of hemicellulose from alkali pretreated almond shell is as shown in Table 7.1. As evident from the data, alkali concentration and particle size play an important role in governing the recovery of hemicellulose. At 4% NaOH concentration, maximum recovery of 35.5 ± 4.4% was observed for fraction A. However, the recovery was not significantly different ($p<0.05$) from those obtained for fraction B (35.1 ± 4.0) and fraction C (29.7 ± 1.2). The lowest recovery of 5.7 ± 2.0% was observed for fraction F, having the particle size above 1000 microns. The fraction E having particles in the range of 500-1000 microns was found to give 7.9 ± 0.1% of hemicellulose recovery.

Table 7.1: Percentage relative recovery of hemicellulose upon alkaline extraction of different fractions

Alkali concentration (%w/v)	Temperature (°C)	Time (h)	Fraction label	% Relative recovery*
4	121	1	A	35.4 ± 4.4^{h}
			B	35.0 ± 4.0^{hi}
			C	29.7 ± 1.2^{i}
			D	15.0 ± 0.3^{j}
			E	5.7 ± 2.0^{k}
			F	7.8 ± 0.1^{k}
8	121	1	A	93.5 ± 2.5^{ab}
			B	96.6 ± 3.1^{a}
			C	90.7 ± 4.9^{b}
			D	61.7 ± 0.4^{d}
			E	44.6 ± 2.8^{g}
			F	50.0 ± 4.4^{efg}

*values sharing an alphabet are not significantly different ($P<0.05$)

However, the difference was not significantly different ($p<0.05$). An increase of alkali concentration from 4% to 8%, resulted in a substantial increase in the recovery of hemicellulose. Upon treatment with 2 M NaOH, fractions A, B and C produced more than 90% of available hemicellulose. The highest recovery was observed for fraction B (96.6 ± 3.1%) as compared to fraction A (93.5 ± 2.5%) and fraction C (90.8 ± 4.9%). However, the difference was not significant ($p<0.05$). The insignificant difference in recovery in case of fraction A, B, and C for both 1 and 2 M NaOH concentration can be attributed to the fact that particle size smaller than 120 μm did not pose any mass transfer challenge. Based on the data, it can be concluded that fraction A, B, and C having particle smaller than 120 microns were able to recover maximum hemicellulose upon alkaline pretreatment with 8% NaOH.

In the present work, the usage of 8% alkali is significantly low for recovery of above 90% of available hemicellulose as compared to those reported for bagasse (Jayapal et al., 2013), corn

(Samanta, Senani, et al., 2012), grass (Samanta, Jayapal, et al., 2012b) rice husk (Khat-udomkiri et al., 2018).

7.2.4. Hemicellulose characterization:

The extracted hemicellulose upon hydrolysis with acid was found to contain 3.5-5% acid insoluble lignin, thus, producing about 95% purity hemicellulose. The monosaccharide composition was 58.6 ± 0.3% xylose and 8.5 ± 1.7% glucose with a negligible amount of arabinose. Acetic acid was found to be 2.6 ± 0.1%. As can be observed, xylose makes the abundant of almond shell hemicellulose, making xylan as major C5 polysaccharide.

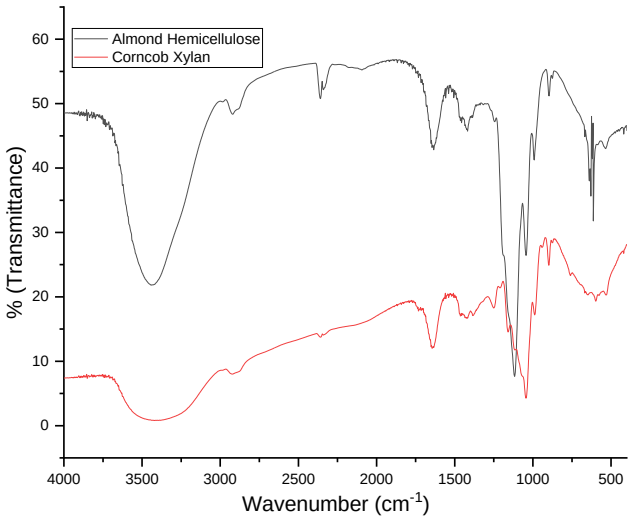

Figure 7.3: FTIR Spectra of extracted hemicellulose and its comparison with commercial corncob derived xylan

The FTIR spectra of extracted hemicellulose were similar to that of corncob xylan (Figure 7.3). However, a slight shift in peak values was observed, which may be attributed to the difference between branches and the presence of associated lignin. The FTIR spectra show peaks at 2920, 1417, 1117, 1043 cm^{-1} which are attributed to xylan molecules. The peak

observed at 896 cm^{-1} is characteristic of β- glycosidic linkages between sugar (Buslov et al., 2010).

7.3. Part B: Production of xylooligosaccharides:

7.3.1. Immobilized enzyme assisted XOS production:

7.3.1.1. Synthesis and activation of magnetic nanoparticles:

A $FeCl_3$ and $FeSO_4$ based magnetic nanoparticles (MNP) were prepared under basic conditions as previously reported and characterized (Talekar et al., 2017). Briefly, $FeSO_4.7H_2O$ and $FeCl_3.6H_2O$ (1:2 molar ratio of Fe^{2+} and Fe^{3+}) were heated at 90°C, in 25ml NaOH (5M). The black sediment was washed thoroughly with distilled water until neutral and dried under vacuum. The activation of prepared MNP using APTES was as reported by (Liu et al., 2013). The schematic for activation and immobilization of enzyme onto magnetic support is as depicted in Figure 7.4. Briefly, MNP (0.5g) was dispersed in 1:1 ethanol-water mixture (100 ml) followed by addition of APTES (2 ml) and incubated at 60°C for 4 h. The activated amino coated MNP (APTES-MNP) were recovered by magnetic decantation and washed with the ethanol-water mixture and dried overnight at 50°C.

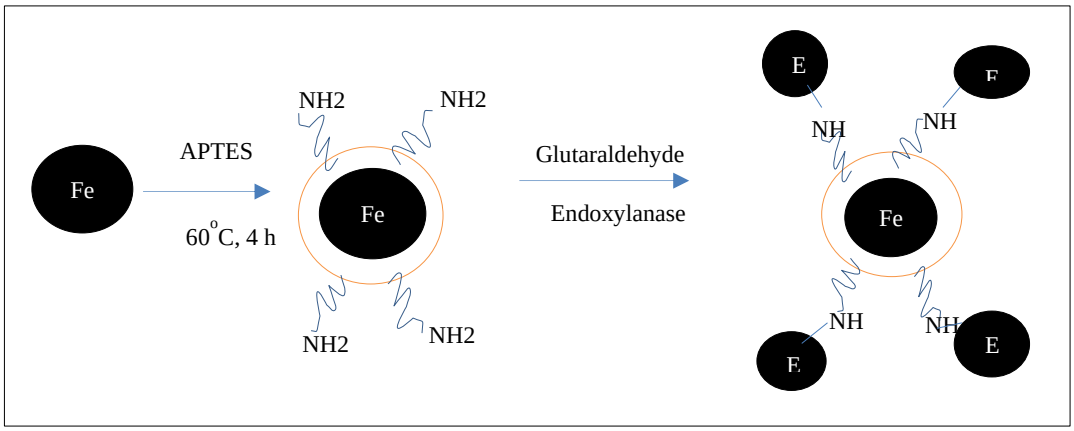

Figure 7.4: Pictorial Representation for activation of magnetic nanoparticles using APTES and enzyme immobilization

7.3.1.2. Immobilization of endoxylanase:

The endoxylanase from *Thermomcyes lanuginosus* (X2753, expressed in *Aspergillus oryzae*, Merck, USA) was immobilized onto the APTES-MNP using glutaraldehyde (GDA) induced covalent binding. The MNP (10 mg) was mixed with 1 ml of enzyme solution (20mg/ml in sodium acetate buffer, pH 5.8) containing GDA at a different molar concentration (5, 10, 25, 50, 75 and 100 mM). The mixture was incubated at 30^{o}C, 150 rpm for 5 h to activate the support by offering aldehyde groups and linkage of the enzyme. The prepared enzyme coated MNP (E-MNP) was then separated from the mixture by decantation using magnet to capture E-MNP. The product was then washed thrice with the buffer to remove free enzyme. The activity of the immobilized system was evaluated by measuring the amount of reducing sugar (xylose equivalent) liberated from xylan using 3,5- dinitrosalicylic acid (DNS) reagent. The activity was compared to that of the free enzyme under optimal conditions. Briefly, 1 ml of buffer (pH 5.8, 50mM) containing 1mg/ml xylan was incubated at 50^{o}C, and then known amount of free enzyme or immobilized enzyme was added to the reaction mixture and reaction continued for 60 min. After completion of the reaction, the released sugar concentration was determined using DNS assay.

7.3.1.3. Characterization of immobilized enzyme:

The activity and stability of the immobilized enzyme were measured under different pH and temperature conditions and compared with the free enzyme. The effect of pH on the activity was evaluated at 6 different pH conditions (3, 4, 5, 6, 7, and 8) at 50^{o}C. The activity and stability of the immobilized system were evaluated at 5 temperature conditions, namely, 20, 30, 40, 50, and 60^{o}C. The storage stability of the immobilized system in dry form was evaluated by measuring the activity after storage at 4^{o}C for a week. The Michaelis Menten constant (Km) and the maximum reaction velocity (Vmax) of the free enzyme and immobilized enzyme were determined at different substrate concentration and the same enzyme dose. The initial reaction rates at the different concentration (2-12 mg/ml) were measured and used to obtain the reaction kinetics by non-linear regression fitting in

GraphPad Prism 8 software. The morphology of MNP, APTES-MNP, and E-MNP was determined using FEG-SEM (JSM-7600F) after iridium coating. The FTIR spectra were recorded using 3000 Hyperion Microscope with Vertex 8 FTIR system (Bruker, Germany) to detect the presence of characteristic functional group and ascertain attachment of enzyme onto the magnetic support. The XRD data was obtained by scanning the samples in 2-theta ranging 10-70^{o} using Equinox 100 X-Ray Diffractometer (Thermo Fischer, USA).

7.3.1.4. Production of Xylooligosaccharides:

The extracted almond shell hemicellulose was used for producing xylooligosaccharides using free enzyme and immobilized enzyme. Briefly, hemicellulose (2%) in 50mM acetate buffer (pH 5.8) was incubated with a suitable dose of free enzyme and equivalent immobilized enzyme at desired temperatures. Aliquots were periodically withdrawn and kept in boiling water for 5 min to deactivate the enzyme. The hydrolysis was performed for 48 h, based on preliminary and previous experience where 48 h was found to be optimal for maximum XOS production, above which no significant increase in yield was seen. The samples were analyzed by HPLC for determining the content of xylobiose, xylotriose, and monosaccharides.

7.4. Results and Discussion:

7.4.1. Synthesis of enzyme coated magnetic nanoparticles:

In this work, the magnetic nanoparticles were activated by (3-aminopropyl) trimethoxysilane (APTES) to obtain aminopropyl- functionalized MNPs. The addition of glutaraldehyde as a crosslinker for enzyme and activated MNP was studied at different concentrations (5, 10, 25, 50, 75 and 100 mM). The activity obtained from free enzyme under the optimal conditions (50^{o}C, pH 5.8) was considered 100% and used as a basis for comparison of the activity of the immobilized enzyme (Figure 7.5).

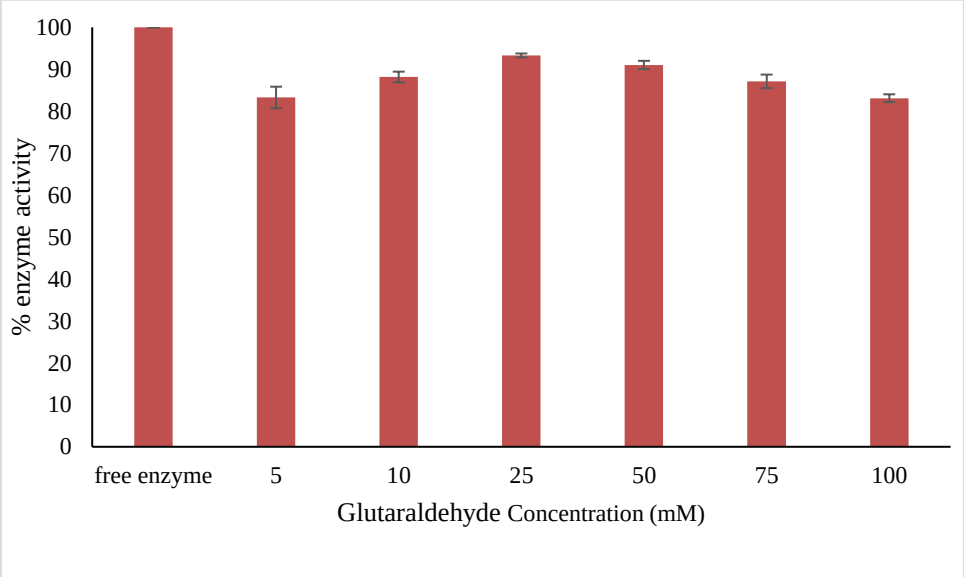

Figure 7.5: Xylanase activity upon immobilization on magnetic nanoparticles using different concentration of glutaraldehyde

It was observed that enzyme activity increases with an increase in glutaraldehyde concentration up to a certain level after which the activity decreases. From Figure 7.5, it can be observed that optimal glutaraldehyde concentration to recover maximum activity was 25 mM, at which about 93.3% of enzyme activity could be recovered when compared to free enzyme. An increase of GDA concentration to 50 mM gives enzyme coated magnetic nanoparticles with 91.0 ± 1.0% of free enzyme activity. At the highest GDA concentration of 100 mM used in this study, the enzyme activity of 83.1 ± 1.0% could be obtained. Hence, based on the above data, a glutaraldehyde concentration of 25 mM was found to be optimal for producing more than 90% of enzyme activity in comparison to free enzyme.

7.4.2. Characterization of immobilized xylanase:

7.4.2.1. Effect of pH on enzyme activity:

The activity of the enzyme is dependent on the pH conditions and is affected by the variation of pH of the reaction medium. An equivalent E-MNP was weighed based on the activity, so that enzyme dose is the same as that of free enzyme. The activity of xylanase immobilized on

magnetic nanoparticles was evaluated under different pH conditions ranging from 3-8 while keeping the temperature constant at 50^{o}C and compared with free xylanase (Figure 7.6a). The pH above 8 was not studied as sugars are susceptible to degradation at alkaline pH.

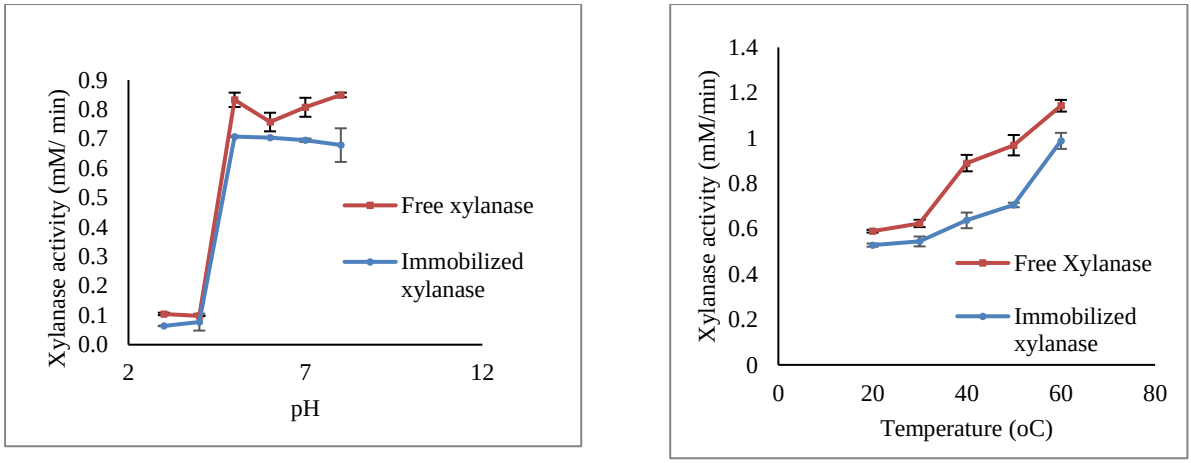

(a) (b)

Figure 7.6: Characterisation of immobilized enzyme, a) effect of pH on the activity of free and immobilized xylanase, b) effect of Temperature on the activity of free and immobilized xylanases

As evident, both free and immobilized xylanase show similar pH-dependent activity profile. At low pH values (3 and 4) the activity of the enzyme was seen to be severely affected, showing less than 10% of the enzyme activity. However, both the free and immobilized enzyme shows good activity at a pH range of 5-8. The activity of the immobilized enzyme was also higher as compared to that to the free enzyme at pH 7 and 8. This can be attributed to the stabilization of enzyme active groups upon linkage to magnetic support (Xu et al., 2014).

The xylanase activity was found to be retained upon immobilization onto magnetic nanoparticles, indicating that the adsorption did not alter the physical nature of the enzyme. Along with pH, the temperature is another critical variable governing the activity and stability of the enzyme. Hence, immobilized xylanase activity was evaluated in the temperature range

of 20-60^{o}C and compared with free xylanase. As can be observed in Figure 7.6b, both free and immobilized enzyme showed similar trends in the given temperature range. In general, an increase in temperature increased xylanase activity for both enzyme forms. However, the activity of both enzymes varied at a constant temperature. For example, at lower temperatures (20 and 30^{o}C), immobilized enzyme activity was in the range of 85-89% of that of free enzyme. With an increase in temperature to 40 and 50^{o}C, the immobilized enzyme's activity reduced as compared to the free enzyme (25% reduction). However, a further increase in temperature to 60^{o}C enabled the immobilized system to exhibit improved activity. Improved stability at higher temperature is characteristic of an immobilized system which is observed in this work. As described in the later section (Figure 7), it was observed that upon XOS production, nearly similar yields were obtained at 50 and 60^{o}C. Also, a further increase in temperature may have improved enzyme activity of E-MNP for shorter reaction time, but it will also increase energy demand, and hence, higher reaction temperature was not evaluated. An improved pH and temperature stability and retention of 80% activity were reported for *Aspergillus niger* xylanase A immobilized on Fe_3O_4 coated chitosan MNP using layer by layer assembly (Liu et al., 2014).

7.4.2.2. Reaction Kinetics:

The values for Km and Vmax are shown in Table 7.2. The free enzyme and the immobilized enzyme show Michaelis-Menten behavior at the substrate concentration studied in this work. The Km value of immobilized enzyme (5.1) is slightly higher as compared to the free enzyme (4.4). As Km represents the affinity between enzyme and substrate, it can be concluded that immobilized enzyme has slightly reduced affinity as compared to free enzyme. This may be ascribed to the rigidity of enzyme and hindrance in mass transfer between bound enzyme and substrate.

Table 7.2: Kinetic parameter (Km and Vmax) of free and immobilized enzyme

Enzyme form	Km	Vmax (mg/min)
Free enzyme	4.4	1018
Immobilized enzyme	5.1	1027

Moreover, the Vmax of the free enzyme (1027 mg/min) and immobilized enzyme (1018 mg/min) were similar, which indicates that both forms of the enzyme can work at similar reaction rate. It can also be observed that at low substrate concentration, the reaction rate doubles when the concentration is doubled, however further increase in concentration (above 6mg/ml) the reaction reaches a maximum (Figure 7.7).

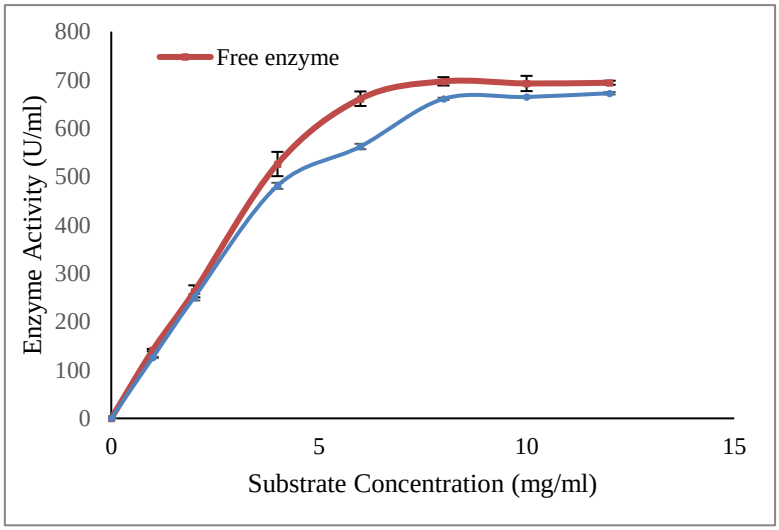

Figure 7.7: Enzymatic activity of free enzyme and immobilized enzyme at different substrate concentration, pH 5.8 and 50^{o}C

7.4.2.3. Storage Stability of immobilized enzyme:

The prepared immobilized xylanase was evaluated for its stability at 4^{o}C by storing the system in dry form. The residual activity was then measured under optimal conditions (50^{o}C, pH 5.8) every 7 days for a month. The residual activity observed upon storage was termed as % retained enzymatic activity and was compared to the original activity, as shown in Figure 7.8 As seen, the residual activity decreased with storage for a month. The residual activity upon storage for 7 days was 90.1 ± 3.2% of the initial, which decreases to 78.1 ± 0.1% at 30

days. Thus, though there is a decrease in activity, about 80% of activity can be observed upon storage until 30 days in dry form. As the free enzyme is supplied in powder form, the activity upon storage was not determined for the same.

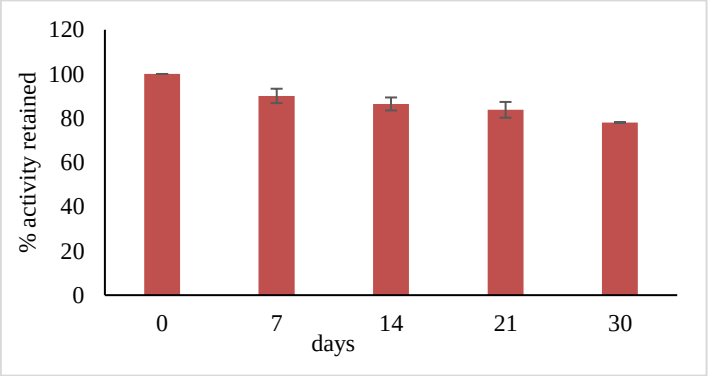

Figure 7.8: Percentage residual activity after storage for 30 days at 4^{o}C

7.4.2.3. Morphology and functional group analysis:

The FTIR spectra of MNP, APTES-MNP, and E-MNP is, as shown in Figure 7.9. In all the spectra, the peak can be observed in the region of 560-580 cm^{-1}, which can be ascribed to the Fe-O stretching of Fe_3O_4, thus indicating the presence of magnetic core (Silva et al., 2013). In case of E-MNP however, additional bonds were seen around 560-580 cm^{-1} the reason of which is not apparent. The presence of an absorption band at 3400 cm^{-1} is due to OH stretching and can be observed in all spectra. The band is more pronounced in case of E-MNP due to the presence of a higher concentration of OH groups in endoxylanase as compared to MNP or APTES-MNP. The bands at around 1018-1033 cm^{-1} can be because of stretching vibrations of Fe-O-Si bonds (Y. Liu et al., 2013), thereby indicating amino attachment onto magnetic support. Also, the bands at 2922 cm^{-1} and 1300-1600 cm^{-1} can be due to absorption by C-H and N-H bonds present in endoxylanase (Roberge et al., 2003). From the obtained data, it is inferred that amino groups were linked to the magnetic core upon APTES treatment, which enabled immobilization of endoxylanase.

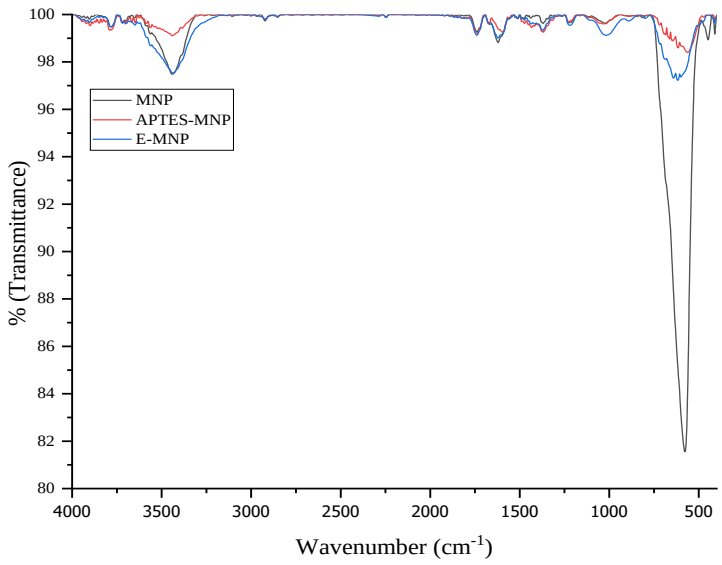

Figure 7.9: FTIR spectra of MNP, APTES-MNP and E-MNP showing characteristic peaks

The morphology of MNP, APTES-MNP, and E-MNP was visualized using Field Emission Gun-Scanning Electron Microscopes (FEG-SEM) and shown in Figure 7.10. The MNP was observed to be quasi-spherical. Due to sub-micron size and magnetic properties of iron oxide, the particles were mostly observed as aggregates. As can be observed from the figure, the APTES coating and enzyme linkage on the support did not produce a change in the structure of nanoparticles. However, in the case of E-MNP, an increased agglomeration of particles could be observed. Therefore, it is suggested that the E-MNP should be sonicated before use to break the agglomerate for efficient contact between enzyme and substrate.

The XRD analysis shows peaks at 30.3º, 35.7º, 43.4º, 57.4º, and 63º 2-theta degrees (Figure 7.11). From literature, it is suggested that the peaks represent the crystal structure of magnetite. The planes which have been ascribed to the aforementioned 2-theta values correspond to (220), (311), (400), (511) and (440) (Bumb et al., 2008). The XRD pattern of APTES-MNP and E-MNP also shows the presence of 2-theta degrees similar to uncoated MNP, thereby suggesting no difference in the structure of the magnetic core during activation

and enzyme linkage. Thus, the data from FTIR and XRD confirms the presence of the magnetic center and enzyme cross-linking on to the support.

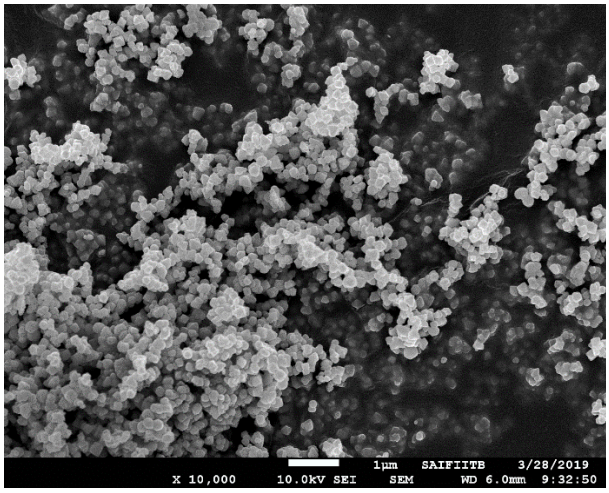

(a)

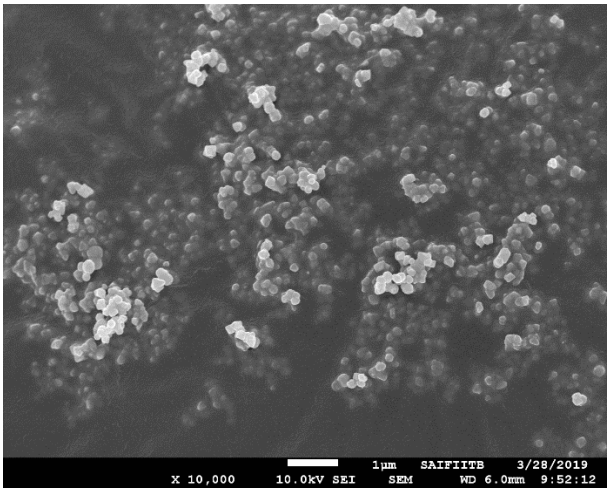

(b)

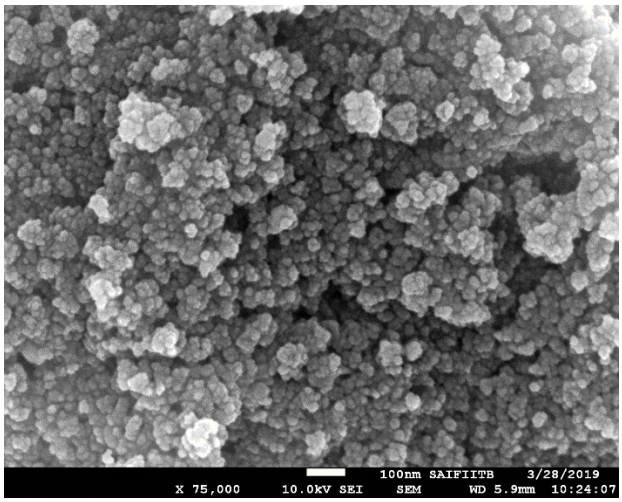

(c)

Figure 7.10: FEG-SEM images of (a) MNP, (b) APTES-MNP, (c) E-MNP

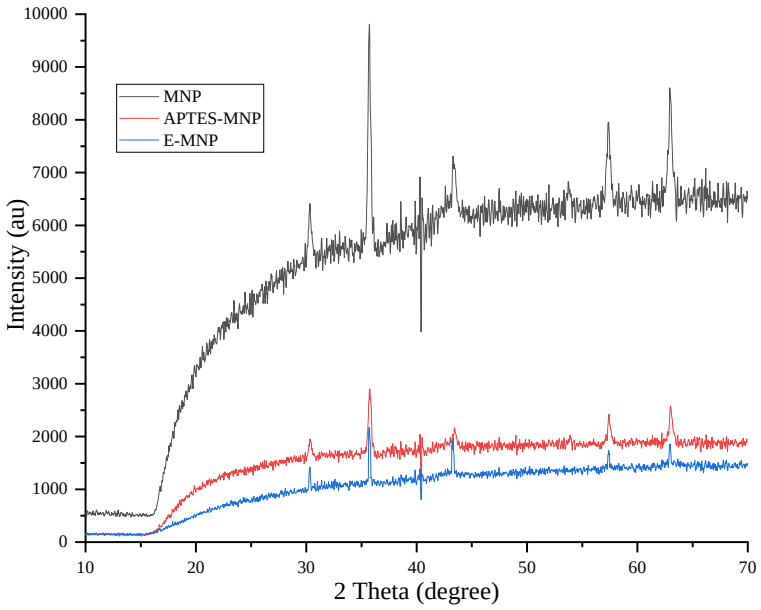

Figure 7.11: XRD pattern of iron oxide MNP, APTES-MNP, and E-MNP

7.4.2.4. Enzymatic production of Xylooligosaccharides:

The free and immobilized enzyme was used for hydrolysis of extracted hemicellulose for production of XOS. Figure 7.9a represents the yield of XOS (sum of xylobiose and xylotriose) produced at 50^{o}C. As evident, the yields of XOS increased with time and reached a maximum of 34.7 ± 1.8 g/100g of hemicellulose for the free enzyme.

In comparison, the immobilized system could produce 23.4 ± 2.8 g/100, amounting to 67.4% of free enzyme. For both the cases, xylobiose was predominant, representing 26.4 ± 2.9 g/100g for free enzyme and 22.6 ± 2.8g/100g for the immobilized system, respectively. For free enzyme, the amount of xylotriose was 8.3 ± 0.3g/100g as compared to 1.1 ± 0.1 g/100g

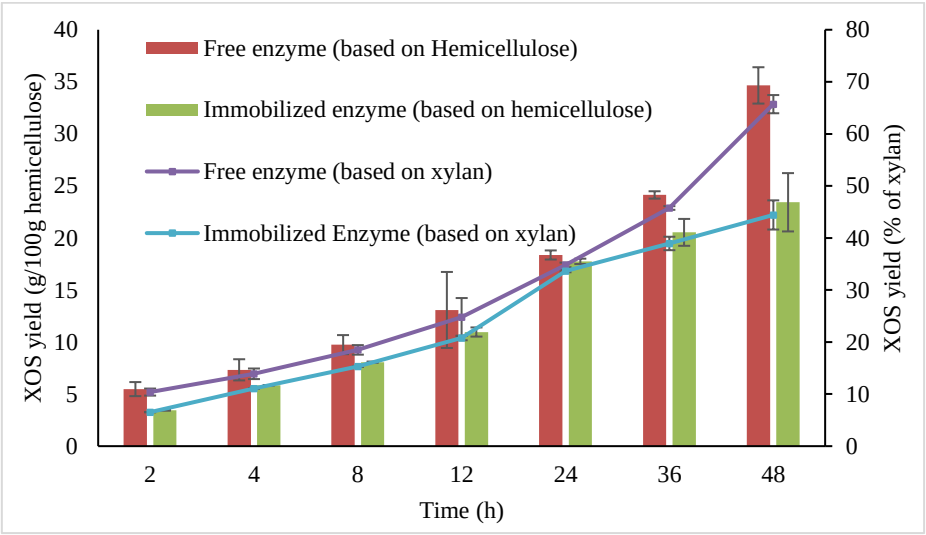

(a)

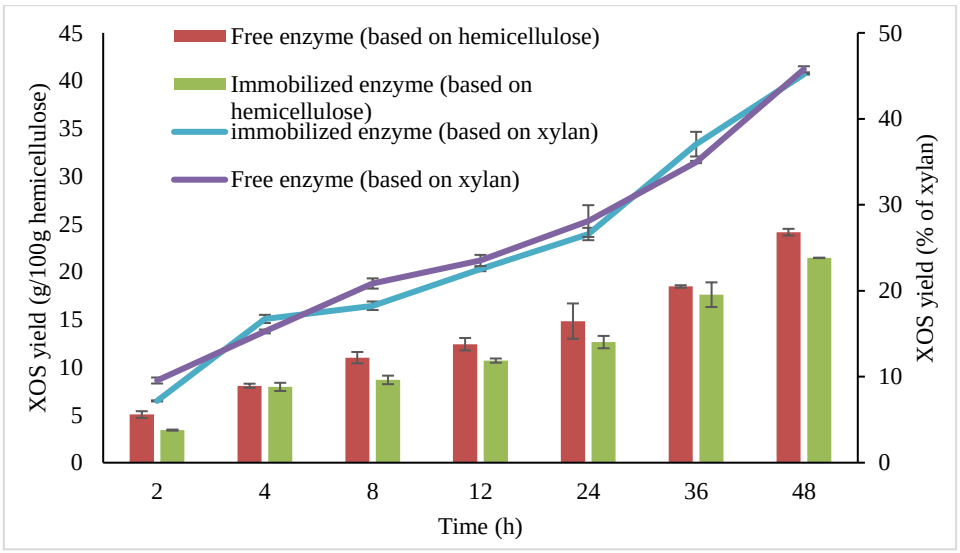

(b)

Figure 7.12: Comparison of XOS produced by free xylanase and xylanase immobilized on magnetic nanoparticles at: a) 50oC and b) 60oC. The bar graph represents XOS yield concerning hemicellulose, and line graph denotes XOS yield concerning xylan

for the immobilized system. The lower yield of XOS and variation in XOS product of the immobilized system as compared to the free enzyme may be due to the hindrance of mass transfer and contact of hemicellulose particle with the solid immobilized system. The

percentage conversion of xylan into XOS was found to be 65.7% and 44.4% for free and immobilized enzymes, respectively. The xylanase from *Thermomyces lanuginosus* is reported to produce predominantly xylobiose (Singh S et al, 2003), which is evident in this work. As observed in Figure 7.9b, the activity of the immobilized enzyme is closer to that of the free enzyme at 60^{o}C, also, the xylanase from *T. lanuginosus* is thought to be effective at higher temperatures (50-80^{o}C). Hence, enzymatic hydrolysis was also studied at 60^{o}C. As evident from Figure 7.9b, at the end of 48 h, the amount of XOS produced was 24.1 ± 0.4 g/100g, which is less as compared to that produced at 50^{o}C. Interestingly, the amount of XOS produced by the immobilized system was 21.4± 0.1 g/100g, which represents 88.9% of free enzyme XOS yield. In both cases, the overall conversion of xylan into XOS was found to be 45%. The conversion level was found to be similar at 50 and 60^{o}C for an immobilized enzyme which may be due to improved thermal stability imparted by immobilization support. However, a decrease in xylan conversion is seen for free enzyme due to possible thermal instability for a longer period. Thus, immobilization seems to be a good approach for enzymatic hydrolysis wherein the longer residence time is required.

Xylanase obtained from *Penicillium occitanis* was immobilized on nickel-chelate Eupergit C and used for the production of XOS (Driss et al., 2014). The author reported XOS yields of 21.3% and 34.2% w/w from the immobilized and free enzyme. However, the paper does not discuss the reusability of the immobilized enzyme upon 24 h cycle. Similarly, for endoxylanase immobilized on alginate beads, the author reports reusability for seven cycles while retaining above 62% of initial activity (Rajagopalan, Shanmugavelu, & Yang, 2016).

However, reusability data upon 24 h cycle, which was necessary to obtain maximum XOS in the study is not presented. The immobilized xylanase was used for the production of XOS from Meranti wood sawdust, wherein at the end of 60 h, 0.36 mg/ml XOS was obtained. The author reported that upon reuse of immobilized enzyme for next cycle, the XOS yield was 70% of the initial cycle, which further decreases to about 50% at the end of the third cycle (Sukri & Mimi Sakinah, 2018). In the author's view, limited to none literature is available

wherein the immobilized enzyme has been evaluated for reusability upon full hydrolysis period necessary to maximize XOS yield. The suitability and applicability of such a system lie in its ability to retain activity upon use for full reaction time. Thus, in this work, the immobilized enzyme was evaluated for its reusability using fresh substrate for full reaction period (48 h). Figure 7.10 represents results of recycling of enzyme for 48 h of the enzymatic reaction. As evident, there is a significant decrease in the XOS yield upon reuse of the immobilized enzyme. Upon cycle two the XOS yield was 53.7 ± 1.0 % of cycle 1 and further decreases to 41.6 ± 4.9% at cycle 3.

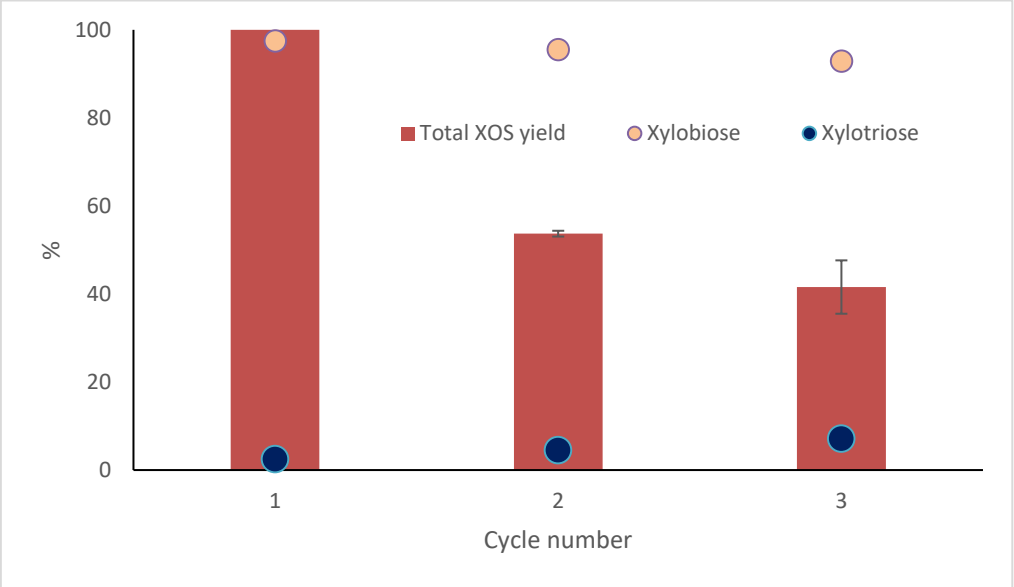

Figure 7.13: XOS yields produced after three successive cycles of enzymatic hydrolysis using same immobilized enzyme on fresh substrate

As the enzyme is noted to maximize xylobiose concentration, it was predominant oligosaccharide in each cycle. The % xylobiose of total XOS in each cycle was found to be a range of 92-98, while that of xylotriose was 2.5-7%. The observed results indicate that though immobilized enzyme allows for re-use of the enzyme, the yield of XOS decreases with several cycles. A possible intervention to obtain similar yield in the consecutive cycle can be supplementation with a fresh immobilized enzyme to make up for the decrease in the

enzyme active over longer reaction time. The cost of the enzyme is important variable contributing to the overall cost of production of XOS and other lignocellulosic-based biomolecules (Klein-Marcuschamer et al. 2012; Chang et al., 2017), thus, supplementation of a fraction of enzyme dose may have a significant impact on the cost of the process in a commercial setting.

This approach, however, warrants a thorough techno-economic analysis to evaluate the feasibility and benefit of using the immobilized system over free enzyme. The concentration of monosaccharides (xylose, glucose) released upon hemicellulose hydrolysis was found to be very low for both free and immobilized enzyme at both temperatures. The concentration of xylose for the free enzyme was found to be in the range of 0.5-3.6% and 0.3-1.9% at 50^{o}C and 60^{o}C.

Part C: RSM based optimization of enzyme dose and substrate concentration

7.5. Optimization of enzymatic hydrolysis:

The enzymatic hydrolysis of almond shell extracted hemicellulose was performed using endoxylanase from *Thermomyces lanuginosus* (Sigma, USA) for production of xylooligosaccharides. Briefly, the extracted hemicellulose at desired dose was added to 50 mM sodium acetate buffer (pH 5.5) and incubated at 50^{o}C with the desired dose of the enzyme. At periodic time interval (2, 4, 8, 12, 24, 32 and 48 h) an aliquot of liquor was withdrawn and heated in boiling water for 5 min to inactivate the enzyme. The aliquot was then filtered and diluted appropriately for analysis of produced xylooligosaccharides and neutral sugar by HPLC.

Table 7.3: Central composite design generated for variables, predicated and experimental values of XOS yield

Run	Factors		XOS yield	
	Enzyme dose (U) (X1)	Substrate concentration (%) (X2)	Predicted value (%)	Experimental value (%)
1	10	1.17	39.8	40.6 ± 0.1
2	10	4	27.6	28.2 ± 0.6
3	15	2	36.9	36.2 ± 1.9
4	10	4	27.8	27.2 ± 0.1
5	5	6	20.0	20.4 ± 0.9
6	10	4	27.2	26.9 ± 0.2
7	2.9	4	21.6	21.5 ± 1.4
8	10	4	28.1	27.6 ± 0.4
9	10	4	27.9	28.1 ± 0.2
10	15	6	25.5	25.6 ± 0.1
11	5	2	31.6	31.2 ± 1.6
12	17.07	4	29.2	29.6 ± 1.9
13	10	6.8	23.5	23.2 ± 0.4

The parameters studied for the production of oligosaccharides include enzyme concentration (5, 10, and 15 U) and substrate concentration (2%, 4%, and 6%). The parameters were optimized using response surface methodology employing central composite design (CCD) having 2 factors and 3 levels. The enzyme dose and substrate concentration were considered as an independent factor and their effect evaluated on XOS yield considered as the response variable. The experimental design is as depicted in Table 7.3. A total of 13 randomized experiments were performed, and the relation between response and factor was estimated using the following equation:

$$Y = \beta_0 + \beta_1 X_1 + \beta_2 X_2 + \beta_2 X_1^2 + \beta_3 X_2^2 + \beta_4 X_1 X_2$$

where Y is the response as XOS yield, β_0 is constant, X_1 represents enzyme dose, X2 represents substrate concentration, β_1 β_2, β_2, β_3, and β_4 are interaction constants.

9.6. Results: Optimization of enzymatic hydrolysis:

The extracted hemicellulose was enzymatically hydrolyzed using endoxylanase from *Thermomyces lanuginosus* to produce xylooligosaccharides. The central composite design approach was used to optimize the enzyme and substrate concentration. The regression equation for the production of XOS can be depicted by the following:

$$Y = 37.7097 + 1.39636\ X_1 - 7.03740\ X_2 - 0.0436171\ X_1^2 + 0.515128\ X_2^2 + 0.00391422\ X_1X_2$$

The observed predicted and adjusted R^2 value for the equation was observed to be 0.98 and 0.95 and 0.97, respectively. The observed high values for R^2 indicates a good agreement between the observed XOS yield, and the model generated predicted yield. The analysis of variance for the XOS yield is as shown in Table 7.4. It can be observed that p-value for single variable including enzyme dose and substrate concentration is below 0.05, thereby indicating a significant effect of both on the XOS yield. As observed the p-value for interaction term was 0.9, which may suggest an insignificant effect of the interaction between enzyme dose and substrate concentration. The contour plot and 3D surface plot were generated using the Minitab Statistical Software to explore the potential interaction between the variables and XOS yield. As observed from Figure 7.9A and B, to obtain high XOS yield, a low substrate concentration is favorable. The maximum XOS yield can be obtained when the enzyme dose above 10 U is used at lower substrate concentration (2% or below). An increase in substrate concentration tends to lower the XOS production, which may be due to increased viscosity of the medium, limiting the mass transfer and depletion of water molecules. However, a yield between 25-30 g can be obtained by using 4% substrate with low enzyme dose of 5 U but preferably 10 U.

Table 7.4: Analysis of Variance (ANOVA) test for the experimental XOS yield obtained from hemicellulose hydrolysis

Source	DF	Sum of squares	Mean square	F value	P Value
Regression	5	731.554	146.311	154.80	0.000
Linear	2	646.323	323.116	341.91	0.000
Enzyme dose	1	116.501	116.501	123.26	0.000
Substrate concentration	1	529.822	529.822	560.55	0.000
Square	2	85.219	42.609	45.08	0.000
Enzyme dose*enzyme dose	1	26.148	16.543	17.50	0.000
Substrate concentration*substrate concentration	1	59.071	59.071	62.50	0.000
Interaction	1	0.012	0.012	0.01	0.910
Enzyme dose*substrate concentration	1	0.012	0.012	0.01	0.910
Residual error	20	18.903	0.945		
Lack of fit	3	3.334	1.111	1.21	0.335
Pure error	17	15.569	0.916		
Total	25	750.457			

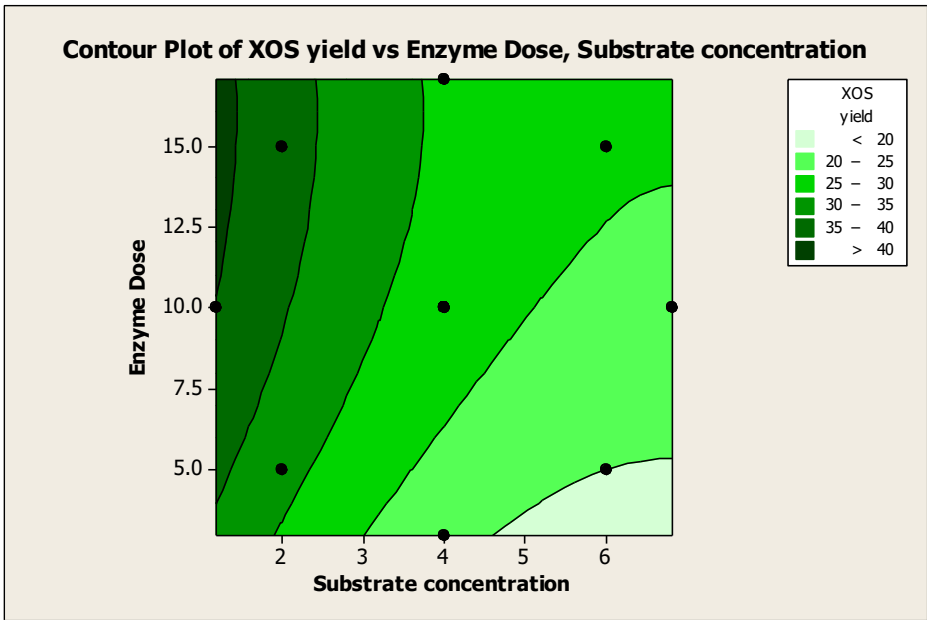
Contour Plot of XOS yield vs Enzyme Dose, Substrate concentration
Enzyme Dose
15.0
12.5
10.0
7.5
5.0
2
3
4
5
6
Substrate concentration
XOS yield
< 20
20 – 25
25 – 30
30 – 35
35 – 40
> 40

A)

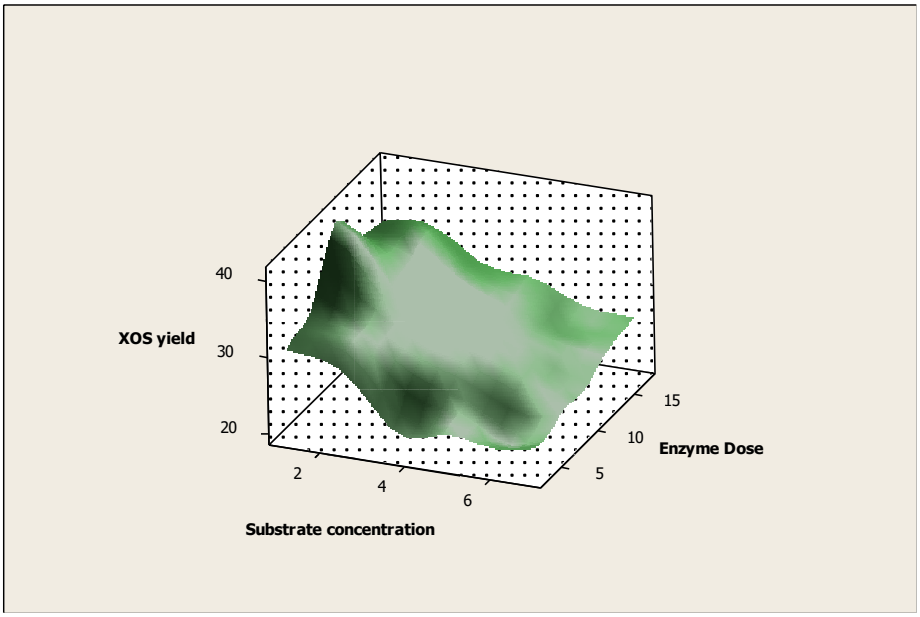
XOS yield
40
30
20
2
4
6
Substrate concentration
5
10
15
Enzyme Dose

B)

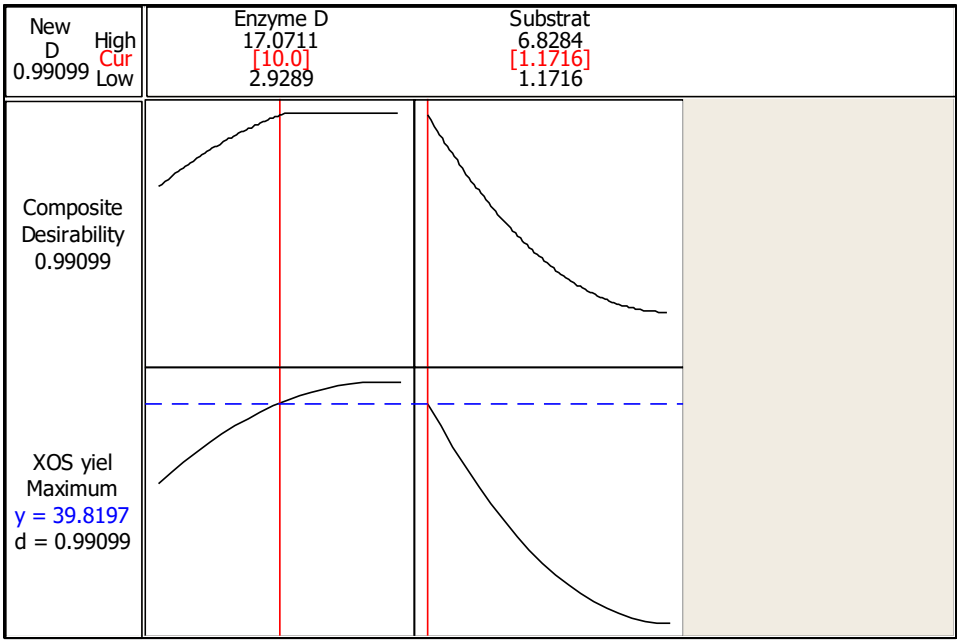
New
D
0.99099
High
Cur
Low
Enzyme D
17.0711
[10.0]
2.9289
Substrat
6.8284
[1.1716]
1.1716
Composite
Desirability
0.99099
XOS yiel
Maximum
y = 39.8197
d = 0.99099

C)

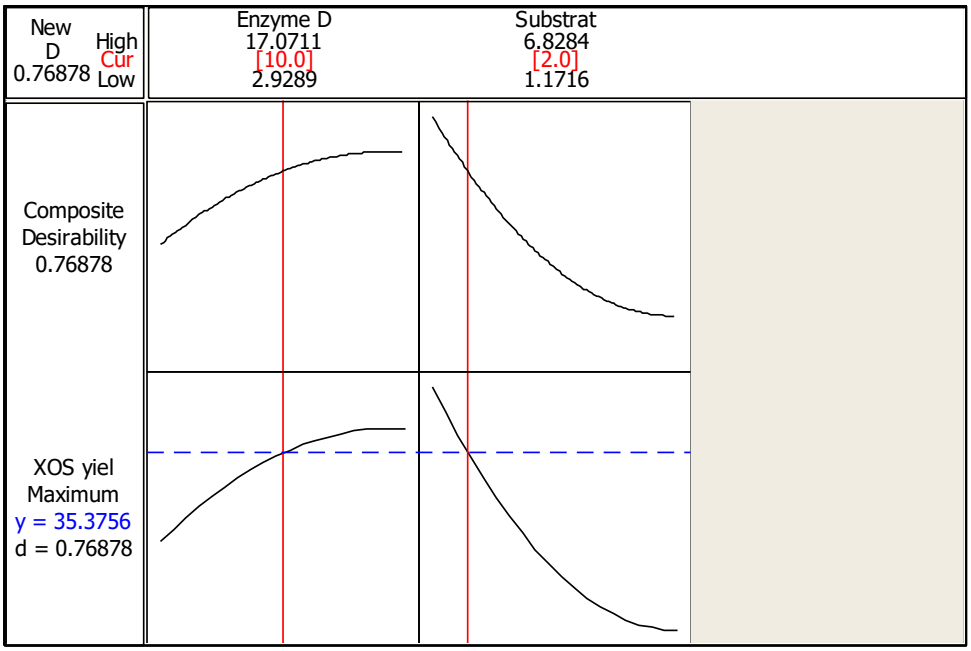
New
D
0.76878
High
Cur
Low
Enzyme D
17.0711
[10.0]
2.9289
Substrat
6.8284
[2.0]
1.1716
Composite
Desirability
0.76878
XOS yiel
Maximum
y = 35.3756
d = 0.76878

D)

Figure 7.14: Contour, 3D surface plot and desirability estimate of XOS production. A) Contour plot describing the effect of enzyme dose and substrate concentration on XOS yield; B) 3D surface plot describing the effect of enzyme dose and substrate concentration on XOS yield; C) Response optimization plot describing the desirability of XOS production at enzyme dose of 10 U and 1.17% substrate concentration; D) Response optimization plot describing the desirability of XOS production at enzyme dose of 10 U and substrate 2%.

The response optimizer option from Minitab Statistical software was used to predict the desirability of XOS yield for a few selected enzyme dose and substrate concentration. As observed from Figure 7.9C and D, for an enzyme dose of 10 U and 1.17% substrate, the desirability was 0.99 to give high XOS yield (39.8g). However, when substrate concentration was increased to 2%, the desirability decreases to 0.77, giving a yield of 35.4g. The verification experiment using 2% substrate at 10 U confirms the prediction wherein yield of 34.7 ± 1.75g XOS was obtained.

7.7. Conclusion:

It was observed that particle size plays a vital role in determining the maximum recovery of hemicellulose upon alkaline pretreatment. With ball milling, when milling was conducted for higher time (2, 4 h), the fraction consisted mostly of particle size less than 120 µm. In this case, 8% alkali was able to recover more than 90% hemicellulose. On the other hand, when the shell was milled, it was again observed that particle size less than 120 µm gives more than 90% recovery at 2 M NaOH.

Additionally, 4% NaOH was not suitable as recovery was less than 50%. Thus, it can be concluded that optimal particle size is less than 120 µm for maximum recovery of available hemicellulose. The observed results also provide an opportunity of choosing between ball milling and grinding for particle size reduction. As ball milling is an energy-intensive process, it may be economical to use grinding of the shell for size reduction, thereby reducing the overall cost of the process. Additionally, as near complete recovery is observed at alkali concentration of 8%, this is lower as compared to that reported in the literature (12-16%), and that observed for arecanut husk (10%). This reduction in alkali loading will have a significant

influence on process cost and downstream processing in case of upscale technology or commercial viability.

The observation from the use of immobilized enzyme system indicates that immobilization does impart temperature stability to the enzyme when the reaction period is of 48 h. This is evident from the fact that immobilized enzyme could produce near similar XOS yields at 50^{o}C and 60^{o}C in comparison to a free enzyme where the yield decreased from 34.65% to 24.14%. However, for cases like XOS production, immobilized enzymes do not seem to be a good option as the yield of XOS was observed to decrease with an increase in cycle number. This can be attributed to the reaction period of 48 h, which was necessary to maximize XOS yield. Although supplementation of loss in activity with either free enzyme or immobilized enzyme can be evaluated, however, it needs further experimentation and techno-economic analysis.

The response surface methodology based optimization of enzyme dose and substrate concentration indicates that maximum XOS yield is obtained when the substrate concentration is low (preferably less than 2%). The optimum enzyme dose was observed to be 10 U. With an increase in substrate concentration, the desirability of higher XOS production decreases as indicated in the response optimizer plots.

Thus, this chapter provides a process wherein maximum hemicellulose was recovered at low chemical usage and converted into XOS.

Chapter 8 Autohydrolysis pretreatment for XOS production

The *in-situ* generated hydronium ion during autohydrolysis process induces cleavage of glycosidic linkages, thereby liberating oligosaccharides into solution. The experimental condition is controlled to minimizing sugar degradation and by-product formation. Thus, autohydrolysis gives an opportunity of developing a greener process for lignocellulose valorization.

The autohydrolysis process has been studied to produce XOS from numerous substrates including almond shell, rye straw, bamboo culm, rice straw. However, it was observed that the XOS produced has wide DP range. It has also been reported that the rate and extent of fermentation of XOS depend on DP and lower DP XOS are used preferentially as a source of energy. Hence, in this chapter, a combination of autohydrolysis and enzymatic hydrolysis was evaluated for the production of XOS with a high concentration of low DP XOS. The autohydrolysis process has been reported for biomass such as Miscanthus x giganteus (Chen et al., 2014), vine prunings (Jesus, Romaní, Genisheva, Teixeira, & Domingues, 2017), almond shell (Nabarlatz, Farriol, & Montané, 2005), palm empty fruit bunches (Ho et al., 2014). A different in yield was observed based on difference in biomass composition and experimental condition employed. However, in most cases a wide degree of polymerisation XOS product was obtained. It has been reported that with respect to XOS, a narrow and low DP product is beneficial, due to better prebiotic properties. As it is difficult to obtain a narrow and low DP product with autohydrolysis, an additional step of enzyme reaction was used to obtain low DP product. For purification, various approaches such as adsorption on activated carbon and ethanol elution (Chen et al., 2016), ultrafiltration (Vegas et al., 2006) has been proposed. As membrane filtration is economical and can be upscaled easily, it was evaluated in the present work.

8.1. Methodology:

The almond shell was used for the production of XOS using autohydrolysis process. The general procedure is depicted as a schematic description in Figure 8.1.

8.1.1. Reactor system and autohydrolysis:

The autohydrolysis was performed in a SS 316 reactor having a nominal volume of 1 liter provided with forced auto-cooling (Trident Labotek, India). The temperature in the desired range was controlled using PID controller. For each experiment, the reactor was loaded with biomass (15 g), and the required amount of distilled water was added and mixed to prevent lump formation. The reactor was then assembled by tightening the screws, and the overhead motor was affixed to the stirrer drive. The reactor was heated to reach the desired temperature for the specified period. After the reaction period, cold water was forced through tubes in the reaction medium to decrease temperature up to 60^{o}C. The reaction mixture was then filtered using a muslin cloth; the residue was washed with 100 ml distilled water and pressed to collect all liquor. The washing was combined with autohydrolysate and termed original liquor. The liquor was then centrifuged to obtain clear original liquor. A part of liquor was used for determination of sugar, XOS and degradation products. An aliquot of autohydrolysis liquor was subjected to hydrolysis using the appropriate amount of 4% sulphuric acid based on liquor pH to convert soluble oligosaccharides into monosaccharides (Sluiter, Hames, Ruiz, & Scarlata, 2006). The increase in xylose concentration was used to estimate the extent of oligosaccharides present in the liquor and hence, used to determine the degree of hydrolysis of xylan into XOS.

The parameters evaluated include:

Reaction temperature: 180, 200 and 220^{o}C

Reaction Time: 2.5- 40 min (for different reaction temperature)

Solid: liquid: 1:10

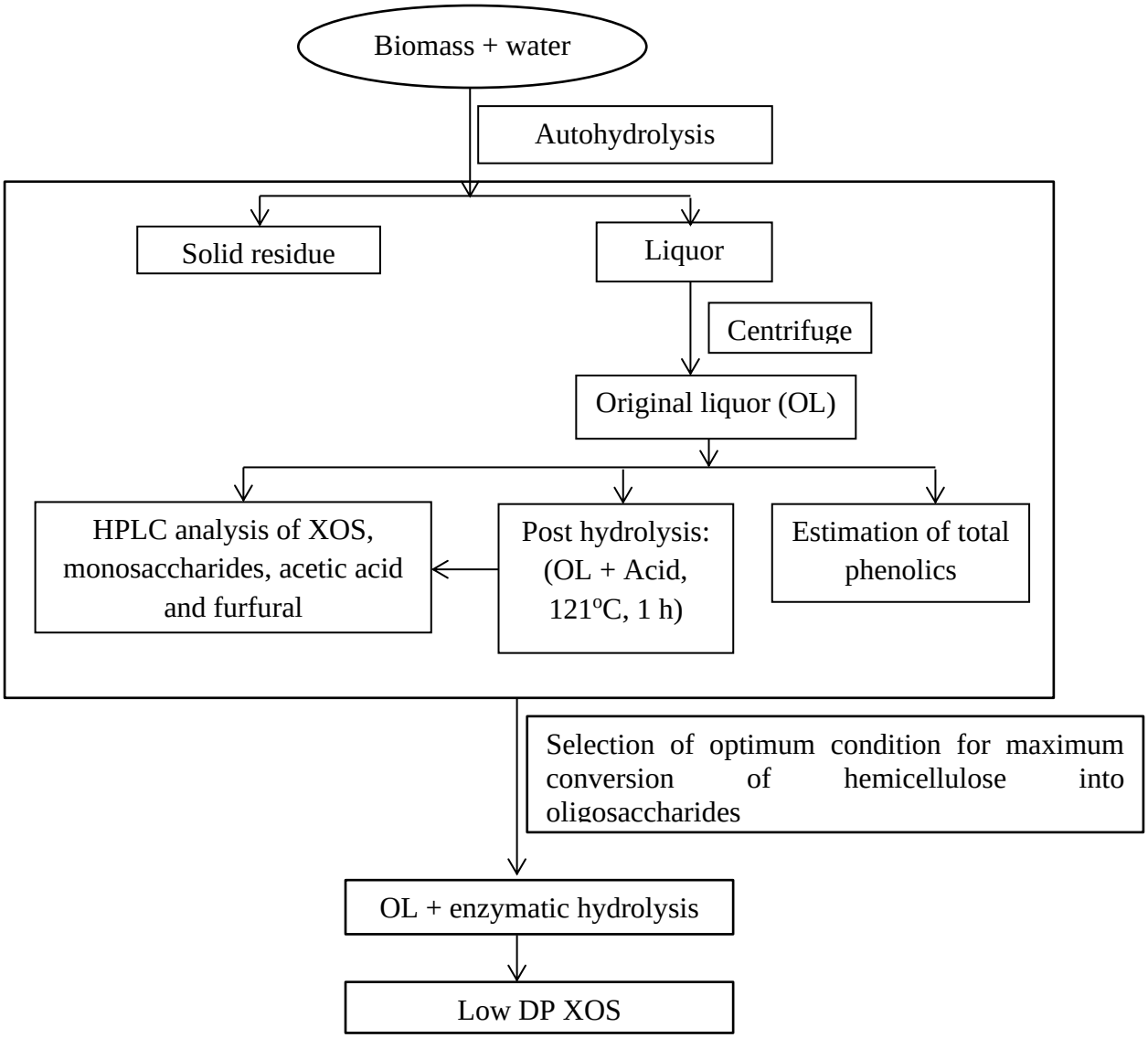

Figure 8.1: Schematic description of the process for autohydrolysis and maximizing low DP XOS production

8.1.2. Enzymatic hydrolysis of original liquor:

The clear autohydrolysate was enzymatically hydrolyzed using endoxylanase from *Thermomyces lanuginosus* (expressed in *Aspergillus oryzae*) at 50 ± 1 °C (temperature decided based on preliminary experiments) after adjusting pH to 5.8. For enzymatic hydrolysis, the liquor was incubated with the desired dose (5U, 10U and 15U) of the enzyme at 70 rpm to ensure mixing. An aliquot was withdrawn at a fixed time interval (2, 4, 8, 12, 24,

36, 48 h) and the enzyme inactivated by heating the aliquot in boiling water bath for 5 min. The aliquot was filtered through a 0.2 µ membrane filter and used for the analysis of low DP xylooligosaccharides. The outcome of enzymatic treatment was analyzed by conducting ANOVA analysis.

8.1.3. Membrane assisted refining of XOS liquor:

The enzymatically hydrolyzed liquor containing XOS was refined using 1 kDa and 250 Da membrane (47 mm) in an ultrafiltration system (HP 4750 Stirred Cell, Sterlitech Corporation, USA). The membranes were preconditioned using HPLC grade water at the required pressure designated for the membrane before each experiment. For ultrafiltration, 90 ml of liquor was added to the vessel provided with a Teflon coated magnetic bar to prevent concentration build-up. The filtration was performed using 1 kDa membrane at 100 psi (using nitrogen gas) until about 96-97% of feed was permeated. For the next step, the liquor was passed through 250 Da membrane at 150 psi, until about 65% feed was permeated. The ml of permeate collected was recorded at regular interval and used to determine the flux. An aliquot of permeate and retentate was analyzed by HPLC for its composition as compared to feed. The composition of feed and permeate was used to determine the retention (R) by using the following formula:

$$R= [(Cf-Cp)/Cf] \times 100$$

where Cf is the concentration of the constituent in feed, Cp is the concentration of the component in the permeate.

8.2. Result and Discussion:

8.2.1. Effect of autohydrolysis on xylan hydrolysis:

The average time required to reach the desired temperature was 16 min, 20 min and 24 min for 180^{o}C, 200^{o}C, and 220^{o}C, respectively. The pressure attained during the reaction was observed to be 8-9 kg/cm^2 for 180^{o}C, 12-14 kg/cm^2 for 200^{o}C and 18-20 kg/cm^2 for 220^{o}C. After the reaction time, the reaction mixture was cooled to 60^{o}C by forced cold water circulation (within 5-7 min). The percentage xylan depolymerized and resulting in oligosaccharides is as shown in Figure 8.2.

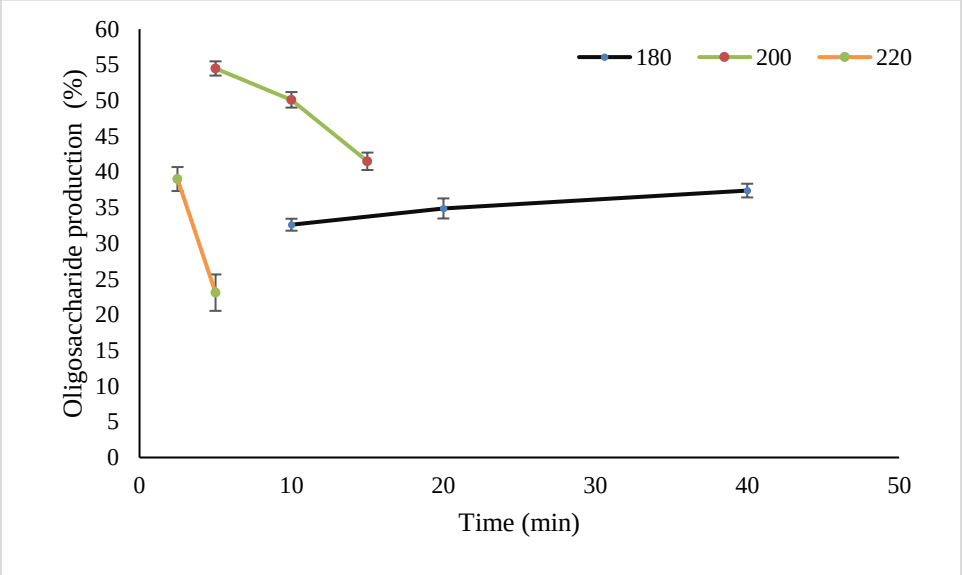

Figure 8.2: The effect of temperature and holding time on depolymerization of xylan and formation of oligosaccharides (% of xylan)

At 180^{o}C, the percent hydrolysis of available xylan into oligosaccharides was observed to be 32.6 ± 0.8% at 10 min, 34.9 ± 1.4% at 20 min and 37.4 ± 1.0% at 40 min of reaction time. With an increase in temperature to 200^{o}C, the percent hydrolysis was found to increase to 54.5 ± 1.0% at 5 min, 50.1 ± 1.1% at 10 min and 41.5 ± 1.2% at 15 min. A further increase in temperature to 220^{o}C resulted in a decrease in percent hydrolysis, with 39.0 ± 1.7% at 2.5 min and 23.1 ± 2.6% at 5 min of reaction time. Thus, based on obtained data, it can be concluded that the increase in temperature does increase percentage hydrolysis. However, temperature above 200^{o}C is not suitable. Therefore, a reaction at 200^{o}C for 5 min can be considered optimal for maximum hydrolysis of almond shell xylan into oligosaccharides, which can be translated to 10.97% oligomers from dry biomass.

For autohydrolysis pretreatment, severity factor has been commonly used to observe the effect of experimental conditions on the outcome. The severity factor (Ro), presents an equation which combines the effect of temperature (^{o}C) and time (min) and is expressed as

$$Ro = t*\exp[(T-T_{ref}) / \omega)].$$

where T is set temperature, T_{ref} is the reference temperature which is generally considered as 373.15 K and ω is the empirical parameter representing activation energy required for hemicellulose solubilization. The activation energy (ω) is calculated using the following formula

$$\omega = RT_{ref} / Ea$$

where R is the ideal gas constant (8.314 J/mol K), Ea is the activation energy of hemicellulose (J/mol). In literature, the value of ω for hemicellulose solubilization has been suggested as 14.75 K (Jesus et al., 2017). The severity factor in this work was in the range of 3.3-4.2. As can be observed from Figure 8.3, the percentage hydrolysis of xylan into oligosaccharides increases with increase in severity factor up to 3.9, after which the value decreases. At a constant temperature of 180^{o}C, increase in reaction time increases the severity and also slightly increases the oligosaccharide production. At 200^{o}C, an opposite trend is observed wherein an increase in reaction time; thus, the severity leads to the reduction in oligosaccharide production. A similar trend was observed for 220^{o}C. Also, for nearly the same severity factor of 3.64 and 3.66, a significant difference in oligosaccharide yield is observed. This is due to the difference in reaction temperature and time. Thus, the maximum xylan solubilization or oligosaccharide production was observed at log Ro value of 3.64. A similar trend in change of xylose concentration with severity factor was observed and presented in Table 8.6. The log Ro value for hazelnut shell was 3.92 (190^{o}C, 5 min) producing about 62% xylan solubilization (Surek & Buyukkileci, 2017). Similarly, log Ro of 3.59 (210^{o}C) has been reported for rice straw to produce XOS yield of 40% (Sluiter et al., 2011) and log Ro of 3.96 for wheat straw has been proposed to give 64% solubilization of arabinoxylan (Carvalheiro, Silva-Fernandes, Duarte, & Gírio, 2009). As autohydrolysis results in cleavage of hemicellulose sugar backbone, the concentration and composition of released soluble oligosaccharides depend on the reaction temperature and time. The total XOS (sum of xylobiose and xylotriose) and content of xylobiose and xylotriose produced upon autohydrolysis is as presented in Figure 8.4. At 180^{o}C, the liquor was composed of 1.9 ± 0.1% xylobiose at 10 min, which increases to 2.2 ± 0.1% at 40 min. The concentration of

xylotriose was however, found to be in the range of 1.2-1.3 % in the same time range. When the reaction temperature was set at 200°C, the yield of xylobiose was 2.1 ± 0.1% at 5 min, which increases to 3.1 ± 0.1% at 15 min of reaction time. The xylotriose yield was observed

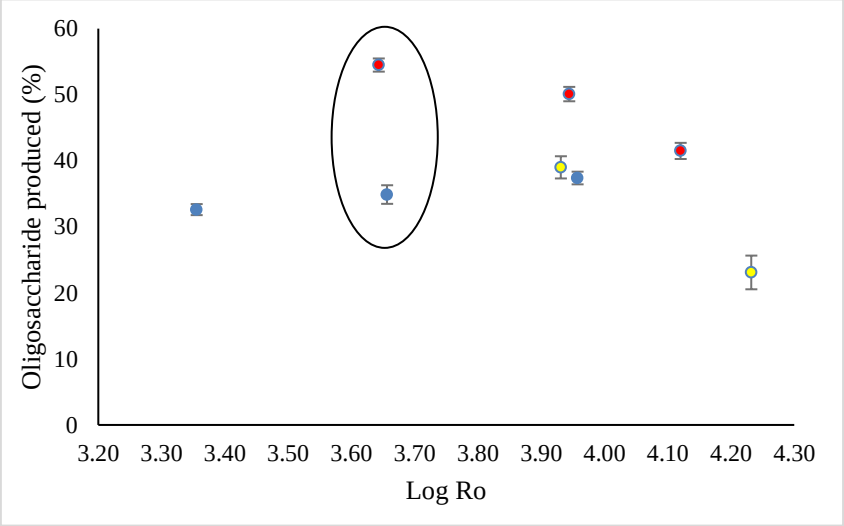

Figure 8.3: The influence of severity factor upon xylan depolymerization and generation of oligosaccharides (% of xylan). ● represents 180°C, ● represents 200°C and ● represents 220°C

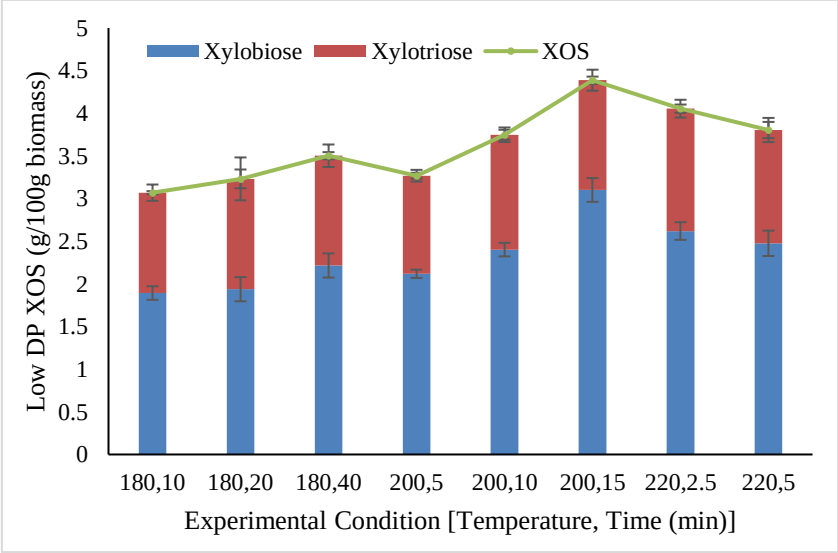

Figure 8.4: The percentage of total XOS and the corresponding levels of xylobiose and xylotriose produced upon autohydrolysis at different experimental conditions

in the range of 1.1-1.6%, which was almost similar at each reaction time. The yield of xylobiose at 220^{o}C, 2.5 min was observed to be 2.6 ± 0.1% and 2.5 ± 0.2% at 5 min reaction time, whereas the xylotriose yield was 1.3-1.4%.

8.2.2. Composition of autohydrolysis liquor:

The autohydrolysis also brings about cleavage of susceptible bonds, thereby releasing monosaccharides, acids, and their degradation products. The liquor was composed of sugars such as xylose, glucose, and arabinose resulting from the backbone of hemicellulose. The severity factor and corresponding sugar content are as shown in Table 8.1. The xylose content was found to increase with an increase in the severity factor and was observed to be in the range of 2.4-3.4%. A similar trend was observed for glucose content, which was found to be in the range of 2.5-3.9%. The presence of glucose can be ascribed to the possible glucose substituent on xylan backbone or hydrolysis of the amorphous region of cellulose. The lower concentration of glucose at all severity factor indicates minimal glucan hydrolysis, which is advantageous when the objective is producing XOS. The content of arabinose was found to be nearly similar for all studied concentration and might be originating from hemicellulose structure. Also, as seen in Table 8.1, the amount of acetic acid produced was dependent on the reaction severity and increased with increase in reaction temperature and time. The amount of acid produced at different reaction condition is reflected in the variation of liquor pH (Table 8.1). The lignin content of biomass is considered to be resistant to autohydrolysis pretreatment and is considered to undergo limited to none degradation or hydrolysis. However, certain susceptible groups may be liberated upon autohydrolysis, which are present as phenolics. The total phenolics content of the autohydrolysate liquor was found to be in the range of 0.15-0.28 mg/ 100g biomass, thus indicating a negligible breakdown of lignin. The concentration of furfural in the autohydrolysate liquor was also found to be very low in concentration and less than 1mg/ml. The typical behavior of biomass under autohydrolysis condition involves the formation of oligosaccharides which subsequently is hydrolyzed into monosaccharides and ultimately degrades to furfural and hydroxymethyl-furfural (Ruiz,

Rodríguez-Jasso, Fernandes, Vicente, & Teixeira, 2013). In this work, under the studied conditions of autohydrolysis, maximum oligosaccharides were obtained with a lower concentration of monosaccharides and degradation products.

Table 8.1: The content of monosaccharide, acetic acid and corresponding liquor pH upon autohydrolysis

Experimental Condition		Severity factor (log R_o)	Xylose	Glucose	Arabinose	Acetic acid	pH
Temperature (^oC)	Time (min)						
180	10	3.36	2.5 ± 0.1	2.5 ± 0.2	2.7 ± 0.1	0.4 ± 0.1	4.31
180	20	3.66	2.6 ± 0.2	2.6 ± 0.1	2.8 ± 0.1	0.6 ± 0.1	4.01
180	40	3.96	2.8 ± 0.1	3.0 ± 0.1	2.5 ± .01	1.2 ± 0.1	3.72
200	5	3.64	2.5 ± 0.1	3.7 ± 0.1	2.9 ± 0.1	0.6 ± 0.1	3.84
200	10	3.94	2.6 ± 0.1	3.8 ± 0.2	2.6 ± 0.3	0.8 ± 0.2	3.56
200	15	4.12	3.0 ± 0.1	3.9 ± 0.2	2.4 ± 0.2	1.4 ± 0.1	3.42
220	2.5	3.93	3.3 ± 0.1	3.8 ±0.1	2.5 ± 0.2	1.1 ± 0.2	3.35
220	5	4.23	3.4 ± 0.1	3.9 ± 0.2	2.5 ± 0.1	1.6 ± 0.1	3.21

units for constituents: g/100g biomass

8.2.3. Enzymatic hydrolysis of liquor:

As mentioned, upon autohydrolysis, about 10.97 g of xylan was solubilized into XOS, out of which the content of low DP XOS (xylobiose and xylotriose) was 3.3 ± 0.1 g/100g biomass. To maximize low DP XOS concentration, the clear liquor was treated with the enzyme at three different doses after adjusting pH of liquor to 5.8 ± 0.1. During preliminary runs, it was observed that the enzyme shows decreased activity at pH value below 4, which was the pH of autohydrolysate. As the optimum pH value of enzyme is 5.5-5.8, the pH was adjusted to 5.8 using 2M NaOH. As observed in Figure 8.5, the concentration of low DP XOS increases upon enzymatic hydrolysis. The maximum XOS yield was observed at an enzyme dose of 15 U upon hydrolysis for 36 h (8.3± 0.1), the yield, however, was not significantly different ($p<0.05$) from that obtained at 10 U (8.2 ± 0.1). Interestingly, a low enzyme dose of 5 U produces 7.7 ± 0.3% XOS within 36 h of enzymatic hydrolysis. Thus, 10 U of the enzyme dose can be considered optimal for producing maximum low DP concentration. Under the

optimal conditions, the liquor was composed of 5.3 ± 0.1% xylobiose and 3.0 ±0.1% xylotriose as compared to 2.2% xylobiose and 1.4% xylotriose present in original liquor.

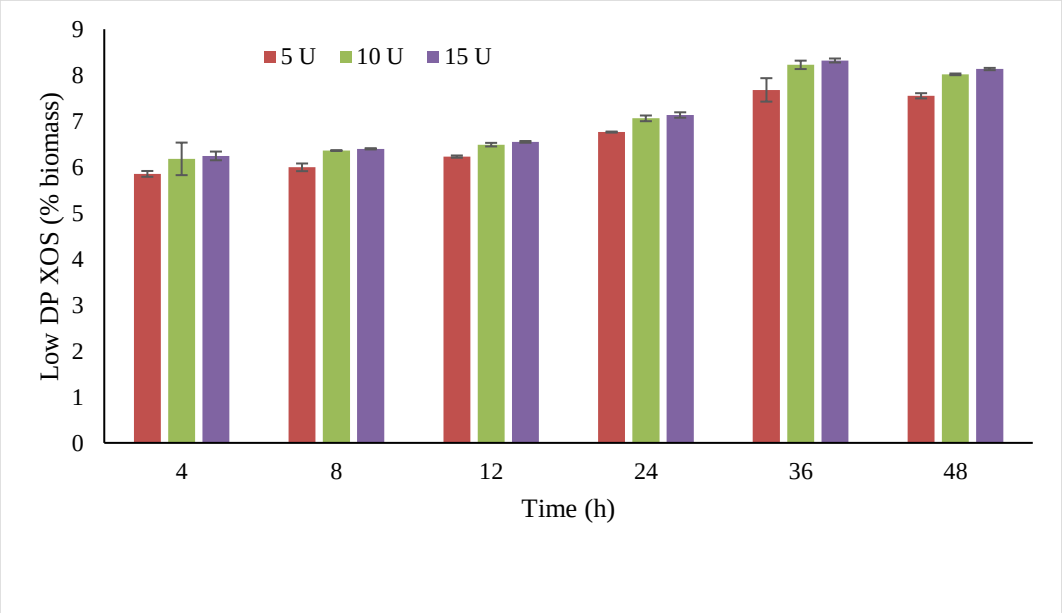

Figure 8.5: Enzymatic hydrolysis of autohydrolysate to increase the composition of low DP XOS (sum of xylobiose and xylotriose) at three different enzyme doses of 5 U, 10 U, and 15 U

The enzymatic liquor was also composed of 3.3 ± 0.2% xylose and 0.9% acetic acid, majorly arising due to autohydrolysis treatment. The Two-way ANOVA test presents an R-sq value of 0.99 and adjusted R-sq of 0.98, indicating a good agreement for the obtained results. Table 8.2 presents the results of Two-way ANOVA for XOS yield using different enzyme dose.

Table 8.2: Analysis of Variance test for experimental response upon enzymatic hydrolysis

Source	DF	Seq SS	Adj SS	Adj MS	F	P
Enzyme dose	2	1.4042	1.4042	0.7021	53.86	0.000
Time	5	22.0464	22.0464	4.4093	338.23	0.000
Enzyme*Time	10	0.0966	0.0966	0.0097	0.74	0.679
Error	18	0.2347	0.2347	0.0130		
Total	35	23.7819				
R-Sq	99.01%					
R-Sq (adj)	98.08%					

As can be observed, the individual factor (enzyme dose and reaction time) has a significant influence on XOS yield. However, the effect of the interaction term was not significant ($p<0.05$). The ANOVA was tested for XOS yield obtained at each sampling time to determine the time from where a significant difference in XOS yield occurs at different enzyme dose. The test reveals that similar XOS yields were observed at 4 h for all three enzyme doses tested. From 8-48 h, it was observed that the highest XOS yield was obtained with 15 U, though it was not significantly different from that obtained at 10 U. However, a significantly lower yield was observed with 5 U of enzyme dose. Thus, the enzyme dose of 10 and 15 U produces gives nearly similar XOS yield after 8 h of hydrolysis. The main and interaction effects plots are as shown in Figure 8.6a and 8.6b, respectively. The figure shows that as enzyme dose increases from 5 U to 10 U the yield of XOS increases with time, reaching a maximum at about 36 h of the enzymatic reaction.

Further increase in enzyme dose does not give a higher XOS yield, as supported by the ANOVA analysis. The contour plot as shown in Figure 8.6c, helps to visualize the effect of a change in enzyme dose and reaction time on XOS yield. The plot suggests that a reaction time above 35 h and enzyme dose above 7.5 U can enable the production of more than 8g/100g XOS from biomass. Thus, the optimal condition for enzymatic hydrolysis is 10 U for 36 h, which enables to increase low DP XOS concentration from 3.5 ± 0.1% present in original liquor to 8.2 ± 0.1 %. Importantly, the obtained liquor has a narrow spectrum of DP. Thus, in this work, 10.97g soluble oligosaccharides were produced upon autohydrolysis of the almond shell of which low DP XOS represented 31.9%. After enzymatic hydrolysis, the concentration of low DP XOS increases to 76.8%. In other words, 8.2 g of low DP XOS (xylobiose and xylotriose) could be obtained from 100g of dry biomass.

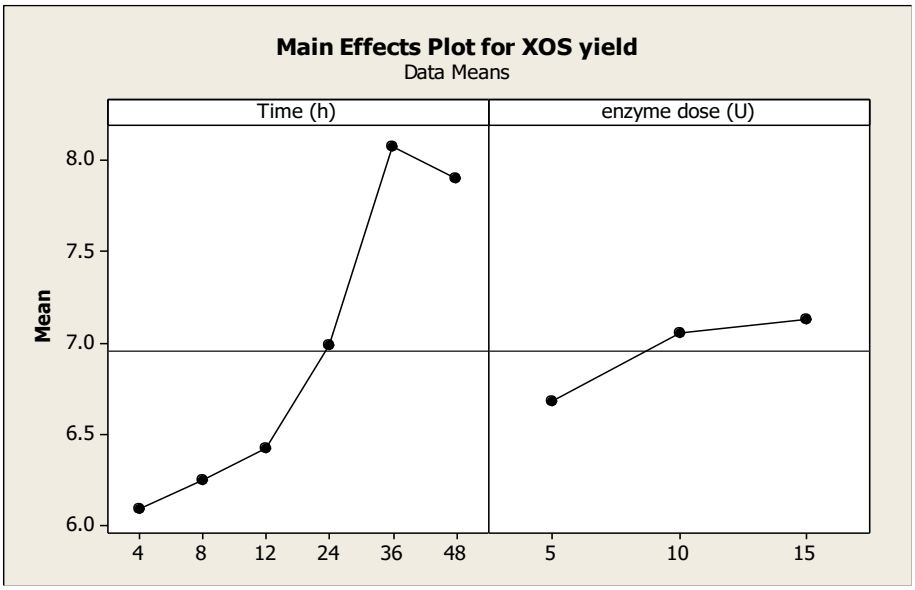
Main Effects Plot for XOS yield
Data Means
Time (h)
enzyme dose (U)
Mean
8.0
7.5
7.0
6.5
6.0
4
8
12
24
36
48
5
10
15

(a)

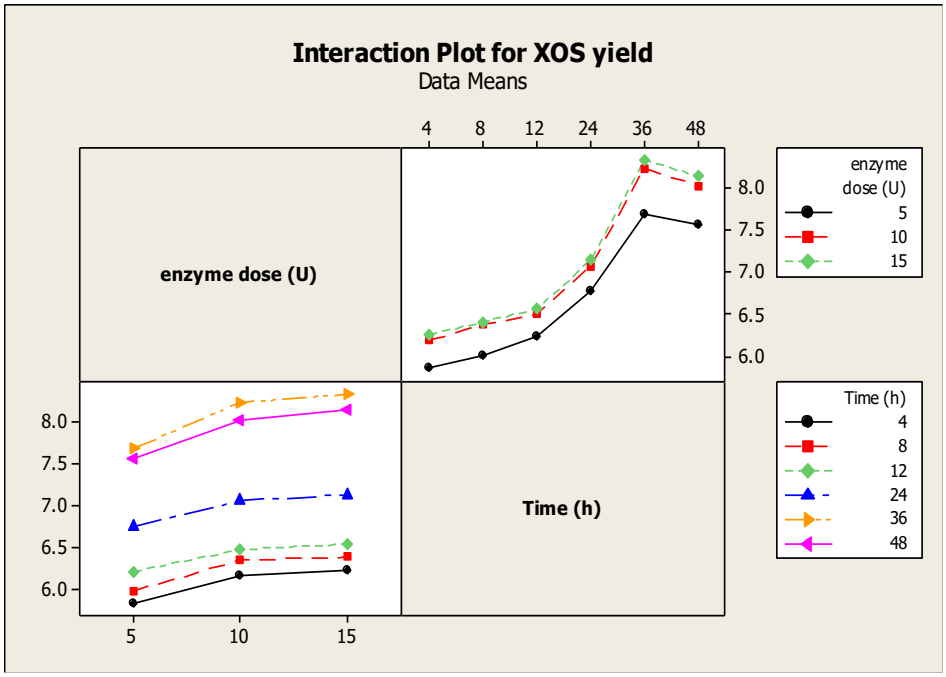
Interaction Plot for XOS yield
Data Means
enzyme dose (U)
Time (h)
4
8
12
24
36
48
5
10
15
8.0
7.5
7.0
6.5
6.0
enzyme dose (U)
5
10
15
Time (h)
4
8
12
24
36
48

(b)

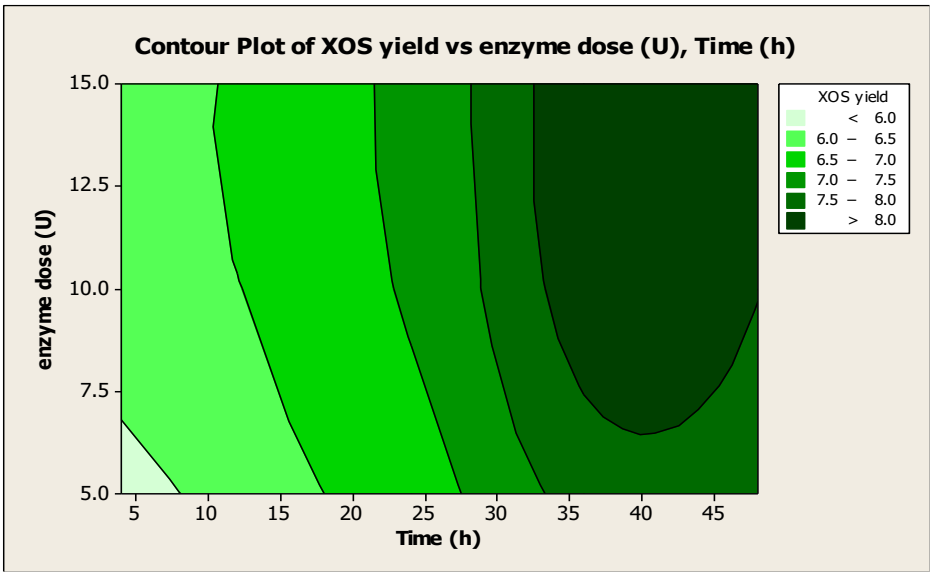

(c)

Figure 8.6: Statistical analysis of enzymatic hydrolysis of autohydrolysate showing (a) main plot (b) interaction plot and (c) contour plot

8.2.4. Membrane assisted refining of enzymatic XOS liquor:

Enzymatic hydrolysis liquor was subjected to sequential membrane separation following the scheme (as shown in graphical representation) to concentrate low DP oligosaccharides. XOS liquor was purified using ultrafiltration and nanofiltration by employing membranes with MWCO of 1 kDa and 250 Da, respectively, the properties of the membrane are described in Table 3. The feed, the permeate, and the retentate obtained for each membrane were evaluated using HPLC for its individual low DP oligosaccharides, sugars, and acetic acid content. The schematic of the sequence of membrane filtration and the flux of the pure water and liquor upon filtration using 1 kDa and 250 Da membrane is as shown in Figure 8.7. The first step was to reject high molecular weight solids such as xylose polymers (DP>9) if any, proteins, enzyme, and higher molecular weight lignin degradation products using 1 kDa and allow XOS, sugars and acetic acid to permeate through the membrane. The resulting permeate (P1) from 1 kDa membrane was subjected to 250 Da membrane to concentrate low DP XOS in the retentate. Pure water flux (Javg=93 LMH) was determined by measuring the

cumulative permeate volume using distilled water as a feed. Subsequently, feed stream (enzymatic liquor) was passed through the membrane. Permeate flux of liquor declined from 55.4 to 30.1 LMH in 100 min of operation with the 1 kDa membrane.

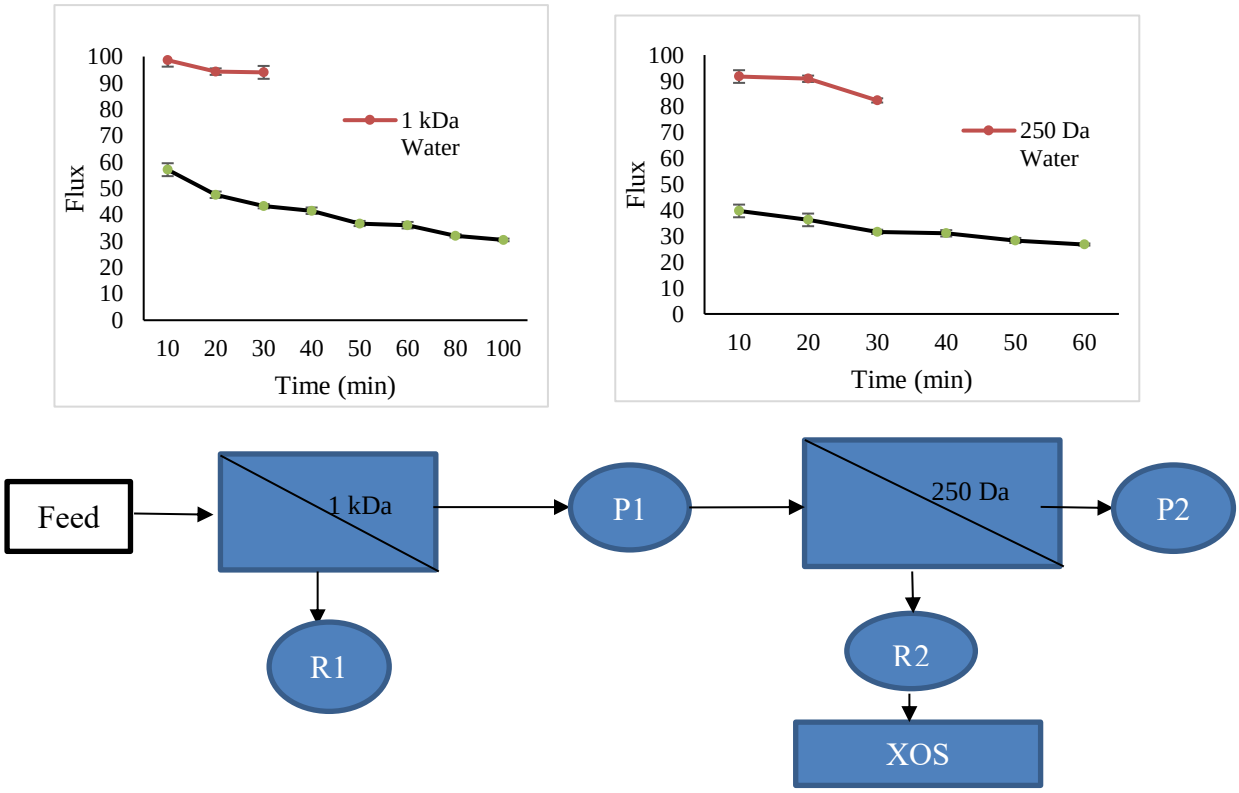

Figure 8.7: The flux rate observed during membrane filtration using 1 kDa and 250 Da membrane

This decline was due to concentration polarization, and membrane fouling in the stirred cell. Since enzymatic hydrolysate was centrifuged, most of the suspended solids were removed, which helped in reduced fouling during membrane separation. The selection of the membrane was dependent on the molecular weight of XOS and monosaccharides. Since low DP XOS (DP2, DP3) molecular weight are above 282 g/mol, 250 Da membrane should be able to retain these while allowing passage of most of the monosaccharides and acetic acid with a molecular weight less than 180 g/mol in permeate stream (P2). Subsequent refining of P1

stream using tighter cut-off (250 Da) membranes allowed the concentration of low DP XOS in the retentate. For 250 Da, the permeate flux decreased gradually from 38.1 to 27.1 L/m^2.h in 60 min of operation, during which 31-33% of feed was retained as retentate (R2).

Table 8.3 and Figure 8.8 represents the mass balance of membrane separation, indicating the percentage of xylobiose, xylotriose, xylose, glucose, arabinose, and acetic acid in the initial feed and permeate or retentate.

Table 8.3: Mass balance of components upon membrane assisted refining of XOS liquor

Component	**Feed**	**1 kDa**		**250 Da**	
		Permeate	**Retentate**	**Permeate**	**Retentate**
Xylobiose	441.1 ± 5.5	397.8 ± 5.0	18.5 ± 0.2	N.D	375.0 ± 4.7
Xylotriose	248.7 ± 2.2	238.0 ± 2.1	7.8 ± 0.1	N.D	104.7 ± 0.9
Xylose	299.8 ± 5.7	277.1 ± 5.3	10.5 ± 0.2	137.9 ± 2.6	149.8 ± 2.9
Glucose	317.2 ± 0.6	306.3 ± 0.6	10.6 ± 0.1	194.5 ± 0.4	103.6 ± 0.2
Arabinose	265.3 ± 3.3	253.3 ± 3.2	8.8 ± 0.1	157.1 ± 2.0	104.1 ± 1.3
Acetic acid	7.7 ± 0.2	6.7 ± 0.2	0.2 ± 0.0	4.4 ± 0.1	2.5 ± 0.1

Values are in mg, mean ± s.d.
Volume of feed: 90 ml, Volume of 1 kDa permeate: 87 ml, Volume of 1 kDa retentate: 3.3 ml, Volume of 250 Da permeate: 55.96 ml and Volume of 250 Da retentate: 27.34 ml.
N.D.: Not detected

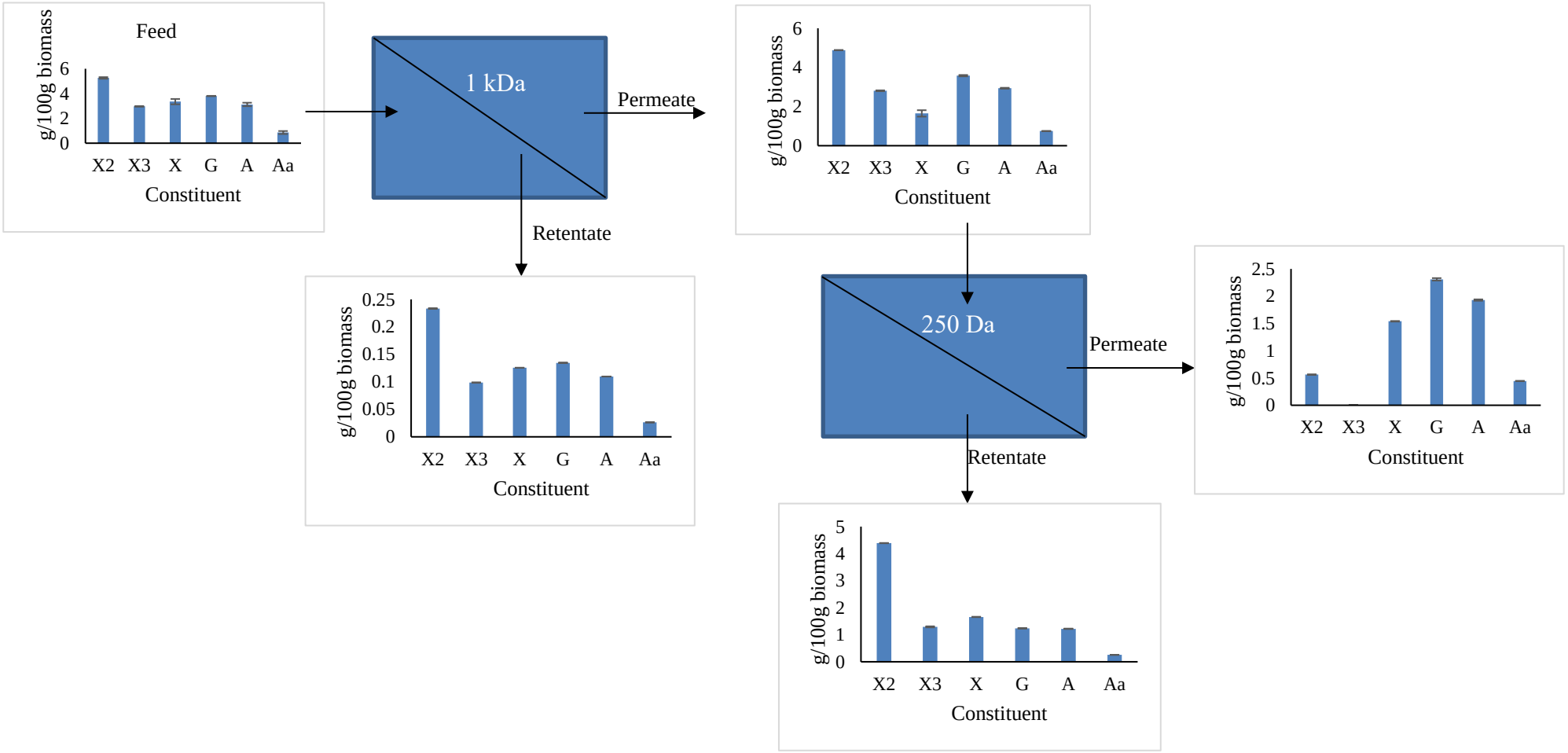

Figure 8.8: Mass balance of constituent upon membrane assisted refining using 1 kDa and 250 Da membranes. X2: Xylobiose, X3: Xylotriose, X: Xylose, G: Glucose, A: Arabinose and Aa: Acetic acid. Y axis is in g/100g biomass

In the first step, when the XOS feed was filtered through 1 kDa membrane, about 93-95% of xylobiose and xylotriose from the feed was collected as permeate fraction. Also, about 94-95% of monosaccharides (xylose, glucose, arabinose) was detected in the permeate fraction along with 87% of acetic acid. The rejection (R) on 1 kDa membrane was as follows: xylobiose: 7%; xylotriose: 5.3%;xylose: 6.4%; glucose: 5.9%; arabinose: 5.9% and acetic acid 13%. As the objective was to remove high molecular weight impurities including enzymes, the filtration was continued to recover the maximum of each constituent while keeping values of retention low. The permeate obtained from 1 kDa was then subjected to filtration using 250 Da. The concentration of xylobiose increased from 4.9 mg/ml (feed) to 13.7 mg/ml in 250 Da retentate (R2) with a VCR ~ 3.0 and 85% recovery. Similarly, the concentration of xylotriose change from 2.8 mg/ml to 3.8 mg/ml, with a recovery of about 42%. It was observed that negligible xylobiose and xylotriose were detected in 250 Da permeate (P2). Based on mass balance data, it is speculated that the xylobiose and xylotriose deficit may be due to thin layer formation of solids on the membrane, which subsumed a small amount of xylobiose and xylotriose.

The rejection (%) for 250 Da membrane was 54% for xylose, 38.7% for glucose, 40.8% for arabinose and 42.9% for acetic acid. In other words, the percent removal of xylose was 46% along with 61.3% glucose, 59.2% arabinose, and 57.1% acetic acid. The permeate (P2) volume represents about 62% of feed volume containing monosaccharides and acetic acid. Since enzymatic hydrolysis of autohydrolysis liquor was performed at the very low solid-liquid ratio, the solids and monomers concentration in the P2 stream was too low to meet the requirement of economical fermentation of sugars for any value addition. Total solids content (based on mass balance data) was less than 0.3%. Therefore, it would be prudent to recycle P2 in the process to meet more than 50% of the water requirement of autohydrolysis step, which could potentially reduce fresh water need by 50% in the process. However, further studies are warranted using this approach to determine the actual number of cycles as the sugar and acid concentration will keep building.

Thus, upon refining using sequential membranes, a concentrated low DP XOS (xylobiose and xylotriose) liquor source containing 69.1 ± 0.1% of the initial XOS (after enzymatic hydrolysis) could be obtained. Recently, XOS refining and purification has been reported for

Miscanthus XOS, with alcohol: water mixture as the eluting solvent (M. H. Chen et al., 2016). This process will require an additional energy-intensive unit operation for alcohol recycling. The membrane separation process developed in the current work provides a greener approach for obtaining XOS syrup rich in a low degree of polymerization xylooligosaccharides. For further purification of low DP XOS, diafiltration and hybrid membrane-resin based systems could be used, but these would require careful and detailed analysis and process optimization. The final decision needs to be taken based on the techno-economic feasibility of the process.

8.3. Conclusion:

In this chapter, a greener alternative of autohydrolysis was used for the production of XOS. Further enzymatic hydrolysis was used to obtain a product containing a maximum of low DP XOS.

For the almond shell, out of the available xylan 54.5 ± 1.0% was hydrolyzed to give soluble oligosaccharides. However, the percentage of low DP XOS (Xylobiose and xylotriose) was 3.5%. After enzymatic hydrolysis, the amount of low DP XOS was observed to be 8.2 ± 0.1g/100g biomass. The optimum condition for enzymatic hydrolysis was observed to be 10 U of enzyme dose, pH 5.8. Thus, 10.97g soluble oligosaccharides was produced upon autohydrolysis of the almond shell containing 31.9% as low DP XOS, which increases to 74.8% after enzymatic hydrolysis. The membrane purification process enabled recovery of 69.1 ± 0.1% of total low DP XOS while removing most of the monosaccharide and acetic acid. The membrane refined liquor has only about 50% of initial xylotriose, most of which is supposed to be lost due to entrapment in membrane pores, as none was detected in the permeate. This can be beneficial when the process is run at a pilot scale as the blocked pores may prevent further loss of xylotriose, thereby increasing the recovery of XOS. Thus, a green process was developed for production and refining of XOS product, predominantly rich in xylobiose.

Chapter 9 Membrane assisted refinement and *in-vitro* fermentation of XOS

This chapter describes the process developed for refining of XOS obtained from alkaline extraction of almond shell hemicellulose and subsequent enzymatic hydrolysis. The refined XOS product was used to study the fermentation characteristics. The *in-vitro* fermentation was carried out using human fecal inoculum as well as individual bacteria belonging to the *Lactobacillus* species.

Alkaline pretreatment or autohydrolysis have been commonly used for the production of XOS from biomass. However, the recovery of XOS is challenging due to the complex nature of the alkaline solution or autohydrolysate (Vázquez et al., 2000). Downstream processing approaches including solvent precipitation, solvent extraction, chromatographic methods have been used for refining and purification of XOS, however, they may not be suitable for commercial application. Membrane filtration is a promising technology for oligosaccharide refinement or purification. Ultrafiltration allows to separate the oligosaccharides from higher molecular weight impurities while nanofiltration enables concentration and removal of low molecular weight compounds including monosaccharides, phenolics (Pinelo, Jonsson, & Meyer, 2009). A two-step membrane separation process using 10 kDa and 3 or 1 kDa membrane, has been reported to produce an oligosaccharide rich permeate from enzymatically obtained XOS liquor (Akpinar, Ak, Kavas, Bakir, & Yilmaz, 2007). Similarly, nanofiltration using 1 kDa membrane allowed to obtain XOS concentrate from rice husk autohydrolysate (Vegas et al., 2006). However, in these studies, as nanofiltration with tighter molecular weight cut-off membrane (MWCO) is not used, the product may be considered to be composed of monosaccharides and other low molecular weight impurities.

Bifidobacterium and *Lactobacillus* are resident of the human gut and commonly used target for prebiotic activity. Such bacteria can ferment a broad range of carbohydrate substrates, including XOS, to provide health benefits (Singh, Banerjee, & Arora, 2015). A difference in the rate of fermentation among the bacterial strains is observed based on the substrate, substrate branching, substitutions, and degree of polymerisation (Aachary & Prapulla, 2011).

For this work, the objective was to develop a downstream process and realise the prebiotic potential of XOS derived upon enzymatic hydrolysis of almond shell hemicellulose. Membrane separation, including ultrafiltration and nanofiltration, was used to refine and

concentrate XOS. In this work, a tighter membrane (150 Da) was used for nanofiltration to concentrate XOS while minimising the concentration of the monosaccharides and low molecular weight impurities. The difference and extent of fermentability of the XOS concentrate was evaluated with strains of *Lactobacillus* and *Bifidobacteria*. The residual XOS concentration after fermentation was measured to hypothesize the preference of bacteria for the degree of polymerisation of XOS.

9.1. Methodology:

9.1.1. Membrane assisted refinement of enzymatic XOS liquor:

The enzymatic liquor containing XOS (as described in Chapter 7, section 7.5) was refined using a dead-end ultrafiltration process by using HP 4750 Stirred Cell (Sterlitech Corporation, USA), containing a 300 ml capacity 316L stainless steel, chemically resistant vessel with a maximum pressure rating of 1000 psig (69 bar) and maximum temperature of 121^{o}C at 55 bars. This assembly was provided with a Teflon coated magnetic stirrer to prevent "build-up" on the membrane surface and also to ensure even concentration of the liquor throughout. This assembly could support a membrane of 47-49 mm diameter (active membrane area of 14.6 cm^2). The filtration was carried out using compressed nitrogen gas, and the inlet pressure was regulated using a pressure regulator and visualized by a pressure gauge. The decompression valve attached to nitrogen gas hose allowed for releasing pressure to halt ultrafiltration. The ultrafiltration was carried out using commercial membranes having a molecular mass cut- off of 10 kDa (polyether sulphone), 1 kDa (Hydrophilized Polyamide) and 150 Da (Hydrophilized Polyamide). The cell was filled with liquor and stirred at 800 rpm, and filtration was carried at the desired pressure to allow about 90-95% of the liquor to permeate. Before each run, the membrane was allowed to saturate with double distilled water with the same conditions as that of liquor. All the experiments were performed in duplicate and at room temperature. The permeate and retentate were then analyzed for its xylooligosaccharides content. One part of the enzyme liquor, of permeate and of retentate was used to measure total solid. The colour intensity of liquor permeate was determined by measuring optical density between 200-1100 nm using UV-Vis spectrophotometer (Thermofischer). The absorption at OD 230 and 280 nm were also measured to estimate the level of phenolic impurities and colour pigments.

9.1.2. *In-vitro* human fecal fermentation study:

9.1.2.1. Participants

The fecal samples from healthy adults (n = 3) with no known gastrointestinal diseases or significant comorbidities were collected. Notable exclusion criteria for participants included the use of antibiotic therapies and consumption of either prebiotics or probiotics in the month preceding the study. Once enrolled in the study, participants were instructed not to alter their diets during the collection period. All participants provided written informed consent prior to the sample collection. Ethical approval was obtained from the Monash University Human Research and Ethics Committee (ID: 11491) to undertake this study. The fermentation characteristics of almond shell XOS (this study) in human fecal samples was compared with substrates with established fermentation characteristics. The other fiber substrates used in the study include fructooligosaccharide (FOS) (Orafti P-95, Beneo); medium-chain inulin (Orafti GR, Beneo); and XOS derived from corn (Xylooligosaccharide 95%, Huangzhou Focus Corporation).

9.1.2.2. In vitro fermentation

The *in-vitro* fermentation protocol was adapted from (Yao et al., 2018). Fresh feces were collected into a sealed container and immediately transported to the laboratory. The sample was immediately gassed with oxygen-free nitrogen upon arrival, kept at 37°C in a water-bath, and used in the preparation of the fecal inoculum within 30 minutes of passage. The inoculum was prepared by mixing the freshly passed fecal samples from each volunteer with sodium phosphate buffer (pH 7) to make up a 16% fecal slurry (weight/volume) and homogenized in a household blender for 2 minutes. The slurry was then filtered through four layers of muslin cloth to remove particulate materials. Aliquots (50 ml) of fecal slurry were transferred to 250 ml bottles containing either 10ml of sodium phosphate buffer alone, as the blank control, or 10 ml of sodium phosphate buffer spiked with 1 gram of fiber substrate. The headspace of the bottles was then gassed with N_2 before incubation and then sealed. Each bottle was incubated in a shaking water bath at 37°C, shaking at 50 shakes per minute, for four hours.

The substrate fermentations were undertaken in triplicate with fecal slurries from individual donors (n=3) to capture possible individual variations in fecal bacterial metabolism and if

necessary, exclude for outliers. Before, and immediately following the four-hour incubation, 25 ml aliquots of fecal slurry were transferred to sterile fecal containers and frozen immediately at -80°C for analysis of short-chain fatty acid (SCFA) content.

9.1.2.3. Assessment of gas production in response to fiber substrates

The gas produced upon fermentation of carbohydrate substrate by fecal microbiota were measured via automated headspace sampling over the four-hour incubation period. Total gas produced upon fermentation was measured via a pressure sensor (ANKOM^{RF} Gas Production System, ANKOM Technology) at 15-second intervals over the four hours. Gas production was adjusted for total headspace volume, converted from pressure (psi) into volume in mL using the 'ideal' gas and Avogadro's laws, and expressed as a volume (mL/g fiber). Cumulative gas produced at the end of the four-hour incubation period was used to assess the total extent of fermentation.

11.1.2.4. Short chain fatty acid concentrations:

Frozen samples of fecal slurry were defrosted overnight at -4°C. A 5 ml aliquot of the defrosted slurry was spiked with an internal standard (1.68 mM heptanoic acid) at 1:3) (sample to an internal standard, volume/volume), homogenized and then centrifuged (2000 g, 10min, 4°C). After centrifugation, 300 µL of supernatant was added to a 0.2 µL filter vial containing 10 µL of 1 M phosphoric acid. The vials were then analyzed for SCFA content via gas chromatography. All samples were analyzed using an Agilent GC6890 coupled to a flame-ionization detector (FID) with helium used as the carrier gas. An Agilent FFAP column (30 m x 0.53 mM [internal diameter] x 1.00 µM [film thickness]) was installed for analysis, with a constant flow rate of 4.0 mL/min. A split-less injection technique was used, with 0.2 µL of sample injected. The oven was held at 90°C for 1 minute and then raised to 190°C at 20°C per minute and held for 3 minutes. The samples were analyzed in triplicate, with a coefficient of variation (CV) less than 15% within triplicate samples used for quality control.

9.1.2.5. Statistical analysis:

The data was statistical analysis using GraphPad Prism version 7.0 software. Data were presented as mean (standard deviation) of cumulative gas production per gram of fiber at different time points over the four hours. Differences in the following endpoints at the end of the incubation period were analyzed using one-way ANOVA and, where significant

differences were identified between substrates, multiple comparisons were performed using Fisher's Least Significant Difference (LSD): total gas production; slurry pH; total and individual SCFA concentrations; and the proportion of individual SCFAs relative to total SCFAs produced.

9.1.3. *In-vitro* bacterial fermentation:

The bacterial fermentation of almond XOS was performed using different strains of *Lactobacillus*. The bacterial strains were procured from National Dairy Research Institute, Karnal, India in freeze-dried form and stored at -20^{o}C throughout the study. Before the fermentation study, the *Lactobacillus* strains were pre-cultured in MRS (De Man, Rogosa, Sharpe) broth under a static condition at 37^{o}C except for *L. brevis*, which was cultivated at 30^{o}C. The MRS broth was sterilized by treatment at 121^{o}C for 20 min. To the sterile broth, the freeze-dried bacterium was inoculated to obtain seed culture. Once the seed culture was obtained, it was used to prepare slant culture on MRS broth containing agar and remaining seed culture was stored at -20^{o}C for further use. The slant agar culture was then incubated at the required temperature overnight to obtain colonies of bacteria. From the agar, colonies were inoculated into sterile MRS broth and cultured overnight to obtain a working bacterial culture. The culture was then centrifuged to obtain cell pellets, washed with 0.9% saline, and then reconstituted into 0.9% saline to obtain OD in a range of 0.7 to 0.9.

The composition of the MRS broth used for fermentation study was 2g/L dipotassium hydrogen phosphate, 20g/L glucose, 0.2g/L magnesium sulfate heptahydrate, 0.05g/L manganous sulfate tetrahydrate, 8g/L meat extract, 10g/L peptone, 5g/L sodium acetate trihydrate, 2g/L triammonium citrate, 4g/L yeast extract and the pH was adjusted to 7 (if required). For the substrate fermentation study, the MRS broth was prepared by dissolving each constituent in water except for glucose. The glucose was replaced with the required carbohydrate substrate at a final concentration of 0.5%.

The fermentation study was carried out using four different carbohydrate substrates including almond XOS; corncob derived commercial XOS (Xylooligosaccharide 95%, Huangzhou Focus Corporation), xylose, glucose (as a positive control) and blank (without carbohydrate source). At regular intervals of 0, 2, 4, 6, 12, 24, 48 h, the tubes were taken out, and the OD measured. The pH of the medium was determined and the medium centrifuged to obtain clear

supernatant, which was used for SCFA, and residual XOS estimation by HPLC. All the study was performed in duplicates.

9.2. Results and discussion:

9.2.1. Membrane assisted refinement of XOS:

The applicability of a membrane assisted separation process for refining the enzymatically produced XOS was evaluated using membranes with different molecular weight cut-offs. A schematic that illustrates the sequence of membrane filtration steps along with the flux obtained for water and liquor is shown in Figure 9.1. The 10 kDa membrane was used in the first step to remove the higher molecular weight impurities including enzyme, higher DP XOS (if present) and the colour impurity possibly arising due to lignin contamination. The filtration was continued to collect more than 90% of liquor as permeate (P1) to recover maximum XOS. The enzymatic liquor was dark brown in colour indicating the presence of a high concentration of dissolved constituents and impurities. Hence the flux ($J=L/hm^2$) changed from 14.7 at the start of filtration to 9 towards the end. The increase in the concentration of impurities in retentate (R1) as the filtration progressed may have increased the viscosity, which possibly explains the decrease in permeation rate. The permeate (P1) from 10 kDa was light yellow in colour and was used as feed for the 1 kDa membrane. It was observed that no significant difference in the colour or change in the concentration of XOS and monosaccharide upon filtration was found using the 1 kDa membrane. Hence, this step can be neglected/ omitted from the process as some loss of XOS is observed in the retentate. The permeate (P2) obtained from the 1 kDa membrane was then used as feed for the 150 Da membrane. As XOS has DP above 282 g/mol, it can be assumed that 150 Da membrane will cause retention of XOS while allowing monosaccharides to permeate. For 150 Da, the flux changed from 23.8 to 15.4, during which about 70% of liquor could permeate while retaining about 29% of the feed. The observation of membrane purification is shown in Table 9.1, and the mass balance is depicted in Figure 9.2. Initially, the enzymatically produced XOS liquor containing the product along with enzymes and residual hemicellulose was centrifuged to collect clear supernatant. It was observed that the permeate obtained from the 10 kDa was yellowish as compared to the dark brown feed. This may be because of the removal of color imparting phenolic/ lignin impurity and high molecular weight components. As observed in Table 9.1, 10 kDa membrane brought about decoloration and removal of impurities without

significant loss of XOS, xylose, and acetic acid, as more than 90% was observed in permeate. The retention (R) for 10 kDa membrane was xylobiose: 3.4%; xylotriose: 8%; xylose: 4.3% and acetic acid: 4.6%.

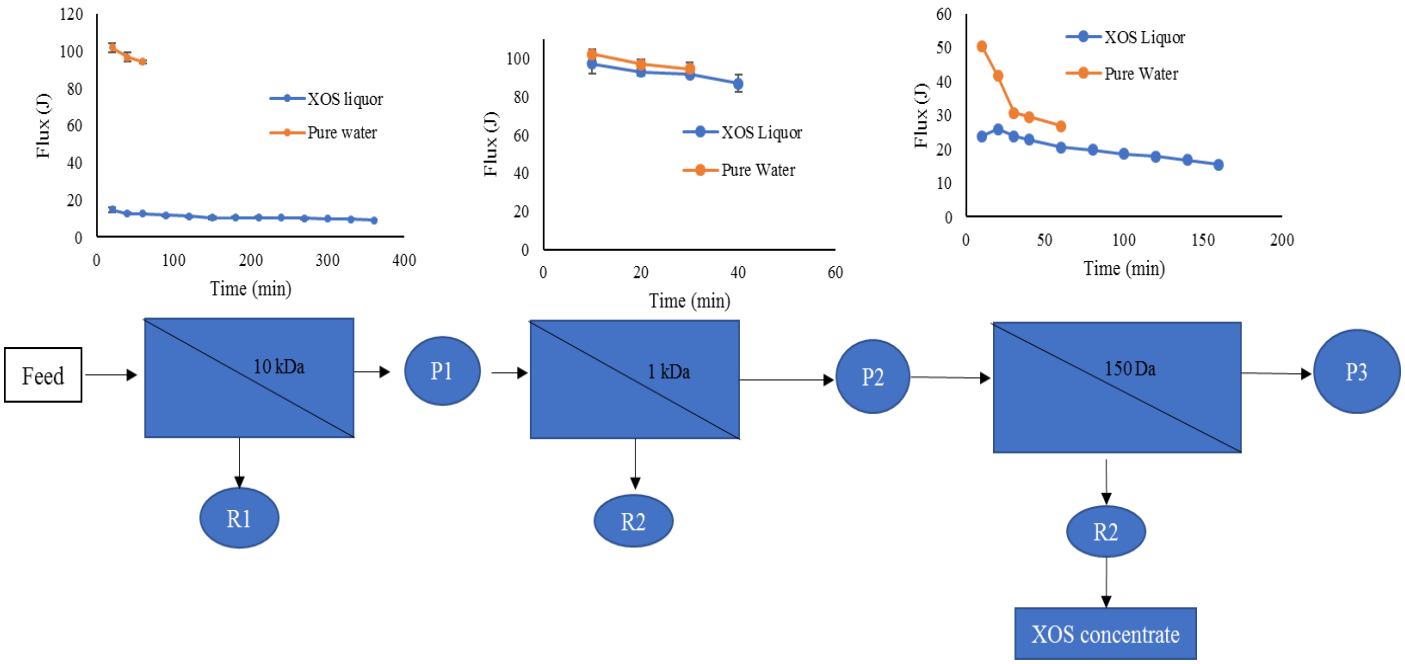

Figure 9.1: Schematic of membrane filtration sequence and the observed flux

Table 9.1: The composition of permeate and retentate upon membrane filtration using different molecular weight cut-off

Membrane	Fraction	Xylobiose (%)	Xylotriose (%)	Xylose (%)	Acetic acid (%)
10 kDa	Permeate	96.6 ± 2.8	91.8 ± 1.9	95.6 ± 2.2	95.4 ± 2.6
	Retentate	5.3 ± 3.4	4.7 ± 3.0	4.7 ± 3.2	3.5 ± 1.9
1 kDa	Permeate	89.9 ± 2.8	88.6 ± 2.1	90.6 ± 1.4	85.5 ± 1.7
	Retentate	3.6 ± 1.0	3.8 ± 0.5	3.9 ± 0.6	3.7 ± 0.8
150 Da	Permeate	12.8 ± 0.3	N.D.	55.6 ± 0.3	42.7 ± 7.1
	Retentate	79.1 ± 0.2	41.3 ± 3.4	36.1 ± 2.6	40.7 ± 2.9

N.D: not detected

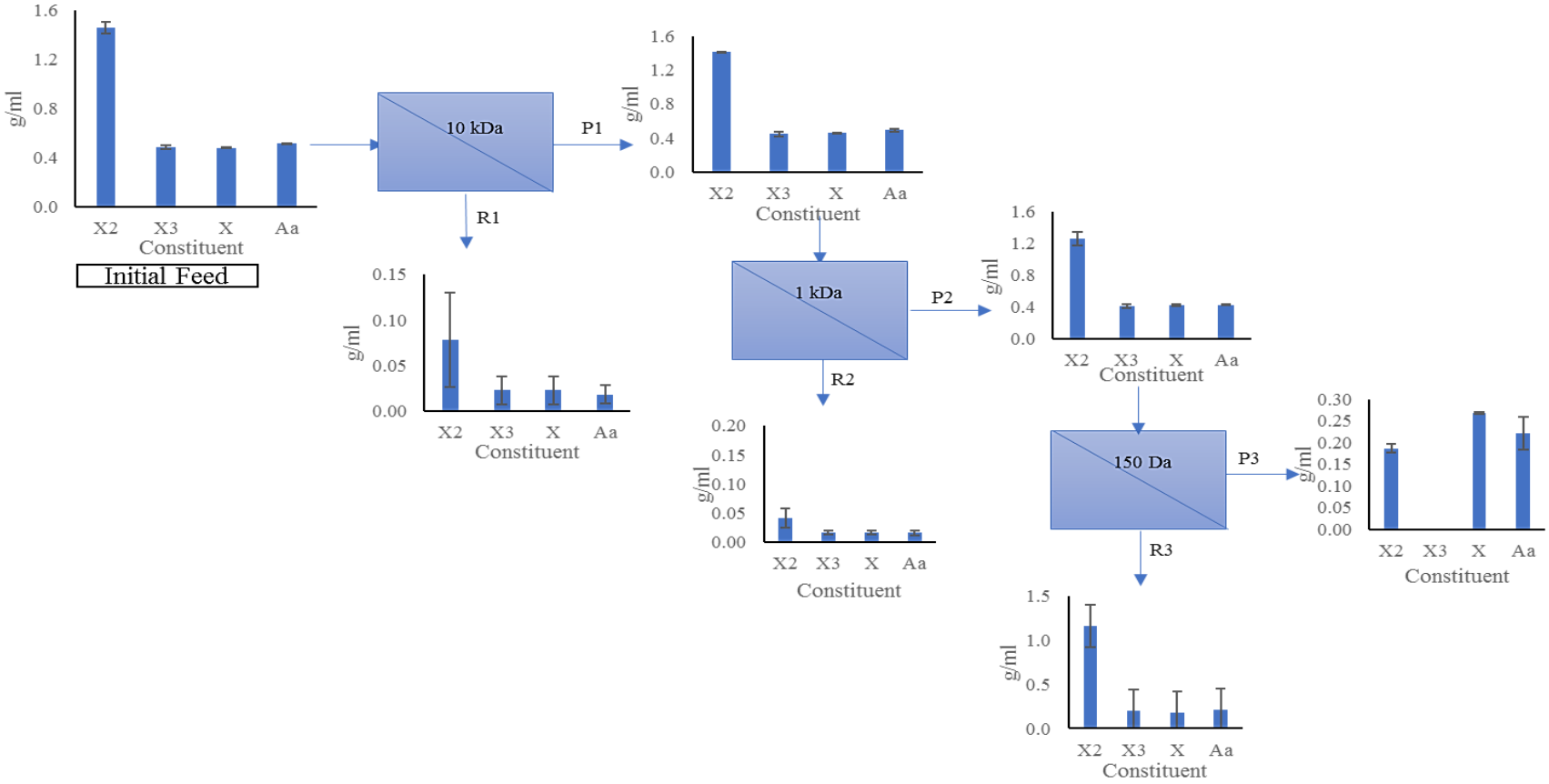
1.6
1.2
0.8
0.4
0.0
g/ml
X2 X3 X Aa
Constituent
Initial Feed
10 kDa
P1
R1
0.15
0.10
0.05
0.00
1 kDa
P2
R2
0.20
0.15
0.10
0.05
0.00
150 Da
P3
R3
1.5
1.0
0.5
0.0
0.30
0.25

Figure 9.2: Mass balance of membrane separation of enzymatically produced XOS.

For 1 kDa membrane, the rejection was xylobiose: 7%, xylotriose: 3.4%; xylose: 5.2% and acetic acid: 11%. Finally, for 150 Da the rejection was xylobiose: 86%; xylose: 39% and acetic acid: 50%. In other words, more than 50% of xylose and acetic acid could be removed from 150 Da feed. However, for 150 Da, about 79% of xylobiose could be observed in retentate (R3). The analysis of permeate (P3) indicates the presence of xylobiose, which could permeate through the membrane. The pattern of loss of constituent upon filtration through 150 Da is, as shown in Figure 9.3. As can be observed from the Figure, the loss of xylobiose at the initial stage nearly doubles with an increase in permeation time and subsequently the difference in loss decreases and at the end of filtration about 14% could be detected in permeate. As evident, no xylotriose was detected in permeate (P3), and the loss can be due to entrapment in the pores of the membrane as seen in SEM image. For xylose and acetic acid, the loss increases with time. As xylobiose and xylotriose loss was observed during permeation, the permeation was stopped, and diafiltration not attempted.

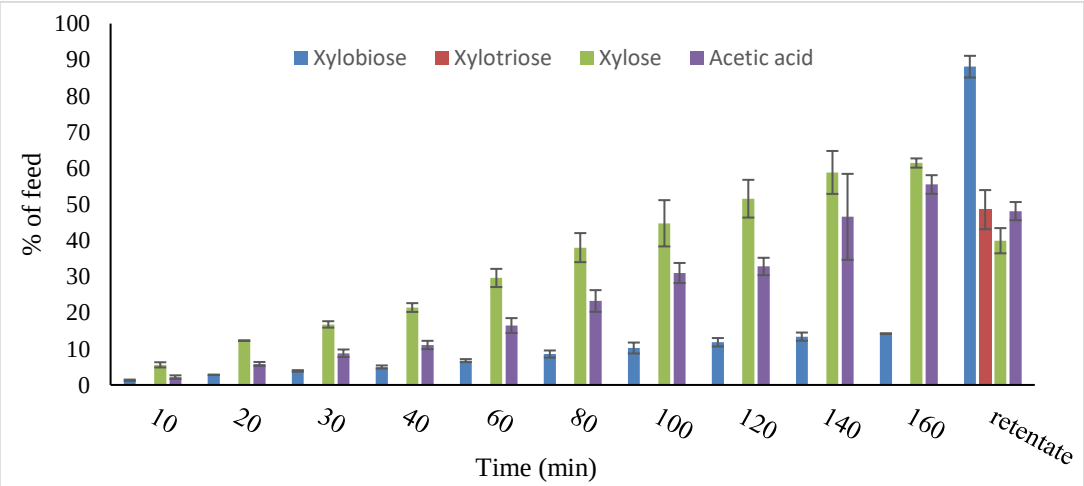

(a)

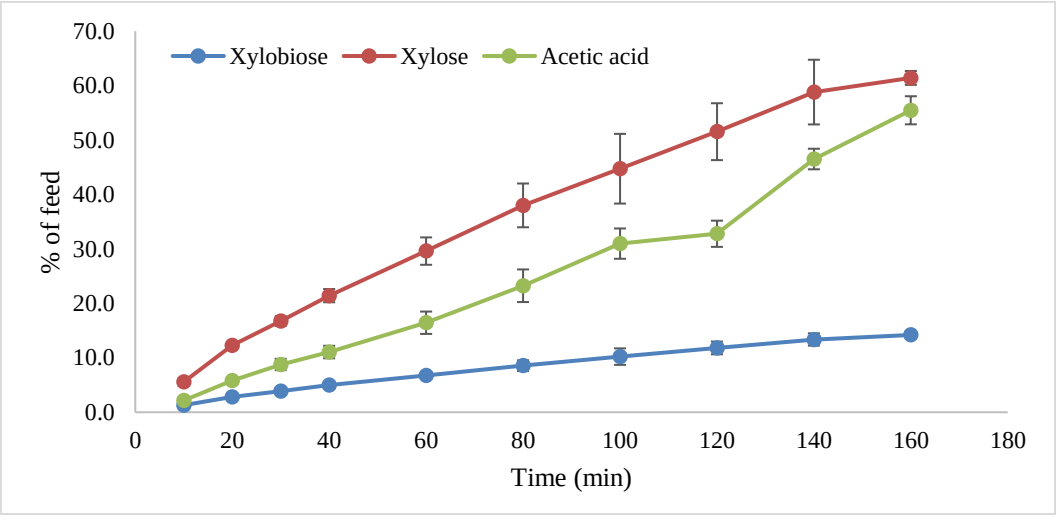

(b)

Figure 9.3: The percentage permeation of each component with time upon filtration through 150 Da

The loss of xylobiose and xylotriose in the pores may be because the membrane used had a molecular weight cut-off of 150-300 Da, with the maximum pore of 150 Da. Although the loss of xylotriose is high, it can be beneficial when the process is upscaled or used for several batches as the blocked pores may prevent further loss. At the end of filtration through 150 Da, the composition of permeate (P3) was 12.8% xylobiose, 55.6% xylose, and 42.7% acetic acid. Thus, the retentate was enriched in xylobiose (79.1%) and xylotriose (41.3%) along with 36.1% xylose and 40.7% acetic acid. Out of all the XOS present in the original feed, it was observed that about 69.6 ± 3.8% could be recovered with a VCR of about 4. The concentration of xylobiose increases from 7.1 mg/ml (in feed) to 49.1 mg/ml in 150 Da retentate (R3) whereas, the concentration of xylotriose rises from 2.3 mg/ml to 9.1 mg/ml.

The 150 Da filtered liquor was observed to be light yellow (Figure 9.4). Hence for decoloration and further removal of an organic acid, the liquor was treated with Diaion WA-30 resin. Diaion is a weak base resin, which is reported to remove colorant and organic acid. After treatment with resin, a part of liquor was evaporated to measure the total solid content, and another part was used for measurement of XOS by HPLC.

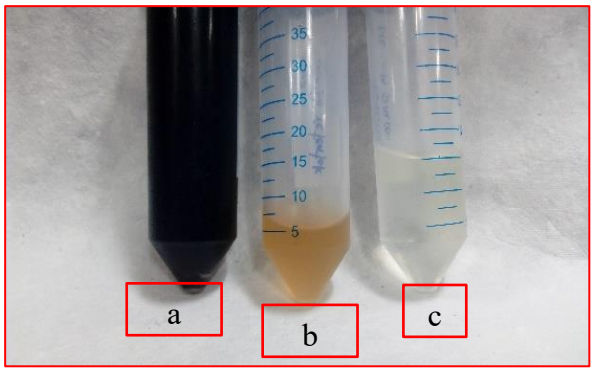

Figure 9.4: Colour of (a) feed (b) 150 Da retentate and (c) Diaion treated liquor

It was observed that the Diaion treated liquor was composed of 72.2% of XOS, composed of xylobiose and xylotriose. Thus, indicating the purity of 72% concerning XOS. The total xylose sugar-based molecules constitute 76.9% including, XOS and xylose. Interestingly, the liquor obtained after resin treatment was colorless, which indicates the removal of color imparting impurities. However, the liquor was still observed to be composed of about 10% acid.

The change in absorbance of the feed, the permeates, and the Diaion treated XOS liquor is as shown in Figure 9.5. It can be observed that the absorbance decreases upon filtration. However, there was an increase in absorbance for 150 Da retentate. It was observed that the color of 150 Da retentate was slightly darker than the 1 kDa permeate, which may be due to the concentration of color imparting phenolics, which was not filtered. The amount of phenolic impurity was estimated by measuring absorbance values at 230 and 280 nm. It was observed that the absorbance decreases from about 4 to 0.9 and 1, at 230 and 280 nm, respectively (Table 9.2). The decrease in absorbance value indicates a reduction of color imparting impurities.

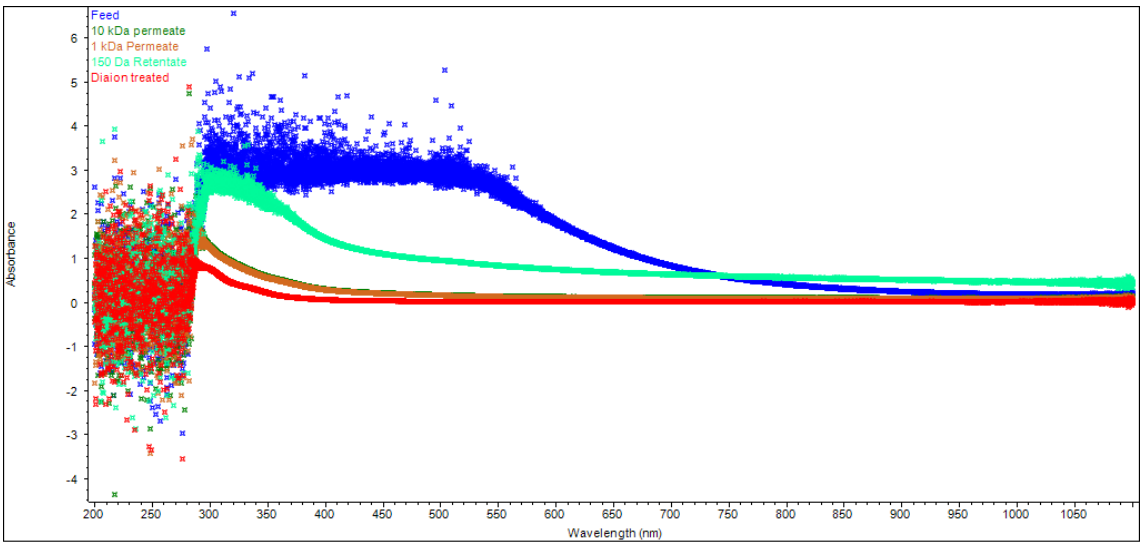

Figure 9.5: UV-Vis spectra of membrane refined XOS at different stages of filtration

Table 9.2: Absorbance at 230 and 280 nm of samples at a different stage of membrane refining

Sample	230 nm	280 nm
Feed	3.9	3.8
10 kDa permeate	1.8	1.9
1kDa permeate	1.7	1.4
150 Da retentate	2.5	2.2
Diaion treated	0.9	1.0

The cross-section of the membranes used for the filtration process was visualized using FEG-SEM and shown in Figure 9.6. As seen in the figure, the 10 kDa membrane shows the presence of asymmetric pores of nearly uniform size and also the presence of contaminants. These contaminants are possibly due to the higher molecular weight impurities present in the enzymatic liquor which were unable to pass through the membrane. The 1 kDa membrane allowed nearly all the constituents to pass through and hence does not show the presence of contaminants or blockage of membrane pores. As per the vendor's label, the 150 Da membrane has MWCO in range of 150-300 Da. Hence, different pore size could be observed in FEG-SEM. Interestingly, it can be observed that the particles are larger than the pores and hence were either retained on the surface or entrapped in the pores. This may be the reason for the loss of xylotriose upon filtration, as no xylotriose was observed in permeate.

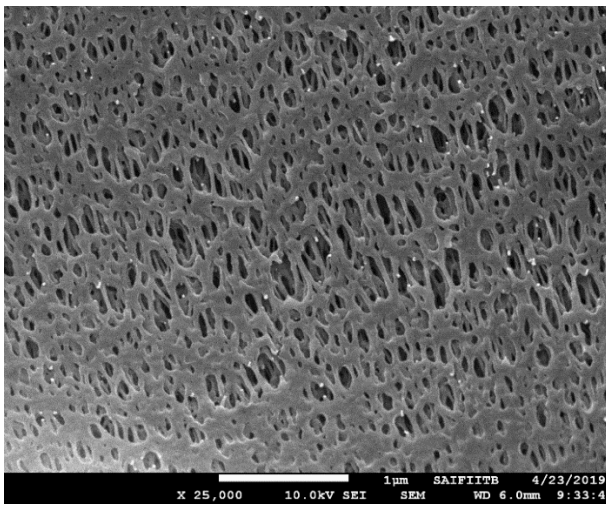

(a)

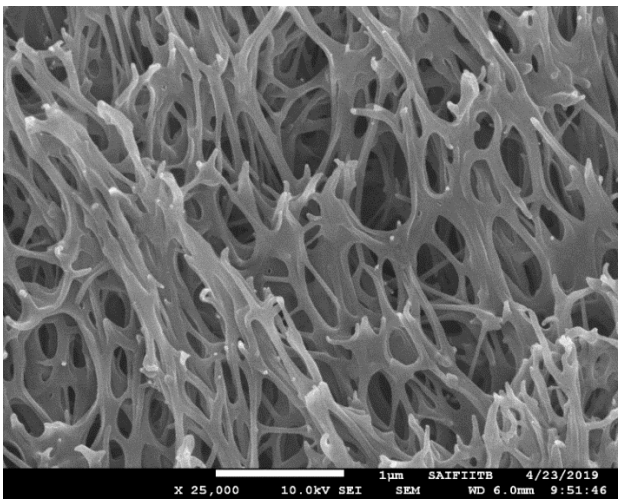

(b)

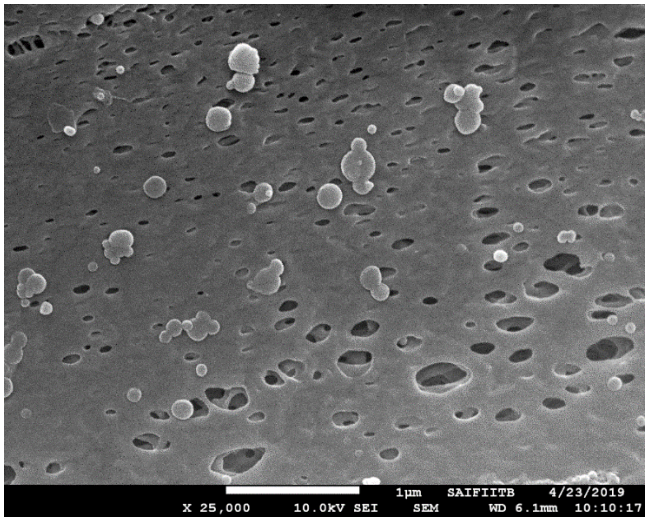

(c)

Figure 9.6: FEG-SEM images of membranes after filtration process (a) 10 kDa, (b) 1 kDa and (c) 150 Da

9.2.2. *In-vitro* human fecal fermentation:

Various studies about prebiotic oligosaccharides have measured the extent of SCFA produced upon fermentation using feces and its implication on health (Morrison & Preston, 2016). Apart from SCFA, gases (including carbon dioxide, hydrogen) are produced upon prebiotics microbial fermentation and are considered as an influential clinical deterrent for consumption (Cummings, Macfarlane, & Englyst, 2001). Hence, in this study, we measured the total SCFA concentration and gas production upon human fecal fermentation of almond XOS and compared with commercial XOS, FOS, and inulin. The in- vitro fermentation of fiber in

human fecal was studied in three healthy adults (male, mean age 25 y). The total volume of gas produced along with pH and SCFA concentration at the end of 4 h incubation in response to varying fiber is as shown in Table 9.3. The total SCFA concentration was not found to be significantly different among the fiber at the end of 4 h incubation, however levels of acetate were found to be significantly different. The XOS from corn and almond produced significantly higher acetate as compared to inulin and FOS, whereas, a higher level of butyrate was observed for inulin and FOS. The bacterial species belonging to *Bifidobacterium* phyla are thought to be specialized in uptake and metabolism of short-chain carbohydrates or oligosaccharides to produce acetate (Rivière, Selak, Lantin, Leroy, & De Vuyst, 2016).

Table 9.3: Magnitude of gas production, differences in pH and SCFA at the end of the four hours experimental period for each fiber substrate.

Parameter	FOS	Inulin	XOS (corn)	Almond XOS	*p* value
Total gas production (ml/g)	82.1 ± 19.1	87.2 ± 39.5	63.2 ±5.5	32.1 ± 12.1	0.07
pH	5.3 ± 0.1^{a,b}	5.3 ± 0.2^{b}	5.2 ± 0.1b	5.6 ± 0.1^{a}	0.01
pH change (% from baseline)	-24.5 ± 2.0	-23.2 ± 2.5	-27.1± 2.6	-19.3 ± 1.5	-
Total SCFA (umol/g)	79.3 ± 7.7	75.9 ± 12.0	108.0 ± 31.0	83.0 ± 14.0	0.21
Acetate (umol/g)	47.0± 4.3^{b}	45.0 ± 12.0^{b}	74.0 ± 18.0^{a}	68.0 ± 8.2^{a,b}	0.01
Propionate (umol/g)	5.3 ± 2.4	7.4 ± 5.0	9.6 ± 1.3	8.4 ± 2.6	0.85
Butyrate (umol/g)	33.0 ± 7.2	30.0 ± 6.8	25.0 ± 13.0	15.0 ± 5.5	0.13
Acetate (% total SCFA)	53.6 ± 2.3^{b}	52.5 ± 4.4^{b}	65.7 ± 1.8^{a}	68.3 ± 4.0^{a}	<0.01
Propionate (% total SCFA)	10.8 ± 3.2	13.0± 4.1	11.0 ± 2.6	11.5 ± 4.1	0.87
Butyrate (% total SCFA)	34.1 ± 3.2^{a}	32.9 ± 3.1^{a,b}	21.8± 4.8^{b,c}	18.9± 6.2^{c}	<0.01

Values shown represent mean (SD) of three replicate experiments.[1] Differences between fibers evaluated using one-way ANOVA. Significant differences ($p < 0.05$; Tukey's test) between fibers highlighted with the use of different superscripts. The means are compared across the column.

This can be the reason attributed to higher levels of acetate with shorter DP oligosaccharides such as corn cob XOS and Almond XOS. As shown in Figure 9.6, the mean total gas

production was highest for FOS followed by inulin; corn derived XOS and XOS produced in this study. As can be observed from Figure 9.7, the fermentation of XOS produces lower gas volume as compared to FOS and inulin. The difference in gas production upon fermentation of a carbohydrate source can be ascribed to a difference in the backbone and structural composition, chain length or the degree of polymerization. Among the XOS, gas production upon almond XOS fermentation was low than commercial XOS. This can be ascribed to the difference in purity (not determined), and composition. However, as can be observed, no major significant difference in gas production was observed between the fiber substrates ($p = 0.07$). Nonetheless, the lower volume of gas being produced may be clinically relevant, potentially reducing the level of discomfort following consumption, thereby giving XOS can have higher acceptance rate among consumers. However, such outcomes need to be verified by a human intervention study.

The changes in pH of the fecal slurry, both absolute and as a percentage from baseline, were proportional to other endpoints assessed namely, total gas production and SCFA concentrations.

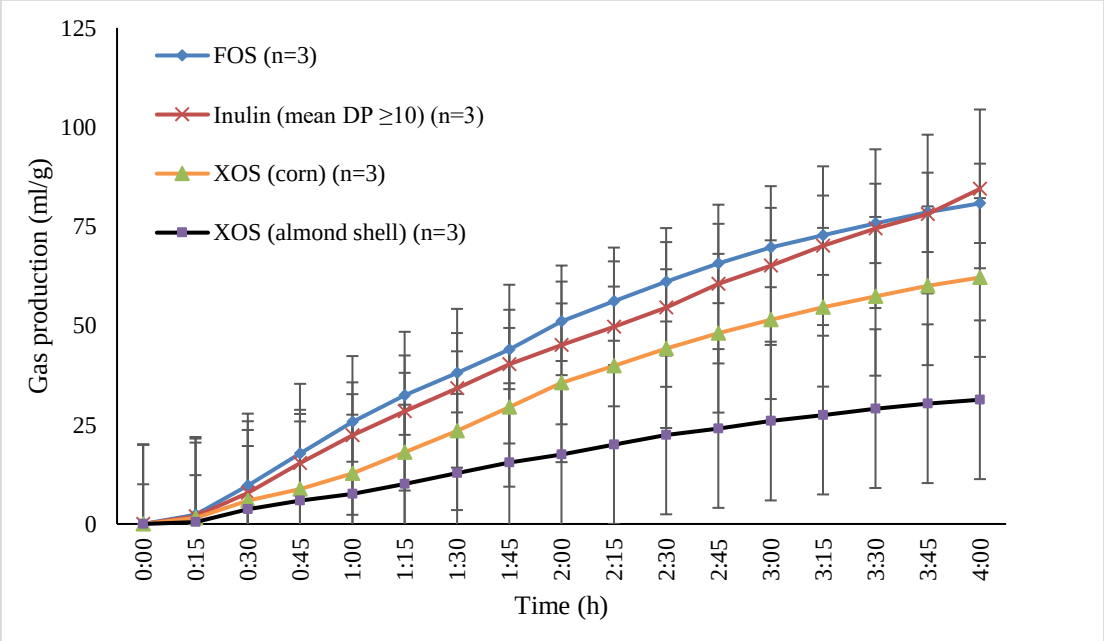

Figure 9.7: Kinetics of total gas production over four hours for different fiber substrates. Values are mean (n = 3) ± SD

9.2.3. *In-vitro* bacterial fermentation:

The *Lactobacillus* strains such as *L. acidophilus, L. paracasei, and L. rhamnosus* was used to determine the prebiotic ability of almond XOS.

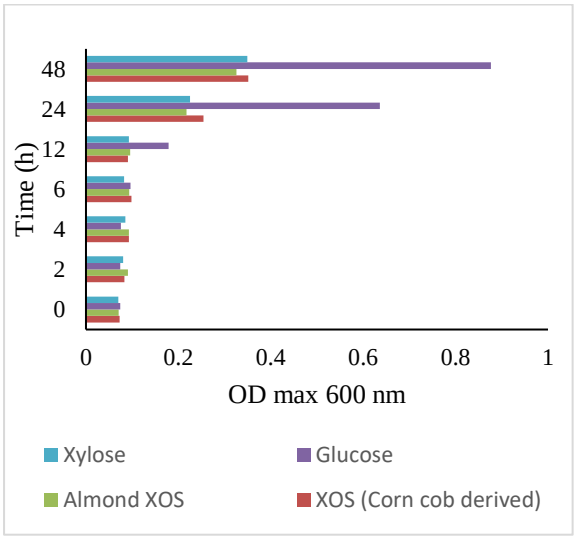

L. acidophilus

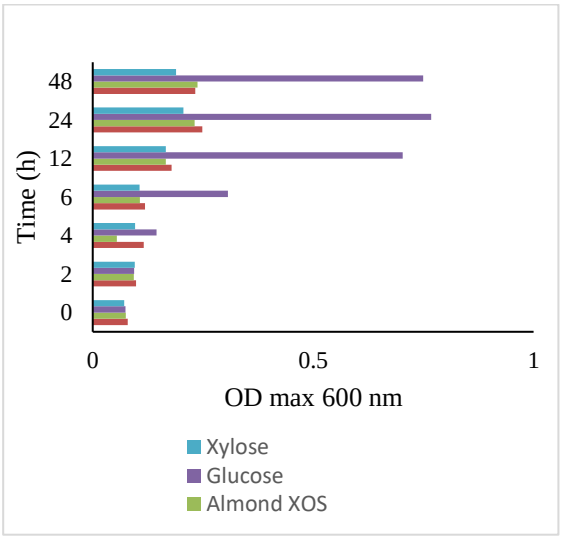

L. paracasei

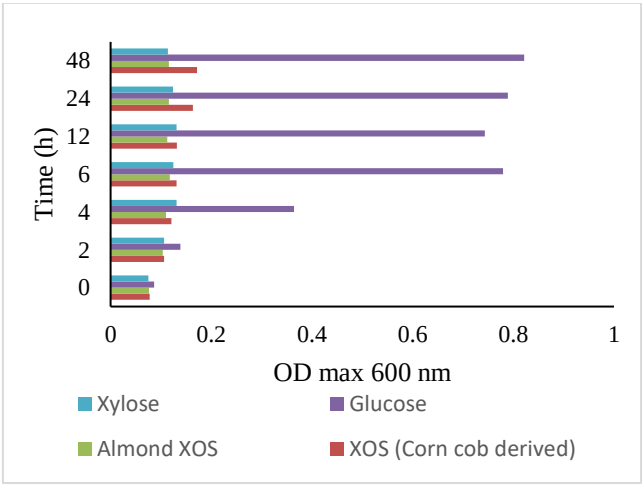

L. rhamnosus

Figure 9.8: Optical density measured upon fermentation of carbohydrates by *Lactobacillus spp.*

The growth of bacteria was determined as optical density (OD) measured at 600 nm. The OD of various strains on different carbohydrate substrates is as shown in Figure 9.8. It was observed that all the strains which were tested, were able to grow significantly on XOS. Also, the growth on almond XOS was similar to that observed for commercial XOS. For *L. acidophilus*, the OD upon almond XOS fermentation increases from 0.07 to 0.87, indicating a

12 fold increase in a bacterial cell population in 48 h. Similarly, for *L. paracasei*, and *L. rhamnosus*, a ten-fold increase was observed.

However, the increase in cell population was similar to that of xylose, indicating that *Lactobacillus species* can utilize both xylose monomer and oligomer for an energy source. As *Lactobacillus* possess high ability to ferment glucose, a very high increase in bacterial cell population was observed for all strains. However, it can be argued that as glucose is primarily used as a source of energy for human, the relative abundance in the proximal part of gut or colon may be low. Moreover, as evident from this work, almond derived XOS can be used as a source of energy by gut bacteria for growth. Another indication of the growth of bacteria is the pH of the medium. As fermentation proceeds, short chain fatty acids are produced, which lowers the pH of the medium. It has been suggested that a decrease in the pH below 5 should be considered as an endpoint of fermentation as most of the gut bacteria start dying below pH 5. This was observed during fermentation using human fecal samples. The change in pH as fermentation proceeds is depicted in Figure 9.9 for different carbohydrates studied. It was observed that for glucose, the pH decreases to below 5 after 24 h of fermentation, owing to preferential uptake and utilization by *Lactobacillus*. However, for xylose based molecules, the pH fall was not significant, and a decrease of 0.2-0.4 units was observed from initial pH. As mentioned, the putative health claims of prebiotics are, to an extent ascribed to the short chain fatty acids produced upon fermentation by gut bacteria. Hence the SCFA including, acetate, propionate, butyrate, was measured at the end of fermentation (48 h). The concentration of SCFA's produced is as shown in Table 9.4.

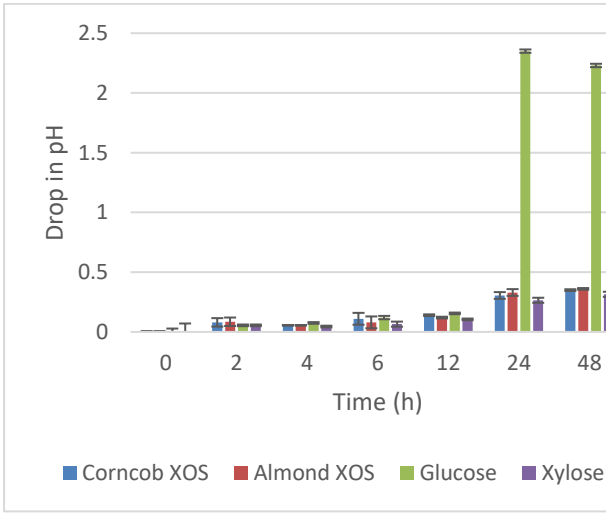

L. acidophilus

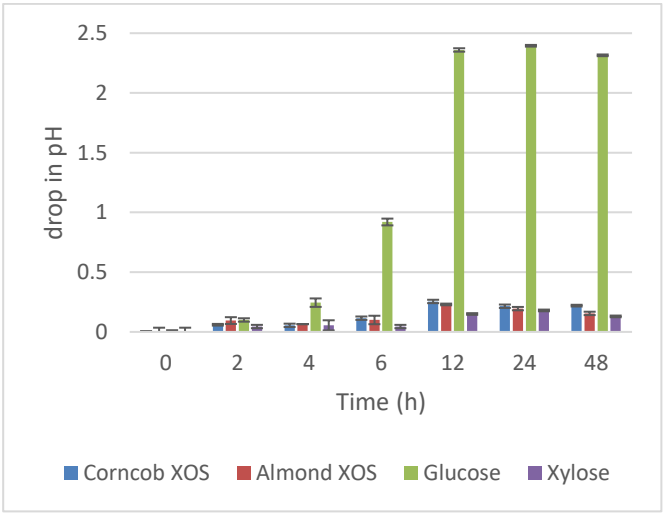

L. paracasei

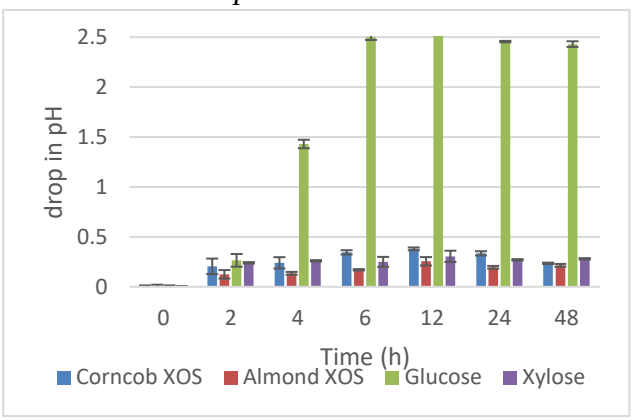

L. rhamnosus

Figure 9.9: Drop in pH as measured upon fermentation of carbohydrates by *Lactobacillus spp.*

At the end of fermentation, the residual XOS was estimated to determine if there is preferential utilization of particular DP. The results are shown in Figure 9.10. It was observed that for commercial XOS which was composed of xylobiose, xylotriose and xylotetrose; xylobiose was consumed maximum by *L. acidophilus* and *L. paracasei*. The residual xylobiose was found to be 57% and 61%. The findings of bacterial fermentation corroborate the results of human faecal fermentation in terms of maximum acetate production by XOS. With all the carbohydrate evaluated, the *Lactobacillus* predominantly produces acetate, representing 90% of total SCFA produced. Within the bacterial strains evaluated, it can be seen that *L. paracasei* gave a higher concentration of acetate for all carbon source as compared to other strains.

Table 9.4: The SCFA level produced upon fermentation of carbohydrates by *Lactobacillus spp*

Substrate	Bacterial species	SCFA (µmol)			
		Acetate	Propionate	Butyrate	Total
Corncob XOS	*L. rhamnosus*	7.23 ± 0.44	0.35 ± 0.01	0.04 ± 0.02	7.62 ± 0.25
	L. acidophilus	14.0 ± 0.8	0.5 ± 0.3	0.1 ± 0.1	14.6 ± 0.8
	L. paracasei	22.15 ± 0.96	0.96 ± 0.10	0.08 ± 0.04	23.19 ± 0.51
Almond XOS	*L. rhamnosus*	6.49 ± 2.59	0.12 ± 0.06	0.03 ± 0.01	6.74 ± 1.50
	L. acidophilus	14.9 ± 5.3	0.4 ± 0.1	0.1 ± 0.1	15.4 ± 1.5
	L. paracasei	30.58 ± 3.11	0.59 ± 0.04	0.02 ± 0.02	31.19 ± 1.78
Glucose	*L. rhamnosus*	14.52 ± 2.92	0.14 ± 0.09	0.06 ± 0.02	14.72 ± 1.65
	L. acidophilus	16.0 ± 0.3	0.2 ± 0.1	0.1 ± 0.1	16.3 ± 1.7
	L. paracasei	46.97 ± 0.12	0.85 ± 0.33	0.29 ± 0.10	48.12 ± 0.13
Xylose	*L. rhamnosus*	3.96 ± 0.72	0.37 ± 0.04	0.07 ± 0.02	4.39 ± 0.02
	L. acidophilus	14.0 ± 0.9	0.2 ± 0.1	0.1 ± 0.0	14.2 ± 0.4
	L. paracasei	17.51 ± 1.56	0.78 ± 0.24	0.04 ± 0.03	18.33 ± 0.83

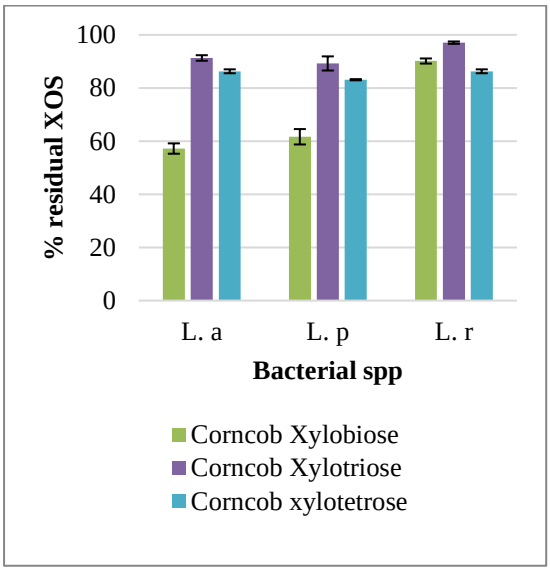

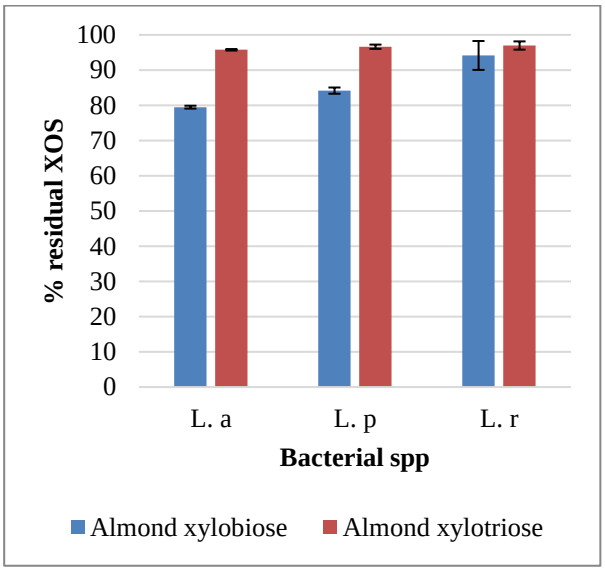

Figure 9.10: The residual XOS content at the end of fermentation

The residual xylotriose and xylotetrose level were 85-90% at the end of fermentation. In the case of almond XOS, produced in this study, the product was composed of xylobiose and xylotriose, and it was seen that about 15-20% xylobiose was consumed by *L. acidophilus* and *L. paracasei*. The residual xylotriose level was above 90% in all cases. Thus, the findings indicate that among XOS, xylobiose is preferably utilized by bacteria in comparison to

xylotriose and xylotetrose. Thus, the production of low DP XOS, as was the objective, in this study is justified.

9.3. Conclusion:

The alkali extracted hemicellulose was enzymatically converted to XOS. The enzymatic liquor was refined using 10 kDa, 1 kDa, and 150 Da membranes in an ultrafiltration cell. The 10 kDa membrane was successful in removing the higher molecular weight impurities, including the enzyme. Upon filtration, more than 90% of each constituent was present in permeate. Further, refining using 1 kDa membrane did not produce a significant influence on the liquor concerning composition or color intensity. The liquor was finally treated with 150 Da, wherein a slight increase in color was observed possibly due to the concentration of small molecular weight phenolics. At the end of the filtration process, 79% of xylobiose, 41% of xylotriose was retained as compared to initial feed. The liquor was also composed of 36-40% xylose and acetic acid hence was further treated with Diaion resin to assist in de-coloration and de-acidification. Upon resin treatment, the color intensity and impurities as measured by absorption at 230 and 280 nm was reduced from 3.8 to 0.9-1. Also, about 10% of acetic acid could be removed. The final purity of enzymatically produced XOS (sum of xylobiose and xylotriose) was about 72%.

The *in-vitro* fermentation of almond derived XOS using human fecal matter shows that XOS is rapidly fermented to produce SCFA and gases. The total SCFA produced upon fermentation was about 93 umol/g with acetate as predominant SCFA. The total gas produced upon fermentation of XOS was 32 ml/g. The fermentation products of almond XOS was observed to be similar to commercial XOS. The *in-vitro* fermentation of XOS using Lactobacillus could increase the bacterial population, thereby indicating that XOS acts as an energy source. The SCFA composition corroborates the finding from the fecal fermentation study, as acetate was the predominant metabolite. It was also observed that among xylobiose, xylotriose, and xylotetrose, Lactobacillus consumed xylobiose to a considerable extent. Thus, it can be concluded that XOS can be used as an energy source for gut bacteria, and production of low DP XOS is justified.

Chapter 10 Conclusion and Future work

Annually, billions of tonnes of lignocellulosic residues are generated. Though not all of it can be considered as waste. In India, after accounting for fodder, feed, and other uses, the surplus quantity from agricultural, forestry, the wasteland was estimated to be about 240 million tonnes in 2010-11 and expected to increase to 281 million tonnes by 2030 (Purohit & Chaturvedi, 2018). In Australia, the major source of lignocellulose includes bagasse, forestry waste, and crop stubble. It is reported that the production of the two dedicated energy crops, *Arundo donax,* and *Forage sorghum*, is about 51 tonnes and 14 tonnes per hectare, respectively. Among the major fruit industry, banana and pineapple are considered to produce huge quantum of lignocellulosic waste. In 2013-14, banana production was reported to be 372000 tonnes. As one tonne of banana generates about 4 tonnes of pseudo-stem, the lignocellulosic waste can be accounted for about 1.4 million tonnes. In the case of pineapple, the stem and leaves amount to 50% of pineapple fruit weight. Approximately 85000 tonnes of pineapples were produced in the year 2009-10, thus giving about 42500 tonnes of waste. Among the agricultural industry, sugarcane is the dominant contributor to lignocellulosic waste in Australia where the production scores above 30 million tonnes. As about 3 tonnes of bagasse is generated from 10 tonnes of sugarcane, approximately 9 million tonnes of bagasse is available for valorisation (Kosinkova et al., 2017). Though limited literature is available to provide a total estimate of lignocellulosic residue in Australia, the above examples provide an insight into the potential of raw material availability for valorisation. The huge quantity of surplus biomass is a matter of concern due to improper disposal, cost incurred for disposal or burning, thereby leading to an environmental concern.

The looming danger of depletion of fossil fuels and the associated adverse effect of its use on climate has accelerated research in search of alternative fuels. The lignocellulosic biomass has received increased interest because of cellulose, the most abundant biopolymer in nature. In a commercial setting, the cellulose is converted to glucose and finally into ethanol for blending with petrol. In this process, the hemicellulose is discarded as waste, possibly due to the increased difficulty of converting xylose into ethanol. However, techno-economic and environmental assessment studies for woody biomass and sugar beet pulp industry (González-García et al., 2016; Gonzalez-Garcia et al., 2018) have suggested utilization of low

value streams for value addition to achieve a successful bio-economy. Similarly, valorisation of hemicellulose can contribute to a lignocellulose-based circular economy. Also, hemicellulose represents about 25% of the biomass, thereby providing a abundant raw material. The hydrolysis product of hemicellulose, namely, xylooligosaccharides are classified as a functional food, more specifically as a prebiotic. Commercially available prebiotics such as fructooligosaccharides, inulin, galactooligosaccharides have documented health benefits. However, they are obtained from limited natural resources and thus, synthesized chemically. XOS offers an advantage of abundantly available, cheaply available starting material.

In this work, arecanut husk and almond shell were used as a substrate, as they both possess different physical forms but has similar hemicellulose and lignin content of about 25%. Arecanut husk is generated predominantly in India, which accounts for 53% of global production. The husk represents 60-80% of the total weight of nut. In 2016-17, about 0.7 million tonnes of arecanut was produced (National Horticultural Database, 2017), thus generating about 0.5 million tonnes of husk. A fraction of husk is used as a solid fuel for household application, and the maximum is discarded as waste. The global production of the almond shell in 2018-19 recorded 1.4 million tonnes on the shelled basis. As shell constitutes about 50% of the total nut, the quantity of shell generated was about 1.4 million tonnes. A process enabling efficient production of XOS from high lignin biomass can also be used for another biomass. Thus, biomass with higher lignin content was used in this study. In this work, alkaline pretreatment and autohydrolysis process of production of XOS was evaluated. Alkaline pretreatment for extraction of hemicellulose and subsequent enzymatic hydrolysis of hemicellulose to XOS has been reported for several biomass. It was observed that 12-16% of alkali is reported optimal for more than 90% recovery of hemicellulose. Also, the reported biomass had lignin content of less than 20%. As alkali and enzyme are the important factors governing efficacy and economics of the process, in this work, efforts were concentrated to minimize the chemical loading and enzyme cost. With autohydrolysis as a process, it was observed that wide DP range XOS product is obtained. As a narrow and low DP XOS is more beneficial as an energy source for the bacterium, the objective was to maximize low DP XOS in the liquor.

The alkaline pretreatment of arecanut husk was studied using different alkali concentration with and without heat assistance. It was observed that when biomass was soaked in alkali (20%) for 16 h and then subjected to hydrothermal treatment (121^{o}C, 1 h), about 82% of hemicellulose could be recovered while achieving about 70% delignification of biomass. Whereas about 75% hemicellulose was recovered when biomass was treated with alkali (20%) for 1 h at 121^{o}C, without any incubation. By further increasing hydrothermal time to 1.5 h, about 83-86% hemicellulose could be recovered at 15% w/v alkali. Thus, decreasing alkali concentration was possible by increasing reaction time. In case of microwave irradiation used as an energy source, the highest hemicellulose recovery was 52% of the available hemicellulose with 3 min as reaction time. As the microwave irradiation was performed using home-use microwave oven, the presence of open system prevents studying higher reaction time, due to loss of solvent. With microwave irradiation, about 82% of lignin from biomass could be dissolved into alkali solution. The residue obtained after pretreatment was cellulose-rich and could be enzymatically hydrolyzed to sugars. Upon enzymatic hydrolysis, 75-79% reducing sugar was released consisting of 69.2 ± 1.3% of glucose. Thus, alkaline pretreatment enabled to develop a biorefinery prospective for arecanut husk. As reaction time, temperature were important parameters governing hemicellulose recovery, further optimization of process was carried out by studying different incubation time, incubation temperature, alkali concentration, and assistance of hydrothermal treatment. With 25^{o}C as incubation temperature, the recovery of hemicellulose increases with an increase in alkali concentration and incubation time. The maximum which could be recovered was 19.01 ± 0.58% at 20% alkali. Increase in incubation temperature to 50^{o}C increases the recovery to 54.01 ± 2.75%, whereas the incubation temperature of 65^{o}C gave 67.12 ± 1.42% hemicellulose relative recovery. The observation of data reveals that upon incubation of biomass for 8-24 h and 65^{o}C, alkali concentration of 10% was able to recover 40-50% of hemicellulose. Hence, these conditions were selected for hydrothermal assisted extraction. The obtained results suggest that hydrothermal treatment for 1 h of incubated biomass could recover more than 90% of the available hemicellulose. The ANOVA analysis indicates alkali concentration, hydrothermal time, incubation period having a significant influence on hemicellulose recovery. The interaction term of hydrothermal time-alkali concentration and hydrothermal time-incubation period also significantly influences hemicellulose recovery.

Thus, the optimal condition for more than 90% hemicellulose recovery from arecanut husk was incubation of biomass at 65^{o}C for 8 h in 10% alkali and subsequent hydrothermal treatment for 1 h. The enzymatic hydrolysis of extracted hemicellulose was performed using endoxylanase at different pH, temperature, and enzyme dose. The optimal condition was 10 U of enzyme dose, 50^{o}C and pH 4, under which the XOS yield was 35.2 ± 1.3 g/100g xylan. The liquor was composed of XOS with DP 2-4, with xylobiose being the predominant oligosaccharide accounting to 71% of total XOS, followed by 26.2% of xylobiose and 2% of xylotetrose. The ANOVA analysis indicates good fit between observed and model predicted values, where the linear and the interaction terms were significant. Thus, the study was able to develop a process for the valorisation of arecanut husk into XOS, where the reported alkali concentration is lowest for maximum recovery of hemicellulose. This can be translated as a reduction in the cost of chemical consumed during the process.

The extraction of hemicellulose from the almond shell using alkaline pretreatment was studied after particle size reduction, to visualize the effect of particle size on alkali concentration. The particle size was reduced using either a ball mill or grinding. The shell was ground in ball mill for different time (0.5-4 h) after which the material was sieved to determine particle size range. In both the milling process, particle size was found as an important variable for maximum recovery of hemicellulose at alkali concentration of 8%. Upon ball milling for 4 h maximum particles were below 120 µm and in this case, more than 90% hemicellulose was extracted at 8% w/v NaOH in 1 h at 121^{o}C. A similar observation was reported for ground samples, wherein particle size below 120 µm gave above 90% recovery under similar experimental conditions. Thus, it can be inferred that irrespective of the mechanism of milling, if the particles are smaller than 120 µm, maximum hemicellulose can be extracted. This implies that ball milling, which is an expensive and energy-intensive process can be substituted with grinding. For enzymatic hydrolysis, endoxylanase from *Thermomyces lanuginosus* was employed. To minimize the cost of enzymes, immobilization of the enzyme on magnetic nanoparticles was studied to allow reuse of enzyme. The immobilized enzyme was found to be at par with the free enzyme in terms of pH and temperature profile, and reaction kinetics. For free enzyme, it was observed that XOS yield decreases with an increase in temperature from 50 to 60^{o}C; however, in case of an

immobilized enzyme similar yields could be obtained at both temperatures. This suggests that immobilized enzyme have better thermal stability and can be applied for reaction with longer residence time. Interestingly, upon reuse of immobilized enzyme using fresh substrates, the yield of XOS decrease to 41% of the initial cycle at cycle 3. Thus, it is inferred that the immobilized enzyme has limited applicability for XOS production, as longer reaction time is warranted to maximize XOS yield. Hence, interventions such as supplementation of loss in enzyme activity with the free enzyme or the immobilized enzyme in consecutive cycles can be studied. However, a thorough economic analysis of such intervention is a must to validate the usefulness. Further, response surface methodology was used to determine the lowest possible enzyme dose, which can hydrolyse the highest possible substrate while producing high XOS yield. The analysis of results indicates that 10 U of the enzyme is optimal. Also, for maximum conversion of xylan into XOS, the substrate concentration should be below 2%. It was observed that the desirability of high XOS yield decreases with an increase in substrate concentration. This is due to increased viscosity of medium, causing depletion of water molecules for the enzyme and also limiting mass transfer. Thus, based on work done with the almond shell, it can be concluded that particle size is a crucial factor and near complete hemicellulose recovery is possible if the particles are less than 120 µm. Also, immobilized enzyme though has similar physico-chemical properties; it has limited applicability in terms of reusability for XOS production.

The enzymatically obtained XOS was refined using membrane-based ultrafiltration and resin treatment. For membrane refining, 10 kDa, 1 kDa, and 150 Da membranes were used. Upon filtration, most of the impurities present as an enzyme, higher molecular weight phenolics, and particulate matter was retained on 10 kDa, while the permeate was composed of more than 90% of xylobiose, xylotriose, xylose and acetic acid present in the feed. This liquor was then filtered through 1 kDa, wherein no major change in composition and color intensity was observed. The final filtration through 150 Da membrane could retain 79% of initial xylobiose along with 41% of xylotriose. Out of the total xylotriose present in feed of 150 Da, only 41% could be observed in the retentate, and none was detected in permeate. Hence, the loss may be due to entrapment in pores of the membrane. The 150 Da retentate was also composed of 36-40% of initial xylose and acetic acid. Finally, the concentrated XOS liquor was treated

with Diaion WA 30 resin to cause de-coloration and de-acidification. Upon resin treatment, the XOS product with 72% purity was obtained containing about 10% of acetic acid. The color intensity and impurity as determined by absorbance at 230 and 280 nm was reduced from 3.8 to 1.0.

The *in-vitro* fermentation of XOS was studied using human fecal matter and *Lactobacillus* spp. XOS was rapidly fermented by bacteria present in fecal samples as indicated by a decrease in pH below 5 within 4 h of fermentation. The fermentation resulted in the production of SCFA and gases, which was similar to that of commercial corn derived XOS. The *in-vitro* fermentation using Lactobacillus suggest that XOS acts as an energy source for the bacterium, as the bacterial population increases by 10-12 fold in 48 h. The SCFA produced upon fermentation has acetate as a predominant metabolite, similar to that obtained for fecal fermentation. It was also observed that xylobiose was consumed to larger extent (40%) as compared to xylotriose and xylotetrose (less than 20%). Thus, it can be concluded that the obtained almond XOS can act as an energy source for gut bacterium, and based on results, production of low DP XOS is justified.

The in-situ generated hydronium ion during autohydrolysis catalyzes the cleavage of glycosidic linkages of hemicellulose, thus is a greener alternative for XOS production. The autohydrolysis process was studied in the temperature range of 180-220, under which hemicellulose is susceptible to hydrolysis. For the almond shell, 54.5 ± 1.0% of available xylan was hydrolyzed in soluble oligosaccharides, containing only 1.8% of low DP XOS (sum of xylobiose and xylotriose). The pH of the autohydrolysate was adjusted to 5.8, as the endoxylanase from *Thermomyces lanuginosus* shows decreased activity at pH below 4 (the pH of autohydrolysate liquor). Upon enzymatic hydrolysis (10 U), low DP XOS concentration was 8.2% (of biomass), which represents 75% of oligosaccharides obtained from autohydrolysis. The membrane assisted refining of the enzymatic liquor enabled recovery of 69% of produced low DP XOS.

Thus, the work presents an optimized alkaline pretreatment process for recovery of maximum hemicellulose and its efficient conversion to prebiotic XOS. Alternatively, a greener approach has also been proposed for production and refining of XOS. In the future, the

developed process can be replicated at pilot scale to see the variation in yield brought by an increase in efficiency of unit operations. Also, a thorough techno-economic analysis should be performed for alkaline pretreatment and autohydrolysis concerning hemicellulose valorisation. A comparative techno-economic analysis of alkaline pretreatment and autohydrolysis will enable to visualize the better approach for XOS production. The hemicellulose economics can be evaluated in comparison of cellulose utilization for bioethanol production, to determine the effect on ethanol price brought by hemicellulose valorisation. This work supports the prebiotic effect of low DP XOS; however, it can be beneficial to compare the XOS obtained after autohydrolysis with low DP to estimate the change of bacterial growth/ utilization. Also, XOS can be evaluated in the presence of dietary fibers, insoluble fiber such as cellulose and its derivative to determine the overall beneficial effect in gastrointestinal diseases and disorders.

11. References:

AOAC (2000). Association of Official Analytical Chemists, Washington, DC.

A. Sluiter, R. Ruiz, C. Scarlata, J. Sluiter, A., & Templeton, D. (2008). Determination of Extractives in Biomass: Laboratory Analytical Procedure (LAP); Issue Date 7/17/2005 - 42619.pdf. *Technical Report NREL/TP-510-42619*, (January), 1–9. http://doi.org/NREL/TP-510-42621

Aachary, A. A., Gobinath, D., & Prapulla, S. G. (2011). Short chain xylooligosaccharides: a potential prebiotic used to improve batter fermentation and its effect on the quality attributes of idli, a cereal-legume-based Indian traditional food. *International Journal of Food Science & Technology*, *46*(7), 1346–1355. http://doi.org/10.1111/j.1365-2621.2011.02591.x

Aachary, A. A., & Prapulla, S. G. (2009). Value addition to corncob: production and characterization of xylooligosaccharides from alkali pretreated lignin-saccharide complex using Aspergillus oryzae MTCC 5154. *Bioresource Technology*, *100*(2), 991–5. http://doi.org/10.1016/j.biortech.2008.06.050

Aachary, A. A., & Prapulla, S. G. (2011). Xylooligosaccharides (XOS) as an Emerging Prebiotic: Microbial Synthesis, Utilization, Structural Characterization, Bioactive Properties, and Applications. *Comprehensive Reviews in Food Science and Food Safety*, *10*(1), 2–16. http://doi.org/10.1111/j.1541-4337.2010.00135.x

Aagaard, K., Ma, J., Antony, K. M., Ganu, R., Petrosino, J., & Versalovic, J. (2014). The placenta harbors a unique microbiome. *Science Translational Medicine*. http://doi.org/10.1126/scitranslmed.3008599

Aagaard, K., Riehle, K., Ma, J., Segata, N., Mistretta, T. A., Coarfa, C., … Versalovic, J. (2012). A metagenomic approach to characterization of the vaginal microbiome signature in pregnancy. *PLoS ONE*. http://doi.org/10.1371/journal.pone.0036466

Akpinar, O., Ak, O., Kavas, A., Bakir, U., & Yilmaz, L. (2007). Enzymatic production of xylooligosaccharides from cotton stalks. *Journal of Agricultural and Food Chemistry*, *55*(14), 5544–51. http://doi.org/10.1021/jf063580d

Akpinar, O., Erdogan, K., & Bostanci, S. (2009). Production of xylooligosaccharides by controlled acid hydrolysis of lignocellulosic materials. *Carbohydrate Research*, *344*(5), 660–6. http://doi.org/10.1016/j.carres.2009.01.015

Anwar, Z., Gulfraz, M., & Irshad, M. (2014). Agro-industrial lignocellulosic biomass a key to unlock the future bio-energy: A brief review. *Journal of Radiation Research and Applied Sciences*, *7*(2), 163–173. http://doi.org/10.1016/j.jrras.2014.02.003

Aragon, C. C., Mateo, C., Ruiz-Matute, A. I., Corzo, N., Fernandez-Lorente, G., Sevillano, L., … Guisan, J. M. (2013). Production of xylo-oligosaccharides by immobilized-stabilized derivatives of endo-xylanase from Streptomyces halstedii. *Process Biochemistry*, *48*(3), 478–483. http://doi.org/10.1016/j.procbio.2013.01.010

Aragon, C. C., Santos, A. F., Ruiz-Matute, A. I., Corzo, N., Guisan, J. M., Monti, R., & Mateo, C. (2013). Continuous production of xylooligosaccharides in a packed bed reactor with immobilized-stabilized biocatalysts of xylanase from Aspergillus versicolor. *Journal of Molecular Catalysis B: Enzymatic*. http://doi.org/10.1016/j.molcatb.2013.09.017

Arai, S. (1996). Studies on Functional Foods in Japan—State of the Art. *Bioscience, Biotechnology, and Biochemistry*, *60*(1), 9–15. http://doi.org/10.1271/bbb.60.9

Bäckhed, F., Roswall, J., Peng, Y., Feng, Q., Jia, H., Kovatcheva-Datchary, P., … Jun, W. (2015). Dynamics and stabilization of the human gut microbiome during the first year of life. *Cell Host and Microbe*. http://doi.org/10.1016/j.chom.2015.04.004

Bai, Y.-Y., Xiao, L.-P., & Sun, R.-C. (2015). Microwave-assisted conversion of biomass derived hemicelluloses into xylo-oligosaccharides by novel sulfonated bamboo-based catalysts. *Biomass and Bioenergy*, *75*, 245–253. http://doi.org/10.1016/j.biombioe.2015.02.023

Bajury, D. M., Nashri, S. M., King Jie Hung, P., & Sarbini, S. R. (2018). Evaluation of potential prebiotics: a review. *Food Reviews International*, *34*(7), 639–664. http://doi.org/10.1080/87559129.2017.1373287

Bergman, E. N. (1990). Energy contributions of volatile fatty acids from the gastrointestinal tract in various species. *Physiological Reviews*, *70*(2), 567–590. http://doi.org/10.1152/physrev.1990.70.2.567

Berlin, A., Balakshin, M., Gilkes, N., Kadla, J., Maximenko, V., Kubo, S., & Saddler, J. (2006). Inhibition of cellulase, xylanase and beta-glucosidase activities by softwood lignin preparations. *Journal of Biotechnology*, *125*(2), 198–209. http://doi.org/10.1016/j.jbiotec.2006.02.021

Bian, J., Peng, P., Peng, F., Xiao, X., Xu, F., & Sun, R.-C. (2014). Microwave-assisted acid hydrolysis to produce xylooligosaccharides from sugarcane bagasse hemicelluloses. *Food Chemistry*, *156*, 7–13. http://doi.org/10.1016/j.foodchem.2014.01.112

Bloemen, J. G., Venema, K., van de Poll, M. C., Olde Damink, S. W., Buurman, W. A., & Dejong, C. H. (2009). Short chain fatty acids exchange across the gut and liver in humans measured at surgery. *Clinical Nutrition*, *28*(6), 657–661. http://doi.org/10.1016/j.clnu.2009.05.011

Brodeur, G., Yau, E., Badal, K., Collier, J., Ramachandran, K. B., & Ramakrishnan, S. (2011). Chemical and physicochemical pretreatment of lignocellulosic biomass: a review. *Enzyme Research*, *2011*, 787532. http://doi.org/10.4061/2011/787532

Broekaert, W. F., Courtin, C. M., Verbeke, K., Van de Wiele, T., Verstraete, W., & Delcour, J. a. (2011). Prebiotic and other health-related effects of cereal-derived arabinoxylans, arabinoxylan-oligosaccharides, and xylooligosaccharides. *Critical Reviews in Food Science and Nutrition*, *51*(2), 178–94. http://doi.org/10.1080/10408390903044768

Bruggencate, S. J. M. Ten, Bovee-oudenhoven, I. M. J., Lettink-wissink, M. L. G., Katan, M.

B., & Meer, R. Van Der. (2006). Nutrient Physiology , Metabolism , and Nutrient-Nutrient Interactions Dietary Fructooligosaccharides Affect Intestinal Barrier Function in Healthy Men, (October 2005), 70–74.

Bumb, A., Brechbiel, M. W., Choyke, P. L., Fugger, L., Eggeman, A., Prabhakaran, D., … Dobson, P. J. (2008). Synthesis and characterization of ultra-small superparamagnetic iron oxide nanoparticles thinly coated with silica. *Nanotechnology*. http://doi.org/10.1088/0957-4484/19/33/335601

Buslov, D. K., Kaputski, F. N., Sushko, N. I., Torgashev, V. I., Solov'eva, L. V., Tsarenkov, V. M., … Larchenko, L. V. (2010). Infrared spectroscopic analysis of the structure of xylans. *Journal of Applied Spectroscopy*, *76*(6), 801–805. http://doi.org/10.1007/s10812-010-9282-z

Canny, G. O., & McCormick, B. A. (2008). Bacteria in the intestine, helpful residents or enemies from within? *Infection and Immunity*. http://doi.org/10.1128/IAI.00187-08

Carlson, R. (2001). Design of Experiments, Principles and Applications, L. Eriksson, E. Johansson, N. Kettaneh- Wold, C. Wikstrom and S. Wold, Umetrics AB, Umea Learnways AB, Stockholm, 2000, ISBN 91-973730-0-1, xii?+?329 pp. *Journal of Chemometrics*, *15*(5), 495–496. http://doi.org/10.1002/cem.686

Carvalheiro, F., Duarte, L. C., & Gírio, F. M. (2008). Hemicellulose biorefineries : a review on biomass pretreatments, *67*(November), 849–864.

Carvalheiro, F., Silva-Fernandes, T., Duarte, L. C., & Gírio, F. M. (2009). Wheat straw autohydrolysis: Process optimization and products characterization. In *Applied Biochemistry and Biotechnology*. http://doi.org/10.1007/s12010-008-8448-0

Chang, S., Chu, J., Guo, Y., Li, H., Wu, B., & He, B. (2017). An efficient production of high-pure xylooligosaccharides from corncob with affinity adsorption-enzymatic reaction integrated approach. *Bioresource Technology*. http://doi.org/10.1016/j.biortech.2017.06.002

Chapla, D., Pandit, P., & Shah, A. (2012). Production of xylooligosaccharides from corncob xylan by fungal xylanase and their utilization by probiotics. *Bioresource Technology*, *115*, 215–21. http://doi.org/10.1016/j.biortech.2011.10.083

Chen, M.-H., Bowman, M. J., Dien, B. S., Rausch, K. D., Tumbleson, M. E., & Singh, V. (2014). Autohydrolysis of Miscanthus x giganteus for the production of xylooligosaccharides (XOS): kinetics, characterization and recovery. *Bioresource Technology*, *155*, 359–65. http://doi.org/10.1016/j.biortech.2013.12.050

Chen, M. H., Bowman, M. J., Cotta, M. A., Dien, B. S., Iten, L. B., Whitehead, T. R., … Singh, V. (2016). Miscanthus × giganteus xylooligosaccharides: Purification and fermentation. *Carbohydrate Polymers*, *140*, 96–103. http://doi.org/10.1016/j.carbpol.2015.12.052

Chen, M. H., Bowman, M. J., Dien, B. S., Rausch, K. D., Tumbleson, M. E., & Singh, V. (2014). Autohydrolysis of Miscanthus x giganteus for the production of xylooligosaccharides (XOS): Kinetics, characterization and recovery. *Bioresource Technology*, *155*, 359–365.

http://doi.org/10.1016/j.biortech.2013.12.050

Chen, Y., Stevens, M. A., Zhu, Y., Holmes, J., & Xu, H. (2013). Understanding of alkaline pretreatment parameters for corn stover enzymatic saccharification. *Biotechnology for Biofuels*, *6*(1), 8. http://doi.org/10.1186/1754-6834-6-8

Courtin, C. M., Swennen, K., Verjans, P., & Delcour, J. A. (2009). Heat and pH stability of prebiotic arabinoxylooligosaccharides, xylooligosaccharides and fructooligosaccharides. *Food Chemistry*, *112*(4), 831–837. http://doi.org/10.1016/j.foodchem.2008.06.039

Cruz-Bravo, R. K., Guevara-González, R. G., Ramos-Gómez, M., Oomah, B. D., Wiersma, P., Campos-Vega, R., & Loarca-Piña, G. (2014). The fermented non-digestible fraction of common bean (Phaseolus vulgaris L.) triggers cell cycle arrest and apoptosis in human colon adenocarcinoma cells. *Genes and Nutrition*. http://doi.org/10.1007/s12263-013-0359-1

Cummings, J. H., Macfarlane, G. T., & Englyst, H. N. (2001). Prebiotic digestion and fermentation. In *American Journal of Clinical Nutrition*. http://doi.org/11157351

de Figueiredo, F. C., Carvalho, A. F. A., Brienzo, M., Campioni, T. S., & de Oliva-Neto, P. (2017). Chemical input reduction in the arabinoxylan and lignocellulose alkaline extraction and xylooligosaccharides production. *Bioresource Technology*, *228*, 164–170. http://doi.org/10.1016/j.biortech.2016.12.097

De Filippo, C.; Lionetti, P. (2016). Nutrition in pediatrics. In C. (Christopher P. . Duggan, J. B. Watkins, B. (Berthold) Koletzko, & W. A. Walker (Eds.), *Nutrition in Pediatrics* (5 th editi). PMPH-USA. Retrieved from https://openpub.fmach.it/handle/10449/25317?mode=full.252#.XE7W2lUzbIU

den Besten, G., van Eunen, K., Groen, A. K., Venema, K., Reijngoud, D.-J., & Bakker, B. M. (2013a). The role of short-chain fatty acids in the interplay between diet, gut microbiota, and host energy metabolism. *Journal of Lipid Research*, *54*(9), 2325–40. http://doi.org/10.1194/jlr.R036012

den Besten, G., van Eunen, K., Groen, A. K., Venema, K., Reijngoud, D.-J., & Bakker, B. M. (2013b). The role of short-chain fatty acids in the interplay between diet, gut microbiota, and host energy metabolism. *Journal of Lipid Research*, *54*(9), 2325–2340. http://doi.org/10.1194/jlr.R036012

Dhiman, S. S., Jagtap, S. S., Jeya, M., Haw, J.-R., Kang, Y. C., & Lee, J.-K. (2012). Immobilization of Pholiota adiposa xylanase onto SiO_2 nanoparticles and its application for production of xylooligosaccharides. *Biotechnology Letters*, *34*(7), 1307–13. http://doi.org/10.1007/s10529-012-0902-y

Driss, D., Haddar, A., Ghorbel, R., & Chaabouni, S. E. (2014). Production of xylooligosaccharides by immobilized his-tagged recombinant xylanase from penicillium occitanis on nickel-chelate Eupergit C. *Applied Biochemistry and Biotechnology*. http://doi.org/10.1007/s12010-014-0932-0

Driss, D., Zouari-Ellouzi, S., Chaari, F., Kallel, F., Ghazala, I., Bouaziz, F., Chaabouni, S. E.

(2014a). Production and in vitro evaluation of xylooligosaccharides generated from corncobs using immobilized Penicillium occitanis xylanase. *Journal of Molecular Catalysis B: Enzymatic*. http://doi.org/10.1016/j.molcatb.2014.02.004

Driss, D., Zouari-Ellouzi, S., Chaari, F., Kallel, F., Ghazala, I., Bouaziz, F., … Chaabouni, S. E. (2014b). Production and in vitro evaluation of xylooligosaccharides generated from corncobs using immobilized Penicillium occitanis xylanase. *Journal of Molecular Catalysis B: Enzymatic*, *102*, 146–153. http://doi.org/10.1016/j.molcatb.2014.02.004

Duncan, S. H., Barcenilla, A., Stewart, C. S., Pryde, S. E., & Flint, H. J. (2002). Acetate utilization and butyryl coenzyme A (CoA):acetate-CoA transferase in butyrate-producing bacteria from the human large intestine. *Applied and Environmental Microbiology*, *68*(10), 5186–90. http://doi.org/10.1128/AEM.68.10.5186-5190.2002

Englyst, H. N., Hay, S., & Macfarlane, G. T. (1987). Polysaccharide breakdown by mixed populations of human faecal bacteria. *FEMS Microbiology Letters*, *45*(3), 163–171. http://doi.org/10.1016/0378-1097(87)90013-9

Esbensen, K., Guyot, D., Westad, F., & Houmoller, L. P. (1994). *Multivariate data analysis : in practice : an introduction to multivariate data analysis and experimental design*. CAMO. Retrieved from https://books.google.com.au/books?hl=en&lr=&id=Qsn6yjRXOaMC&oi=fnd&pg=PA1&dq=An+Introduction+to+Multivariate+Data+Analysis+and+Experimental+Design.&ots=cC-p4-mTW8&sig=T055CrbEpA5Wqbq6e7bxtTXyKB4#v=onepage&q=An Introduction to Multivariate Data Analysis and Experimental Design.&f=false

Faryar, R., Linares-Pastén, J. A., Immerzeel, P., Mamo, G., Andersson, M., Stålbrand, H., … Karlsson, E. N. (2015). Production of prebiotic xylooligosaccharides from alkaline extracted wheat straw using the K80R-variant of a thermostable alkali-tolerant xylanase. *Food and Bioproducts Processing*, *93*, 1–10. http://doi.org/10.1016/j.fbp.2014.11.004

Fernández, J., Redondo-Blanco, S., Gutiérrez-del-Río, I., Miguélez, E. M., Villar, C. J., & Lombó, F. (2016). Colon microbiota fermentation of dietary prebiotics towards short-chain fatty acids and their roles as anti-inflammatory and antitumour agents: A review. *Journal of Functional Foods*, *25*, 511–522. http://doi.org/10.1016/j.jff.2016.06.032

Galisteo, M., Duarte, J., & Zarzuelo, A. (2008). Effects of dietary fibers on disturbances clustered in the metabolic syndrome. *The Journal of Nutritional Biochemistry*, *19*(2), 71–84. http://doi.org/10.1016/j.jnutbio.2007.02.009

Gill, S. R., Pop, M., DeBoy, R. T., Eckburg, P. B., Turnbaugh, P. J., Samuel, B. S., … Nelson, K. E. (2006). Metagenomic analysis of the human distal gut microbiome. *Science*. http://doi.org/10.1126/science.1124234

Gonzalez-Garcia, S., Gullón, B., & Moreira, M. T. (2018). Environmental assessment of biorefinery processes for the valorization of lignocellulosic wastes into oligosaccharides. *Journal of Cleaner Production*. http://doi.org/10.1016/j.jclepro.2017.02.164

González-García, S., Gullón, B., Rivas, S., Feijoo, G., & Moreira, M. T. (2016).

Environmental performance of biomass refining into high-added value compounds. *Journal of Cleaner Production*. http://doi.org/10.1016/j.jclepro.2016.02.015

Gorbach, S. L. (1996). Microbiology of the Gastrointestinal Tract. In *Medical Microbiology 4th edition*. http://doi.org/NBK7670 [bookaccession]

Grajek, W., Olejnik, A., & Sip, A. (2005). Probiotics, prebiotics and antioxidants as functional foods. *Acta Biochimica Polonica*, *52*(3), 665–71. Retrieved from http://www.ncbi.nlm.nih.gov/pubmed/16086074

Gullón, P., Moura, P., Esteves, M. P., Girio, F. M., Domínguez, H., & Parajó, J. C. (2008). Assessment on the fermentability of xylooligosaccharides from rice husks by probiotic bacteria. *Journal of Agricultural and Food Chemistry*, *56*(16), 7482–7. http://doi.org/10.1021/jf800715b

Hasler, C. M. (2002). Functional Foods: Benefits, Concerns and Challenges—A Position Paper from the American Council on Science and Health. *The Journal of Nutrition*, *132*(12), 3772–3781. http://doi.org/10.1093/jn/132.12.3772

Heerdt, B. G., Houston, M. A., & Augenlicht, L. H. (1997). Short-Chain Fatty Acid-initiated Cell Cycle Arrest and Apoptosis of Colonic Epithelial Cells is Linked to Mitochondrial Function. *Cell Growth & Differentiation*. http://doi.org/10.1063/1.4864657

Heitz, M., Carrasco, F., Rubio, M., Chauvette, G., Chornet, E., Jaulin, L., & Overend, R. P. (1986). Generalized correlations for the aqueous liquefaction of lignocellulosics. *The Canadian Journal of Chemical Engineering*, *64*(4), 647–650. http://doi.org/10.1002/cjce.5450640416

Ho, A. L., Carvalheiro, F., Duarte, L. C., Roseiro, L. B., Charalampopoulos, D., & Rastall, R. A. (2014). Production and purification of xylooligosaccharides from oil palm empty fruit bunch fibre by a non-isothermal process. *Bioresource Technology*, *152*, 526–529. http://doi.org/10.1016/j.biortech.2013.10.114

Holscher, H. D. (2017). Dietary fiber and prebiotics and the gastrointestinal microbiota. *Gut Microbes*. http://doi.org/10.1080/19490976.2017.1290756

Hooper, L. V., Xu, J., Falk, P. G., Midtvedt, T., & Gordon, J. I. (1999). A molecular sensor that allows a gut commensal to control its nutrient foundation in a competitive ecosystem. *Proceedings of the National Academy of Sciences*. http://doi.org/10.1073/pnas.96.17.9833

Hopkins, M. J., Cummings, J. H., & Macfarlane, G. T. (1998). Inter-species differences in maximum specific growth rates and cell yields of bifidobacteria cultured on oligosaccharides and other simple carbohydrate sources. *Journal of Applied Microbiology*, *85*(2), 381–386. http://doi.org/10.1046/j.1365-2672.1998.00524.x

Jakobsson, H. E., Abrahamsson, T. R., Jenmalm, M. C., Harris, K., Quince, C., Jernberg, C., … Andersson, A. F. (2014). Decreased gut microbiota diversity, delayed Bacteroidetes colonisation and reduced Th1 responses in infants delivered by Caesarean section. *Gut*. http://doi.org/10.1136/gutjnl-2012-303249

Jaskari, J., Kontula, P., Siitonen, A., Jousimies-Somer, H., Mattila-Sandholm, T., & Poutanen, K. (1998). Oat beta-glucan and xylan hydrolysates as selective substrates for Bifidobacterium and Lactobacillus strains. *Applied Microbiology and Biotechnology*, *49*(2), 175–81. Retrieved from http://www.ncbi.nlm.nih.gov/pubmed/9534257

Jayapal, N., Samanta, A. K., Kolte, A. P., Senani, S., Sridhar, M., Suresh, K. P., & Sampath, K. T. (2013). Value addition to sugarcane bagasse: Xylan extraction and its process optimization for xylooligosaccharides production. *Industrial Crops and Products*, *42*, 14–24. http://doi.org/10.1016/j.indcrop.2012.05.019

Jensen, J. K., Johnson, N., & Wilkerson, C. G. (2013). Discovery of diversity in xylan biosynthetic genes by transcriptional profiling of a heteroxylan containing mucilaginous tissue. *Frontiers in Plant Science*, *4*(June), 183. http://doi.org/10.3389/fpls.2013.00183

Jesus, M. S., Romaní, A., Genisheva, Z., Teixeira, J. A., & Domingues, L. (2017). Integral valorization of vine pruning residue by sequential autohydrolysis stages. *Journal of Cleaner Production*. http://doi.org/10.1016/j.jclepro.2017.08.230

Khat-udomkiri, N., Sivamaruthi, B. S., Sirilun, S., Lailerd, N., Peerajan, S., & Chaiyasut, C. (2018). Optimization of alkaline pretreatment and enzymatic hydrolysis for the extraction of xylooligosaccharide from rice husk. *AMB Express*. http://doi.org/10.1186/s13568-018-0645-9

Klein-Marcuschamer, D., Oleskowicz-Popiel, P., Simmons, B. A., & Blanch, H. W. (2012). The challenge of enzyme cost in the production of lignocellulosic biofuels. *Biotechnology and Bioengineering*. http://doi.org/10.1002/bit.24370

Kosinkova, J., Ramirez, J. A., Jablonský, M., Ristovski, Z. D., Brown, R., & Rainey, T. J. (2017). Energy and chemical conversion of five Australian lignocellulosic feedstocks into bio-crude through liquefaction. *RSC Advances*. http://doi.org/10.1039/c7ra02335a

Kumar, P., Barrett, D. M., Delwiche, M. J., & Stroeve, P. (2009). Methods for Pretreatment of Lignocellulosic Biomass for Efficient Hydrolysis and Biofuel Production. *Industrial & Engineering Chemistry Research*, *48*(8), 3713–3729. http://doi.org/10.1021/ie801542g

Lasrado, L. D., & Gudipati, M. (2015). Antioxidant property of synbiotic combination of Lactobacillus sp. and wheat bran xylo-oligosaccharides. *Journal of Food Science and Technology*, *52*(7), 4551–7. http://doi.org/10.1007/s13197-014-1481-9

Li, X., Liu, Y., Hao, J., & Wang, W. (2018). Study of almond shell characteristics. *Materials*, *11*(9). http://doi.org/10.3390/ma11091782

Lin, Y. S., Tseng, M. J., & Lee, W. C. (2011). Production of xylooligosaccharides using immobilized endo-xylanase of Bacillus halodurans. *Process Biochemistry*. http://doi.org/10.1016/j.procbio.2011.08.008

Liu, M., Dai, X., Guan, R., & Xu, X. (2014). Immobilization of Aspergillus niger xylanase A on Fe3O4-coated chitosan magnetic nanoparticles for xylooligosaccharide preparation. *Catalysis Communications*, *55*, 6–10. http://doi.org/10.1016/J.CATCOM.2014.06.002

Liu, M. Q., Dai, X. J., Guan, R. F., & Xu, X. (2014). Immobilization of Aspergillus niger xylanase A on Fe3O 4-coated chitosan magnetic nanoparticles for xylooligosaccharide preparation. *Catalysis Communications*. http://doi.org/10.1016/j.catcom.2014.06.002

Liu, Y., Li, Y., Li, X.-M., & He, T. (2013). Kinetics of (3-Aminopropyl)triethoxylsilane (APTES) Silanization of Superparamagnetic Iron Oxide Nanoparticles. *Langmuir*, *29*(49), 15275–15282. http://doi.org/10.1021/la403269u

Maalej-Achouri, I., Guerfali, M., Gargouri, A., & Belghith, H. (2009). Production of xylo-oligosaccharides from agro-industrial residues using immobilized Talaromyces thermophilus xylanase. *Journal of Molecular Catalysis B: Enzymatic*, *59*(1–3), 145–152. http://doi.org/10.1016/j.molcatb.2009.02.003

Macdonald, D. G., Bakhshi, N. N., Mathews, J. F., Roychowdhury, A., Bajpai, P., & Moo-Young, M. (1983). Alkali treatment of corn stover to improve sugar production by enzymatic hydrolysis. *Biotechnology and Bioengineering*, *25*(8), 2067–76. http://doi.org/10.1002/bit.260250815

Macfarlane, S., & Macfarlane, G. T. (2003). Regulation of short-chain fatty acid production. *Proceedings of the Nutrition Society*, *62*(01), 67–72. http://doi.org/10.1079/PNS2002207

Madhukumar, M. S., & Muralikrishna, G. (2012). Fermentation of xylo-oligosaccharides obtained from wheat bran and Bengal gram husk by lactic acid bacteria and bifidobacteria. *Journal of Food Science and Technology*, *49*(6), 745–52. http://doi.org/10.1007/s13197-010-0226-7

Malherbe, S., & Cloete, T. E. (2002). Lignocellulose biodegradation: Fundamentals and applications. *Reviews in Environmental Science and Bio/Technology*, *1*(2), 105–114. http://doi.org/10.1023/A:1020858910646

Manisseri, C., & Gudipati, M. (2010). Bioactive xylo-oligosaccharides from wheat bran soluble polysaccharides. *LWT - Food Science and Technology*, *43*(3), 421–430. http://doi.org/10.1016/j.lwt.2009.09.004

Mayer-Laigle, C., Blanc, N., Rajaonarivony, R. K., & Rouau, X. (2018). Comminution of Dry Lignocellulosic Biomass, a Review: Part I. From Fundamental Mechanisms to Milling Behaviour. *Bioengineering (Basel, Switzerland)*, *5*(2). http://doi.org/10.3390/bioengineering5020041

McIntosh, S., & Vancov, T. (2010). Enhanced enzyme saccharification of Sorghum bicolor straw using dilute alkali pretreatment. *Bioresource Technology*, *101*(17), 6718–27. http://doi.org/10.1016/j.biortech.2010.03.116

Milessi, T. S. S., Kopp, W., Rojas, M. J., Manrich, A., Baptista-Neto, A., Tardioli, P. W., Giordano, R. L. C. (2016). Immobilization and stabilization of an endoxylanase from Bacillus subtilis (XynA) for xylooligosaccharides (XOs) production. *Catalysis Today*. http://doi.org/10.1016/j.cattod.2015.05.032

Moniz, P., Pereira, H., Duarte, L. C., & Carvalheiro, F. (2014). Hydrothermal production and

gel filtration purification of xylo-oligosaccharides from rice straw. *Industrial Crops and Products*, *62*, 460–465. http://doi.org/10.1016/j.indcrop.2014.09.020

Morrison, D. J., & Preston, T. (2016). Formation of short chain fatty acids by the gut microbiota and their impact on human metabolism. *Gut Microbes*. http://doi.org/10.1080/19490976.2015.1134082

Nabais, J. M. V., Laginhas, C. E. C., Carrott, P. J. M., & Ribeiro Carrott, M. M. L. (2011). Production of activated carbons from almond shell. *Fuel Processing Technology*, *92*(2), 234–240. http://doi.org/10.1016/J.FUPROC.2010.03.024

Nabarlatz, D., Ebringerová, A., & Montané, D. (2007). Autohydrolysis of agricultural by-products for the production of xylo-oligosaccharides. *Carbohydrate Polymers*, *69*(1), 20–28. http://doi.org/10.1016/j.carbpol.2006.08.020

Nabarlatz, D., Farriol, X., & Montané, D. (2005). Autohydrolysis of almond shells for the production of xylo- oligosaccharides: Product characteristics and reaction kinetics. *Industrial and Engineering Chemistry Research*. http://doi.org/10.1021/ie050664n

O'Mahony, L. (2015). Host-microbiome interactions in health and disease. *Clinical Liver Disease*. http://doi.org/10.1002/cld.484

Overend, R. P., Chornet, E., & Gascoigne, J. A. (1987). Fractionation of Lignocellulosics by Steam-Aqueous Pretreatments [and Discussion]. *Philosophical Transactions of the Royal Society A: Mathematical, Physical and Engineering Sciences*, *321*(1561), 523–536. http://doi.org/10.1098/rsta.1987.0029

Ozalp, V. C., Bayramoglu, G., & Arica, M. Y. (2015). Magnetic silica nanoparticle–Taq polymerase hybrids for multiple uses in polymerase chain reaction. *RSC Advances*, *5*(106), 87672–87678. http://doi.org/10.1039/C5RA15677G

Patel, A., Falck, P., Shah, N., Immerzeel, P., Adlercreutz, P., Stålbrand, H., Nordberg Karlsson, E. (2013). Evidence for xylooligosaccharide utilization in Weissella strains isolated from Indian fermented foods and vegetables. *FEMS Microbiology Letters*, *346*(1), 20–8. http://doi.org/10.1111/1574-6968.12191

Pereira, D. I. A., & Gibson, G. R. (2002). Effects of consumption of probiotics and prebiotics on serum lipid levels in humans. *Critical Reviews in Biochemistry and Molecular Biology*, *37*(4), 259–81. http://doi.org/10.1080/10409230290771519

Pinelo, M., Jonsson, G., & Meyer, A. S. (2009). Membrane technology for purification of enzymatically produced oligosaccharides: Molecular and operational features affecting performance. *Separation and Purification Technology*. http://doi.org/10.1016/j.seppur.2009.08.010

Purohit, P., & Chaturvedi, V. (2018). Biomass pellets for power generation in India: a techno-economic evaluation. *Environmental Science and Pollution Research*. http://doi.org/10.1007/s11356-018-2960-8

Qi, B., Chen, X., Su, Y., & Wan, Y. (2011). Enzyme adsorption and recycling during hydrolysis of wheat straw lignocellulose. *Bioresource Technology*, *102*(3), 2881–9. http://doi.org/10.1016/j.biortech.2010.10.092

Qu, T., Zhang, X., Gu, X., Han, L., Ji, G., Chen, X., & Xiao, W. (2017). Ball Milling for Biomass Fractionation and Pretreatment with Aqueous Hydroxide Solutions. *ACS Sustainable Chemistry and Engineering*. http://doi.org/10.1021/acssuschemeng.7b01186

Rajagopalan, G., Shanmugavelu, K., & Yang, K. L. (2016). Production of xylooligosaccharides from hardwood xylan by using immobilized endoxylanase of Clostridium strain BOH3. *RSC Advances*. http://doi.org/10.1039/c6ra17085d

Reddy, S. S., & Krishnan, C. (2016). Production of high-pure xylooligosaccharides from sugarcane bagasse using crude β-xylosidase-free xylanase of Bacillus subtilis KCX006 and their bifidogenic function. *LWT - Food Science and Technology*, *65*, 237–245. http://doi.org/10.1016/j.lwt.2015.08.013

Resch, M. G., Baker, J. O., & Decker, S. R. (2015). Low Solids Enzymatic Saccharification of Lignocellulosic Biomass: Laboratory Analytical Procedure (LAP), Issue Date: February 4, 2015.

Richardson, A. J., McKain, N., & Wallace, R. J. (2013). Ammonia production by human faecal bacteria, and the enumeration, isolation and characterization of bacteria capable of growth on peptides and amino acids. *BMC Microbiology*. http://doi.org/10.1186/1471-2180-13-6

Rivière, A., Selak, M., Lantin, D., Leroy, F., & De Vuyst, L. (2016). Bifidobacteria and butyrate-producing colon bacteria: Importance and strategies for their stimulation in the human gut. *Frontiers in Microbiology*. http://doi.org/10.3389/fmicb.2016.00979

Roberfroid, M. (2007). Prebiotics: The Concept Revisited. *J. Nutr.*, *137*(3), 830S–837. Retrieved from http://jn.nutrition.org/content/137/3/830S.full

Roberfroid, M., & Slavin, J. (2010). Nondigestible Oligosaccharides. Retrieved from http://www.tandfonline.com/doi/abs/10.1080/10408690091189239?url_ver=Z39.88-2003&rfr_id=ori:rid:crossref.org&rfr_dat=cr_pub%253dpubmed#

Roberge, M., Lewis, R. N. A. H., Shareck, F., Morosoli, R., Kluepfel, D., Dupont, C., & McElhaney, R. N. (2003). Differential scanning calorimetric, circular dichroism, and Fourier transform infrared spectroscopic characterization of the thermal unfolding of xylanase A from Streptomyces lividans. *Proteins: Structure, Function and Genetics*. http://doi.org/10.1002/prot.10262

Rodríguez, J. M., Murphy, K., Stanton, C., Ross, R. P., Kober, O. I., Juge, N., … Collado, M. C. (2015). The composition of the gut microbiota throughout life, with an emphasis on early life. *Microbial Ecology in Health & Disease*. http://doi.org/10.3402/mehd.v26.26050

Roediger, W. E. W. (1982). Utilization of Nutrients by Isolated Epithelial Cells of the Rat Colon. *Gastroenterology*, *83*(2), 424–429. http://doi.org/10.1016/S0016-5085(82)80339-9

Rowley, J., Decker, S. R., Michener, W., & Black, S. (2013). Efficient extraction of xylan from delignified corn stover using dimethyl sulfoxide. *3 Biotech*, *3*(5), 433–438. http://doi.org/10.1007/s13205-013-0159-8

Rubio, M., Tortosa, J. F., Quesada, J., & Gómez, D. (1998). Fractionation of lignocellulosics. Solubilization of corn stalk hemicelluloses by autohydrolysis in aqueous medium. *Biomass and Bioenergy*, *15*(6), 483–491. http://doi.org/10.1016/S0961-9534(98)00054-3

Ruiz, H. A., Rodríguez-Jasso, R. M., Fernandes, B. D., Vicente, A. A., & Teixeira, J. A. (2013). Hydrothermal processing, as an alternative for upgrading agriculture residues and marine biomass according to the biorefinery concept: A review. *Renewable and Sustainable Energy Reviews*. http://doi.org/10.1016/j.rser.2012.11.069

Saha, B. C. (2003). Hemicellulose bioconversion. *Journal of Industrial Microbiology & Biotechnology*, *30*(5), 279–91. http://doi.org/10.1007/s10295-003-0049-x

Saini, J. K., Saini, R., & Tewari, L. (2014). Lignocellulosic agriculture wastes as biomass feedstocks for second-generation bioethanol production: concepts and recent developments. *3 Biotech*, *5*(4), 337–353. http://doi.org/10.1007/s13205-014-0246-5

Samala, A., Srinivasan, R., & Yadav, M. (2015). Comparison of xylo-oligosaccharides production by autohydrolysis of fibers separated from ground corn flour and DDGS. *Food and Bioproducts Processing*, *94*, 354–364. http://doi.org/10.1016/j.fbp.2014.04.004

Samanta, A. K., Jayapal, N., Kolte, A. P., Senani, S., Sridhar, M., Dhali, A., … Prasad, C. S. (2014). Process for Enzymatic Production of Xylooligosaccharides from the Xylan of Corn Cobs. *Journal of Food Processing and Preservation*, n/a-n/a. http://doi.org/10.1111/jfpp.12282

Samanta, A. K., Jayapal, N., Kolte, A. P., Senani, S., Sridhar, M., Mishra, S., … Suresh, K. P. (2013a). Application of pigeon pea (Cajanus cajan) stalks as raw material for xylooligosaccharides production. *Applied Biochemistry and Biotechnology*, *169*(8), 2392–404. http://doi.org/10.1007/s12010-013-0151-0

Samanta, A. K., Jayapal, N., Kolte, A. P., Senani, S., Sridhar, M., Mishra, S., … Suresh, K. P. (2013b). Application of pigeon pea (Cajanus cajan) stalks as raw material for xylooligosaccharides production. *Applied Biochemistry and Biotechnology*, *169*(8), 2392–2404. http://doi.org/10.1007/s12010-013-0151-0

Samanta, A. K., Jayapal, N., Kolte, A. P., Senani, S., Sridhar, M., Suresh, K. P., & Sampath, K. T. (2012a). Enzymatic production of xylooligosaccharides from alkali solubilized xylan of natural grass (Sehima nervosum). *Bioresource Technology*, *112*, 199–205. http://doi.org/10.1016/j.biortech.2012.02.036

Samanta, A. K., Jayapal, N., Kolte, A. P., Senani, S., Sridhar, M., Suresh, K. P., & Sampath, K. T. (2012b). Enzymatic production of xylooligosaccharides from alkali solubilized xylan of natural grass (Sehima nervosum). *Bioresource Technology*, *112*, 199–205. http://doi.org/10.1016/j.biortech.2012.02.036

Samanta, A. K., Senani, S., Kolte, A. P., Sridhar, M., Sampath, K. T., Jayapal, N., & Devi, A. (2012). Production and in vitro evaluation of xylooligosaccharides generated from corn cobs. *Food and Bioproducts Processing*, *90*(3), 466–474. http://doi.org/10.1016/j.fbp.2011.11.001

Scheller, H. V., & Ulvskov, P. (2010). Hemicelluloses. *Annual Review of Plant Biology*, *61*, 263–89. http://doi.org/10.1146/annurev-arplant-042809-112315

Schloss, P. D., & Handelsman, J. (2004). Status of the Microbial Census. *Microbiology and Molecular Biology Reviews*. http://doi.org/10.1128/MMBR.68.4.686-691.2004

Scott, K. P., Martin, J. C., Duncan, S. H., & Flint, H. J. (2014). Prebiotic stimulation of human colonic butyrate-producing bacteria and bifidobacteria, in vitro. *FEMS Microbiology Ecology*, *87*(1), 30–40. http://doi.org/10.1111/1574-6941.12186

Sender, R., Fuchs, S., & Milo, R. (2016). Revised Estimates for the Number of Human and Bacteria Cells in the Body. *PLoS Biology*. http://doi.org/10.1371/journal.pbio.1002533

Sharma, M., & Majumdar, P. K. (2009). Occupational lifestyle diseases: An emerging issue. *Indian Journal of Occupational and Environmental Medicine*, *13*(3), 109–12. http://doi.org/10.4103/0019-5278.58912

Silva, V. A. J., Andrade, P. L., Silva, M. P. C., Bustamante, A. D., De Los Santos Valladares, L., & Albino Aguiar, J. (2013). Synthesis and characterization of Fe3O4 nanoparticles coated with fucan polysaccharides. *Journal of Magnetism and Magnetic Materials*. http://doi.org/10.1016/j.jmmm.2013.04.062

Silverstein, R. A., Chen, Y., Sharma-Shivappa, R. R., Boyette, M. D., & Osborne, J. (2007). A comparison of chemical pretreatment methods for improving saccharification of cotton stalks. *Bioresource Technology*, *98*(16), 3000–3011. http://doi.org/10.1016/j.biortech.2006.10.022

Singh, R. D., Banerjee, J., & Arora, A. (2015). Prebiotic potential of oligosaccharides: A focus on xylan derived oligosaccharides. *Bioactive Carbohydrates and Dietary Fibre*, *5*(1). http://doi.org/10.1016/j.bcdf.2014.11.003

Singh, R. D., Banerjee, J., & Arora, A. (2015). Prebiotic potential of oligosaccharides: A focus on xylan derived oligosaccharides. *Bioactive Carbohydrates and Dietary Fibre*, *5*(1), 19–30. http://doi.org/10.1016/J.BCDF.2014.11.003

Singh, R. D., Bhuyan, K., Banerjee, J., Muir, J., & Arora, A. (2017). Hydrothermal and microwave assisted alkali pretreatment for fractionation of arecanut husk. *Industrial Crops and Products*, *102*, 65–74. http://doi.org/10.1016/j.indcrop.2017.03.017

Singh, S., Madlala, A. M., & Prior, B. A. (2003). Thermomyces lanuginosus: Properties of strains and their hemicellulases. *FEMS Microbiology Reviews*. http://doi.org/10.1016/S0168-6445(03)00018-4

Sluiter, A., Hames, B., Ruiz, R., & Scarlata, C. (2006). *Determination of sugars, byproducts, and degradation products in liquid fraction process samples*. *NREL Technical Report*.

Sluiter, A., Hames, B., Ruiz, R., Scarlata, C., Sluiter, J., Templeton, D., & Crocker, D. (2008). Determination of Structural Carbohydrates and Lignin in Biomass: Laboratory Analytical Procedure (LAP) (Revised July 2011).

Sluiter, A., Hames, B., Ruiz, R., Scarlata, C., Sluiter, J., Templeton, D., & Nrel, D. C. (2011). Determination of Structural Carbohydrates and Lignin in Biomass Determination of Structural Carbohydrates and Lignin in Biomass, *2011*(July).

Stearns, J. C., Lynch, M. D. J., Senadheera, D. B., Tenenbaum, H. C., Goldberg, M. B., Cvitkovitch, D. G., … Neufeld, J. D. (2011). Bacterial biogeography of the human digestive tract. *Scientific Reports*, *1*, 170. http://doi.org/10.1038/srep00170

Sukri, S. S. M., & Mimi Sakinah, A. M. (2018). Production of High Commercial Value Xylooligosaccharides from Meranti Wood Sawdust Using Immobilised Xylanase. *Applied Biochemistry and Biotechnology*. http://doi.org/10.1007/s12010-017-2542-0

Sun, Y.-G., Ma, Y.-L., Wang, L.-Q., Wang, F.-Z., Wu, Q.-Q., & Pan, G.-Y. (2015). Physicochemical properties of corn stalk after treatment using steam explosion coupled with acid or alkali. *Carbohydrate Polymers*, *117*, 486–93. http://doi.org/10.1016/j.carbpol.2014.09.066

Surek, E., & Buyukkileci, A. O. (2017). Production of xylooligosaccharides by autohydrolysis of hazelnut (Corylus avellana L.) shell. *Carbohydrate Polymers*, *174*, 565–571. http://doi.org/10.1016/j.carbpol.2017.06.109

Talekar, S., Joshi, A., Kambale, S., Jadhav, S., Nadar, S., & Ladole, M. (2017). A tri-enzyme magnetic nanobiocatalyst with one pot starch hydrolytic activity. *Chemical Engineering Journal*, *325*, 80–90. http://doi.org/10.1016/J.CEJ.2017.05.054

Teng, C., Yan, Q., Jiang, Z., Fan, G., & Shi, B. (2010). Production of xylooligosaccharides from the steam explosion liquor of corncobs coupled with enzymatic hydrolysis using a thermostable xylanase. *Bioresource Technology*, *101*(19), 7679–82. http://doi.org/10.1016/j.biortech.2010.05.004

Tomomatsu, H. (1994). Health effects of oligosaccharides. *Food Technology*, *48*(10), 61–65. Retrieved from http://www.scopus.com/inward/record.url?eid=2-s2.0-0028529163&partnerID=tZOtx3y1

Van Laere, K. M., Hartemink, R., Bosveld, M., Schols, H. A., & Voragen, A. G. (2000). Fermentation of plant cell wall derived polysaccharides and their corresponding oligosaccharides by intestinal bacteria. *Journal of Agricultural and Food Chemistry*, *48*(5), 1644–52. Retrieved from http://www.ncbi.nlm.nih.gov/pubmed/10820072

Van Soest, P. J., Robertson, J. B., & Lewis, B. A. (1991). Methods for dietary fiber, neutral detergent fiber, and nonstarch polysaccharides in relation to animal nutrition. *Journal of Dairy Science*, *74*(10), 3583–97. http://doi.org/10.3168/jds.S0022-0302(91)78551-2

Vázquez, M. ., Alonso, J. ., Domínguez, H., & Parajó, J. . (2000). Xylooligosaccharides: manufacture and applications. *Trends in Food Science & Technology*, *11*(11), 387–393.

http://doi.org/10.1016/S0924-2244(01)00031-0

Vázquez, M. J., Alonso, J. L., Domínguez, H., & Parajó, J. C. (2001, November 1). Xylooligosaccharides: Manufacture and applications. *Trends in Food Science and Technology*. Elsevier. http://doi.org/10.1016/S0924-2244(01)00031-0

Veenashri, B. R., & Muralikrishna, G. (2011). In vitro anti-oxidant activity of xylo-oligosaccharides derived from cereal and millet brans – A comparative study. *Food Chemistry*, *126*(3), 1475–1481. http://doi.org/10.1016/j.foodchem.2010.11.163

Vegas, R., Luque, S., Alvarez, J. R., Alonso, J. L., Domínguez, H., & Parajó, J. C. (2006). Membrane-Assisted Processing of Xylooligosaccharide-Containing Liquors. *Journal of Agricultural and Food Chemistry*, *54*(15), 5430–5436. http://doi.org/10.1021/jf060525w

Venema, K. (2010). Role of gut microbiota in the control of energy and carbohydrate metabolism. *Current Opinion in Clinical Nutrition and Metabolic Care*, *13*(4), 432–438. http://doi.org/10.1097/MCO.0b013e32833a8b60

Wang, T.-H., & Lu, S. (2013). Production of xylooligosaccharide from wheat bran by microwave assisted enzymatic hydrolysis. *Food Chemistry*, *138*(2–3), 1531–5. http://doi.org/10.1016/j.foodchem.2012.09.124

Wang, W., Wang, Y., Tu, L., Klein, T., Feng, Y., & Wang, J.-P. (2013). Surface Modification for Protein and DNA Immobilization onto GMR Biosensor. *IEEE Transactions on Magnetics*, *49*(1), 296–299. http://doi.org/10.1109/TMAG.2012.2224327

Westbye, P., Köhnke, T., Glasser, W., & Gatenholm, P. (2007). The influence of lignin on the self-assembly behaviour of xylan rich fractions from birch (Betula pendula). *Cellulose*, *14*(6), 603–613. http://doi.org/10.1007/s10570-007-9178-0

Wyman, C. E. (2007). What is (and is not) vital to advancing cellulosic ethanol. *Trends in Biotechnology*, *25*(4), 153–7. http://doi.org/10.1016/j.tibtech.2007.02.009

Wyman, C. E., Dale, B. E., Elander, R. T., Holtzapple, M., Ladisch, M. R., & Lee, Y. Y. (2005). Coordinated development of leading biomass pretreatment technologies. *Bioresource Technology*, *96*(18), 1959–1966. http://doi.org/10.1016/j.biortech.2005.01.010

Xiao, X., Bian, J., Peng, X.-P., Xu, H., Xiao, B., & Sun, R.-C. (2013). Autohydrolysis of bamboo (Dendrocalamus giganteus Munro) culm for the production of xylo-oligosaccharides. *Bioresource Technology*, *138*, 63–70. http://doi.org/10.1016/j.biortech.2013.03.160

Xu, F., Sun, R. C., Zhai, M. Z., Sun, J. X., She, D., Geng, Z. C., & Lu, Q. (2008). Fractional separation of hemicelluloses and lignin in high yield and purity from mild ball-milled Periploca sepium. *Separation Science and Technology*. http://doi.org/10.1080/01496390802063721

Xu, J., Sun, J., Wang, Y., Sheng, J., Wang, F., & Sun, M. (2014). Application of iron magnetic nanoparticles in protein immobilization. *Molecules*. http://doi.org/10.3390/molecules190811465

Yao, C. K., Rotbart, A., Ou, J. Z., Kalantar-Zadeh, K., Muir, J. G., & Gibson, P. R. (2018). Modulation of colonic hydrogen sulfide production by diet and mesalazine utilizing a novel gas-profiling technology. *Gut Microbes*. http://doi.org/10.1080/19490976.2018.1451280

Yu, X., Yin, J., Li, L., Luan, C., Zhang, J., Zhao, C., & Li, S. (2015). Prebiotic Potential of Xylooligosaccharides Derived from Corn Cobs and Their In Vitro Antioxidant Activity When Combined with Lactobacillus. *Journal of Microbiology and Biotechnology*, *25*(7), 1084–92. http://doi.org/10.4014/jmb.1501.01022

Appendix (i)

Figure 1: HPLC Chromatogram of Xylobiose

Figure 1: HPLC Chromatogram of Xylotriose

Figure 1: HPLC Chromatogram of Xylotetrose

Figure 1: HPLC Chromatogram of Xylose

Figure 1: HPLC Chromatogram of Glucose

Figure 1: HPLC Chromatogram of Arabinose

Figure 1: HPLC Chromatogram of Acetic acid

Figure 1: HPLC Chromatogram of Propionic acid

Figure 1: HPLC Chromatogram of Butyric acid

Figure 1: HPLC Chromatogram of Furfural

Figure 1: UV Spectra of reducing sugar (based on xylose)

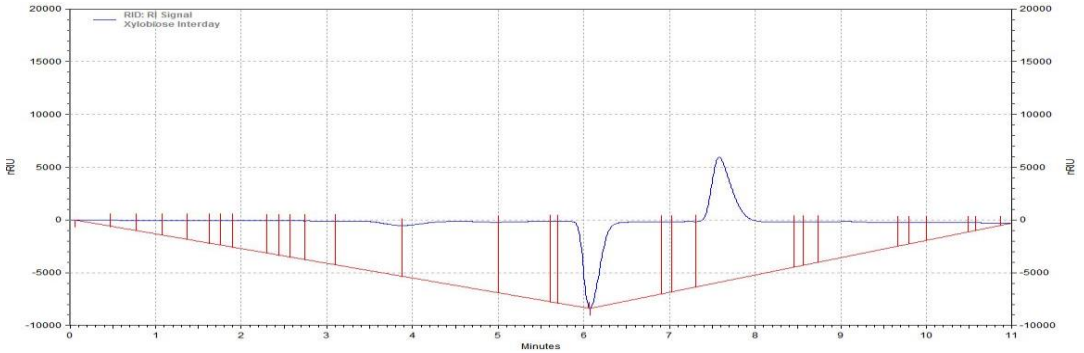

Xylobiose chromatogram

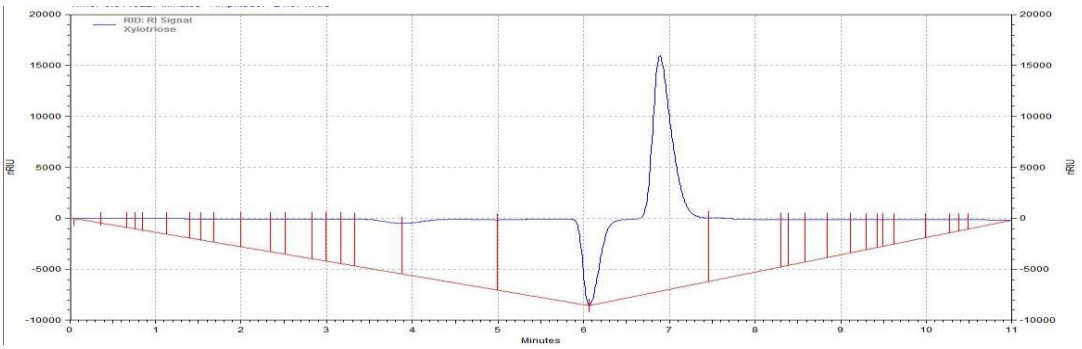

Xylotriose Chromatogram

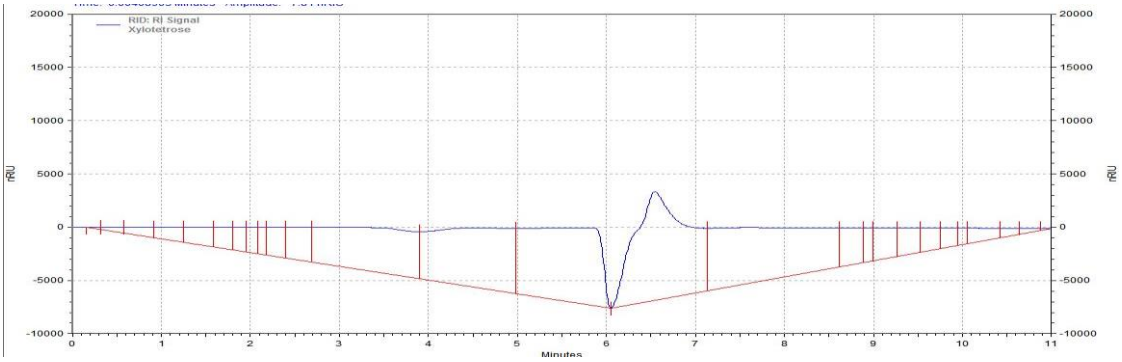

Xylotetrose Chromatogram

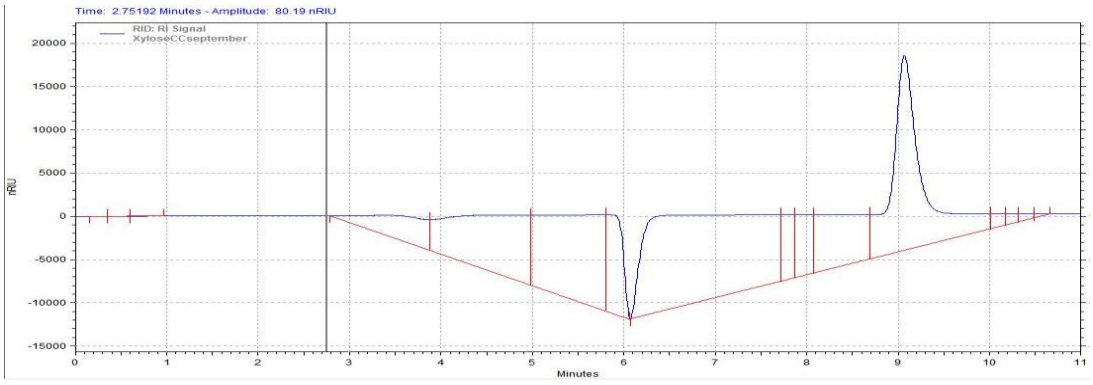

Xylose chromatogram

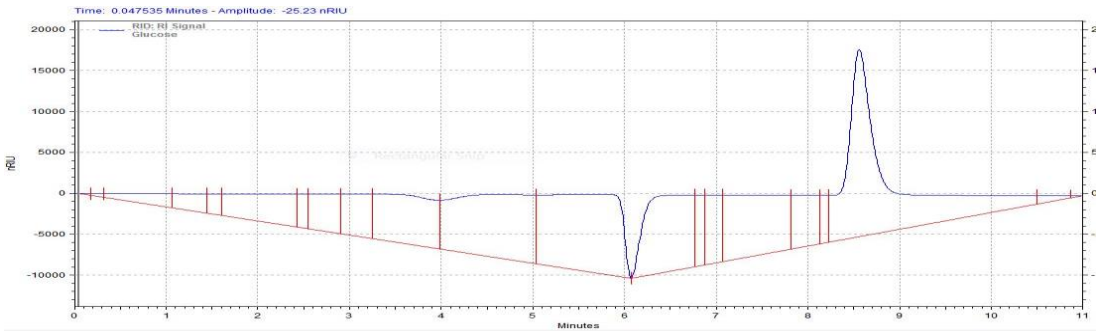

Glucose Chromatogram

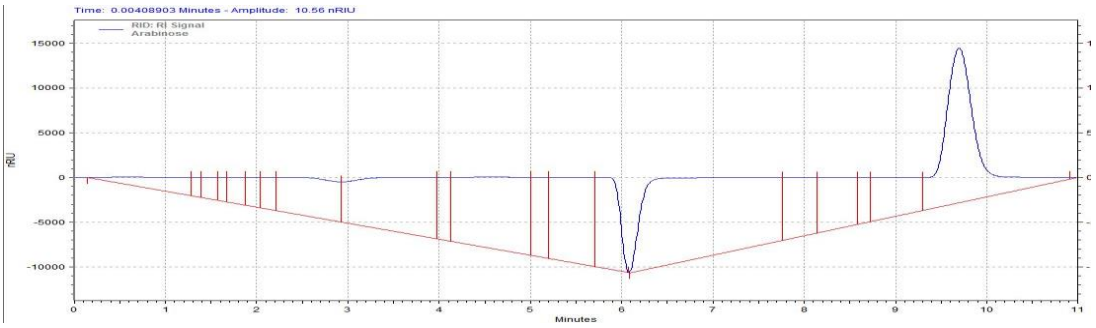

Arabinose Chromatogram

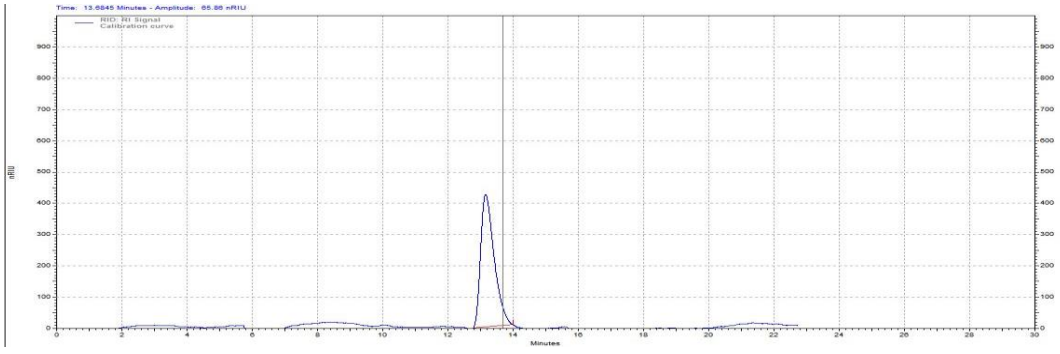

Acetic acid

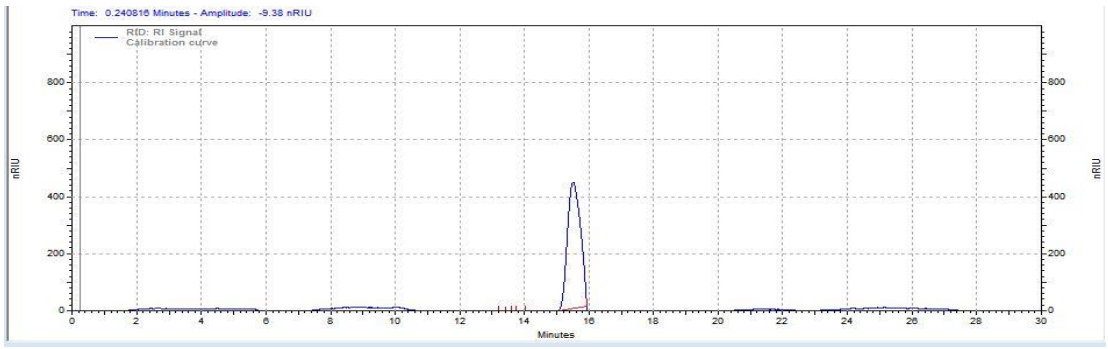

Propionic acid

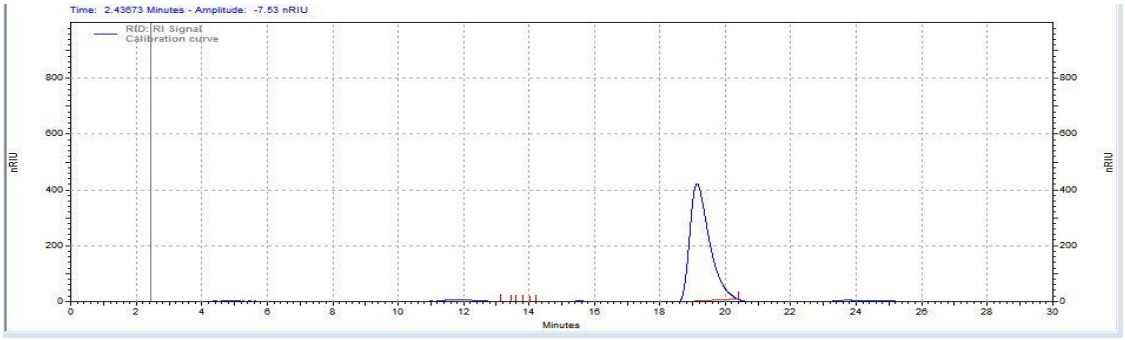

Butyric acid

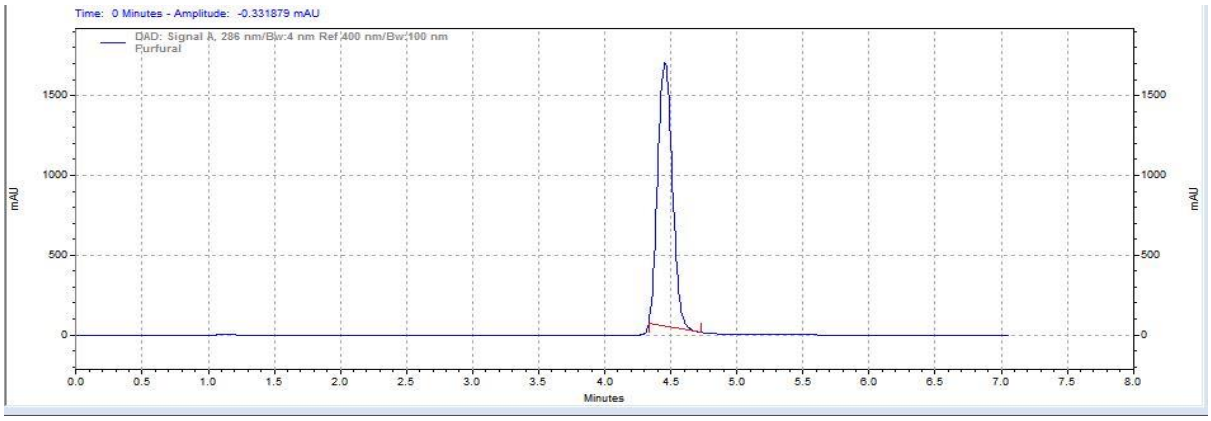

Furfural

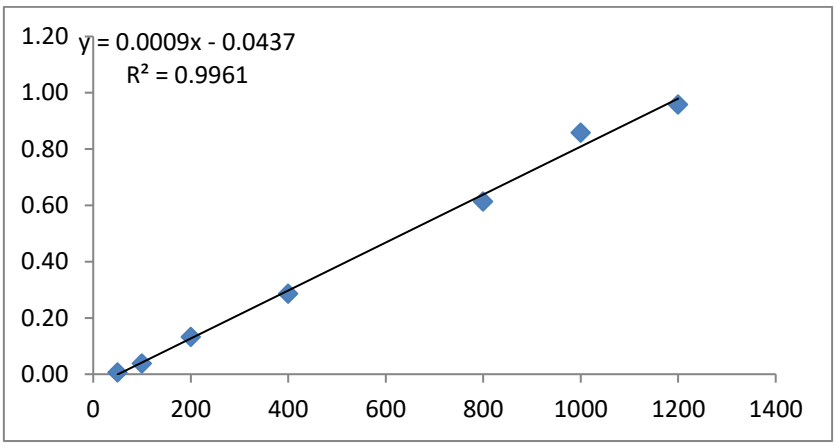

Calibration curve of Xylose (UV)

Appendix ii

Manuscripts:

Sr. No	Description	Status
1	**Ramkrishna D Singh,** Jane Muir, Amit Arora, Low degree of polymerisation xylooligosaccharides: Membrane assisted refinement and assessment of prebiotic potential	To Submit
2	**Ramkrishna D. Singh,** Cresha Gracy Nadar, Jane Muir, Amit Arora, Green and clean process to obtain low degree of polymerisation xylooligosaccharides from waste almond shell, **Journal of Cleaner Production**, Vol 241, 118237	Published
3	**Ramkrishna D. Singh,** Sachin Talekar, Jane Muir, Amit Arora, Low degree of polymerization xylooligosaccharides production from almond shell using immobilized nano-biocatalyst, **Enzyme and Microbial Technology,** 130, 109386.	Published
4	**Ramkrishna D. Singh,** Daniel So, CK Yao, Paul Gill, Naresh Pillai, Jane Muir, Amit Arora, Production and faecal fermentation of pentose oligomers of hemicellulose: Study of variables influencing bioprocess efficiency, **Food Chemistry,** 297, 124945.	Published
5	**R.D. Singh**, J. Banerjee, S. Sasmal, J. Muir, A. Arora, (2018), High xylan recovery using two stage alkali pretreatment process from high lignin biomass and its valorization to xylooligosaccharides of low degree of polymerisation, **Bioresource Technology**, 256, 110-117	Published
6	Jhumur Banerjee, **Ramkrishna Singh**, R. Vijayaraghavan, Douglas MacFarlane, Antonio F. Patti, Amit Arora, (2018), A hydrocolloid based biorefinery approach to the valorization of mango peel waste, **Food Hydrocolloids**, 77, 142-151.	Published
7	Sachin Talekar, Antonio F. Patti, **Ramkrishna Singh**, R. Vijayaraghavan, Amit Arora, (2018), From waste to wealth: High recovery of nutraceuticals from pomegranate seed waste using a green extraction process, **Industrial Crops and Products**, 112, 790-802.	Published
8	**R.D. Singh**, K. Bhuyan, J. Banerjee, J. Muir, A. Arora, (2017), Hydrothermal and microwave assisted alkali pretreatment for fractionation of arecanut husk, **Industrial Crops and Products**, 102, 65-74	Published
9	Jhumur Banerjee, **Ramkrishna Singh**, R. Vijayraghavan, Douglas MacFarlane, Antonio F. Patti, Amit Arora, (2017), Bioactives from fruit processing wastes: Green approaches to valuable chemicals, **Food Chemistry**, 225, 10-22	Published
10	J. Banerjee, **R. Singh**, R. Vijayaraghavan, A. Arora, D. MacFarlane, A. Patti. (2016) Effect of drying methods and extraction time-temperature regime on mango kernel lipids. **International Journal of Food and Nutritional Science**. 3(2): 1- 10.	Published

Patents (As co-inventor, not related to this work)

1. Banerjee J. **Singh, R**., Vijayaraghavan, R., MacFarlane, D., Patti, A., Arora, A., 2017, An integrated process for recovery of pectin and a sugar-polyphenol mixture from horticultural waste. **Indian Patent filed**.
2. Banerjee, J., **Singh, R**., Kapoor, M., Sivaramakrishnan, C., Arora A. 2017. Efficient recovery of oil from pomegranate seeds. ***Indian provisional patent*** (TEMP/E-1/8747/2017-MUM)

Conference/ symposium

1. Daniel So, CK Yao, Naresh Pillai, **Ramkrishna Singh**, Peter Gibson, Jane Muir, 2019, Characterisation of fibres using a rapid *in vitro* fermentation method, 43rd NSA Annual Scientific Meeting, 2-5 December 2019, City Hall Newcastle. (abstract accepted)
2. Daniel So, Paul Gill, Chu Yao, Naresh Pillai, **Ramkrishna Singh**, Peter Gibson, Jane Muir, Evaluating fermentation characteristics of fibre using an *in vitro* fermentation model, Dietitians Association of Australia 36th National Conference, 12-14 August 2019, Gold Coast, Australia. (abstract accepted)
3. **Ramkrishna Singh**, Jhumur Banerjee, Amit Arora, Jane Muir, 2016, Development of functional foods from agricultural waste, International Conference on Emerging Technologies in Agriculture and Food Engineering, IIT-Kharagpur, 27-30 December.
4. J. Banerjee, R. **Singh, R**. Vijayaraghavan, A. Arora, D. MacFarlane, A. Patti. 2016. Nutraceuticals from horticultural processing waste', Emerging Technologies in Agricultural Engineering (ETAE 2016),Kharagpur, India, (29/12/2016)
5. J. Banerjee, R. **Singh, R**. Vijayaraghavan, A. Arora, D. MacFarlane, A. Patti. 2016. Valorisation of mango processing waste using a greener fractionation process, 6th International IUPAC Green Chemistry conference, Venice, Italy, (7/10/2016)
6. J. Banerjee, **R. Singh**, M. Kapoor, R. Vijayaraghavan, A. Arora, D. MacFarlane, A. Patti. 2016. Nutraceutical lipids from Pomegranate processing waste, Food Innovation Network workshop, Monash University, Melbourne, Australia, (17/8/2016)
7. J. Banerjee, R. **Singh, R.** Vijayaraghavan, A. Arora, D. MacFarlane, A. Patti. 2016. Development of integrative biorefinery for mango processing waste, The 5th Asia-Oceania Conference on Green and Sustainable Chemistry, New Delhi, India, (17/01/2015)
8. **Ramkrishna Singh**, Agro- based residues as a source of dietary functional fiber, Symposium on Waste to Wealth, 30-31 March 2016, IIT Bombay, India.